Apoplastic proteins, enzymes and radicals

Doherty, Sean

Apoplastic proteins, enzymes and radicals

A thesis submitted by Sean Doherty B.Sc. in accordance with the requirements for the degree of Doctor of Philosophy in the University of Durham.

Department of Biological Sciences, August 2000

For my Dad

ABSTRACT

Apoplastic proteins, enzymes and radicals.

The soluble and readily extractable part of the plant extracellular matrix has been termed, the apoplast and contains a wide range of components such as, complex carbohydrates, structural proteins, enzymes and radicals that are known to be responsive to stress and developmental pressures.

This thesis describes the development of a technique for the selective enrichment of apoplastic components for a range of subsequent analyses. Using this technique a number of apoplastic proteins were N-terminally sequenced and revealed 2 cell wall related enzymes, an antifungal protein and 3 auxin-binding/germin-like proteins. This technique also provided a novel approach to the further study of auxin-binding proteins via the use of affinity chromatography at their putative site of action, the apoplast. Three potential auxin-binding protiens were identified.

Many attempts were made to subject the material extracted from the apoplast to the highly resolving technique of 2-dimensional electrophoresis, and during the process two unusual 2D systems were developed. These systems could be run in a small format that permitted very rapid analysis and/or using an in-gel loading strategy to subject up to 500μg of protein to 2D separation therefore permitting N-terminal sequencing from single 2D gels. Unfortunately 2D separation of apoplastic proteins was never fully achieved within the time frame of this study due to the vast degree of heterogenity present in the sample material. It did however demonstrate the very complex nature of apoplastic components.

A series of experiments revealed that the tobacco leaf apoplast contained compartment specific antioxidant enzymes, some of which share physical characteristics with similar enzymes from other species. The activity of these enzymes altered in response to stress and according to the developmental age of the tissue. The reduced activity of these enzymes directly correlated to the degree of oxidative modification of apoplastic proteins illustrating that these enzymes are important in the detoxification of apoplastic radicals.

Follow on experiments following the apoplastic generation of the superoxide anion and nitric oxide from impact stressed potato tuber tissue showed that radicals play important roles in the responses of plant tissue to stress, and show the first involvement of nitric oxide in plants in response to abiotic stress.

STATEMENT

No part of this thesis has been previously submitted for any other degree at this or any other university. I declare that, unless otherwise stated, the work presented herein is entirely my own.

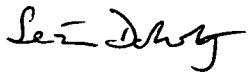

Sean Doherty

MEMORANDUM

Parts of this work have been submitted for publication in the following peer reviewed international journals:

Doherty, S. & Croy, R.R.D.
Tobacco leaf apoplastic superoxide dismutases and peroxidases.
Plant, Cell and Environment
Submitted September 2000; the manuscript is presented in Appendix 1.

Johnson, S.M., Doherty, S. & Croy, R.R.D.
Superoxide radical production in potato tubers: a novel biphasic response to mechanical stress.
Planta
Submitted August 2000; the manuscript is presented in Appendix 1.

Doherty, S. & Croy, R.R.D.
A simple and rapid microtitre plate spectrophotometric assay for superoxide dismutase.
Pre-submission manuscript is presented in Appendix 1.

Parts of this work have been presented at the following International Conferences:

Doherty, S. Johnson, S.M., Shehab, G.M.G. & Croy, R.R.D. (1999)
Radical Responses to stress in potatoes.
Presented at The 13th John Innes Symposium; 'Attack & Defence in Plant Disease'; Norwich, UK, 20-23rd July 1999.

Bowler, K., Bates, T. & Doherty, S. (1998)
Thermal tolerance in adult blowflies protects mitochondria from heat damage and involves production of heat shock proteins.
Presented at the XIX Congress of the European Society from Comparative Physiology and Biochemistry; 'Cellular and Molecular Responses to Environmental Changes'; Turku, Finland, 23-26th August 1998

ACKNOWLEDGMENTS

Grateful thanks to Dr Ron Croy for his supervision of this project, extensive and rapid proof-reading of this manuscript and a seemingly abundant supply of red ink.

Thanks to all the folks who have rustled in and out of Lab 2, special consideration to Dr David Dixon for his particularly large brain and Steven Johnson for involving discussions about sandwich fillings and bruised potatoes. John Gilroy deserves a special mention for his sequencing skills and being available, and in the department 7 days a week.

It is difficult to express enough gratitude to my wife Jacqui for her unerring support, listening ear and ability to distract me at any opportunity, grateful thanks to my best pal. Warm thanks are also due to my mum for a constant supply of boiled potatoes in childhood, my dad for his constant encouragement and never ending inquisitiveness and finally my in-laws for continual interest in all things scientific.

This research was funded by a special studentship from the Biotechnology and Biological Sciences Research Council.

ABBREVIATIONS

ABP	auxin binding protein
AGP	arabinogalactan protein
AOS	active oxygen species
Bis-acrylamide	bis (N,N'-methylene-bis-acrylamide)
BSA	bovine serum albumin
°C	degrees centrigrade
cm	centimetre
CMF	cellulose microfibril
2D	2-dimensional electrophoresis
dH_2O	distilled water
DNPH	dinitrophenylhydrazine
DTT	dithiothreitol
EDTA	ethylenediamine tetra-acetic acid
g	gram
GalA	galacturonosyl acid
GRP	glycine-rich protein
GSH	reduced glutathione
GSSG	oxidised glutathione
GSNO	nitrosoglutathione
H_2O_2	hydrogen peroxide
HPAA	hydroxyphenylacetic acid
HRGP	hydroxproline-rich glycoprotein
ICF	intercellular fluid
IEF	isoelectric focussing
kDa	kilodalton
l	litre
M	molar
M_r	molecular weight
MDH	malate dehydrogenase
NaCl	sodium chloride
NADH	nictotinamide adenine dinucleotide
NADPH	nictotinamide adenine dinucleotide
NEDD	N-(1-napthyl)-ethylenediamine dihydrochloride
$^{\cdot}NO$	nitric oxide
$^{\cdot}OH$	hydroxyl radical
$^{\cdot}OONO^{-}$	peroxynitrite radical
$^{\cdot}OONONOH$	peroxynitrous acid
$OONOCO_2$	nitrosoperoxocarbonate molecule
PAG-IEF	polyacrylamide gel isoelectric focusing phosphate
pI	isoelectric point
PGA	polygalacturonic acid
PMS	phenazine methosulphate
PR	pathogenesis-related
PRP	proline-rich protein
PVDF	polyvinylidene difluoride
QH_2O	deionised water
RG	rhamnogalacturonan
SDS-PAGE	sodium dodecyl sulphate polyacrylamide gel electrophoresis
SULF	sulphanilamide
TE	total extract
Tris-HCl	tris(hydroxymethyl) methylamine hydrochloride
RUBISCO	ribulose bis-phosphate carboxylase
VI	vacuum infiltration
v/v	volume for volume
v/w	volume for weight
XG	xyloglucan
XTT	2,3-bis-[2-methoxy-4-nitro-5-sulphophenyl]-2H-tetrazolium-5-carboxanilide

TABLE OF CONTENTS

SECTION 3 – MATERIALS

SECTION 4 – METHODS

SECTION 5 – APOPLASTIC PROTEINS

SECTION 6 – THE DEVELOPMENT OF 2D ANALYSIS

SECTION 7 – APOPLASTIC ANTI-AOS ENZYMES

LIST OF FIGURES

LIST OF TABLES

SECTION 1

INTRODUCTION

1.1 The Plant Extracellular Matrix

With growing knowledge the antiquated view of the plant extracellular matrix as a relatively inert, static and homogenous compartment has been radically revised to produce a concept of the extracellular matrix as a near extension of the cytosol, with a unique biochemistry and a complex dynamic structure. As an integrated structure, components in the extracellular matrix partly determine the development of the plant form, being essential for morphogenesis, organogenesis and therefore plant growth in its entirety. As would be expected of such a fundamental compartment of a plant, its structure, composition and biochemistry is dynamic during all stages of cell growth, maturation and differentiation.

Intracellular mechanisms exist to respond to temperature fluctuations, drought, changes in salinity, heavy metal presence and elevated levels of atmospheric pollutants. In tandem with intracellular changes, the extracellular matrix is also modified to enable the plant to cope with any such external environmental stress. In an analogous manner, adaptation is evident when a plant is wounded or undergoes pathogen attack. All adaptations are presumed to involve enhancing, restructuring or altering the composition of the extracellular matrix, to protect the plant and increase its overall chances of survival.

For the course of this introduction the plant extracellular matrix will be sub-divided into its two main discrete components, the cell wall and the apoplast. The cell wall is described in section 1.2 and the term apoplast will be fully defined in section 1.3. Figure 1.1 presents a highly simplified diagram to illustrate this sub-division.

1.2 The Plant Cell Wall

The cell wall is well recognised as the principal structural element of the plant that imparts mechanical integrity, for controlling the expansion of cells during development and acting as the primary 'barrier' between the external environment and the intracellular milieu [Braam 1999].

Cellulose is the principal element of the cell wall; it is synthesised at the plasma-membrane and forms long crystals of several dozen glucan chains. Cellulose in

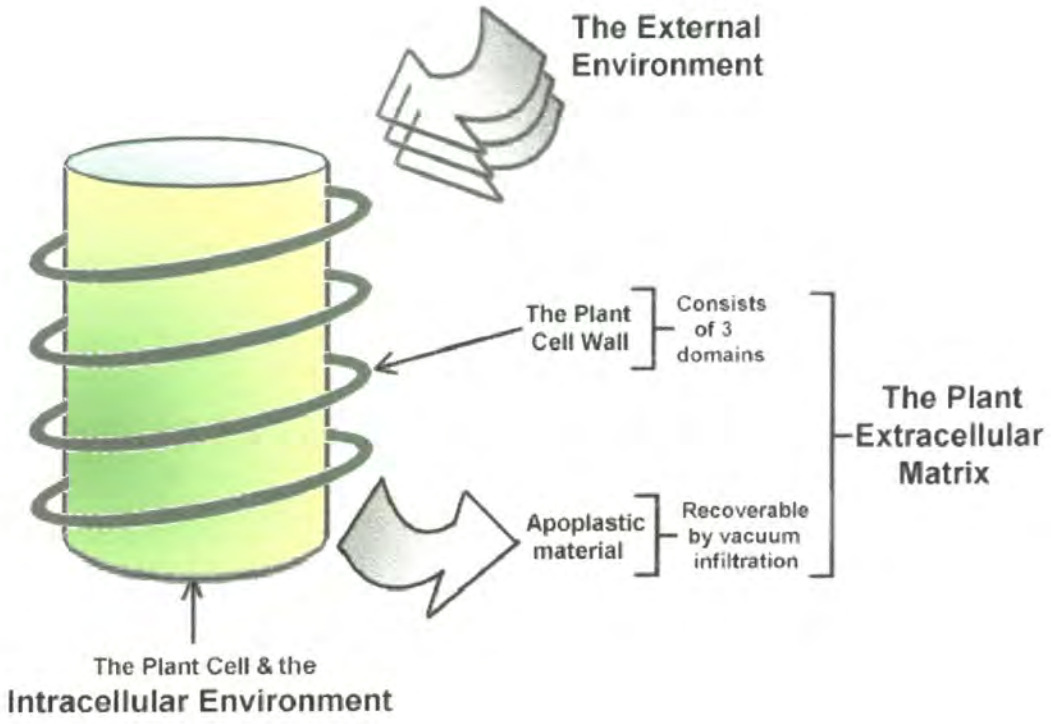

Figure 1.1

Schematic of the intracellular and external environments and the extracellular matrix.

Changes in the external environment can stress the plant and ultimately change both the intracellular environment and the extracellular matrix to cope with the imposed external stress. The plant extracellular matrix can be sub-divided into the plant cell wall, which comprises of 3 independent domains (see section 1.2) and the apoplast (see section 1.3).

conjunction with the heterogeneous xyloglucan group of polysaccharides provides the microfibrilar foundation of the cell wall that encases the cell and houses a diverse range of other non-cellulosic polysaccharides, proteins and enzymes. Indeed, several recent reports have altered the historical view of the cell wall as static and purely structural in function to a virtual continuum of the cytoskeleton [Lin *et al.* 1990; Wyatt & Carpita 1993; Zhu *et al.* 1993; Freshour *et al.* 1996].

Although the primary cell wall's of all plant species contain the fundamental cellulosic microfibrilar structure; other components are extremely diverse [Gibeaut & Carpita 1994]. Leaders in the field of plant cell wall biology, Carpita & Gibeaut [1993] have sub-divided the components that comprise the primary cell walls of plants into three independent, yet, interacting domains (see figure 1.1). Domain 1 comprises the basic structural elements of the plant cell wall, the cellulose-xyloglucan framework, which is embedded within a range of related gelatinous compounds that form the second domain, the pectin matrix. Both of these domains are comprised wholly of carbohydrates. The third independent domain consists of the proteinaecous elements of the plant cell wall.

Carpita & Gibeaut [1993] have also proposed that all plant cell walls can be divided into one of two broad categories; type I, which is typical of most flowering plants, and type II, which is seen primarily in the genus, Poaceae and some monocots. Throughout this research plants with type I cell walls have been utilised for study, consequently, this introduction will be limited to detailing the current consensus of a generalised type I cell wall. Furthermore, instead of constantly referring to the type I cell wall; it will simply be referred to as, the cell wall.

1.2.1 Domains 1 & 2 : The plant cell wall polysaccharides

Cellulose and callose are the only known plant polysaccharides to be synthesised at the plasma-membrane [Delmer 1991]. All other polysaccharides are synthesised by the Golgi apparatus [Driouich *et al.* 1993]. Not a single synthase of the vast array of polysaccharides present in plant cell walls has ever been unequivocally identified because, all plant polysaccharide synthases appear to be membrane-spanning proteins which are uniquely sensitive to solubilisation with respect to their enzymatic activities [see Driouich *et al.* 1993 for a review]. Consequently, it is only very recently, with the advent of new methodologies for polysaccharide sequencing that the myriad of polysaccharides present in the cell wall, are beginning to catalogued and categorised [McCann *et al.* 1994; Watt *et al.* 1999]. Due to the highly heterogeneous nature of cell wall polysaccharide material and relatively scarce information regarding functionality, the description below will be limited to the cellulosic microfibrilar foundation (domain 1) and an overview of some of the more prevalent and well documented polysaccharides found

housed within this framework (domain 2). Figure 1.2 provides a reference for structural information regarding the major polysaccharides discussed within the text.

- **Domain 1 : The cellulose-xyloglucan framework**

The cellulose-xyloglucan framework is a fibrilar network encasing the cell that accounts for approximately 50% of the primary cell wall mass. It forms the structural foundation of the cell wall and is composed of approximately 50% cellulose and 50% xyloglucan [Carpita & Gibeaut 1993].

Cellulose, (1→4)β-D-glucan chains of varying length, is synthesised at the plasma-membrane, by an as yet unidentified cellulose synthase complex and liberated into the extracellular matrix [Brett 2000]. Individual units of cellulose hydrogen bond to each other along their length to form paracrystalline assemblies of relatively huge cellulose microfibrils (CMFs) approximately 5-15nm wide [McCann *et al.* 1990]. Detailed electron microscopy studies have revealed that CMFs are wrapped around the cell like a skeletal cage, with individual fibres regularly spaced approximately 20 to 40 nm apart [McCann *et al.* 1990]. The exact arrangement of the CMF 'cage' alters according to cell and tissue type and developmental stage [Carpita & Gibeaut 1993] (see section 1.2.3).

Xyloglucans (XGs) are synthesised in the Golgi apparatus and secreted at the plasma-membrane surface by the secretory system. XGs have essentially the same glucan 'backbone' structure as cellulose, which comprise of linear chains of condensed (1→4)β-D-glucan monomers approximately 200 nm in length [McCann *et al.* 1990]. The most consistent structural difference is that XGs have numerous α-D-xylosyl units added at the O-6 position of the glucan residues within the backbone [Bacic *et al.* 1988]. However, XGs can be sub-categorised because of a bewildering array of potential tri-, hepta-, undeca- and many other oligomeric additions of monosaccharide units such as, β-D-galactose, α-L-arabinose and α-L-fucose to the xylosyl branch of the glucan backbone [Bacic *et al.* 1988]. The effect of these multitudinous structural differences can only be guessed at, but what is certain is that XGs have a very distinct and different functionality to cellulose, especially with respect to hydrogen bonding characteristics. Computer simulations have predicted that XGs can assume a range of low energy conformations, all with the potential to hydrogen bond to exposed β-D-glucan chains in CMFs [Levy 1991]. Consequently, it has been postulated that XGs can hydrogen bond to one another and to CMFs thereby aiding in spanning, linking and locking the CMF 'cage' around the cell [McCann *et al.* 1992; Carpita & Gibeaut 1993]. Figure 1.3 presents a diagrammatic representation of the current consensus.

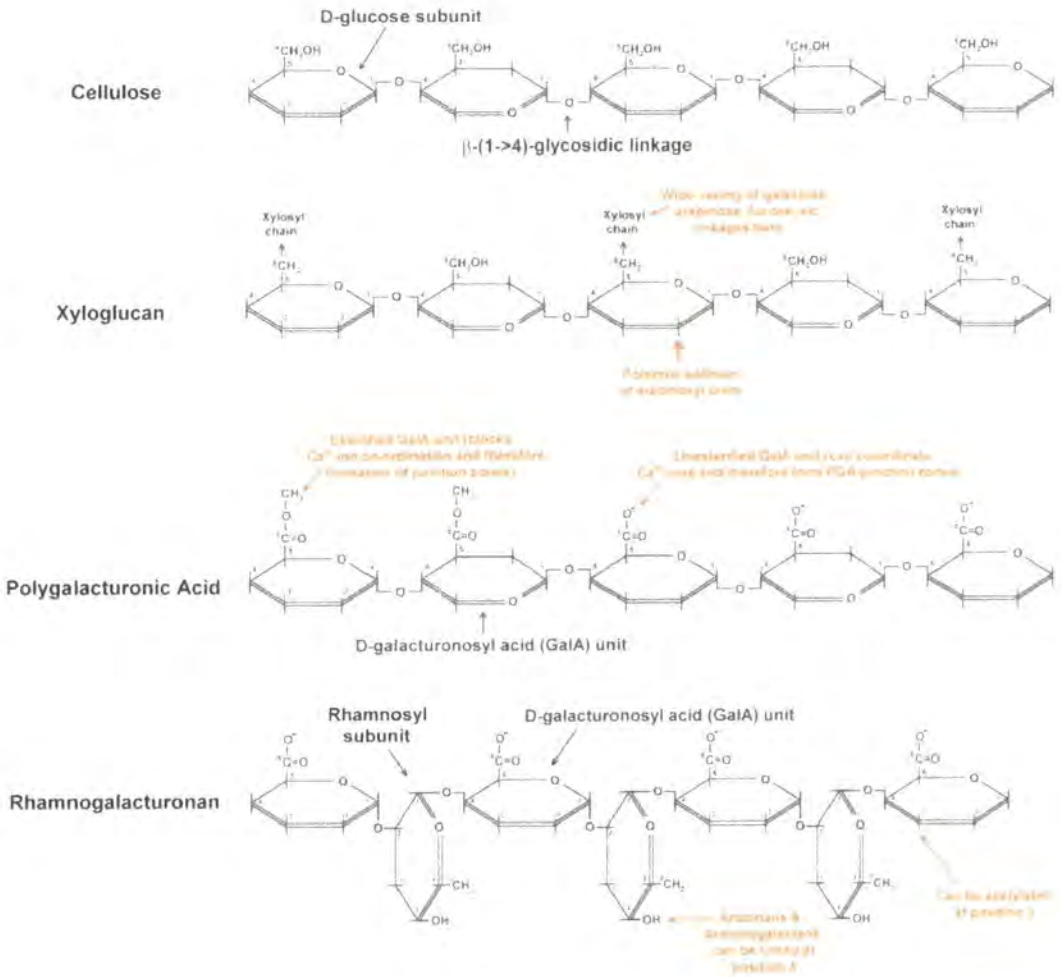

Figure 1.2

Plant cell wall polysaccharides.

Structures of the key plant cell wall polysaccharides described within the text. Red arrows and text indicate sites and description of potential additions and changes to the rudimentary structure that generate a high degree of heterogeneity. Structures are derived from information provided in Carpita & Gibeaut [1993].

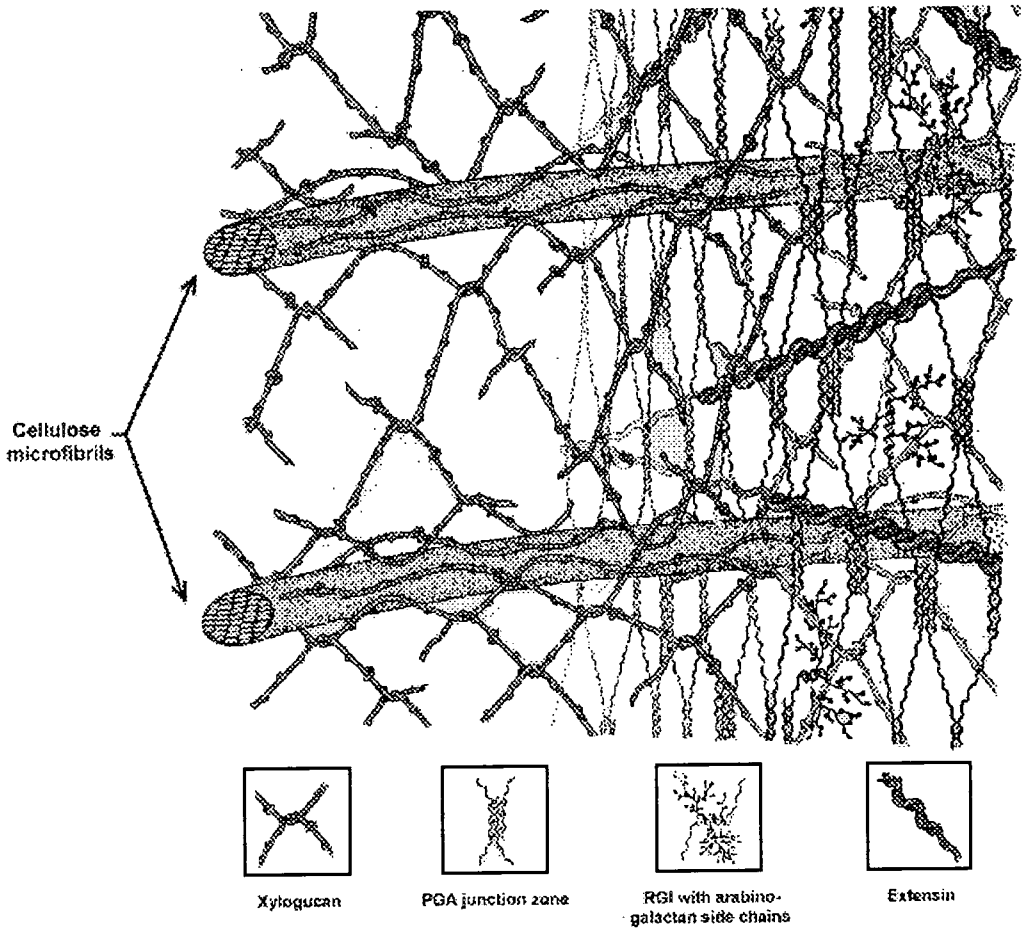

Figure 1.3

The 3 domains of the mature plant cell wall.

The diagram illustrates a single stratum of cellulose microfibrils (CMF's) in parallel arrangement, as they would be around a cell; the various CMF-linking molecules involved in structural integrity are presented in the legends. Several strata would form a full section of cell wall. This image has been adapted from Carpita & Gibeaut [1993].

There are many other non-cellulosic polysaccharides found in association with the cell wall, such as, galactoglucomannans, galactomannans, (1→3)β-D-glucans and glucutono-arabinoxylans, which also have the potential to bind to CMFs, but are found in much smaller amounts relative to XGs [Bacic *et al.* 1988; Maltby *et al.* 1979]. These polysaccharides are found in greater abundance in differentiated tissues and are assumed to be playing highly specialised structural roles.

- **Domain 2 : The pectin matrix**

The pectin matrix constitutes approximately 30% of the cell wall mass, its chemistry and physical properties are extremely complex and alter throughout development [Roberts 1990] and probably in response to environmental stress. The pectin matrix forms a gelatinous liquid that has often been described as a 'jelly' [Roberts 1990; Carpita & Gibeaut 1993] the physical properties of which, are highly dependent upon the local ratio and concentrations of ions and the local temperature [Walkinshaw & Arnott 1981; Nakajima *et al.* 1981]. The pectin matrix is primarily composed of two highly heterogeneous pectinous compounds, polygalacturonic acids (PGA's) and rhamnogalacturonans (RG's).

PGA's are composed of linear chains of 150-250 α(1→4)-glycosidically-linked sub-units of D-galacturonosyl acid. Hundreds of PGA chains can interact via hydrogen bonding to form helical chains that are about 100 nm in length. PGA's have the unique ability of being able to form, 'junction zones', by coordinating anti-parallel chains of unesterified PGA around calcium ions [Rees 1977; Jarvis 1984;] this behaviour markedly alters the physical properties of the whole gel [Powell *et al.* 1982]. The cross-linking of PGA's via calcium ion co-ordination is highly dependent upon the local concentration of Ca^{2+} [Walkinshaw & Arnott 1981], and measurements *in vivo* depict drastic shifts in the ratio and concentrations of magnesium and calcium in plant cell walls during growth and differentiation, these results may indicate development specific roles for PGA's [Nakajima *et al.* 1981].

At a structural level, RG's are contorted rod-like heteropolymers of repeating (1→2)α-L-rhamnosyl-(1→4)α-D-galacturonosyl acid disaccharide units. RG's are often linked to arabinans, galactans and the highly branched arabinogalactans via the O-4; furthermore, many RG's are acetylated at the O-3 position on galacturonosyl acid sub-units. Many more permutations exist; thus, it isn't surprising to find that as a group RG's comprise some of the most complex polysaccharides yet discovered. Consequently, it has been problematic elucidating both structures and functions for RG's [see Carpita & Gibeaut 1993].

Other pectinous compounds found in the pectin matrix at much lower levels are thought to play significant roles in fundamental cell biology. In particular intriguing evidence has accumulated that a particular sub-type of the polysaccharide grouping, arabinogalactan, plays a crucial role in cell differentiation pathways by acting as a specific cell 'marker' molecule [Pennell & Roberts 1990; Stacey *et al.* 1990].

The pectin matrix in conjunction with the cellulose-xyloglucan framework is proposed to modulate porosity, pH, ion balance and the water content of the plant extracellular environment [Jarvis 1984; Gibeaut & Carpita 1994] and may also play a role to generate signalling molecules [McCann *et al.* 1992]. All of these functions are of course extremely important to the plant, but at a fundamental level, the pectin matrix can even functionally replace the cellulose-xyloglucan framework. When tomato cells are grown in the presence of dichlorobenzonitrile (an inhibitor of cellulose synthesis) the pectin matrix becomes tightly cross-linked to form a semi-rigid cell wall [Shedtetzky *et al.* 1990]. Amazingly, the pectin matrix is effectively acting as a functional replacement for cellulose.

1.2.2 Domain 3 : The plant cell wall proteins

The plant cell wall and the general plant extracellular matrix it occupies play host to a wide range of structural proteins and wall associated enzymes. Each protein group may exhibit substantial inter-species sequence differences, which is especially evident in comparisons between monocot and dicot but all plant cell wall proteins identified to date are glycoproteins. Many of the structural proteins have been reasonably well characterised, as have some of the enzyme constituents. However, many proteins and enzymes associated with the cell wall are as yet still unidentified and of unknown function or significance. Broadly speaking several categories of plant cell wall proteins can be discerned based upon the presence of specific and highly repetitive amino acid motifs. The following is a brief overview of the structure, function and localisation of the known major cell wall structural proteins, table 1.1 presents a collated list of some of characteristics of the plant cell wall proteins considered in the text.

1.2.2.1 Hydroxyproline-rich-glycoproteins

The hydroxyproline-rich-glycoprotein (HRGP) family comprise a highly diverse range of glycoproteins found primarily in the extracellular matrix and predominantly in association with the plant cell wall. As the name suggests all HRGP's are rich in hydroxyproline, however, enough distinctive characteristics have been discovered within the broad

Table 1.1 – Characterised plant cell wall proteins; collated for this thesis from the references indicated, Somner-Knudsen *et al.* [1997] and Sachetto *et al.* [2000].

Type/Group	Species	Repetitive Protein Sequence	Protein Structure	Carbohydrate composition	Localisation	References
HRGP - Extensins	Soybean	SPPPPKH	Rigid polyproline II-like structure	50-60% (w/w) arabinose & galactose	Primary cell walls; vascular tissue	Evans *et al.* [1990]; Memelink *et al.* [1993]; Smith *et al.* [1986]
	Rape	SPPPPVK				
	Tobacco	SPPPPKKPYYPP				
	Tomato	SOOOOVKP				
HRGP – AGP's	Maize	$(Ala\text{-}Hyp)_X$ $(Ser\text{-}Hyp)_X$	Predicted partial polyproline II-like structure	>90% (w/w) arabinose & galactose (plus some rhamnose & glucuronic acid)	Vascular bundles; pollen; flowers	Kieliszewski *et al.* [1992]
	Maize					
	Maize					
HRGP – SL's	Daturna	$Ser\text{-}(Hyp)_4$	Predicted single domain with polyproline II-like structure	~50% (w/w) arabinose & galactose	Cell wall; cytoplasm and vacuole	Desai *et al.* [1981]; Kieliszewski *et al.* [1992]
	Potato					
GRP's	Arabidopsis thaliana	GGGX	Predicted keratin type structure of glycine loops or alternatively β-sheets	–	Epidermis; vascular tissue	Quigley *et al.* [1991]; Lin *et al.* [1996]; Condit & Meagher [1986]
	Carrot	GGX				
	Petunia hybridia	GGGX				
	Atriplex canlsceus	GGGX				
PRP's	Soybean	KPPVYK	Predicted β-helices	<3% to >70% (w/w) arabinose & galactose	Vascular tissue; frequently co-localised with extensins	Hong *et al.* [1990]; Stiefel *et al.* [1988]; Chen & Varner [1985]; Caelles *et al.* [1992]
	Maize	KPPTPKP				
	Carrot	PPIHKPP				
	Rice	PPTYKP				

classification of 'HRGP' to distinguish upto 3 individual sub-groupings, the extensins, arabinogalactan proteins and solanaceous lectins.

The extensins are probably the most well known HRGP's and comprise a diverse group of highly basic glycoproteins located in the cell walls of all plants but are particularly prevalent in dicots. They are typically the most abundant protein component, and depending upon the origin of the plant cell wall in question, they may comprise upto 10% of the final dry weight [Cassab & Varner 1988]. Extensins contain upto 40% hydroxyproline, but are also rich in serine, and usually contain some combination of valine, tyrosine, lysine or histidine and a large proportion of the primary amino acid sequence contains the repeating pentapeptide motif, Ser-(Hyp_4) often within the context of a larger repeating motif [Chen & Varner 1985; Memelink 1988]. The carbohydrate components of extensins usually comprise between 50 and 60% of the total mass. Typically, almost all the hydroxyproline residues within an extensin molecule are glycosylated with mono- to tetra- saccharides of (1→4)β-D-arabinose [Akiyama *et al.* 1980], furthermore, many serine residues can be α-linked to a single D-galactopyranose unit [Lamport *et al.* 1973]. In solution mature extensins conform to a rigid polyproline II type helical structure [van Holst & Varner 1984]. Experimental observations have revealed that mature extensins, (secreted >6 hours previously) are impossible to remove from the cell wall by all non-degradative solvents but newly secreted extensins can be leached from the cell wall with salt solutions [Smith *et al.* 1984]. These observations do provide direct evidence for the prevailing consensus regarding extensin function, one in which, Carpita & Gibeaut [1993] have likened to the functional equivalent of 'fixing pins' (see figure 1.3), that are inserted into the cell wall to enhance wall rigidity and strength. The method of extensin fixation appears to be achieved via H_2O_2-mediated formation of covalent tyrosine cross-links to other extensins, or strong ionic extensin-pectin interactions [Epstein & Lamport 1984].

The second major class of HRGP is the highly soluble, highly acidic and heavily glycosylated arabinogalactan proteins (AGP's). To date all AGP's have been located to the plant extracellular matrix, but precise localisation has been difficult because of their extreme solubility [Fincher *et al.* 1983]. However, some have been found in association with the extracellular side of the plasma-membrane [Pennell *et al.* 1989], and are frequently co-localised with glycine-rich-proteins (see section 1.2.2.3). A typical AGP has a protein moiety that comprises only 2-10% of the total mass, the remainder is a heterogeneous carbohydrate mixture composed of D-galactose and L-arabinose, connected to the protein core via hydroxyproline:β-D-galactopyranose linkages [Strahm *et al.* 1981] consequently AGP's can also be classed as proteoglycans [Braam 1999]. The degree of glycosylation observed in AGP molecules ensures that molecular weight estimation is extremely difficult, but all migrate in a pH gradient to exhibit pI's in the

range 2-5. The protein moiety is typically rich in hydroxyproline, serine, alanine, threonine and glycine, and many of the sequenced AGP's exhibit Ala-Hyp repeats towards the N-terminus [Gleeson *et al.* 1989], furthermore, circular dichrometry has revealed that in a similar manner to the extensins a proportion of the protein core (~30%) forms a polyproline II type helix [van Holst & Fincher 1984]. No function has been unequivocally assigned to AGP's, however based on their extracellular location and biochemical and physical properties they have been postulated to act as 'glues' and 'lubricants' [Fincher *et al.* 1983], 'chaperones' of polysaccharide materials during wall remodelling [Gibeaut & Carpita 1994] and cell-cell recognition molecules [Knox *et al.* 1991].

The third class of HRGP, the solanaceous lectins, are extracellular glycoproteins that are structurally similar to extensins and found only in solanaceous plants, the term lectin refers to their ability to bind to carbohydrate materials. Solanaceous lectins can be distinguished from other plant lectins because of their ability to agglutinate oligomers of N-acetyl-β-D-glucosamine [Allen *et al.* 1978; Murray & Northcote 1978], and their unusual amino acid and carbohydrate composition in which hydroxyproline and arabinose are major constituents [Showalter 1993]. Potato tuber lectin is the best characterised of all the solanaceous lectins identified to date. It is a glycoprotein with a molecular weight of 50kDa, and comprises 50% carbohydrate and 50% protein [Matsumoto *et al.* 1983]. The carbohydrate components are primarily tri- and tetra arabinose saccharides linked to hydroxyproline residues, and to a much lesser extent, serine can be linked to individual units of galactose [Ashford *et al.* 1982]. The protein moiety is especially rich in hydroxyproline, serine, glycine and cysteine and in its native state it is exhaustively inter-linked with disulphide bridges so that no free sulphydryl groups are present [Matsumoto *et al.* 1983].

1.2.2.2 Proline-rich-proteins

Proline-rich-proteins (PRP's) are a group of cell wall glycoproteins that have only been identified relatively recently, some members, and perhaps all, contain hydroxyproline, but PRP's can be distinguished from HRGP's because of a much lower degree of proline hydroxylation [Showalter 1993]. PRP's can be sub-categorised into two broad classes that are distinct but not mutually exclusive; those that are normal components of the extracellular environment [Chen & Varner 1985; Datta *et al.* 1989] and those that fall under the special grouping of, 'plant nodulins' [Govers *et al.* 1991]. Both classes can be characterised by a repeating Pro-Pro-Val-X-Lys (X = glutamic acid or tyrosine) motif, which is often incorporated within a variety of other larger repeating units [Hong *et al.* 1990]. PRP's from alfalfa and soybean cell wall's are some of the best characterised to

date and are typified by approximately equal quantities of proline and hydroxyproline [Francisco & Tierney 1990], and are typically only lightly glycosylated [Datta *et al.* 1989].

Developmental-related expression of PRP's has been reported in soybean [Hong *et al.* 1989], potato and tomato [Ye & Varner 1991]. Concurrent data from regulatory studies has indicated extensive PRP involvement in the various stages of development [Jose-Estanyol *et al.* 1992]. PRP's are often found localised at vascular bundles and some can often be found in association with extensins [Wyatt 1992]. PRP's are known to be expressed and oxidatively insolubilised, to form structural wall elements in a similar manner to extensins and glycine-rich-proteins (see section 1.2.2.3) in response to, wounding, endogenous and fungal elicitors, and ethylene treatment [Tierney *et al.* 1988; Marcus *et al.* 1991; Bradley *et al.* 1992].

Plant nodulins are proteins that are specifically produced in plants in response to infection by nitrogen fixing bacteria, and are ultimately constituents of the nodule wall [Franssen *et al.* 1987; Govers *et al.* 1991]. It is proposed that these proteins are involved in nodule morphogenesis and the responses to bacterial infection process in general. Govers *et al.* [1991] hypothesised that plant nodulins may be specifically induced to form an extracellular, 'oxygen barrier' for the O_2-sensitive nodules.

1.2.2.3 Glycine-rich-proteins

The first glycine-rich-protein (GRP) gene was discovered in 1986 by Condit & Meagher, it encoded an extracellular protein that contains 67% glycine, with the repeating motif Gly-X, where X can be alanine or serine. The Gly-X repeat is a very distinctive characteristic of GRP's and results in a glycine content in the range 25 to 70% [Mundy & Chua 1988]. Secondary structure predictions have indicated that GRP's may exist as β-pleated sheets composed of varying numbers of anti-parallel strands dictated by the particular GRP sequence. Two sub-classes of GRP's exist, the first is developmentally regulated, encodes a signal peptide and is ultimately destined for the exterior of the cell [Keller *et al.* 1988], the second, either lacks a signal sequence or encodes an RNA-binding domain and is cytoplasmic [Sturm 1992].

GRP's are typically the second major structural protein associated with the cell wall of dicot plants [Hirose *et al.* 1994; Carpenter *et al.* 1994; Parsons & Mattoo 1994], though much smaller quantities are also found in monocots [Cretin & Puigdomenech 1990; Didierjean *et al.* 1992]. Commonly they are co-localised with PRP's [Condit *et al.* 1990] and have been frequently located to vascular bundles, particularly the xylem, and are also clearly associated with cells that are going to be lignified [Ye & Varner 1991]. GRP's are commonly expressed during wounding and drought stress, and may provide

elasticity with a high tensile strength due to extensive β-pleating, or act as nucleation sites for lignification [Keller *et al.* 1988].

1.2.3 The plant cell wall and development

The plant cell wall changes dramatically throughout development therefore it is commonly divided into three sequential stages, cytokinesis, elongation and maturation. At each stage, the chemistry, biochemistry and resultant structure of the cell wall alters.

1.2.3.1 Cytokinesis

After nuclear and cytoplasmic division has taken place the new cells begin to develop a vestigial cell wall called the phragmoplast that physically divides the two cells from one another. The phragmoplast is formed from coalesced Golgi vesicles that primarily contain the polysaccharide, callose [Kakimoto & Shiboaka 1992].

After the initial phragmoplast separation of the two cells, CMF encasing of the cells begins. Deposition of CMFs is closely associated with the terminal ends of the cytoskeleton, thus tentative similarities to animal cell cytoskeletal-extracellular matrix interactions have been proposed [Zhu *et al.* 1993]. Immediately after cytokinesis, CMFs are arranged around the cell in a relatively random fashion (see figure 1.4a). CMFs re-orientate as the cell progresses towards elongation, leading to bands of CMFs encasing the cell. This banding can be arranged traversely or longitudinally and ultimately produces a CMF arrangement rather akin to a spring in which CMFs are regularly spaced, presumably by cross-linking to XG polysaccharides [Carpita & Gibeaut 1993] (figure 1.4b).

1.2.3.2 Cell wall elongation

In order for the cell to continue developing it must increase its size by elongating. Cross-linked XGs are considered to be the principal tension bearing components of the cell wall (see figure 1.4b & c), therefore elongation cannot occur until this restraining framework is removed or greatly loosened. Hydrolysis of CMFs and breakage of XG-CMF interactions appears to be the logical process by which the CMF-XG cage could be weakened to allow elongation of the cell. At first glance this appears to be exactly what is happening, pea seedling walls lose up to 50% of their total XG content during elongation [Hayashi 1984]. However, this assumption is directly challenged by recent contradictory evidence presented by McQueen-Mason & Cosgrove [1995]; the walls of cucumber cells that were heat-killed could be induced to elongate, without the detectable release of sugars, by two small, non-hydrolytic proteins, which have been dubbed, 'expansins'. They go on to

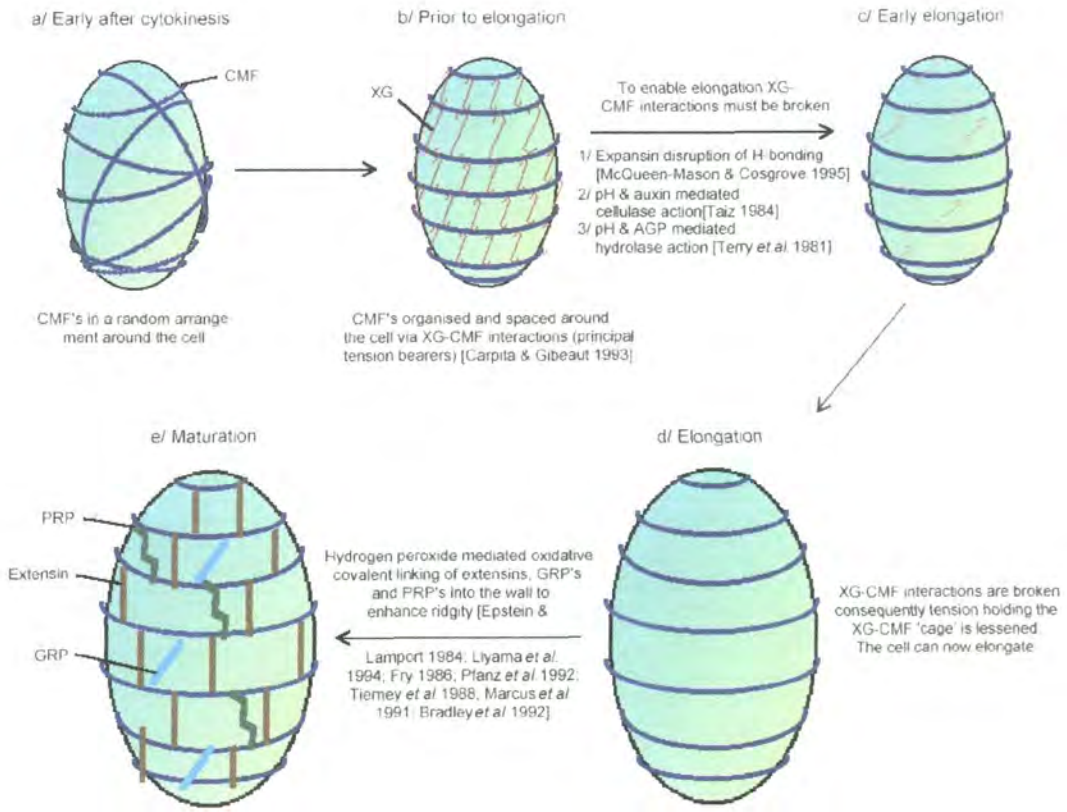

Figure 1.4

The plant cell wall during development.

Information collated and presented in graphical form based on the references quoted.; Terry *et al.* 1981; Epstein & Lamport 1984; Taiz 1984; Tierney *et al.* 1988; Marcus *et al.* 1991; Bradley *et al.* 1992; Pfanz *et al.* 1992; Capita & Gibeaut 1993; McQueen-Mason & Cosgrove 1995.

discuss a possible mechanism of expansin disruption of hydrogen bonding between CMFs and XGs.

Thus the process of cell elongation hasn't yet been fully elucidated and other possible mechanisms have been proposed. Most involve interaction with the pectin matrix. For example, PGA's can be de-esterified by the enzyme pectin methyltransferase, thus indirectly altering the local pH. At specific pHs and under the action of auxin, cellulases can hydrolyse XGs *in vitro* [Taiz 1984]. Alternatively, AGP's may bind specifically to XG-CMF cleavage sites thus preventing access by hydrolytic enzymes, slight alterations in the ionic environment as a result of pectin methyltransferase activity could substantially alter the tenacity of AGP's to bind to such sites [Terry *et al.* 1981] (refer to figure 1.4c).

Interestingly, and of particular relevance to this study Fry [1998] and Schweikert *et al.* [2000] have proposed a new theory of cell wall loosening and elongation via the scission of polysaccharides by active oxygen species (AOS), in particular the hydroxyl radical. This theory details a series of Fenton style reactions (see section 1.5 for an overview) that can generate hydroxyl radicals in the extracellular matrix by the action of cell wall and apoplastic peroxidases, providing there is a constant supply of molecular oxygen and a suitable reductant, such as ascorbate. Hydroxyl radicals have been proven to induce polysaccharide scission *in vitro* [Fry 1998; Schweikert *et al.* 2000] a similar situation *in vivo* may ultimately break the restraining XG-CMF framework and consequently loosen the cell wall around the elongating cell. Although hydroxyl radicals are invariable regarded as detrimental, they are so short lived they may act as site-specific oxidants targeted to play useful roles during wall loosening for cell elongation and fruit ripening. The extracellular generation of hydroxyl radicals by this mechanism is covered more fully in section 1.5.2.

1.2.3.3 Cell wall maturation

Once the cell has fully elongated, the cell wall is 'locked' into place. The extensin group of proteins are thought to be important elements of the locking mechanism because it is well established that they are oxidatively fixed into cell wall (see sections 1.2.2.1, 1.4.1 & 1.4.3). Concurrent with this assumption is the observation that cessation of cell elongation, is accompanied by a large increase in the quantity of extensin in the extracellular environment [Sadava *et al.* 1973]. Extensins are insolubilised into the wall by ionic interactions with pectins, and/or covalent linkages via tyrosine bridges to other extensin molecules and PRP's [Epstein & Lamport 1984; Fry 1986] (see figure 1.4e).

In cells that are subsequently going to be lignified GRP and PRP expression is highly co-localised, coupled with this, both protein types rapidly become insoluble after secretion, in a similar manner to extensins [Tierney *et al.* 1988; Marcus *et al.* 1991; Bradley *et al.*

1992]. This possibly indicates that PRP and GRP molecules may interact and are oxidatively insolubilised together. Several potential covalent linkages are feasible between GRP's and PRP's, as is linkage to extensins via isodityrosine linkages (figure 1.4e).

Thus the prevailing hypothesis follows that immediately after cell division CMFs are randomly wound around the cell, and as the cell wall continues to develop the CMFs re-orientate to become regularly spaced and transiently fixed into place by XG interaction. During elongation, XG interactions with CMFs are disengaged thus permitting the cell to elongate. As the cell begins to approach maturity, extensins, PRP's and GRP's are expressed and are oxidatively fixed into the wall, thus locking the cell wall into its final conformation around the cell.

1.3 The Apoplast

In 1930 Münch first coined the term 'apoplast' to describe the free space between plant cells through which solutions could move relatively unhindered. He used the term in his description of the theory of translocation of solutes over long distances between sources and sinks within a plant. Since then the term apoplast has been utilised in many ways to describe the extracellular matrix surrounding plant cells. In the 1950's researchers working on extracellular ion movement described the apoplast as [Briggs 1957],

"... the free space formed from spaces generated by the continuous wall phase."

Until the late 1950's the term apoplast was used to describe the part of the plant tissue that was essentially, 'non-living' and in which substances in solution could move by diffusion. However during the 1970's plant anatomists further revised the term. They described the apoplast as,

"... *the walls and intercellular spaces that contain not liquid, but gas*".

This definition is distinct from Münch's apoplast and Briggs' free space in that it refers only to the gaseous phase of the intercellular space. During the intervening 20 years the term apoplast has been utilised essentially to refer to the part of the extracellular matrix of plant cells that is distinct from the plant cell wall. Recently Canny [1995] has attempted to clarify and section the apoplast into four distinct types of space with associated putative functions: -

1. **The xylem-lumen apoplast:** carries water from roots.
2. **The water free-space:** is composed of the wet intercellular space and is part of the cell-wall space. The liquid effectively forms a film, which permits diffusion among contacting solutions [Altus *et al.* 1985].
3. **The Donnan free-space:** a further subsection of the wall space. Contains fixed negative charges.
4. **The gaseous intercellular space:** small gas pockets transiently entrapped by water films lining the space.

The apoplast has a multitude of roles to fulfil not least the establishment and maintenance of cell and tissue shape in conjunction with cell walls, turgor development, and uptake and transport of water, ions and metabolites (i.e.: root apoplast and xylem) and gaseous exchange with the external environment. In addition to these many important functions the apoplast is intricately involved in many other cellular reactions and processes, not only under normal growth conditions but also under stress conditions. Abiotic stresses (temperature, ozone, sulphur dioxide, nutrient deficiency or excess, heavy metals, etc) or biotic stress (herbivore and insect induced wounding or bacterial and fungal infections) are known to alter apoplastic functions either as a direct and toxic effect of the stressor or as a reflection of an adaptation to the stress.

The apoplast has an ion and metabolite composition distinct from other cellular compartments, and contains tissue-specific patterns of structural proteins and lytic enzymes. Five distinct processes have been identified that ultimately play roles in defining the metabolic composition of the apoplast [Dietz 1997]:-

1. Physiochemical properties (mostly dictated by the cell wall)
2. Transport characteristics of neighbouring cells
3. Exo- and Endocytotic activity of neighbouring cells
4. Water and solute transport in the xylem-lumen apoplast
5. Environmental factors (biotic and abiotic)

The apoplast as a homogenous compartment almost certainly does not exist because the factors that contribute towards apoplastic composition are many, varied and some, like external environmental stresses are outside the control of the plant [Canny 1995; Dietz 1997]. Unfortunately there are only a few methods which can distinguish microheterogeneity in the apoplast including; pH measurements using fluorescent dyes [Canny 1995] or microelectrodes [Edwards *et al.* 1988] or immunocytochemistry and tissue prints to investigate protein distribution [Ye & Varner 1991]. Methods in operation to directly sample the apoplast, such as vacuum infiltration, offer low spatial resolution

and therefore tend to give average measurements or protein extracts over a relatively large area.

1.3.1 Gaseous exchange

The molecular composition of the apoplastic gas phase is highly dependent upon the composition of the atmosphere, the aperture of the stomata (limits diffusion), the solubilisation profile (gases and salts) of the aqueous phase of the apoplast and the rate of uptake of dissolved material into the cell [Nobel 1983]. The stomata constantly alter aperture size according to the prevailing conditions and thereby restrict equilibrium formation between leaf gas phase and the atmosphere, consequently the water vapour saturation is thought to be approaching 100% in the internal leaf gas space [Farqurhar *et al.* 1981]. The diffusion resistance for other gases can be inferred from the diffusion resistance to water vapour [Pfanz & Heber 1989]. Laisk *et al.* [1989] have calculated that under normal atmospheric conditions the concentrations of potential gaseous toxins, such as, ozone, in the leaf gas phase is close to zero. Consequently when elevated atmospheric toxins are present locally, the diffusion gradient is maximal into the gas phase of the leaves, the only limitation to the influx of potential deleterious gaseous toxins is stomatal aperture size. Current theory therefore suggests that the apoplast acts as a very effective sink for gaseous toxins and accordingly the extracellular matrix and the plasma-membrane are effectively exposed targets for immediate damage by such gaseous toxins.

1.3.2 The volume of the leaf apoplast

In all of these studies an important feature for consideration is the relative volumes of gaseous and liquid filled spaces. Using aqueous solutions of low viscosity and known density, measurements have been made of the increase in leaf weight after complete infiltration with a sorbitol solution [Dietz *et al.* 1992; Winter *et al.* 1993 & 1994] and silicone oil [Luwe & Heber 1995]. Taking weight change data, post-infiltration, provides a measure of the volume of intercellular gas space within leaf material. Another way to measure the volume of the apoplast has been to manually analyse ultrathin cross-sections for the relative areas of both intra- and extracellular compartments [Dietz *et al.* 1992; Winter *et al.* 1994]. Such estimates indicate that intercellular gas spaces in leaves typically occupy 18-46% of the total leaf volume and interestingly, the proportion of intercellular gas space to total leaf volume is responsive to stress (i.e.: heavy metal exposure).

The volume of the aqueous phase of the apoplast can be estimated by infiltrating a known concentration of a marker substance; this is effectively diluted by apoplastic

liquid, reducing the concentration of the marker which can then be recovered and assayed to calculate the dilution factor. From this information it is possible to extrapolate the volume of liquid (diluent) in the apoplast [Speer & Kaiser 1991]. Estimates vary and are extremely species-dependent, presumably because of species-specific morphological differences, but approximately 5-20% of leaf water appears to be apoplastic. Table 1.2 presents compiled data detailing the calculated volumes of apoplastic gaseous and aqueous phases for several different plant species.

1.3.3 pH and solute composition of the leaf apoplast

Typically the pH of the apoplast is lower than that of the cytosol, and usually ranges between 5-7. In 1987 Canny used the pH tracer dye sulphorhodamine, and showed that strong acidification (<pH 4) occurs at bundle cells in soybean, i.e.: microheterogeneity in apoplastic pH is evident. Stress, growth substances and enzyme action can all alter apoplastic pH, so one value, for all tissues does not seem likely, more probable is that pH is highly dependent upon local tissue conditions. Changes in apoplastic pH are particularly important because they affect the activity of plant growth regulators such as indoleacetic acid and abscisic acid. Abscisic acid and indolacetic acid respond to altered growth conditions and stresses by redistribution or changes in metabolic activity [Slovik & Hartung 1992]. Table 1.3 illustrates that depending upon the species in question apoplastic pH can range from 5.2 to 7.5 [Dietz 1997].

Mirmura *et al.* [1992] have proposed that the apoplast acts as an ion reservoir for K^+, Ca^{2+}, Mg^{2+}, Cl^-, NO^{3-} and PO_4^{3-} ions which is ultimately under homeostatic control. Other solutes such as sugars, amino acids, ascorbic acid, dehydroascorbate, phenolic compounds and organic acids can be detected at low but not insignificant levels (see table 1.4). Based on water turnover and solute concentrations detected in the xylem, solutes equivalent to 2 osmol/l^{-1} should accumulate in leaves if no solute recycling mechanism was present. Solute cycling between shoot and root has been established for all major elements [Jeschke & Pate 1991]. Using tracer dyes, Smith and Nobel [1986] have observed that solutes tend to accumulate at the extreme tips and margins of leaves; this is especially important for salt-stressed plants, because apoplastic salt-accumulation is thought to be the primary cause of salt-induced necrotic lesions [Speer & Kaiser 1994].

1.3.4 The working definition of the leaf apoplast

Many reports have detailed the use of various types of vacuum infiltration strategies to selectively remove apoplastic components [Ilett 1998; Hammond-Kosack 1992]. Throughout this project vacuum infiltration has been the method of choice for the

Table 1.2 – Estimates of the volumes of intercellular gas and apoplastic water spaces in leaves from different plant species; adapted from Dietz [1997].

Species	Intercellular gas space ($\mu l\ g^{-1}$)	Apoplastic water volume ($\mu l\ g^{-1}$)	Reference
Carpinus betulus	200	150	Luwe [1994]
Corylus avelana	330	130	Luwe [1994]
Hordeum vulgare	260	53	Winter *et al.* [1993]
Spinacia oleracea	430	70	Winter *et al.* [1993]
Spinacia oleracea	450	110	Speer & Kaiser [1991]
Vicia faba	870	110	Hajibagheri *et al.* [1984]

Table 1.3 – Estimates of apoplastic pH in various species; adapted from Dietz [1997].

Species	pH value	Method	Reference
Beta vulgaris	6.0±0.3	Fluorescence	Pfanz & Dietz [1987]
Gossypium hirsutum	6.7-7.5	Pressure chamber	Hartung *et al.* [1988]
Ruminex lunaria	5.6±0.2	Fluorescence	Pfanz & Dietz [1987]
Spinacia oleracea	6.4±0.3	Fluorescence	Pfanz & Dietz [1987]
Vicia faba	5.2-5.9	Fluorescence	Muhling *et al.* [1995]

Table 1.4 – Ion, metabolite and growth regulator composition of the leaf apoplast; adapted from Dietz [1997].

Compound or ion	Apoplastic concentration	Species	Reference
Amino acids	3.1±0.4 mM 3.2±0.8 mM	*Hordeum vulgaris* *Spinacia oleracae*	Lohans *et al.* [1995]
Ascorbic acid	0.45 mM	*Spinacia oleracae*	Takahama & Oniki [1992]
Glucose	1.0±0.4 mM 4.2±2.3 mM	*Hordeum distichum* *Hordeum vulgaris*	Tetlow & Farrar [1993] Lohans *et al.* [1995]
Glutathione	6.5μM	*Picea abies*	Polle *et al.* [1990]
Malate	5.5±1.4 mM 0.6±0.3 mM	*Hordeum vulgaris* *Spinacia oleracae*	Lohans *et al.* [1995]
Chloride	4±1 mM 6±2 mM	*Spinacia oleracae* *Pisum sativum*	Speer & Kasier [1991]
Magnesium	2±1 mM	*Spinacia oleracae*	Speer & Kasier [1991]
Phosphate	2.5±0.4 mM	*Hordeum vulgare*	Mimura *et al.* [1990]
Potassium	2.4±11.8 mM	*Pisum sativum*	Long & Widders [1990]
Sodium	1±1 mM 2±1 mM	*Spinacia oleracae* *Pisum sativum*	Speer & Kasier [1991]
Abscisic acid	20-100 nM	*Gossypium lirsutum*	Hartung *et al.* [1992]
Cytokinin	~10 nM	*Gossypium lirsutum*	Hartung *et al.* [1992]
Indoleacetic acid	200 nM	*Gossypium lirsutum*	Hartung *et al.* [1992]

selective enrichment of apoplastic materials primarily because of the ease of the technique, the extremely low levels of intracellular contamination and the partial purification achieved during the extraction. As a consequence, with respect to this project, the working definition of the apoplast and derived apoplastic materials, will be defined as, the parts of the extracellular matrix that are recoverable by vacuum infiltration.

1.3.5 Theoretical considerations on the extraction of apoplastic components

Ewald *et al.* [1991] have calculated that the cell walls of higher plants will exhibit sieving properties that will exclude molecules with a Stokes radius larger than 2.9 nm, this corresponds to a molecular mass of 40-45 kDa. Using non-destructive means to extract apoplastic components (i.e.: vacuum infiltration) these sieving effects should be evident. Dietz [1997] reports that a typical whole leaf infiltration eventually subjected to 2-dimensional IEF vs. SDS-PAGE separation will reveal 60-100 major and minor polypeptides with a molecular mass in the range 10-60 kDa. Many of these apoplastic proteins are known to be sub-unit components of larger assemblies with native molecular masses upto 300 kDa [Rohringer *et al.* 1983] for example α-mannosidase of barley is a complex of 270 kDa [Betz *et al.* 1992]. However, contradictory to the theoretical limits imposed by Elwald *et al.* [1991] apoplastic proteins or polypeptides of this size are readily extractable using vacuum infiltration. There is no obvious explanation to clarify why larger proteins are not sieved out by the cell wall fabric [Betz *et al.* 1992; Dietz 1997].

1.4 Apoplastic Proteins

The secretory system, which comprises the Golgi apparatus, rough and smooth endoplasmic reticulum and secretory vesicles, delivers secretory proteins and carbohydrate materials (with the notable exceptions of cellulose and callose) to the plant extracellular matrix [see Chrispeels 1991 for a review]. Therefore, the protein composition of the both the plant cell wall and the apoplast is ultimately under the control of the cytosol, this is most obvious when the protein complement rapidly changes in response to biotic or abiotic stresses [Dietz 1997]. The total protein content of the extracellular matrix consists of a covalently bound fraction which acts primarily in structural roles [Fry 1991], some of the key covalently bound proteins have already been described in section 1.2.2. The remainder fall under the umbrella term of apoplastic, as defined in section 1.3.4, and are therefore either ionically bound or freely soluble [Fry 1991] because they are readily removed from the apoplast by vacuum infiltration. Table 1.5 presents some of the better characterised apoplastic proteins. As can be seen all known apoplastic proteins can be broadly categorised into either cell wall, intercellular

Table 1.5 – Examples of characterised proteins present in the leaf apoplast [compiled and adapted from the references indicated and Dietz 1997 for this thesis].

Functional Grouping	Protein	Characteristics	Specific functions	Reference
Cell wall related	**Expansins**	Soluble 29 & 20kDa	Cell wall elongation	McQueen-Mason and Cosgrove [1994]
	β-Fructofuranosidase	Soluble and cell wall bound forms; 50-60 kDa	Cleavage of sucrose and regulation of photosynthesis	Sturm & Chrispeels [1990]; Tang *et al.* [1996]
	Germin/Oxalate oxidase	Soluble homopentameric glycoprotein of 125kDa	The production of hydrogen peroxide via the oxidation of oxalate oxidase; oxidative linkage of cell wall polysaccharides	Lane [1994]
	β-1→3, 1→4-Glucanase	Soluble cell wall maintenance protein	Normal wall metabolism	Hoj & Fincher [1995]
	Hydrolases	Acid pH optima	Breakdown of pectins during cell growth; hydrolysis of ABA glucose esters	Sawicka & Kacperska [1995]
	Lipid transfer proteins	Hydrophilic, ~9 kDa	Cuticle assembly, pathogen-, ABA-, drought-, heavy metal-induced	Molina *et al.* [1992]]
	α-Mannosidase	270 kDa	Glycosylation and turnover of glycoproteins; may degrade pathogen walls	Betz *et al.* [1992]; Brune *et al.* [1994]
	Phosphatase	Two 70 kDa subunits	Hydrolysis of organic phosphates	Ferte *et al.* [1993]
	Protease	Acidic protein; 70 & 100 kDa	Protein degradation during senescence	Pinedo *et al.* [1993]
Intercellular signalling	**Auxin-binding protein I**	Auxin binding domain and KDEL sequence	Putative extracellular auxin binding activity	Brown & Jones [1994]; Shimomura *et al.* [1999]
	Calmodulin-binding protein	Soluble, apoplastic 21 kDa protein	Putative calmodulin signalling pathway	Jun *et al.* [1996]
Stress related	**Chitinase**	Multigene family	Hydrolysis of fungal cell walls containing chitin as a component. Defence response	Chen *et al.* [1994]
	Defensin (formerly γ-thionin)	Small 5 Da peptide	Involved in pathogen resistance	Broekaert *et al.* [1995]
	β-1→3-Glucanase	Hydrolysis of 1→3-β-glucans	Hydrolysis of 1→3-β-glucans present in fungal cell wall. Defence response	Hoj & Fincher [1995]
	Polygalacturonsidase inhibitor protein	40 kDa	Binds and inactivates fungal polygalacturonsidase	Bergmann *et al.* [1994]
	Osmotin	25-50 kDa	Drought- and salt-induced	Zhu *et al.* [1995]
	Peroxidases	Hydrogen peroxide utilising	Cross-linking of cell wall components; degradation of auxin; lignification; roles in defence and stress responses	Pfanz *et al.* [1992]; Polle *et al.* [1994]
	Superoxide dismutase	CuZn enzyme	Roles in oxidative stress tolerance	Streller & Wingsle [1994]
	Thionin	Basic, cys-rich, low molecular weight proteins	Inhibition of pathogens	Bohlmann & Apel [1991]

signalling or stress-related with respect to their function. Each will be considered in turn.

1.4.1 Cell wall related apoplastic proteins

The plant cell wall is an extremely complex amalgam of polysaccharides and protein materials, (see section 1.2), many cell wall related apoplastic proteins have enzymatic activity which appear to play roles in remodelling cell wall architecture during development.

The cell wall hydrolases are a particular numerous and diverse group of cell wall related apoplastic enzymes that can be found ionically bound to the plant cell wall or freely soluble depending upon the local pH and ionic strength, most characterised apoplastic hydrolases have optimum hydrolytic activity at acidic pH [Hatfield & Nevins 1987; Sawicka & Kacperska 1995]. The grouping is large, and probably contains a repertoire of hydrolases that could potentially break all of the known glycosidic linkages present in the plant cell wall and include examples of cellulases, gluconases, α- & β-galactosidases, β-glucuronosidases, α- & β-mannosidases, β-xylosidases and arabinosidases [Fry 1991]. Some hydrolases, such as the cellulases, were originally considered to play crucial roles hydrolysing the cellulose components of plant cell walls to enable wall loosening and subsequent cell elongation [e.g.: Taiz 1984]. However, this theory has been disputed, most notably by McQueen-Mason & Cosgrove [1995] after the discovery that the small, apoplastic expansin proteins can disrupt CMF-XG interactions, thereby mediating cell wall loosening without recourse to substantial enzymatic digestion of cellulose polymers by cellulases. (Incidentally, Fry [1998] has also proposed a hydroxyl radical theory of plant cell wall loosening described in outline in section 1.2.3.2 and in greater biochemical detail in section 1.5).

Germination, the process of hydration of a dry, mature embryo, that leads to growth of the embryo into a viable seedling involves a huge increase in the mass of the plant, which in wheat escalates from <1 mg to >10 mg with 48 hours, this increase is accompanied by very little cell division but rapid restructuring of the extracellular matrix to accommodate the great increase in cell size [Lane 1994]. Germin is an apoplastic/cell wall associated glycoprotein with a native molecular weight of ~125kDa, that was found to be expressed in tight correlation with the process of germination and cell wall maturation [Lane *et al.* 1992] and was ultimately determined to be an enzyme with oxalate oxidase activity [Lane *et al.* 1993]. Extraction of the protein reveals that there is a tenacious selective association between germin and some members of the arabinogalactan family of extracellular matrix polysaccharides [Lane *et al.* 1987; Jaikaran *et al.* 1990] coupled with the enzymatic production of hydrogen peroxide from oxalate

oxidation the proposed function of germin is the oxidative coupling of polysaccharides into the plant cell wall [Lane 1994].

A range of broad substrate-peroxidases are also proposed to play similar oxidative cell wall strengthening role, and are therefore critical to apoplastic integrity and development. As a group, the apoplastic peroxidases can oxidatively couple polysaccharide-bound phenolic groups including, the *p*-coumaroyl groups of certain polysaccharides and oxidative cross-linking tyrosine residues in extensins and some PRP's and GRP's via isodityrosine bridges to enhance wall rigidity [Epstein & Lamport 1984; Fry 1986]. Furthermore they are integral to lignification via coupling p-hydroxycinnamyl, coniferyl and sinapyl alcohol's [Mader 1980]. Apoplastic peroxidases are often expressed in a tissue-specific, developmental- and stress-related manner; consequently, they are frequently implicated in differentiation, pathogen resistance and wound response [Rao *et al.* 1990; Cordewener *et al.* 1991].

1.4.2 Intercellular signalling related apoplastic proteins

The apoplast almost certainly contains intercellular signalling components that individual cells in a multi-cellular organism require to maintain organism integrity. However, unlike animal cells the extracellular signalling systems have not been as well characterised in plants and the literature tends to report tentative similarities to those of animal systems.

In recent years animal systems have illustrated that calmodulin can function as an extracellular signalling molecule by directly binding to and affecting the activity of other proteins. As an example Inui *et al.* [1990], have shown that calmodulin can actively prevent the binding of thyroid hormone to its target membrane receptor, thereby altering the cellular response to the hormone. Apoplastic calmodulin was first reported by Biro *et al.* [1984] and has since been verified by a number of different workers [Ye *et al.* 1989; Sun *et al.* 1995]. The exact role that calmodulin plays in plant intercellular signalling and control mechanisms is not clear but Sanchez *et al.* [1989] have reported that calmodulin can bind to and inactivate a cell wall peroxidase from *Cicer arietinum*, this evidence may point to an extracellular role for calmodulin in plant cell development, as has been verified in animal systems [MacNeil *et al.* 1988]. Recently, Jun *et al.* [1996] has reported the isolation of a 21 kDa apoplastic calmodulin binding protein and proposes a tentative Ca^{2+}:calmodulin based signalling system similar to the known intracellular system [Trewavas 1991; Jun *et al.* 1996].

The actions of the plant growth substance, auxin are reasonably well characterised after years of research. On the whole plant scale the hormone modulates root and shoot formation, elongation and growth, and at the molecular level induces membrane

hyperpolarisation and acidification of the extracellular matrix. The latter effects may go someway to explaining how auxin can induce cell elongation and growth in auxin-sensitive tissue [see Millner 1995 and Palme & Gälweiler 1999 for reviews]. Despite the efforts of a multitude of researchers, to date, there is no concrete evidence of any of the components of the auxin signal transduction pathway. There have, however, been a number of putative auxin-receptors reported, the most notable and best characterised is auxin-binding protein (ABP) 1 which was isolated from maize in 1985 [Löbler & Klämbt]. ABP1 is a dimer of 40 kDa [Löbler & Klämbt 1985] that contains an auxin-binding motif, a glycosylation site and a carboxy-terminal KDEL signal sequence that targets and retains the protein in the endoplasmic reticulum [Campos *et al.* 1994]. The KDEL targetting sequence is difficult to reconcile with the current consensus on the site of auxin perception, the plasma-membrane [Venis & Napier 1995; Millner 1995] and additionally both standard immunofluorescence microscopy [Napier *et al.* 1992; Brown & Jones 1994] and density gradient fractionation data [Shimomura *et al.* 1988] further indicate that the vast majority of ABP1 is located to the endoplasmic reticulum. However, recently, the use of highly sensitive immunogold-label electron microscopy [Jones & Herman 1993] and silver-enhanced immunofluorescent microscopy [Deikmann *et al.* 1995] has visualised a small sub-population of ABP1 present in the extracellular matrix, in the cell wall and clustered at the outer surface of the plasma-membrane. It is therefore probable that this small sub-population of ABP1 is functionally resident in the apoplast [Brown & Jones 1994], and although unidentified at the present, the ABP1-auxin complex is proposed to interact with a plasma-membrane receptor, thus mediating the auxin signal to the cell.

In addition to the obvious role of ABP's in trafficking auxin from the apoplast to the plasma-membrane to induce cellular changes, auxin is also likely to interact with the proteins involved in auxin metabolism and extracellular and apoplastic auxin related effects [Cohen & Bandurski 1982; MacDonald *et al.* 1991]. In support of this hypothesis photoaffinity labelling has revealed a number of enzymes that are capable of binding auxin, these include, a hydrolase [Brzobohaty *et al.* 1993], a 1,3-β-glucanase [MacDonald *et al.* 1991], a glutathione-S-transferase [Bilang *et al.* 1993; Reinard & Jacobsen 1995] and a superoxide dismutase [Feldwisch *et al.* 1994].

1.4.3 Stress related apoplastic proteins

Any stress whether abiotic or biotic disturbs the normal physiological functioning of any organism. Typically, stress responses are transmitted primarily from the cells to the apoplast, but in certain cases, such as pathogen invasion and ozone stress, mediators are generated or liberated in the apoplast and transmitted to the cell. Plants, like other organisms, have developed appropriate responses to deal with stresses that ultimately

serve to re-establish normal physiology and in effect remove or reduce the stress. A common adaptation to a variety of stresses is the alteration of the extracellular matrix; this includes physical restructuring and alteration of the biochemical properties of the plant cell wall, modulation of the solute composition of the apoplast and changes to the apoplastic protein complement. Drought, excessive salinity, heavy metals, excessive cold, air pollutants, pathogens, and other stressors have all been shown to modify both qualitatively and quantitatively the protein composition of the apoplast. Salt, heavy metal stress, pathogen invasion, ozone, elevated SO_2 [Pfanz *et al.* 1989] and cold-hardening [Marentes *et al.* 1993] all produce increases in apoplastic protein levels, whereas, drought reduces the quantity of extractable apoplastic protein. Stress can be divided into two groupings, biotic, which involves attack from a biological agent and in which the plant has a specific set of defensive reactions (see section 1.4.3.2 & 1.5.2) and abiotic, primarily stemming from a local environmental change that instigates a variety of adaptations to ensure survival (section 1.4.3.1).

1.4.3.1 Abiotic stress

- **Temperature**

Chilling-sensitivity (6-4°C) in plants arises primarily because of two factors; firstly, at a critical temperature, lipids present in the membrane phase shift from a liquid-crystalline state to a solid state, this critical temperature is determined by the ratio of unsaturated to saturated fatty acids in the membrane [Quinn 1988]. Many chilling- and frost-tolerant plants can increase the relative quantity of unsaturated fatty acids, thus permitting membranes to remain fluid and therefore functional at lower temperatures. The second major factor is the inadvertent generation of excessive quantities of active oxygen species; this will be discussed further in section 1.5.2.

Frost-tolerance in plants enables survival below freezing temperatures; thus, additional protective mechanisms other than adjustment to membrane fatty acid composition must be active. Frost-tolerant plant cells are known to dehydrate by losing water to small ice crystals that form in their apoplast. Recently, Marentes *et al.* [1993] and Griffith *et al.* [1992] have reported the isolation of apoplastic antifreeze, and ice-nucleation proteins from rye. The Puma and Musketeer rye varieties can survive temperatures as low as –29°C [Fowler *et al.* 1977] because as the temperature drops, the ice-nucleation and antifreeze proteins are secreted into the apoplast. The ice-nucleation proteins promote the formation of many ice crystals while the antifreeze proteins bind to the surface of these crystals and inhibit excessive crystal growth. The actions of both apoplastic proteins ensure that any ice crystals that do form are very small and numerous, consequently these proteins prevent physical damage to the cells from unstrained ice

crystal formation. The roles these proteins play in controlling ice crystal formation are crucial for the plant to survive sub-zero temperatures.

All organisms respond to rapid increases in environmental temperature by transcriptional activation of genes that encode heat shock proteins. Heat shock proteins function to protect the cell from the damaging effects of over-heating by: -

1. Switching gene expression programmes [Craig *et al.* 1994].
2. Binding to incorrectly folded proteins and refolding them into the correct conformation [Jacob & Buchner 1994].
3. Aiding in compartment targetting and secretion [Parsell & Lindquist 1993].

No evidence appears to have been proposed to suggest how elevated temperatures may affect apoplastic components, though, the stress responses of plants to prolonged periods of elevated temperatures may be similar to that observed in drought, because of increased water loss (see below).

- **Drought**

Plant growth is immediately affected by sub-optimal water supply, this effect is not due to lowered turgor but seems to stem from alterations to the physical properties of cell walls [Zhu & Boyer 1992]. No consensus appears to have been reached detailing the exact changes to cell walls during drought stress. However, a temporary cessation of leaf elongation, for approximately 30 minutes, was observed when roots were exposed to a hyperosmotic solution of mannitol. Leaf elongation quickly recovered because of changes to the elastic properties of the cell wall [Serpe & Matthews 1992] the exact molecular basis for such rapid modulation of cell wall structural properties is unknown. Changes to the apoplastic protein complement have been observed during drought. Covarrubias *et al.* [1995] extracted two basic polypeptides of 33 and 36 kDa from bean seedlings, which are cell wall associated, induced, and secreted into the apoplast in response to drought stress. Unfortunately, no function has yet been attributed to either polypeptide.

One important component of the drought stress response is undoubtedly abscisic acid. Abscisic acid induces stomatal closure and promotes genetic adaptation to drought [Bray 1990]. Computer simulations modelling drought stress show that abscisic acid would be redistributed in a pH-dependent fashion, with a particular increase in the levels of apoplastic abscisic acid. In turn, elevated levels of apoplastic abscisic acid are known to trigger stomatal closure [Slovik *et al.* 1995] that ultimately reduces water loss and consequently lessens drought stress.

- **Salt**

An elevated level of salt at the roots results in an accumulation of ions in the shoot apoplast of sensitive species. This accumulation of ions produces the common symptoms of salt-stress, wilting and necrotic lesions on leaves, presumably due to altered osmotic and turgor properties [Niu *et al.* 1995]. These symptoms may be due to the deposition of excess chloride ions in the apoplast, which in turn, would affect the osmotic potentials and the ionic properties of the plant cell wall; 18-day old pea (*Pisum sativum)* seedlings were watered with a 50mM NaCl solution and for the next four days the concentration of apoplastic solutes from leaves remained relatively stable. After day 4 apoplastic chloride ion concentration abruptly rose from 4mM to a maximum of 120mM, and additionally, the concentrations of a range of other ions were also increased by a factor of 10 [Speer & Kaiser 1994]. The authors speculate that this general accumulation of ions in the apoplast results from a non-specific release of intracellular solutes.

More rapid and drastic changes occur to the cell wall and apoplastic protein complement during salt-stress situations. Bressan *et al.* [1990] investigated these effects on tobacco cell cultures. Salt-adapted cells had walls containing, 50% less polysaccharides, 40% less pectins, three times as much insoluble protein. Exactly how this affects plant cell wall structure has not yet been determined, but, a similar study with the algae, *Nitella*, has revealed that more than 50% of the walls' cation exchange capacity was completely lost [Gillet *et al.* 1992]. Salt-adapted tobacco cells also secreted seven times more protein into the medium, similarly, apoplastic extracts from the intact leaves of salt-stressed tobacco plants exhibit quantitative and qualitative changes in protein complement [Ramanjulu & Dietz, unpublished data]. One of these proteins is probably osmotin [Singh *et al.* 1987]. Osmotin and osmotin-like proteins are induced by abscisic acid, NaCl, wounding, ethylene, viral infection and fungal pathogens, their exact role in salt-stress responses is undetermined [Zhu *et al.* 1995].

- **Heavy metals**

At elevated levels, Cd, Ni, Zn and Al all affect plant growth [Woolhouse 1983; MacNair 1993]. All heavy metals eventually accumulate in the root, shoot, and most notably in the leaf apoplast and the vacuole, unless the plant has specific excretion mechanisms [Brune & Dietz 1995]. The apoplast and vacuole appear to act as an effective, 'repository' to ensure that metal ions do not accumulate in the cytoplasm at levels that would cause cellular disruption and ultimately cell death.

Accumulation of metal ions in the apoplast alters the physical and chemical properties of the cell wall. The concentration of metal ions in the apoplast dictates whether the ions will displace Ca^{2+} from anionic sites in the cell wall. The ionic cross-linking that exists in the cell wall is extremely important to normal wall structure and function. This mechanism has been proposed as the primary cause of the Al-dependent reduction of root elongation observed at sub-toxic concentrations [Jones 1995].

Heavy metals appear to induce more quantitative than qualitative changes in the complement of apoplastic proteins. 1 and 2-dimensional patterns of heavy metal stressed apoplastic extracts, reveal enhanced levels of proteins in the 15-30 kDa range. It is possible that heavy metal stress may induce an elevated secretion of all apoplastic proteins in this molecular weight region and ^{35}S-methionine labelling and assay of apoplastic protein does appear to confirm elevated production and secretion of proteins into the apoplast [Brune *et al.* 1994; Blinda *et al.* 1997]. However, Blinda *et al.* [1997] have noted that a more probable reason for apparently elevated levels of apoplastic proteins is that the altered properties of the cell wall, induced by exposure to the heavy metal ions, would probably permit the easier extraction of associated proteins.

1.4.3.2 Biotic stress

Bostock & Stermer [1989] define a wound as;

> *"... an internal or external injury that breaks the outer protective layer of a plant, that ultimately leads to cell destruction in a specific area of tissue."*

Plants can be wounded by a variety of abiotic (wind, rain, hail, freezing) and biotic (abrasion during growth, herbivores, pathogens) means. Consequently, it is not surprising that Jongsma *et al.* [1994] and Baron & Zambryski [1995] have speculated that only one signal transduction pathway produces the wound response, irrespective of the means of wounding. This wound-defence response is exclusively induced by 'elicitor' compounds, which are present, either as a result of localised physical damage, (cell wall oligosaccharides and other wall components [Bishop *et al.* 1984; Darvill & Albersheim 1984; Lamb *et al.* 1989]) or, originate from an invasive pathogen (glycans, oxalic acid, salicylic acid or hydrolytic enzymes [Lamb *et al.* 1989; Davis *et al.* 1992; Bi *et al.* 1995; Ebel & Cosio 1994]). Examples of plasma-membrane receptors for both microbial and plant cell wall derived elicitors have been isolated [Apostol *et al.* 1989; Horn *et al.* 1989]. Additionally, there is also evidence that certain AOS may also act as 'secondary elicitors', the strongest evidence so far points to hydrogen peroxide produced during the oxidative burst [Tenhaken *et al.* 1995] (see below).

The initial rapid defence response has been suitably called the 'oxidative burst', because large quantities of active oxygen species (AOS) are liberated in the extracellular matrix [Wojtaszek 1997] (the biochemical side of this topic is dealt with in greater detail in section 1.5 but see figure 1.5 for a diagrammatic overview). AOS's are toxic intermediates of successive reductions of molecular oxygen, generating, superoxide anions, hydrogen peroxide and the hydroxyl radical [reviewed in Mehdy 1994]. The hydroxyl radical is extremely reactive and can cause lipid peroxidation, enzyme inactivation and degradation of nucleic acids, consequently it is a very effective anti-microbial agent. Typically, AOS's are the first response to a wound or potential infection, for instance, in soybean suspension cultures H_2O_2 in the medium is detected after <5 minutes of exposure to an elicitor [Apostol *et al.* 1989]. The oxidative burst generates many of the characteristics of the early response. For instance, 2-5 minutes after the production of H_2O_2 has begun, existing proline- and tyrosine-rich proteins are oxidatively insolubilised into the cell wall [Bradley *et al.* 1992; Brisson *et al.* 1994] and localised programmed cell death of pathogen infected cells begins to occur [Levine *et al.* 1994]. Furthermore, Matern *et al.* [1995] have reported the rapid deposition of wall strengthening, lignin-like and phenylpropanoid materials in the apoplast in and around the infection site that once deposited greatly reduce the digestibility of the tissue. On a gross scale all of these early responses ultimately deprive the pathogen of nutrients thereby limiting its potential to establish an infection and spread.

Elicitors are potent inducers of defence gene expression, for example, the elicitor, hepta-β-glucoside, can induce phytoalexin synthesis in soybean at only $1x10^{-8}$ M concentration [Albersheim *et al.* 1992]. Defence-related genes are induced both locally and distally in response to the infection process [Stintzi *et al.* 1993], this requires the activation of gene expression programmes and the transcription and translation of new mRNAs, thus these responses typically become apparent hours after the initial insult [Brisson *et al.* 1994].

General defence-related proteins such as, serine proteinase inhibitors [Graham *et al.* 1986], prosystemin [McGurl *et al.* 1992], polyphenol oxidase [Constabel & Brisson 1995], leucine aminopeptidase and cysteine proteinase inhibitors [Hildmann *et al.* 1992] are synthesised and secreted into the apoplast. In additon, specific pathogenesis-related proteins are also synthesised in response to pathogen infection. In general, these proteins are able to inhibit the growth and the spread of the pathogen and are resistant to the harsh conditions in and around the infection site (acidic pH and proteolytic cleavage by pathogen enzymes) [Niderman *et al.* 1995]. Pathogenesis-related proteins can be classified into several categories, lytic enzymes such as, chitinases and β–1,3-glucanases [Fleming *et al.* 1991; Rasmussen *et al.* 1992; Hoj & Fincher 1995] which digest microbial cell walls, ribosome-inactivating proteins [Leah *et al.* 1991], chitin-binding proteins [Hejgaard *et al.* 1992] and thaumatin-like proteins [Vigers *et al.* 1991].

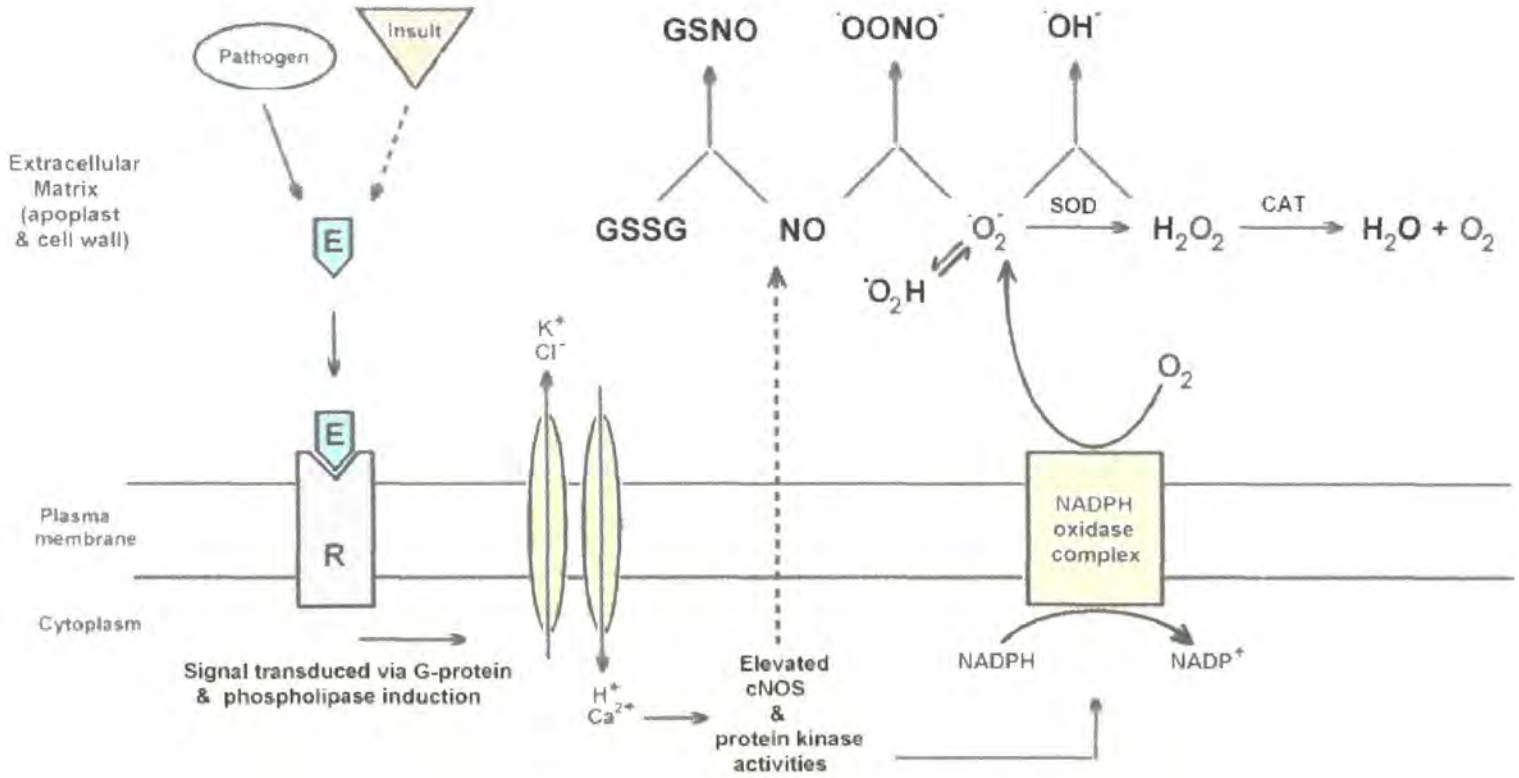

Figure 1.5

Events leading to the production of active oxygen species (AOS) and nitric oxide (NO).

Figure prepared for this thesis; refer to the text for a more detailed explanation of the figure. Solid arrows indicate identified pathways and events. Broken arrows indicate probable pathways and events. Key: E=elicitor; R=receptor; cNOS=constituitively expressed nitric oxide synthase; NO=nitric oxide; O_2=molecular oxygen; H_2O_2=hydrogen peroxide; H_2O=water; GSSG=glutathione; GSNO=nitroso-glutathione; O_2^-=superoxide anion; $^{\cdot}OH$=hydroxyl radical; $^{\cdot}OONO^-$=peroxynitrite radical; O_2H=hydroperoxyl radical; SOD=superoxide dismutase; CAT=catalase.

However, other anti-microbial compounds are also produced in response to pathogen attack. Phytoalexins and the α–, β– and, γ–thionins [Bohlmann 1991] are a range of low molecular weight anti-microbial compounds with a diverse range of action. The thionins are extremely important in most plant species, and are thought to act by binding to ion channels, thus throwing microbial signalling into disarray.

1.5 Active Oxygen Species & Nitric Oxide

Active oxygen species (AOS) as a group comprise the superoxide anion ($^{\cdot}O_2^-$), hydrogen peroxide (H_2O_2) and the hydroxyl radical ($^{\cdot}OH$), all of which are potentially dangerous to macromolecules because of their strong oxidising properties; the redox chemistry of AOS is detailed in section 1.5.1. Even though AOS are potentially deleterious, there are mechanisms in place in plants to purposefully produce appreciable quantities of AOS during defence responses and development, and many of the normal processes of life generate AOS as by-products; these are discussed in section 1.5.2. However, due to their inherent toxicity, plants have developed an array of anti-AOS mechanisms to 'mop up' any excess in order to prevent cellular damage, however, in times of stress these defences may be overcome. Section 1.5.3 illustrates that this phenomenon is common to many types of stress that ultimately perturb the redox state of cells. Recently, evidence has been accumulated that the radical nitric oxide (NO) is also implicated in active oxygen metabolism and signalling, these ideas will be explored in section 1.5.4.

1.5.1 The redox chemistry of active oxygen species

The generation of active oxygen species in biological systems is not an unexpected phenomenon. The oxygen molecule itself is a di-radical, because it contains two electrons that reside in different orbitals, these electrons are not spin paired, therefore, thermodynamically, two more electrons are required to fill the orbitals. However, the oxygen molecule cannot accept spin matched pairs of electrons until one of its unpaired electrons undergoes spin reversal; at ambient pressure and temperature the collision period between molecules is so short that spin reversal faces a large kinetic barrier. Enzymatic oxidation systems effectively remove this kinetic barrier because the collision period between oxygen and the substrate is lengthened at the active site producing a controlled oxidation of the substrate molecule [reviewed in McCord 2000]. However, in biological systems one electron transfers are common (eg: cytochrome chains or photosynthesis) and consequently it is relatively easy for molecular oxygen to undergo a one step reduction and form the superoxide anion ($^{\cdot}O_2^-$), this molecule rapidly establishes an equilibrium with a proton to form the superoxide anion-hydroperoxyl radical ($^{\cdot}O_2H$) acid-base pair:-

$$e^- + O_2 \rightarrow {\cdot}O_2^- \quad (1)$$
$$H^+ + {\cdot}O_2^- \leftrightarrow {\cdot}O_2H \quad (2)$$

The half-life of the superoxide anion-hydroperoxyl radical acid-base pair is less than 1 second at neutral pH and rapidly shortens as the pH becomes more acidic [Sutherland 1991]. The pair spontaneously dismutates into another AOS, hydrogen peroxide (H_2O_2):-

$$2\,H^+ + 2\,{\cdot}O_2^- \rightarrow H_2O_2 + O_2 \quad (3)$$

However, while the superoxide anion does exist it can also act as a reducing agent for transition metals such as, Fe^{3+} and Cu^{2+}:-

$$Fe^{3+} + {\cdot}O_2^- \rightarrow Fe^{2+} + O_2 \quad (4)$$
$$Cu^{2+} + {\cdot}O_2^- \rightarrow Cu^+ + O_2 \quad (5)$$

The generation of the reduced forms of copper and iron opens up the possibility of Fenton style reactions to generate the most reactive and deleterious of all AOS, the hydroxyl radical (${\cdot}OH^-$):-

$$Fe^{2+} + H_2O_2 \rightarrow Fe^{3+} + {\cdot}OH^- + OH^- \quad (6)$$
$$Cu^+ + H_2O_2 \rightarrow Cu^{2+} + {\cdot}OH^- + OH^- \quad (7)$$

These latter reactions are particularly avid, for instance, even metal ions that are complexed within proteins or chelators are capable of generating the hydroxyl radical from hydrogen peroxide-mediated oxidation [Mehdy 1994].

1.5.2 The biological production of active oxygen species

Figure 1.6 diagrammatically presents the major known sources of AOS in plants. Two important intracellular sites of constant AOS production are the mitochondria and chloroplasts. Mitochondria typically convert 1-2% of the total molecular oxygen used for respiration into the superoxide anion, specifically, complex I, partially reduced ubiquinone and cytochrome *b* in complex III are all energetically favourable points within the electron transfer chain that single electron reduction of molecular oxygen can readily occur [Richter *et al.* 1995; McCord 2000]. It has been calculated that a single mitochondrion, operating normally would generate $3x10^7$ superoxide anions per day [Richter *et al.* 1995]. Similarly, the involvement of molecular oxygen in photosynthesis exposes the photosynthetic apparatus to the inadvertent production of AOS. In fact, the single electron reduction of oxygen to form the superoxide anion is known to occur primarily in photosystem I [Asada *et al.* 1974] and more recently discovered in photosystem II during strong illumination [Klimov *et al.* 1993; Ananyev *et al.* 1994].

The production of AOS during plant-pathogen interaction has been briefly covered in section 1.4.3.2 and figure 1.5 diagrammatically illustrates the current consensus

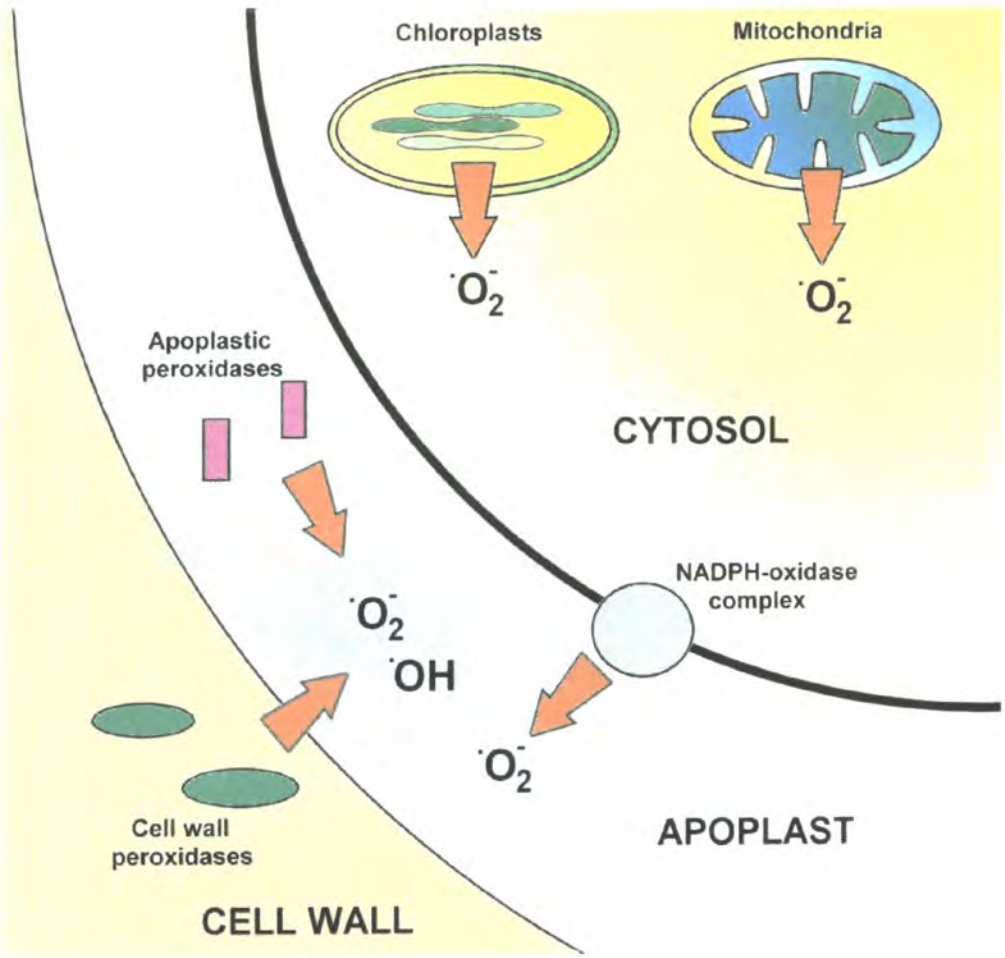

Figure 1.6

Sources of active oxygen species in plants

Figure prepared for this thesis; refer to section 1.5.2 for detail. Active oxygen species are generated at five known sites in plants; mitochondria, chloroplasts, by a putative plasmamembrane NADPH-oxidase complex [Sutherland 1991; Vera-Estrella *et al.* 1992], and by apoplastic and cell wall derived peroxidases [Fry 1998]. Key- $^{\cdot}O_2^-$=superoxide anion; $^{\cdot}OH$=hydroxyl radical.

mechanism. In brief, the interaction of the pathogen with the extracellular matrix leads to the release of elicitor compounds [Bishop *et al.* 1984; Darvill & Albersheim 1984; Lamb *et al.* 1989; Bi *et al.* 1995; Ebel & Cosio 1994] which bind to and activate plasma-membrane receptors [Apostol *et al.* 1989; Horn *et al.* 1989], triggering the G-protein mediated opening of ion channels that induce hyperpolarisation of the plasma-membrane and the influx of calcium ions. Elevated cytosolic calcium may activate a nitric oxide synthase enzyme (see section 1.5.4) and a putative plasma-membrane-associated NADPH-dependent oxidase complex [Sutherland 1991; Vera-Estrella *et al.* 1992]. The latter transfers single electrons from the NADPH molecule to molecular oxygen thereby generating and liberating the superoxide anion into the apoplast. Once in the apoplast the superoxide anion either undergoes spontaneous (see section 1.5.1) or enzymatic dismutation (see figure 1.5, table 1.6 and section 1.5.3), to hydrogen peroxide, as a consequence, hydrogen peroxide is the major AOS observed during the defence response to pathogens.

The hydroxyl radical generated by the Fenton reaction (see section 1.5.1) is known to be able to decompose cellulose-containing materials such as straw and sawdust [Halliwell 1965]. Miller [1986] illustrated that certain cell wall polysaccharides could undergo mild non-enzymatic scission when incubated with hydrogen peroxide. Recently, Fry [1998] has extended these observations to prove that hydroxyl mediated scission of polysaccharides is possible in simple reactions mixtures that deliberately resemble the apoplast; the basic requirements are molecular oxygen, a transition metal such as Cu^{2+}, an appropriate electron donor such as ascorbate and a source of hydrogen peroxide - all are found in the apoplast. The hydroxyl radical is proposed to be formed via the Fenton reaction (reaction scheme 7, section 1.5.1) and the reduced form of the copper ion from the redox reaction with ascorbate:-

$$\text{ascorbate} + Cu^{2+} \rightarrow Cu^{+} + \text{dehydroascorbate}$$

However, the entire mechanism pre-supposes a ready supply of hydrogen peroxide. Germin (an enzyme that readily generates large quantities of hydrogen peroxide during germination in barley) [Lane 1994], some peroxidases when provided with a suitable reductant [Wojataszek 1997] and the putative plasma-membrane NADPH-oxidase complex [Sutherland 1991; Vera-Estrella *et al.* 1992; Fry 1998] can all generate substantial quantities of hydrogen peroxide. The hydroxyl radical appears to cause scission of the glycosidic linkages in the polysaccharide 'backbone' [Schuchmann & von Sonntag 1978]; this has prompted Fry [1998] and Schweikert *et al.* [2000] to propose that this is a potential mechanism of cell wall loosening during cell elongation (see section 1.2.3.2).

1.5.3 Anti-AOS defences & oxidative stress

The mitochondria and chloroplasts are constantly exposed to constitutively generated AOS, consequently, both organelles are especially rich in molecules capable of scavenging AOS such as, ascorbate, vitamin E, glutathione and ubiquinol-10 [Chance *et al* 1979; Richter 1995] and contain high levels of superoxide dismutases, peroxidases and catalases for the enzymatic breakdown of AOS (see table 1.6 for mechanisms of action). Under physiologically ambient conditions, these mechanisms for the management of AOS are sufficient to ensure that no overt cellular damage arises from AOS generated by either organelle. However, under stress these mechanisms can be swamped and may lead to macromolecular oxidation, cellular injury and ultimately the symptoms of stress [Purvis *et al.* 1995; O'Kane *et al.* 1996].

AOS are specifically generated in the apoplast during the biotic stress response and at specific stages of development (see section 1.5.2 and figure 1.5). The apoplast does contain a range of anti-AOS defences, such as, ascorbate, phenolic substances and glutathione [Polle *et al.* 1990; Takahama *et al.* 1992; Luwe *et al.* 1995] which are effective scavengers of AOS, and anti-AOS enzymes such as, superoxide dismutases, catalase, ascorbate peroxidase and glutathione reductase enzymes [Edwards & Dixon 1991; Streller & Wingsle 1994; Vanacker *et al.* 1999], that are capable of catabolising AOS. The actions of these molecules and enzymes are listed in table 1.6. The percentages of these components and enzymes in the apoplast is rather low when compared to whole leaf extracts, but their concentration in this small compartment with such a low water volume per gram of tissue (see table 1.2) is actually relatively high [Streller & Wingsle 1994; Vanacker *et al.* 1999].

These apoplastic anti-AOS mechanisms are responsive to oxidative stress generated from the external environment, biotic attack and development. As an example, atmospheric ozone concentrations have steadily increased over the past 50 years [Chameides *et al.* 1994] and elevated levels can cause foliar injury, reduce shoot and root growth, induce premature senescence, reduce photosynthetic capacity [Heath 1994] and produce increased susceptibility to infection. Ozone enters the plant via the stomata (see section 1.3.1), and is rapidly dissolved into the apoplastic liquid where it readily degrades into several AOS, most notably the hydroxyl radical ($^{\cdot}OH$) which can oxidise most chemical and biological molecules. Luwe *et al.* [1993] have demonstrated that apoplastic levels of ascorbate fall from 420μM to 50μM within 6 hours of treatment with 640μg m^{-3} ozone (very high levels) in spinach leaves. Luwe & Heber [1995] later

Table 1.6 – Characterised anti-AOS defences; compiled from the references indicated for this thesis.

Type of anti-AOS	Name	Mode of action	Location	References
Enzymatic	**Superoxide dismutases**	$2 \cdot O_2^- + 2H^+ \rightarrow H_2O_2 + O_2$	Apoplast and intracellular locations.	Streller & Wingsle [1994]
	Peroxidases	$_{red}$compound + $H_2O_2 \rightarrow$ $_{ox}$compound + H_2O	Apoplast and intracellular locations.	Willekens *et al.* [1995]; Takahama & Oniki [1992]
	Catalases	$2\ H_2O_2 \rightarrow H_2O + O_2$	Apoplast and intracellular locations.	Willekens *et al.* [1995]
Scavenging	**Ascorbate**	ascorbate (red) → dehydroascorbate (ox)	Apoplast and intracellular locations.	Luwe [1996]; Polle *et al.* [1990];
	Glutathione	$_{red}$glutathione → $_{ox}$glutathione	Apoplast and intracellular locations.	Luwe [1996]; Vanacker *et al.* [1998]
	Polysaccharides	$\cdot OH^-$ mediated scission of carbohydrate chains	Apoplast	Fry [1998]; Schweikert *et al.* [2000]
	Phenolics	$_{red}$phenolic compound → $_{ox}$phenolic compound	Apoplast	Takahama & Oniki [1992]
	Ubiquinol	$_{red}$ubiquinol → $_{ox}$ubiquinol	Membranes	Arroyo *et al.* [1998]

Note - AOS are indicated in bold type; key; red=reduced; ox=oxidised.

conducted a series of experiments at ozone levels more representative of those found in certain ozone 'hotspots' in the atmosphere and no significant alterations in apoplastic ascorbate redox state were found, but the leaves still eventually developed the symptoms of ozone toxicity. One explanation of this seemingly contradictory data are that the localised depletion of ascorbate in and around the apoplast of the sub-stomatal cavity did occur and therefore contributed to cell damage and ultimately chlorosis but because infiltration techniques, with the inherent problem of low spatial resolution, were used to sample the apoplast, it is unlikely that the authors would be able to detect changes in very small areas.

Anyhow, the assumption that apoplastic ascorbate is crucial to cellular protection from AOS pre-supposes that mechanisms exist to continually replenish apoplastic stocks. In fact, Horemans *et al.* [1994] and Rautenkranz *et al.* [1994] have reported that dehydroascorbate, the oxidised product of ascorbate, is continually being recycled by a reductive mechanism, when tissues are exposed to sub-toxic levels of ozone. Two potential mechanisms of ascorbate recycling have therefore proposed and are diagrammatically presented in figure 1.7. The first, the ascorbate exchange theory (figure 1.7 [A]) proposes that apoplastic ascorbate could be maintained in a reduced state by continual replenishment from neighbouring cells, thus, the redox state of the apoplast would be directly coupled to that of the local cytoplasm. In support Rautenkranz *et al.* [1994] have reported that barley protoplasts are able to transport ascorbate and dehydroascorbate across their plasma-membranes, and perhaps tellingly, the rate of transfer into the cytoplasm is approximately twice as fast for dehydroascorbate when compared to ascorbate. The alternative mechanism rests with the fact that the plasma-membrane of plant cells contains a cytochrome *b* complex (figure 1.7 [B]). Horemans *et al.* [1994] have inserted this complex into the membranes of vesicles containing ascorbate. When dehydroascorbate is added externally, the ascorbate solution inside the vesicle is rapidly reduced to dehydroascorbate. A similar mechanism may be in action at the plasma-membrane to replenish apoplastic ascorbate *in vivo*.

1.5.4 The chemistry and the roles of nitric oxide

In 1992 the molecule, nitric oxide (NO) was recognised by Science magazine as, 'Molecule of the Year', because of its fundamental and wide ranging effects in animal systems [Wink 1998]. Until relatively recently the effects of NO in plants had primarily focused upon NO as an atmospheric pollutant, its uptake into leaves and subsequent metabolism and toxicity [Hufton *et al.* 1996]. However, the production of biologically active NO in plants is undisputed [Durner & Klessig 1999] but the exact mode of NO production is still under debate. In animal systems NO is exclusively generated by the enzymatic oxidation of L-arginine: -

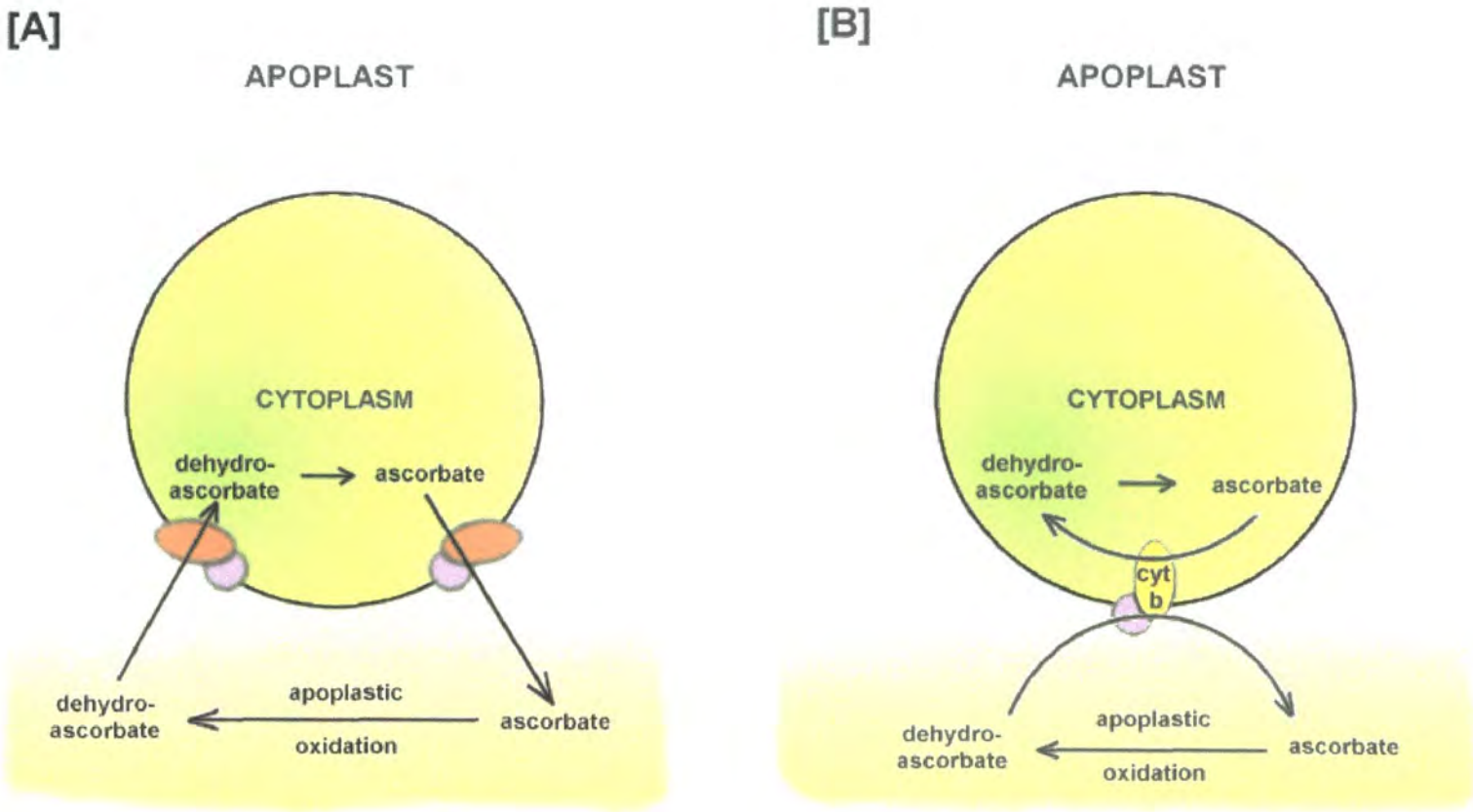

Figure 1.7

Ascorbate recycling theories.

Figure prepared for this thesis; see section 1.5.3 for detail. [A] = diagrammatic representation of the ascorbate exchange theory [Rautenkranz *et al.* 1994]; [B] = diagrammatic representation of the ascorbate regeneration theory [Assard *et al.* 1992; Horemans *et al.* 1994].

$$\text{L-arginine} + O_2 \rightarrow \text{L-citrulline} + NO \quad (1)$$

The reaction is catalysed by the enzyme nitric oxide synthase with the aid of NADPH, flavin, thiol and tetrahydrobiopterin cofactors [Poulos & Raman 1998]. Similar enzyme activity has been reported in plants [Cueto *et al.* 1996; Ninnemann & Maier 1996] but neither the protein nor the gene encoding the protein has been identified [Wojtaszek 2000] furthermore, the co-factor tetrahydrobiopterin is currently not known to be synthesised in plants [Durner & Klessig 1999]. However, plants are already known to contain a range of enzymes with the potential to generate NO, the NAD(P)H-dependent nitrate or nitrite reductases, therefore these enzymes have also been proposed to produce the bulk of NO in plants [Yamasaki *et al.* 1999].

The biological effects attributed to NO primarily arise because of the molecules ability to oxidise the sulphydryl groups of proteins to form S-nitrothiols via S-nitrosylation of cysteine residues [Simon *et al.* 1996; So *et al.* 1998]:-

$$2\,NO + R\text{-}S\text{-}S\text{-}R \rightarrow 2\,R\text{-}S\text{-}NO \quad (3)$$

For example, S-nitrosylation of c-Jun N-terminal kinase 2 [So *et al.* 1998] and upto seven different caspases [Jianrong *et al.* 1997] can reversibly inhibit these enzymes thereby rescuing animal cells that were undergoing programmed cell death.

The reaction between the superoxide anion ($^{\cdot}O_2^-$) and NO to form the highly reactive and therefore very toxic peroxynitrite radical ($^{\cdot}OONO^-$) is only limited by diffusion [Beckman *et al.*1994] and only prevented by the anti-AOS enzyme superoxide dismutase:-

$$NO + {}^{\cdot}O_2^- \rightarrow {}^{\cdot}OONO^- \quad (4)$$

The peroxynitrite radical quickly establishes an acid-base pair in mildly alkaline and neutral solutions thus forming peroxynitrous acid ($^{\cdot}OONOH$) and can rapidly react with any dissolved carbon dioxide (CO_2) to form the nitrosoperoxocarbonate adduct ($OONOCO_2^-$):-

$$^{\cdot}OONO^- + H^+ \rightarrow {}^{\cdot}OONOH \quad (5)$$

$$^{\cdot}OONO^- + CO_2 \rightarrow OONOCO_2^- \quad (6)$$

The formation of the peroxynitrite and nitrosoperoxocarbonate radicals also leads to the oxidation of protein bound sulphydryl groups in a similar, but more reactive manner to NO [Beckman *et al.* 1994; Radi *et al.* 1991], however, these radicals can additionally inactivate proteins via their reactions with the catalytic iron-sulphur centres of metalloproteins [Stamler *et al.* 1992; Castro *et al.* 1994] to form iron-nitrosyl complexes that are generally inhibitory, eg: plant cell wall peroxidases [Ferrer & Ros Barcelo 1999].

The strong oxidant properties of the peroxynitrite radical are well documented [Gatti *et al.* 1994; van der Vliet *et al.* 1994; Ischiropoulos *et al.* 1995] and in fact the oxidation/nitration of tyrosine residues within proteins is considered to be a specific marker of peroxynitrite presence [Gow *et al.* 1996] in the same manner that protein-carbonyl formation is indicative of AOS, and specifically the hydroxyl radical:-

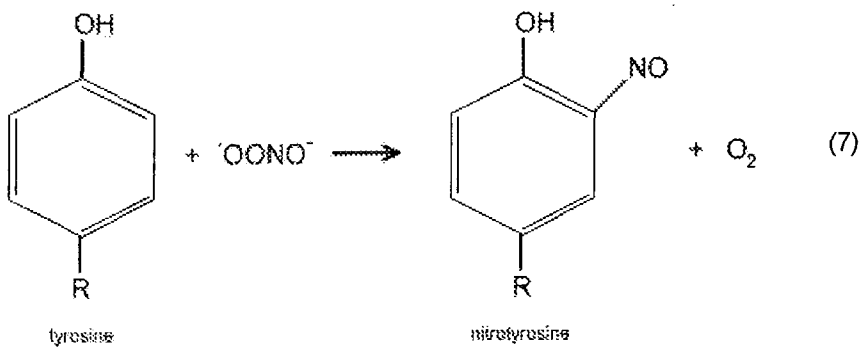

This specific protein modification induced by the peroxynitrite radical can prevent the deliberate enzymatic phosphorylation of tyrosine residues and consequently has the potential to modulate protein activity, for example, Kong *et al.* [1995] have shown that peroxynitrite mediated nitration of a single tyrosine residue of the cell cycle kinase, cdc2 ultimately blocks tyrosine phosphorylation and thus alters the relative duration of the cell cycle phases. This is a novel and potentially substantial protein controlling mechanism because upto 130 individual proteins can be nitrated at tyrosine residues by chemically generated peroxynitrite [Nielsen 1995]; whether the same process is occurring *in vivo* is unknown. The nitration of organic ring structures is not purely limited to protein bound tyrosine residues, and in fact, many plant phenolic compounds have been experimental used as antioxidants against the action of the peroxynitrite radical [Sandova *et al.* 1997].

The exact roles that NO plays in plants have not yet been clearly identified because of the relative infancy of the field, but some generalisations and inferences can be made between the more advanced animal studies and the scant plant data.

In animal systems intracellular NO signals are typically designated as cyclic guanylate monophosphate (cGMP) dependent, because a major effect of NO in animal cells is the activation of the soluble, cytosolic guanylate cyclase enzymes via iron-nitrosyl formation at the active site or S-nitrosylation of cysteine residues [McDonald & Moss 1994]. cGMP has been unequivocally discovered in plant cells [Brown & Newton 1992] and NO treatment has been shown to affect the cytosolic levels of cGMP [Pfeiffer *et al.* 1994] furthermore, cGMP has been proven to induce the transcription of genes, including some pathogenesis-related proteins and phenylalanine ammonia lyase [Durner *et al.* 1998] and to alter the production of secondary metabolites [Bowler *et al.* 1994]. All of these data

point towards similar roles of NO in plants as have been discovered in animals, but it should be noted that no guanylate cyclase enzymes or genes have yet been identified in plants, therefore the data should be interpreted tentatively.

NO can readily traverse phospholipid membranes and has therefore been touted as a potential extracellular molecule. Durner *et al.* [1998] have even proposed that NO may act as the long distance messenger molecule that triggers the acquisition of systemic resistance because of similarities with animal systems. Systemic acquired resistance requires the pathogen induced movement of a phloem-mobile signal to move from the point of infection systemically through the plant [Dempsey *et al.* 1999]. In mammals NO circulates in the blood as S-nitrothiol adducts of serum albumin and haemoglobins or as low molecular weight nitrosoglutathione (GSNO) the latter is believed to act as an effective intra- and inter-cellular NO carrier (see figure 1.5) [Jia *et al.* 1996]. What is intriguing is that glutathione is present in the apoplast [Polle *et al.* 1990] and is also a major constituent of the phloem, furthermore, GSNO has been found to be an extremely powerful inducer of plant defence responses [Durner *et al.* 1998].

In animal systems, AOS act synergistically with NO to induce programmed cell death [Brüne *et al.* 1998] and to directly execute microbial pathogens inside the macrophage vacuole [Mayer & Hemmens 1997], via the formation of the peroxynitrite radical. A similar programmed cell death response is known to occur during the pathogen-induced hypersensitive response in plants, and a parallel can once again be drawn to animal systems because this response is compromised by nitric oxide synthase inhibitors and mimicked by the addition of endogenously added peroxynitrite [Delledonne *et al.* 1998; Durner *et al.* 1998]. These results together with the recent discovery of homologues of the mammalian NADPH-oxidase complex in plants [Scheel 1998] reveal that very similar systems in both plants and animals that are responding to pathogen induced stress by the production of AOS and NO.

SECTION 2

PROJECT OBJECTIVES & TIMELINE

2.1 Project Objectives

The ultimate objective of this project was to utilise relatively simple techniques such as vacuum infiltration to study the leaf apoplast in plants. The overall proposed outcome was the identification of *changes* in the leaf apoplast. This project did not set out to explore any areas of apoplastic carbohydrate biochemistry, and was specifically focused on the quantitative and qualitative assessment of changes in the protein complement and enzyme activity of the apoplast and the generation of apoplastic radicals in the leaf apoplast in response to developmental changes and abiotic stress.

The initial position was therefore to provide a suitable apoplastic 'standard' to measure change, and from this, it was established that it would be necessary to optimise the original small-scale vacuum infiltration strategy adopted by previous students. Furthermore, because this strategy yielded low quantities of apoplastic extract it would be pertinent to develop a larger-scale, bulk procedure to selectively extract apoplastic components. It was hoped that the following specific questions would be answered during the course of the work: -

1. An initial identification and cataloguing of tobacco leaf apoplastic proteins using 1D electrophoresis.
2. The establishment of a complementary analysis of apoplastic proteins using a 2D system of electrophoretic separations to produce, 'protein maps'.
3. Using the above systems to identify proteins that change in response to stress and development.
4. The identification and cataloguing of enzymes present in the apoplast.
5. The identification of radicals either generated by, or released into the apoplast during stress.

It was hoped that N-terminal protein sequencing and database searches would be utilised to identify specific protein components. Identification of individual protein components involved during developmental processes and in response to stress would either fall within current models of the roles of the apoplastic compartment or shed light on 'new' apoplastic processes.

From conception, the need for highly resolving gel techniques had been identified as crucial to resolving small changes in apoplastic protein components. 2-dimensional (2D) electrophoresis is the most highly resolving of all electrophoretic techniques. Consequently, a major early objective of this project was to achieve good 2D separation of apoplastic protein components hopefully for further identifying analysis. Any 2D-system developed had to reflect the requirements of the project, in that the system had to cope with a high enough protein loading so that N-terminal sequencing could be attempted from individual 2D gels. N-terminal sequencing was chosen as the preferred method for protein identification because of the huge availability of database sequences for comparison. MALDI-TOF mass spectrometry was considered but the lack of comparable databases for sequence searches and access to suitable equipment dissuaded further development of this approach. Attempting to develop a 2D system with high protein loading is a relatively difficult challenge as the first dimension of 2D is typically very sensitive to protein load. Consequently, it was envisaged early in the project that the development of such a 2D-system would take up a large part of the project.

During the course of the project it was identified that many stresses whether caused by biotic or abiotic processes, ultimately result in the production active oxygen species (AOS), and when concentrations of such species are high enough result in the phenomenon of oxidative stress. Superoxide dismutase, peroxidase and catalase have been identified in many reports as the rudimentary and fundamental enzymes involved in resistance and tolerance to oxidative stress. The apoplast has been identified as a compartment were AOS are liberated in response to certain developmental stimuli and in response to stress. Consequently, analysis of apoplastic materials for these enzymes and radicals was a major focus of this project.

Some of the work within this thesis provides an excellent starting point for further work on apoplastic processes.

2.2 Project Timeline

The diagram below indicates the approximate time allocated to each major area of study in this project.

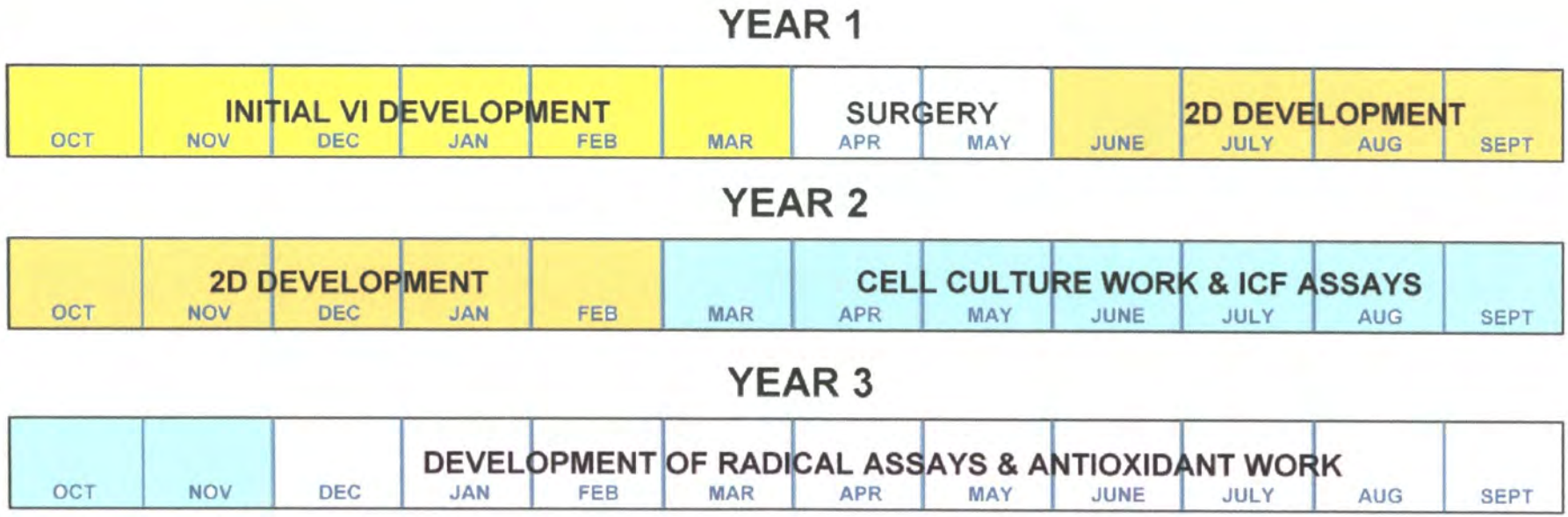

SECTION 3

MATERIALS

3.1 Glassware and plasticware

All glassware used for protein manipulations was washed in a dishwasher using commercial detergents and purified water rinses. Prior to use glassware was rinsed with purified water (Elgastat, UHQPS, Elga Ltd, Buckinghamshire, UK) and allowed to dry. Microcentrifuge tubes, pipette tips, cuvettes and 96 well microtitre plates were obtained from Sarstedt Ltd (Leicester, UK). Petri dishes were supplied by Bibby Sterilin Ltd (Staffordshire, UK).

3.2 Plant material

Nicotiana tabacum (SR-1) seeds were supplied by Dr R.R.D. Croy (Department of Biological Sciences, University of Durham, UK). Potato varieties were supplied by the Potato Research Council, Sutton Bridge, Lincs., UK.

3.3 Buffers and solutions

All buffers and solutions were prepared with purified (Elgastat, UHQPS, Elga Ltd, Buckinghamshire, UK) or distilled water.

3.4 Chemical and biological reagents

Chemical reagents were supplied by BDH Ltd (Leicestershire, UK) and were of AnalaR grade. Other reagents were obtained from the following sources: -

- Sigma (Poole, Dorset, UK)

  Acrylamide, ammonium persulphate, bis-acrylamide, Bovine serum albumin, bromophenol blue, Coomassie brilliant blue R250 CI 42660, dithiothreitol, DNAse, glycerol, molecular weight markers (MW-SDS-70L and MW-SDS-200), RNAse A, SOD from bovine erythrocytes, sodium dodecyl sulphate, TEMED, Tween-20, XTT, NBT, PMS.

- BioRad (Hemel Hempstead, Hertfordshire, UK)

  Bradford protein assay kit, silver stain kit.

- National Diagnostics (Hull, UK)

  Protogel, 30%(w/v) acrylamide: 2.7%(w/v) cross-linked with methylene bisacrylamide (37.5:1 ratio) in distilled water, ammonium persulphate.

- Amersham Pharmacia, Uppsala, Sweden

  Carrier ampholytes (ranges 5-7 & 3-10); native IEF marker proteins; carbamylation standards.

- Micron Separations (MA, USA)

  Problott PVDF transfer membrane.

SECTION 4

METHODS

4.1 Plant growth and potato storage conditions

Seeds of SR-1 tobacco (*Nicotiana tabacum*) were sown in trays containing Levington M3 compost (Levington, UK). The seedlings that had emerged after 14 days were transferred to 2 litre pots and grown in a controlled environment room at 23/20 ± 2°C day/night temperatures, 16 hour photoperiod (20:00-12:00 h), 100μE s^{-1} m^2 (50 W m^2) light intensity (cool-white fluorescent tubes) and 70 ± 5% relative humidity. The plants were fertilised weekly with 1% (w/v) Phostrogen (Phostrogen, UK) and watered once every three days.

Potatoes of various varieties were either bought from a local supermarket or supplied by the potato research council from Sutton Bridge, Lincolnshire. Potatoes were routinely stored in lightproof containers at 10°C. For the 24-hour period before potatoes were exposed to impact stress they were moved to lightproof containers at 4°C.

4.2 Extraction and preparation of apoplastic components

The principle of vacuum infiltration (VI) to recover apoplastic components was essentially the same as that described by Hammond-Kosack [1992] with adaptations made by Dr C. Ilett, Dr R. Croy and during the course of this study. Initially air present in apoplastic spaces was removed by the application of a vacuum to the surface of a liquid into which the tissue had been submerged. The slow release of the vacuum caused the liquid to flood into the apoplast (see the working definition of the term apoplast in section 1.3.4) after which the intercellular fluid (ICF) was collected by low speed centrifugation. The ICF collected contains polysaccharides, apoplastic proteins and a range of other components [Hammond-Kosack 1992]. A small scale technique had been in use by a previous student but it was only capable of isolating small volumes of ICF. Therefore, a large scale technique was developed to extract larger quantities of ICF, the developmental process is outlined in section 5. Both techniques were used in tandem to extract ICF during the project, these methods are described in sections 4.2.1 and 4.2.2. To ensure that the ICF recovered is uncontaminated by intracellular components, comparisons had to be made between it and the total soluble proteins (TE's) present in the leaf, the extraction process for TE's is detailed in section 4.2.3. ICF is typically very dilute, consequently, several approaches were taken to concentrate ICF for further analysis, these are described in sections 4.2.4 and 4.2.5.

4.2.1 Small scale VI protocol

Upto 50 tissue strips of approximately $2cm^2$ were cut from leaves with a sharp blade. Care was taken to avoid the major veins, tissue strips were then washed for >15 minutes in 4°C-chilled dH_2O. The tissue was then dried off using paper towel and then submerged under 4°C-chilled infiltration buffer (200mM NaCl, pH 7.5) in a vacuum jar using a wire mesh and 1 kg weight. The gas was removed from apoplastic spaces by the application of a vacuum (8.5×10^4 Pa (Nm^{-2})) for 75 seconds using a KNF Neuberger pump (model number NO35AN) attached to the vacuum jar, see figure 4.1 [A]. The vacuum jar was gently agitated throughout gas removal so that bubbles were dislodged from the tissue surfaces. The apoplast was then flooded by slow release of the vacuum over a 15-second period. Each leaf strip was then individually dried on paper towel to remove any excess buffer, carefully rolled and inserted into a 0.5-ml eppendorf tube with a small hole cut in the bottom; this arrangement was then placed inside an intact 1.5-ml eppendorf and centrifuged (Beckmann GS-15R, F3602 rotor, 4°C, 900g) for 10 minutes. Any ICF that had a green colouration was discarded, (because it indicated cellular damage and therefore intracellular leakage), the remaining ICF was pooled and either stored at –20°C or dialysed overnight against dH_2O at 4°C, lyophilised and stored at -20°C in a parafilm sealed container (see 4.2.4). A small aliquot (<100µl) of ICF was retained after every VI and assayed for malate dehydrogenase-activity, this was used to calculate the degree of intracellular contamination of ICF (see section 4.3.1) and if required a Bradford assay was also undertaken to quantify the protein concentration (see section 4.3.2). The Bradford assay was only carried out on small scale recovered ICF because large scale ICF were too dilute.

4.2.2 Large scale VI protocol

Leaf tissue strips were prepared, washed and dried as described above (section 4.2.1) - the major difference here is the quantity of tissue, the large scale method permits VI to be carried out on upto 200 tissue strips at a time. The tissue strips were then arranged along a length of nylon mesh (10cm x 1m – supplied by Lockertex, UK) and rolled to form a 'Swiss roll' taking care not to crush or tear the tissue. The Swiss-roll was held in place with a loosely fitting elastic band and infiltrated as described as above (section 4.2.1), excess buffer was allowed to drain from the tissue and nylon mesh after wrapping each roll in tissue paper and standing end up. Each Swiss-roll was then inserted into a sterile blood sample tube with a 3-4 mm hole cut in the bottom; the blood sample tube was then placed into an intact 50-ml Falcon tube. Figure 4.1 [B]-[D] illustrates the large scale VI method. The assembly was then subjected to centrifugation at 2000 rpm for 10 minutes (4°C, Sigma-204 centrifuge, 50ml swing-out rotor) permitted recovery of ICF. Any ICF that had a green colouration was discarded, (because it indicated cellular damage and

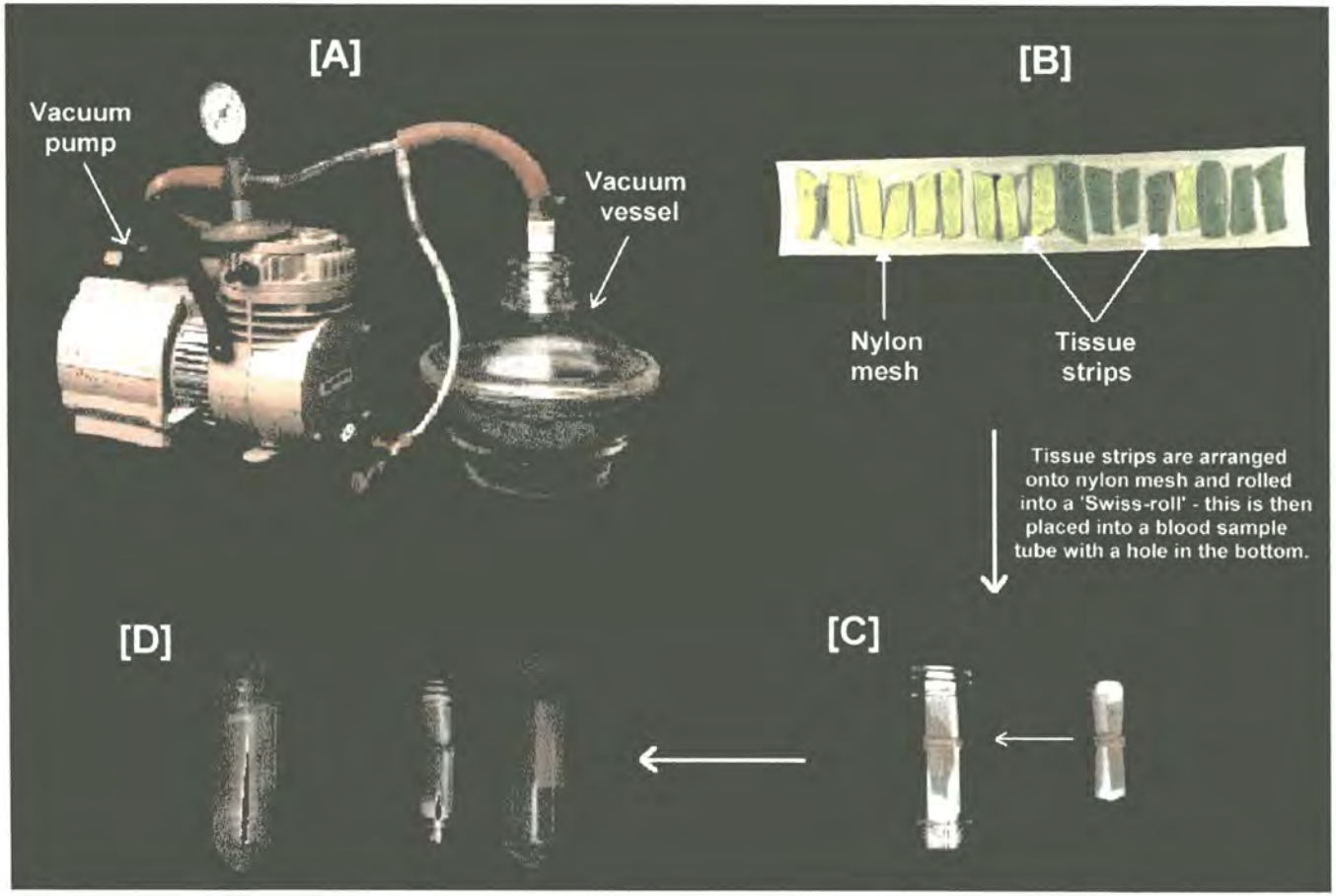

Figure 4.1

Photographs of the equipment and methodology of the large scale VI method

[A] vacuum pump and jar utilised for VI protocols described in sections 3.6.1 and 3.6.2; [B] tobacco leaf strips arranged onto nylon mesh; [C] rolled nylon mesh-tissue strip 'Swiss' roll inside sample tube; [D] the whole assembly is inserted into a 50-ml Falcon tube.

therefore intracellular leakage), the remaining ICF's were pooled and either stored at –20°C or dialysed overnight against dH_2O at 4°C, lyophilised and stored at -20°C in a parafilm sealed container (see 4.2.4). A small aliquot (<1ml) of ICF was retained after every VI and assayed malate dehydrogenase-activity, this was used to calculate the degree of intracellular contamination of ICF (see section 4.3.1).

4.2.3 Total soluble protein extraction

For comparisons between apoplastic and intracellular proteins to be made total soluble protein extracts (TE's) were required. TE's also formed the basis for calculating relative malate dehydrogenase activity (see section 4.3.1). All leaves selected for TE preparation were healthy, clean, dry and developmentally and physiologically identical (as judged by the investigator) to those used in the ICF preparation. $2cm^2$ strips of leaf tissue were excised, taking care to avoid major leaf veins and then weighed. The tissue was then ground to a fine powder in a pestle with quartz sand and liquid N_2. When the N_2 had boiled off buffer was then added to the ground tissue (the same as utilised for VI plus 1 mM DTT) at a ratio of 1.5-ml per 1 gram of original tissue, this mixture was then ground. The resultant slurry was aliquoted into 1.5 ml eppendorf tubes and centrifuged (benchtop, Eppendorf centrifuge at 15,000 rpm) for 5 minutes at 4°C to pellet out sand and large cellular debris. The resultant supernatants were then decanted, pooled and ultracentrifuged at 50,000 rpm, 4°C for 60 minutes. The final supernatant was aliquoted into eppendorf tubes (1ml volumes), the protein concentration estimated (section 4.3.2) and the malate dehydrogenase activity assayed (section 4.3.1). Aliquots were stored at -20°C. If thought necessary for comparative purposes, TE was dialysed overnight against 4°C-chilled dH_2O, lyophilised and the solids stored in parafilm sealed containers at -20°C (section 4.2.4).

4.2.4 Lyophilisation of recovered ICF and TE

Typically ICF has a very low protein concentration, dialysis, to remove salts from the apoplast and those used in the infiltration buffer, followed by lyophilisation was a useful method to concentrate apoplastic components and was used throughout this project. Dialysis was carried out immediately after ICF had been recovered by centrifugation (sections 4.2.1 & 4.2.2), using narrow width dialysis tubing (M_r cut-off 10 kDa from Sigma, UK) against 2-3 changes of dH_2O for a minimum of 8 hours, at 4°C. The material was recovered after dialysis and assayed for protein content using the Bradford assay (section 4.3.2). According to the Bradford assay results appropriate aliquots (200-800µl containing 100µg of protein material) of dialysed ICF were placed into 1.5ml-eppendorf tubes with 2-3 small holes piercing the lid. Samples were quickly frozen in liquid N_2 and

placed into the freeze-drier overnight and lyophilised. Dried solids were stored in parafilm sealed eppendorf tubes at -20°C until required.

4.2.5 Acetone precipitation of recovered ICF and TE

Acetone precipitation was utilised early in the project to concentrate ICF, but was later abandoned because of the potential of acetone to N-terminally block proteins, this would ultimately reduce the number of proteins that could effectively be sequenced, 100% acetone, -20°C cooled was added to ICF at a ratio of 2:1 and mixed; proteins were allowed to precipitate for 15 minutes at –20°C. Precipitates were then separated out by centrifugation (benchtop, Eppendorf centrifuge at 15,000 rpm) for 5 minutes. The supernatant was discarded and the pellet of precipitated proteins was washed in –20°C chilled 70% (v/v) acetone at a ratio of 2:1 of the original volume of sample. Following a repeat 5-minute centrifugation the supernatant was discarded and the pellet was air-dried for 20 minutes. Dried solids were stored at –20°C until required.

4.3 Assay analysis of ICF and TE

To assess the degree of intracellular contamination caused by cellular damage and leakage, all ICF's & TE's were routinely assayed for the activity of the cytoplasmic/mitochondrial enzyme malate dehydrogenase (section 4.3.1). When required the Bradford assay (section 4.3.2) was used to provide an estimate of protein concentration in all samples. Other assays were performed in order to assess the extracellular activities of enzymes of interest (see sections 4.3.3 to 4.3.6).

4.3.1 Malate dehydrogenase (MDH) assay for estimating intracellular contamination of ICF preparations

Malate dehydrogenase (MDH, EC 1.1.1.37) activity was assayed in both TE's and ICF's by a method described in Biochemica Catalogue Enzymes [1968]. A reaction cuvette containing 943µl of 0.1 M phosphate buffer, pH 7.5, 33µl of 2mg/ml oxaloacetate in phosphate buffer, 17µl of 10 mg/ml NADH (sodium salt) in dH_20, was first zeroed against a duplicate mixture. The assay was initiated by the addition of 7µl of either TE or ICF to the reaction cuvette which was quickly inverted twice to mix the reagents and sample. The reaction was followed by measuring the decrease in absorbance at 340nm for 60 seconds. In order to 'quantify' the degree of intracellular contamination of the ICF, TE readings were normalised to 100% of the MDH-activity present in the tissue [Ilett 1998]: -

$$\frac{\Delta Ab_{340} \text{ of ICF} \times 100}{\Delta Ab_{340} \text{ of TE}} = \text{Relative MDH-activity}$$

Only ICF's with <1% relative MDH-activity were used for apoplastic analysis.

4.3.2 Bradford Assay for the quantification of protein

The spectrophotometric dye-binding assay based upon the work of Bradford [1976] and Spector [1978] was used to estimate protein concentration in all samples. The principle of the assay is based on the observation that the maximal absorbance for an acidic solution of Coomassie brilliant blue G-250 shifts from 465nm to 595nm when protein binding occurs. Bradfords' reagent was purchased from BioRad (Poole, Dorset, UK).

In order to quantify the total protein content of an unknown sample a series of standard bovine serum albumin (BSA) solutions ranging from 0.5μg to 10μg per assay volume were used to produce standard curves. 100μl volumes of sample, standards and water blanks were added to 900μl of Bradfords' reagent in micro-cuvettes and allowed to stand at room temperature for 7 minutes. Absorbencies at 595nm were measured using the Unicam UV2 spectrophotometer (ATI Unicam, Cambridge, UK) after zeroing using the water blanks, standard curves and quantification of unknown samples was accomplished using Prism GraphPad software (Prism Software, USA).

For speed of throughput a microtitre plate version of the above assay was established. A 1mg/ml stock solution of BSA in infiltration buffer (see sections 4.2.1 and 4.2.2) was used to produce a range of calibration standards between 100 and 1000μg/ml. ICF and TE samples are diluted as necessary with infiltration buffer. 10μl of each standard and an appropriate volume of ICF or TE sample was added and each well was then diluted by the addition of infiltration buffer to a total volume of 160μl. 40μl of Bradford reagent was added to each well and the plate is shaken for 30 seconds and left to incubate for a further 7 minutes. After the incubation the absorbance of each well was measured against an infiltration buffer blank using the Dynatech MR5000 microtitre plate reader (Dynatech, UK) at 570nm. The quantification of unknown samples and the construction of the calibration curve was accomplished using Prism GraphPad software (Prism Software, USA).

4.3.3 Superoxide Dismutase Assay

Superoxide dismutase (SOD) activity in ICF's was quantified using an assay developed during the course of this research [see memorandum, page iii]. A series of SOD calibration standards were prepared from a commercial preparation of SOD (Sigma, Poole, Dorset, UK), dissolved in 50mM phosphate buffer, pH 8.2. The SOD calibration standards (ranging from 0.01U (2.875ng) to 100U (28.75μg)), experimental samples (prepared in 50mM phosphate buffer, pH 8.2) and blanks (50μl of 50mM phosphate

buffer, pH 8.2) were added to the wells of a microtitre plate in a 25μl aliquot, in triplicate. 200μl of 50mM phosphate buffer, pH 8.2, containing 0.1mM EDTA, 98μM NADH, 150μM 2,3-bis-[2-methoxy-4-nitro-5-sulphophenyl]-2H-tetrazolium-5-carboxanilide (XTT) was then added to each well. The reaction was initiated with 25μl of a 28μM solution of phenazine methosulphate (PMS) in 50mM phosphate buffer, pH 8.2. This mixture had final concentrations of 80μM EDTA, 78.4μM NADH, 120μM XTT and 2.8μM PMS. Absorbance readings were taken at λ_{max} (450nm) for 2 minutes from which the mean blank absorbance value was initially subtracted and then the adjusted initial rate (Δ_{450}/min) was calculated using data derived from the Dynatech MR5000 microtitre plate reader (Dynatech, UK). A calibration curve of known SOD units (calibration standards) versus Δ_{450}/min was constructed and quantification of experimental samples was achieved by reading initial rate values from this standard curve (Prism GraphPad software - Prism Software, USA).

4.3.4 Guaiacol Peroxidase Assay

The activities of peroxidases (POD's) that can utilise the artificial substrate, guaiacol were quantified in ICF. The reaction mixture comprised of 2.9ml of 0.1 M phosphate buffer, pH 7.0, 50μl of 0.0022% (v/v) guaiacol in 0.1 M phosphate buffer, pH 7.0, and 40μl of 0.03% (v/v) hydrogen peroxide in 0.1 M phosphate buffer, pH 7.0. The reaction mixture was initially zeroed against a duplicate mixture and the assay begun by adding 10μl of an ICF preparation (prepared in 0.1 M phosphate buffer, pH 7.0) to the reaction cuvette which was then quickly inverted twice to mix the reagents and sample. The reaction was followed by measuring the increase in absorbance at 470nm using a Unicam UV2 spectrophotometer (ATI Unicam, Cambridge, UK). Experimental sample enzyme activities were then calculated either from the published extinction coefficient for guaiacol of 26.6×10^6 M^{-1} cm^{-1} [George 1953] or from a calibration curve of known POD standards and reading unknowns from the curve (Prism Software, USA).

4.3.5 Superoxide Anion quantification from tissue

Tuber tissue was excised from potatoes as small cores (~5 mm diameter x 3 mm long) weighing in the order of 30-35mg each. After extensive washing with dH_2O to remove any intracellular materials that would have been released during core excision, the tuber cores were each placed into a 200μl volume of 50mM phosphate buffer, pH 8.2 containing, 120μM XTT in an eppendorf tube. The mixture was incubated for 20 minutes in the dark, at room temperature after which the tuber core tissue was removed and the solution was centrifuged (benchtop, Eppendorf centrifuge at 15,000 rpm) for 5 minutes to pellet any cell debris that may interfere with subsequent absorbance measurements. The supernatant was withdrawn and the absorbance measured at 450nm against a reagent-

tissue blank using the Beckman DU7500 (Beckman Instruments, UK). Superoxide anion concentration was calculated using the published extinction coefficient for XTT, of 2.16 x 10^4 M^{-1} cm^{-1} [Sutherland & Learmonth 1997].

4.3.6 Nitric Oxide quantification from tissue

Tuber cores were prepared as described in section 4.3.5 and after extensive washing with dH_2O, the tuber cores were each placed into a 200µl volume of 50mM phosphate buffer, pH 7.8, containing 114mM sulphanilamide (SULF) and 2.4mM N-(1-napthyl)-ethylenediamine dihydrochloride (NEDD). The mixture was incubated for 20 minutes in the dark, at room temperature after which the tuber core tissue was removed and the solution was centrifuged (benchtop, Eppendorf centrifuge at 15,000 rpm) for 5 minutes to pellet any cell debris that may interfere with subsequent absorbance measurements. The supernatant was withdrawn and the absorbance measured at 496nm against a reagent-tissue blank using the Beckman DU7500 (Beckman Instruments, UK). Nitric oxide concentration was calculated using the published extinction coefficient for the SULF-NEDD reagent, of 1.25 x 10^4 M cm [Nims *et al.* 1995].

4.4 1D gel analysis strategies

ICF and TE preparations were subjected to 1D gel analysis for visualisation of protein banding patterns (sections 4.4.1 to 4.4.4), in gel enzyme activity assessments (sections 4.4.5 to 4.4.7), for subsequent N-terminal sequencing (section 4.4.11), antibody probing (section 4.4.9) or oxyblotting for the detection of oxidatively modified protein components (section 4.4.10).

4.4.1 SDS-PAGE

Polypeptides were size fractionated by SDS-PAGE performed essentially as described by Laemmli (1970). 1.5 to 0.75 mm-thick vertical slab gels were cast and electrophoresed using the BioRad Mini-Protean II system. Unless otherwise stated, 12% (w/v) acrylamide/bis-acrylamide (37.5:1) separating gels (containing 375mM Tris-HCl, 0.1% (w/v) SDS) and 4% (w/v) acrylamide/bis-acrylamide stacking gels (containing 125mM Tris-HCl, 0.1 (w/v) SDS) were used throughout these studies. Liquid sample (i.e.: TE's) were prepared by diluting the sample with 2x sample loading buffer (125 mM Tris-HCl pH6.8, 6%(w/v) SDS, 0.01% (v/v) β-mercaptoethanol, 10% (v/v) glycerol, 0.05% (w/v) bromophenol blue) at a ratio of 1:2. Solid protein material (i.e.: ICF's) was reconstituted in a suitable volume of 1x sample loading buffer. Samples were denatured just prior to loading onto a gel by incubating for 5 minutes in a boiling heating block. Electrophoresis was carried out with 1x running buffer (3 g/l Tris-HCl pH 8.3, 14.4 g/l

glycine, 1 g/l SDS), initially at 70V until the marker dye front had just entered the separating gel, then at 170V until the dye front had reached the bottom of the gel.

4.4.2 Native-PAGE

Proteins were separated based on three physical properties, electrical charge, overall mass, and shape by native-PAGE. The native-PAGE protocol used was essentially an adapted non-denaturing version of the SDS-PAGE protocol presented in section 4.4.1 0.75 mm-thick vertical slab gels were cast and electrophoresed using the BioRad Mini-Protean II system. Unless otherwise stated, 12% (w/v) acrylamide/bis-acrylamide (37.5:1) separating gels (containing 375 mM Tris-HCl) and 4% (w/v) acrylamide/bis-acrylamide stacking gels (containing 125 mM Tris-HCl) were used throughout these studies. Liquid sample (i.e.: TE's) were prepared by diluting the sample with 2x native sample loading buffer (125 mM Tris-HCl pH6.8, 10% (v/v) glycerol, 0.05% (w/v) bromophenol blue) at a ratio of 1:2. Solid protein material (i.e.: ICF's) was reconstituted in a suitable volume of 1x native sample loading buffer. Samples were not heated. Electrophoresis was carried out with 1x running buffer (3 g/l Tris-HCl pH 8.3, 14.4 g/l glycine), initially at 70V until the marker dye front had just entered the separating gel, then at 170V until the dye front had reached the bottom of the gel.

4.4.3 Coomassie based protein staining

Protein bands were visualised by submerging gels in 0.1% (w/v) Coomassie blue R250, in 40% (v/v) methanol, 10% (v/v) glacial acetic acid, and destained with 40% (v/v) methanol, 10% (v/v) glacial acetic acid. Alternatively a more sensitive Coomassie based stain was also utilised, 'Fast Stain' from Zoion, (Mass., USA), following the manufacturers instructions.

4.4.4 Silver staining of proteins

Protein bands were visualised by silver staining with the BioRad silver staining kit following manufacturers instructions. Briefly, the rapid silver staining protocol was adopted following the sequence of; submerging the gel in fixative (40% (v/v) methanol, 10% (v/v) glacial acetic acid) for >30 minutes; submerging the gel in oxidiser for 5 minutes; washing the gel extensively with QH_2O for 15 minutes; submerging the gel in silver reagent for 20 minutes; washing the gel with QH_2O for 1minute; developing the bands by submerging in developer reagent; and finally, stopping development by submerging the gel in 5% (v/v) acetic acid solution.

4.4.5 In gel activity staining for catalase

After native electrophoresis (section 4.4.2) the gel was removed from the cassette, submerged into a substrate solution comprising of either 3% (v/v) or 0.3% (v/v) hydrogen peroxide, and incubated in the dark with agitation for 15 minutes. The solution was then removed and the gel washed for >1 minute with dH_2O. The gel was then submerged in the staining solution which comprised 1% (w/v) potassium ferricyanide and 1% (w/v) ferric chloride. Yellow to pale blue bands of catalase activity should appear on a blue background.

4.4.6 In gel activity staining for peroxidase

After native electrophoresis (section 4.4.2) the gel was removed from the cassette and submerged into a staining solution of 0.0225% (v/v) hydrogen peroxide and 0.001% (v/v) guaiacol in 50mM sodium acetate buffer at pH 5.0. The gel was incubated in the dark until peroxidase bands of activity were stained red-brown.

4.4.7 In gel activity staining for superoxide dismutase

After native electrophoresis (section 4.4.2) the gel was removed from the cassette and submerged into a staining solution of 0.98μM nitroblue tetrazolium, 1.57μM phenazinemethosulphate and 5.9μM magnesium chloride contained in 50mM Tris-HCl at pH 8.5. The gel was incubated under direct light (a lamp is ideal) while being agitated. Superoxide dismutase activity bands were detected as clear zones on a dark blue background.

4.4.8 Gel drying for storage

After any of the treatments detailed above gels were routinely dried down for storage. The procedure was based on the protocol provided with the BioRad gel drying apparatus and consisted of, incubating the gel for >1 hour in many changes of dH_2O. Rehydrating sheets of gel wrap in water and sandwiching the gel between 2 sheets of gel wrap using the gel-drying frame as described in the manufactures instructions. The gel-drying frame was placed into the drying apparatus until gels were dehydrated.

4.4.9 Electroblotting from gels for antibody probing

After electrophoresis was complete the enclosing glass plates were removed and the gel was submerged in 1x transfer buffer (0.965g/l Tris base, 4.5g/l glycine) for 15-20 minutes. Suitably sized pieces of nitrocellulose membrane (Micron Separations, MA,

USA) were cut and wetted in methanol for 2 minutes and then placed into 1x transfer buffer for 5 minutes to equilibrate. Four pieces of 3MM blotting paper were cut to the same size as the nitrocellulose membrane and dampened with 1x transfer buffer. The BioRad Mini-Protean II Wet Blotting system was utilised to effect protein transfer, the manufacturers instructions were followed. Briefly, the two electroblotter sponges were submerged in 1x transfer buffer and squeezed to exclude as much trapped air as possible. The electroblotter unit was assembled as described in the manufacturers instructions and inserted into the tank. Electroblotting was undertaken with 1x transfer buffer for 30-60 minutes at 100 V. The unit was then disassembled, the supporting matrix removed, and stained briefly with Coomassie or Ponceau S to ensure protein transfer. It was usual to stain the gel to ensure that protein transfer had been efficient.

4.4.10 Oxyblot analysis

The oxyblotting kit was purchased from Oncor (Oncor, France) and enabled the detection of oxidatively modified proteins, specifically those modified by the action of the hydroxyl radical. The kit was used essentially as described by the manufacturers.

Briefly, the protein solution to be oxyblotted was derivatised with an acidic solution of dinitrophenylhydrazine (DNPH), this procedure induces DNPH-protein complexes at sites of hydroxyl-radical mediated oxidation, specifically carbonyl groups. The derivatisation reaction was stopped after 5 minutes by the additon of 2M Tris-base (neutralisation solution). The protein solution was then loaded onto a standard SDS-PAGE gel (see section 4.4.1) and electrophoresed. After electrophoresis the separated proteins were electroblotted from the gel (see section 4.4.9) and antibody probed (next paragraph).

Primary antibodies were provided by the manufacturer. The antibody probing procedure followed these steps:-

1. 45 minute incubation in blocking buffer (tris buffered saline (TBS) containing 3% non-fat dried milk).
2. 45 minutes in blocking buffer containing 1:150 anti-DNPH primary antibody.
3. 3 x 5 minute washes in TBS-Tween.
4. 45 minutes in blocking buffer containing alkaline phosphatase linked secondary antibody.
5. 3 x 5 minute washes in TBS-Tween.
6. Bands were visualised using Sigma BCIP/NBT tablets prepared as per manufacturers instructions.

4.4.11 Electroblotting from gels for N-terminal sequencing

Proteins were separated as in standard SDS-PAGE (see section 4.4.1) except that the gel was either cast at least 12 hours before use and stored, or pre-run for 30 minutes at 50V with 200μM thioglycolic acid in the upper buffer chamber. These measures ensure that any reactive amines present in the gel matrix have either fully derivatised or are scavenged thereby lessening the chances of inadvertent N-terminal blocking of proteins.

After electrophoresis was complete the enclosing glass plates were removed and the gel was submerged in 1x transfer buffer (2.213g/l 3-(cyclohexylamino)-1-propanesulphonic acid, 10% (v/v) methanol, pH 11) for 15-20 minutes. Suitably sized pieces of PVDF (polyvinylidene fluoride) membrane (Micron Separations, MA, USA) were cut and wetted in methanol for 2 minutes and then placed into 1x transfer buffer for 5 minutes to equilibrate. Four pieces of 3MM blotting paper were cut to the same size as the supporting matrix and dampened with 1x transfer buffer. The BioRad Mini-Protean II Wet Blotting system was utilised to effect protein transfer, the manufacturers instructions were followed. Briefly, the two electroblotter sponges were submerged in 1x transfer buffer and squeezed to exclude as much trapped air as possible. The electroblotter unit was assembled as described in the manufacturers instructions and inserted into the tank. Electroblotting was undertaken with 1x transfer buffer for 30-60 minutes at 100 V. The unit was then dismantled, the supporting matrix removed, and stained briefly with Coomassie blue or Ponceau S to ensure efficient protein transfer had occurred.

4.5 2D gel analysis strategies

ICF and TE preparations were subjected to separation in a variety of different 2D-gel systems in an attempt to produce high resolution protein maps (see sections 4.5.6 and 4.5.7 for the most successful). Throughout these experiments ICF components continually precipitated and interfered dramatically with the separation therefore a variety of sample preparation techniques were employed to try and circumvent this problem. These are presented in sections 4.5.1 to 4.5.3. The isolation of ICF was extremely laborious and time-consuming and a more convenient control mixture of proteins isolated from mitochondria was available (section 4.5.4) therefore this preparation was used for the development of the 2D systems described in this thesis.

4.5.1 Standard TE and ICF sample preparation for 2D analysis

Known quantities of lyophilised or acetone precipitated TE (sections 4.2.4 and 4.2.5) or lyophilised ICF proteins (section 4.2.5) were reconstituted in a suitable quantity of isoelectric focussing (IEF) sample loading buffer (dependent upon IEF and 2D

technique). Precipitate was pelleted by centrifugation (benchtop, Eppendorf centrifuge at 15,000 rpm) for 5 minutes prior to loading the sample onto the IEF.

4.5.2 ESA based TE and ICF sample preparation for 2D analysis

Samples were heat denatured by the addition of 100µl of boiling 0.3% (w/v) SDS, 200mM DTT, 28mM Tris-HCl, 22mM Tris-base, followed by 5 minutes in a 100°C heating block. Samples were then cooled on ice for 5 minutes, treated with 10µl of enzyme mixture (24mM Tris-Base, 476mM Tris-HCl, 50mM $MgCl_2$, 1mg/ml DNAse I) and chilled for a further 10 minutes. Protein material was then removed from solution by incubating on ice for 20 minutes with ice cold acetone (80%(v/v)) followed by centrifugation at 15,000 rpm for 10 minutes, the resultant pellet was air-dried. Samples were then resuspended in a suitable volume of sample loading buffer (7.92M urea, 0.06% SDS, 1.76% ampholytes, 120mM DTT, 3.2% Triton X-100, 22.4mM Tris-HCl, 17.6mM Tris-Base).

4.5.3 Ammonium Sulphate-PVP TE and ICF sample preparation for 2D analysis

For TE preparation leaf tissue was initially cut up into small pieces, weighed and then placed into a 4°C-chilled blender. Liquid nitrogen was added and the tissue fragmented further with a clean spatula. At a ratio of 3ml per 1g of tissue 0.1 M phosphate buffer (pH7.5, 1mM DTT, 2mM EDTA) and at 1g per 10ml of buffer (i.e.: 10% (w/v)) insoluble PVP were then added. The mixture was blended for 2 minutes then strained through Miracloth into a beaker placed on ice and the volume was recorded. Ammonium sulphate was added spatula-wise with constant stirring to 80% relative saturation. Following centrifugation (4°C, 10,000 g, JA-14 rotor, Beckman J2-HC centrifuge) the supernatant was removed and spatula-sized quantities of pellet were collected and placed into eppendorf tubes. This ammonium sulphate stabilised preparation was routinely stored at –20°C for extended periods with no obvious detrimental effects. When required for analysis 1 spatula worth of ammonium sulphate stabilised TE was resuspended in 3-4ml of 0.1M Phosphate buffer (pH7.5 containing 1mM DTT and 2mM EDTA) and then microfuged for 2 minutes to remove any PVP. The supernatant was then decanted and a Bradford protein estimate obtained. A 2.5ml volume of sample was then loaded onto a QH_20 pre-equilibrated PD-10 column (Pharmacia Biotech) and once it had entered the Sephadex bed a further 3.5ml of QH_20 was added. The second and third millitre volumes off the column were collected and assayed to determine the protein concentration. 400µl centricons (spun at 4°C, 2000g, using the F2402 rotor in a Beckman GS-15R centrifuge for 60-120 minutes) were then utilised to reduce the volume and salt concentration and concurrently increase the protein concentration. Sample was then collected from the filter

insert of the centricon, assayed for protein concentration, and was finally stored frozen at –20°C until required for 2D-analysis.

ICF was collected as described in section 4.2.1 or 4.2.2, ammonium sulphate precipitation was not possible because ICF is very dilute. PVP was added at a concentration of 10% (w/v) and was removed after 30 minutes by centrifugation (benchtop, Eppendorf centrifuge at 15,000 rpm) for 5 minutes. The supernatant was collected, dialysed, lyophilised and then prepared as described in section 4.2.4.

4.5.4 2D standard control protein mixture (from blowfly mitochondria)

Control flies were grown at a constant 24°C. Flies were heat-shocked by incubating batches at 37°C for 40 minutes. After heat treatment, they were returned to a constant 24°C chamber for 4 hours to permit the heat-shock responses to develop. Blowfly muscle mitochondria were isolated from both control and heat shocked flies as described previously [Elwadawi *et al.* 1995]. Briefly, thoraces were collected and flight muscles removed and disrupted using a mortar and pestle. Mitochondria were centrifuged at 3,600 rpm (RCF = 1500g) in a Beckman Avanti 30 (F2402 rotor). The mitochondrial pellet was resuspended in 0.15M KCl, 1mM EDTA, 10mM Tris and stored frozen at –80°C. Kind thanks are extended to Judith Chambers (Dept. of Biological Sciences, University of Durham) for the supply of this material.

4.5.5 Preparation of coloured pI markers

After many polyacrylamide-isoelectric focussing (PAG-IEF) trials that did not exhibit adequate protein separation a mixture of coloured proteins and a dye was concocted in order to quickly and visually assess the formation of the carrier ampholyte pH gradient. 6mg, 1mg and 3mg of commercial preparations of cytochrome C, myoglobin and the acidic dye methyl red were weighed on an analytical balance, respectively. Each was solubilised with the addition of 1ml, 800µl and 1ml of QH_20, respectively. The optimal mix of coloured pI markers was determined experimentally and the final combination used was 200µl of cytochrome C preparation, 100µl of myoglobin preparation, 20µl of methyl red preparation and 200µl of QH_2O. A typical loading of this solution onto a PAG-IEF gel for visualisation was of the order 5-15µl.

4.5.6 In-house adaptation of ESA 2D system

This method is an in-house adaptation of the ESA/Oxford GlycoSystems Investigator™ 2D electrophoresis system. 750µl aliquots of gel solution (9.5M urea, 2%(w/v) triton X-100, 4.1% acrylamide, 5mM CHAPS) were prepared and 46µl of 40(w/v) ampholytes and

5µl of 10%(w/v) APS were added and mixed thoroughly. Using a piece of rubber tubing attached to a 1ml syringe the tubing was secured to a suitably dimensioned capillary tube (1.7mm id x 17cm or x 8.5cm) and the free end placed into an eppendorf containing the gel solution. The gel solution was carefully draw up the capillary so that the gel was the desired length (6.5 or 15cm) polymerisation was then allowed to proceed for 60 minutes. Once polymerised the syringe and tubing were removed and any excess gel was cleaned from the bottom of the capillary tube. Anodic buffer (10 mM phosphoric acid) filled the lower chamber of the electrophoresis tank and the capillary gels were inserted into the apparatus ensuring that the bottom of the gels were in full contact with the buffer. The upper chamber was then filled with cathodic buffer (100 mM NaOH) and the ends of the gels were washed several times with buffer using a Hamilton syringe. Sample is prepared and loaded onto the cathodic end of the gels in a 10-30µl volume using a Hamilton syringe and 10µl of sample overlay solution (0.5M urea, 0.2%(w/v) triton X-100, 0.1% ampholytes, 50 mM DTT) applied to protect proteins. IEF gels were electrophoresed at 500V, 3mA/gel, 0.25W/gel, 7.5hrs for 6.5cm gels, and at 500V, 3mA/gel, 0.25W/gel, 17.5hrs for 15cm gels. After the run the gels were extruded using a water filled syringe into either 10%(v/v) glycerol for storage at –20°C or, transfer solution (0.3M Tris-base, 0.075M Tris-HCl, 3% SDS, 50 mM DTT, 0.01%(w/v) bromophenol blue) prior to loading on top of a 12% SDS-PAGE separating gel.

4.5.7 Barent & Elthon based 2D system

This protocol was adapted from the Barent & Elthon [1992] PAG-IEF with slight changes to the ampholyte composition. The gel mixture consisted of 335µl of stock acrylamide solution (28.4%(w/v) acrylamide, 1.6%(w/v) bis-acrylamide containing 5%(w/v) BioRad AF501-X8 ion exchange resin), 0.5ml stock triton X-100 (10%(w/v) triton X-100 containing 5%(w/v) BioRad AF501-X8 ion exchange resin) and 130µl of 40%(w/v) ampholytes (broad range 3-10 supplemented 45%(v/v) 5-8 ampholytes from Pharmacia) this was added to 1g of UltraPure urea. This mixture was placed into a water bath at 37°C to allow the urea to dissolve. Lyophilised samples were reconstituted in 20µl volumes of QH_2O and 200µl of the gel mixture was added to each sample, 1µl of 10%(w/v) APS and 1µl of TEMED were then pipetted to initiate polymerisation. Immediately a 1.5mm i.d. x 5cm capillary tube was filled with this mixture by holding the tube horizontally and slowly dispensing the gel-protein mixture into the tube, polymerisation was usually complete within 30 minutes.

Capillary tubes were placed into the apparatus which contained anodic buffer (10mM phosphoric acid), the upper chamber was then filled with cathodic buffer (degassed 10mM sodium hydroxide). PAG-IEF was achieved by applying a constant 3mA/gel current (max 150V, max 1W) for 10 minutes switching to 300V for a further 10 minutes

then finally running at a constant 450V (max 3mA/gel, 1W max). Gels were extruded from the capillaries using a water filled syringe into 2x SDS-PAGE sample loading buffer and equilibrated for 5minutes. After equilibration they were then loaded onto a 12% SDS-PAGE separating gel and overlaid with 2x SDS-PAGE sample loading buffer, alternatively they were placed into 10%(v/v) glycerol for storage at –20°C.

4.5.8 Ampholyte removal solution

A constant problem with free carrier ampholyte PAG-IEF systems is that the ampholytes migrate into the SDS-PAGE second dimension and stain deeply into a large smear that can obscure upto 20% of the gel. The ampholyte smear can be removed by incubating the PAG-IEF gel prior to equilibration or the second dimension SDS-PAGE gel after electrophoresis, in a solution of 47.5%(v/v) ethanol, 3%(v/v) acetic acid for >5 minutes.

4.6 Miscellaneous methods

A number of other methods were utilised during this research. The production of anti-TE antibodies was an attempt to show that ICF is truly of apoplastic origin and components do not appear in total extract (see section 5). The auxin affinity column methods were attempted towards the end of the project.

4.6.1 Production of rabbit anti-TE antibodies

In order to produce the maximum immune response from the rabbits a final protein concentration in the range 0.8 to 1.2 mg/ml is desirable. Tobacco TE was prepared as described in section 4.2.3 after 4 repeated VI's (see section 4.2.1) to remove soluble apoplastic proteins and polypeptides from the TE preparation. After ultracentrifugation the protein concentration was estimated using the BioRad protein estimation kit (section 4.3.2). A resultant concentration of 1.7 mg/ml of protein was calculated when read off a BSA standard curve (GraphPad Prism Software), i.e.: enough for injection. Antibodies were raised against both native proteins and denatured polypeptides to ensure that antibody probing could be carried out on native or denatured materials. Therefore the sample preparation included untreated native TE proteins and denatured TE proteins that had been boiled and contained 2% (w/v) SDS. An emulsion of this protein mixture was produced using the mineral oil, 'Freund's adjuvant' because it greatly enhances the immune response by prolonging immune system exposure to the antigens. This suspension was then injected into the rabbit; the injection regime was as follows: -

Native-TE preparation for injections (- SDS)

1. 1.0ml of 1.7mg/ml TE containing 1mM DTT
2. Stored at –20°C until required for injection.
3. Thaw TE preparation.
4. 1.0ml of Freund's adjuvant; added in 100μl aliquots, with vortexing and sonication.
5. Load 1ml into a 1ml syringe. Refreeze remaining millilitre for booster injection.

Denatured-TE preparation for injections (+ SDS)

1. 1.0ml of 1.7mg/ml TE containing 1mM DTT
2. 200μl of 10%(w/v) SDS (approximately 1.7mg/ml TE, 1mM DTT, 2%(w/v) SDS).
3. Place into a boiling water bath for 5 minutes.
4. Stored at –20°C until required for injection.
5. 1.0 ml of Freund's adjuvant; added in 100μl aliquots, with vortexing and sonication.
6. Load 1ml into a 1ml syringe. Refreeze remaining millilitre for booster injection.

Day 0 – Primary Injection

1. 0.5ml of +SDS administered intramuscularly into right leg thigh.
2. 10 x 50μl of +SDS administered subcutaneously along spine.
3. 0.5ml of -SDS administered intramuscularly into left leg thigh.
4. 10 x 50 μl of -SDS administered subcutaneously along spine.

Day 15 – Booster Injection

1. 0.5ml of +SDS administered intramuscularly into right leg thigh.
2. 10 x 50μl of +SDS administered subcutaneously along spine.
3. 0.5ml of -SDS administered intramuscularly into left leg thigh.
4. 10 x 50 μl of -SDS administered subcutaneously along spine.

4.6.2 Generating and packing the auxin affinity column

Preparation of the epoxy-sepharose 6B was carried out as per manufacturers instructions (Pharmacia, Uppsala, Sweden). Briefly, 3g of sepharose was weighed into a 50ml Falcon tube and 20ml of QH_2O added. The sepharose was incubated for >30 minutes with agitation in order to re-swell the gel, (it swells to 4ml per original g of dried material). The sepharose was then filtered and washed for >1 hour with >600ml of QH_2O on a sintered glass funnel. It was calculated (see section 5.2.3.1) that 300μM concentration of hydroxyphenylacetic acid (HPAA) would adequate to saturate the

reactive oxirane groups contained within the gel. Consequently the gel was split into 2 equal weights and resuspended in the coupling solution (300μM HPAA) in a glass beaker and agitated at 45°C for > 24hours. After incubation the gel was washed extensively with >600ml of QH_2O on a sintered glass funnel. Excess reactive groups were then blocked by incubating the gel in an excess of 1M triethanolamine >12 hours with agitation at 45°C. After blocking, the gel was washed with >600ml of QH_2O and ligand coupling efficiency was assessed in one of two ways: -

Indirect – 536μl (approximately equivalent to 100mg of re-swollen sepharose) was centrifuged at 100g for 3 minutes. 400μl of supernatant was removed; the pellet was retained for the direct measurement. The absorbance of the supernatant was read against the original coupling buffer at the λ_{max} for HPAA of 277nm.

Direct – The pellet of sepharose from the indirect measurement (see above paragraph – 'Indirectly'), was washed by resuspension in 1ml of QH_2O, centrifugation at 100g for 3minutes, and decanting of the supernatant this washing step was repeated 3 times. After washing the pellet was resuspended in 1ml of glycerol (the sepharose becomes optical clear) and the absorbance of the gel at λ_{max} for HPAA (277nm) was read against gel that had not been exposed to the coupling reagent and had been blocked with 1M triethanolamine.

The column was setup by utilising a peristaltic pump to the pack 2 x 5ml volumes of the auxin-sepharose into a 2 x 10ml syringe barrels at 133% of the maximum expected flow rate during usage – packing was therefore carried out at 1.33 ml/minute.

4.6.3 Running the auxin affinity column

The column was attached to a Pharmacia GradiFrac chromatography system at 4°C, equipped with a UV detector, fraction collector and a trace. The column was equilibrated with >4 column volumes (20ml) of 1M citrate-phosphate buffer, pH 5.5 containing 0.1M NaCl, at 1ml/minute, until a constant baseline was achieved at 280nm. Fresh ICF that had undergone dialysis for >24 hours against several changes of 1M citrate-phosphate buffer, pH 5.5 containing 0.1M NaCl was loaded (1-5ml volumes) at a flow rate of 0.3-0.5ml/minute. This sample was recollected and re-circulated through the column at 0.3-0.5ml/minute 3 times. The column was then washed with >300ml of 1M citrate-phosphate buffer, pH 5.5 containing 0.1M NaCl at 1ml/minute and elution of bound protein material carried out in one of two ways: -

Elution Method No. 1 – was achieved by changing the buffer to 1M Tris-HCl, 0.5M NaCl, pH8.0 at a flow rate of 0.3-0.5ml/minute. The advantage of this method of elution

was the absence of UV absorbing materials except eluting proteins consequently detection and subsequent collection of UV absorbing fractions is relatively simple.

Elution Method No. 2 – was achieved by changing to 1M citrate-phosphate buffer, pH 5.5 containing 0.1M NaCl and 10mM phenylacetic acid. This elution method was much more specific because the auxin (phenylacetic acid) specifically displaced any bound protein material from the column. Hence, one can report that eluted material can definitely bind to an auxin and it is therefore highly likely that the material is indeed an auxin-binding protein.

4.6.4 Cleaning and storing the auxin affinity column

The column was washed to remove any residual material with 100ml of 1M phosphate buffer at pH 8.0 containing 1M NaCl at 0.3-0.5ml/minute. For storage 50ml of 0.02% (w/v) sodium azide was passed through the column at 0.3-0.5ml/minute. The column was then sealed in parafilm and stored at 4°C.

SECTION 5

PROTEINS OF THE APOPLAST

5.1 Introduction

The technique of choice utilised throughout this research to extract the complement of proteins and enzymes present in the apoplast was vacuum infiltration (VI). This technique relies on the vacuum assisted infiltration of buffer into the apoplastic spaces to solubilise components followed by recovery of this intercellular fluid (ICF) with low speed centrifugation [Hammond-Kosack 1992]. This relatively simple technique is a powerful method to extract selectively and therefore partially purify apoplastic components primarily because the infiltration buffer is only in contact with the apoplast and therefore permits the selective extraction of apoplastic materials only. Ultimately, the major advantage of utilising a VI technique to extract apoplastic materials is that one can have a high degree of confidence that a particular component is actually present in the apoplast *in vivo*.

Contamination of ICF by intracellular components can and does occur and in order to confirm the apoplastic nature of materials extracted using VI it was common to use three 'assays' to confirm the apoplastic nature of the ICF. The first involved a visual assessment of ICF, if it was green it was discarded because intracellular contamination of ICF had undoubtedly occurred. The second was an assay for the intracellular enzyme, malate dehydrogenase (MDH) [Hammond-Kosack 1992], if the value contained in any ICF preparation exceeded 1% of the assay value of the total extract, it was deemed too high and was discarded [Ilett 1998]. The final assay was visual, and rested upon the fact that the large sub-unit of one of the most abundant leaf proteins, ribulose-1,5-bisphosphate carboxylase (RUBISCO), [Chen *et al.* 2000] was readily identifiable as a prominent band at approximately 50 kDa on a SDS-PAGE gel. The presence of the RUBISCO large sub-unit in SDS-PAGE separated ICF preparations indicated that intracellular contamination had occurred and that any other polypeptides were not necessarily apoplastic in origin [Alexander 1995; Ilett 1998]. VI was the method of choice because other methods for the isolation of apoplastic/cell wall materials rely on the separation of these materials from whole cell and tissue extracts [eg: Shimuzi *et al.* 1997] and consequently will invariably contain higher levels of contamination from intracellular components than ICF.

In section 1.4 some of the wide range of proteins and enzymes contained within the apoplast that potentially can be selectively extracted using VI have been detailed. During

the course of this research two methods were employed to attempt to identify or attribute characteristics to VI extracted apoplastic proteins: -

1. N-terminal sequencing of polypeptides separated on SDS-PAGE gels
2. Spectrophotometric or in-gel enzyme assays (see section 7)

The ultimate aim was to catalogue and identify as many of the VI-extractable proteins and polypeptides as possible].

One group of proteins speculated to be present in the apoplast are the auxin-binding proteins (ABP's), see section 1.4.2. The apoplast is the proposed, but not yet clearly identified, site of action of ABP's. The highly selective nature of VI provided a very novel extract from which to attempt the isolation of ABP's. To the authors knowledge ICF has never been subjected to such a study and positive results would provide direct evidence of ABP presence in the apoplast *in vivo*.

5.2 Results

5.2.1 Efficacy, optimisation and development of VI techniques

The small scale vacuum infiltration (VI) technique previously used in Durham was initially trialed to ensure that it could provide the necessary selective enrichment of apoplastic polypeptides, this is detailed in section 5.2.1.1. The technique was then optimised to provide the largest quantity of apoplastic polypeptides with the lowest possible contamination from intracellular components (section 5.2.1.2). Section 5.2.1.3 depicts the data from VI's using buffers with differing properties in order to maximise the extraction of apoplastic proteins. Ultimately, any analysis of ICF extracted utilising the small scale VI technique was limited because of the relatively low quantities of material recovered, consequently, a large scale VI technique was developed which quadrupled the volumes of intercellular fluid (ICF) recovered (see section 5.2.1.4 and appendix 1).

5.2.1.1 The selective enrichment of apoplastic components

The first point within the small scale VI technique at which it was possible to make a qualitative assessment on the degree of intracellular contamination was immediately after centrifugation. Consequently, all recovered ICF's were subjected to a visual assessment of intracellular contamination based solely upon the colouration of the liquid. Leaf tissue was especially suited to such a 'quality assessment' because of the very high concentration of chlorophyll present in leaves, therefore any leakage of intracellular components (i.e.: the plasma-membrane and chloroplasts) during VI would impart a

green colour to the recovered ICF thus making a visual assessment of contamination relatively simple. Ultimately, any green colouration would bear a relationship to the degree of intracellular contamination present in the ICF and consequently, should improve the overall selective enrichment of apoplastic components achieved during VI.

To illustrate this point, three independent VI's were conducted on tobacco leaf tissue and the resultant ICF's were categorised as containing either LOW, MID or HIGH levels of intracellular contamination based purely on the visual assessment of the colouration of the liquid when viewed against a white background. Each category was then scanned over the visible spectrum, assayed for the intracellular enzyme malate dehydrogenase (MDH) from which the relative-MDH activity was calculated (section 4.3.1), the data are presented in figure 5.1. The scan revealed the presence of a peak at 682 nm in all ICF's which corresponded with the λ_{max} of chlorophyll a [Moberg *et al.* 2000] this was especially evident in the ICF visually assessed with a HIGH degree of intracellular contamination, but was also present to some degree in both MID and LOW ICF's. Similarly, the relative-MDH activity data (see the graph on figure 5.1) also reported the same trend of increasing intracellular contamination of ICF which 'matched' with the visual assessment and subsequent categorisation into LOW, MID and HIGH levels of contamination.

Polyacrylamide gel separation of ICF was the primary method of analysis to be utilised throughout this project, therefore equal protein loadings of the LOW, MID and HIGH visually assessed ICF samples were subjected to SDS-PAGE alongside tobacco leaf total extract (TE). Figure 5.2 illustrates the resultant gel. The TE lane contains a heavily stained band at ~50 kDa, this corresponds to the major sub-unit (the minor sub-unit is at ~15 kDa) of the most abundant tobacco leaf protein, RUBISCO [Chen *at el.* 2000], the band is arrowed on the figure. Due to the high abundance of RUBISCO in tobacco leaf any leakage of intracellular components during VI would be evident in ICF preparations because of the characteristic ~50 kDa polypeptide band. The conspicuous absence of RUBSICO in ICF preparations has been used previously to validate the apoplastic nature of ICF [Ilett 1998]. This polypeptide was definitely present in the HIGH ICF preparation and to a lesser degree in the MID ICF preparation. However, this band was not present in the ICF preparation that had been categorised as having a LOW level of intracellular contamination. All of these data therefore confirm that VI can selectively enrich components from the apoplast providing that these precautions for minimising intracellular contamination of ICF are undertaken: -

Figure 5.1

Spectrophotometric and malate dehydrogenase enzyme assay of visually assessed intracellular contamination in ICF's.

3 vacuum infiltration's were carried out on tobacco leaf tissue using the small scale method (see section 4.2.1). The resultant ICF's were visually assessed for 'quality' (ie: lack of intracellular contamination) and categorised as having HIGH (obviously green in colour), MID (a hint of green colouration) or LOW (no obvious green colouration) levels of intracellular contamination dependent upon the degree of colouration. Each grouping was then pooled and scanned in the region 400-800nm in a Beckman DU7500 spectrophotometer (Beckman Instruments, UK) against infiltration buffer blank. A representative scan is shown top right. The same ICF's were also subjected to the MDH assay and the relative MDH-activity calculated as described in section 4.3.1, the results are presented on the graph, bottom right. Data are the means of ± SD of three measurements.

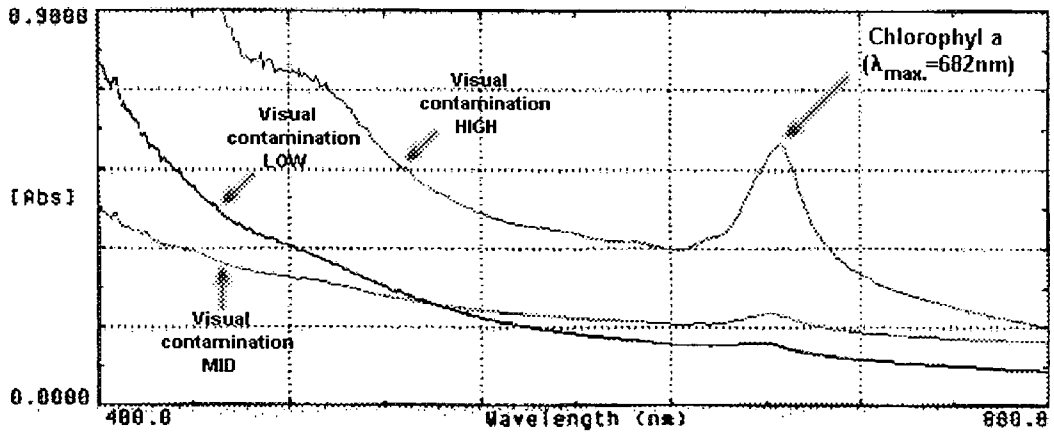

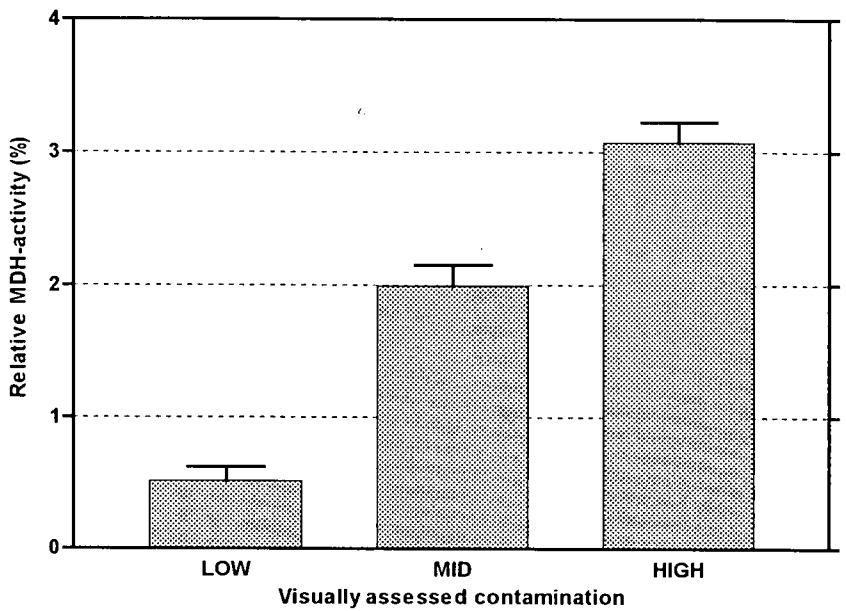

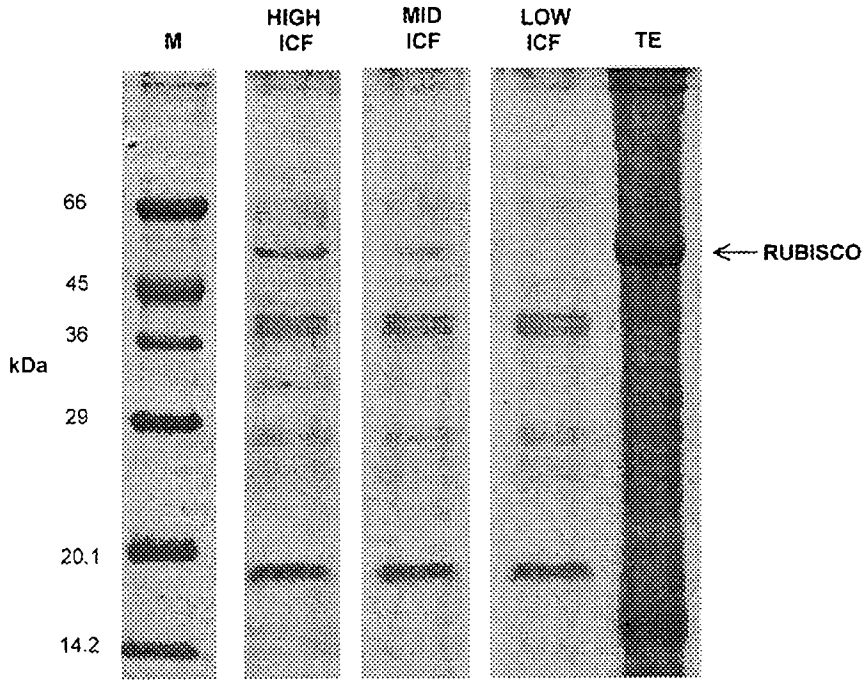

Figure 5.2

SDS-PAGE analyses of ICF with varying degrees of intracellular contamination.

ICF was extracted from tobacco leaf tissue as described in section 4.2.1 and was categorised into either having LOW, MID or HIGH levels of intracellular contamination by visual assessment of colour. Each of the categories of ICF was dialysed overnight and then subjected to protein quantification (section 4.3.2), aliquoted into volumes that contained 50μg of protein and then lyophilised (section 4.2.4). The lyophilised solid was reconstituted in 50μl of SDS-PAGE sample buffer and subjected to SDS-PAGE as described in section 4.4.1. Key: M=denotes a 10 μl loading of marker proteins; HIGH ICF=15μl (15μg) loading; MID ICF=15μl (15μg) loading; LOW ICF=15μl (15μg) loading; TE=35μg loading. The gel was Coomassie stained (section 4.4.3).

1. Visual assessment of ICF for green colouration prior to pooling,
2. Ensuring that the relative MDH-activity is <1% of that found in TE, and,
3. The major sub-unit of RUBISCO is not present in the ICF during gel analysis.

Previous work [Alexander 1995; Ilett 1998] had utilised anti-RUBISCO antibodies to establish the level of intracellular contamination present in ICF preparations. Unfortunately, these antibodies were not available for this study and as a consequence a different approach was taken. Native and denatured TE proteins were prepared from tissue that had been vacuum infiltrated four times in order to remove the majority of the soluble apoplastic protein & polypeptide complement as possible. This protein and polypeptide mixture was then injected into a rabbit to obtain an immune response (see section 4.6.1) the ultimate aim was to generate a spectrum of antibodies that had affinity for intracellular proteins only. TE and ICF proteins were subjected to SDS-PAGE and electroblotted for antibody probing as described in section 4.4.9. The optimal titre of primary and secondary antibodies was assessed by probing 16 individual TE blots with varying combinations of both antibodies, see figure 5.3; primary antibody titre number 2 and secondary antibody titre group B were determined to give the best banding patterns for subsequent analysis. Therefore, 1:1000 dilution of primary antibodies and 1:15,000 secondary antibody were used to probe an ICF blot (figure 5.3). Unfortunately, apoplastic proteins were also recognised by antibodies raised against TE proteins, presumably because the complete extraction of soluble apoplastic proteins may not been achieved or there was enough apoplastic protein material inside/outside the cells to cause a cross-reaction. Ultimately these antibodies were not used again due to the high cross-reactivity.

5.2.1.2 Optimisation of the small scale VI conditions

It was noted that both the vacuum conditions and the developmental age of the leaf tissue played roles in the observed degree of infiltration; i.e., as the tissue was increasingly infiltrated with buffer it gradually becomes more, 'water-logged' and therefore darker in colour. A 'checker-board' experiment was set-up to optimise the observed degree of buffer infiltration into immature (top of plant, <10cm long) and mature (bottom of plant >20cm) tobacco leaf tissue exposed to the vacuum for varying lengths of time. Figure 5.4, illustrates the data from this experiment, and clearly shows that as exposure to vacuum increases so does the observed degree of buffer infiltration into the tissue. Furthermore, it was evident that immature tobacco leaves infiltrated to a greater extent than mature tobacco leaves. This presumably indicates that the apoplast of immature tissue has greater continuity for the conduction of liquids [Canny 1995]. As a

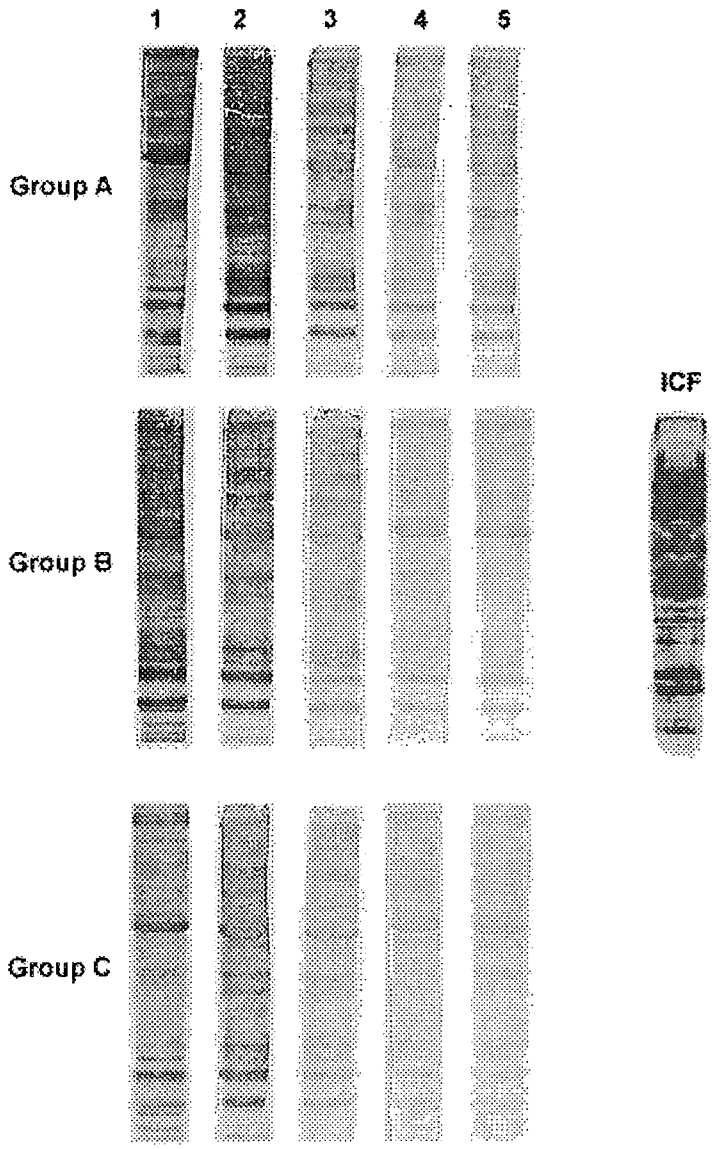

Figure 5.3

Anti-TE antibody probing of TE blots to assess optimum titre for probing ICF blot.

Anti-TE antibodies were prepared as described in section 4.6.1. A total extract was prepared (section 4.2.3) and subjected to SDS-PAGE (section 4.4.1) and then blotted to nitrocellulose membrane (section 4.4.9) for antibody probing. Each number (1-5) represents a different dilution of primary rabbit anti-TE antibodies, as follows; number 1=1:100; number 2=1:1000; number 3=1:5000; number 4=1:10,000; number 5=1:25,000. Each group (A-C) represents a different dilution of secondary anti-rabbit conjugated alkaline phosphatase antibody (Sigma, UK), as follows; group A=1:5000; group B=1:15,000; group C=1:30,000. The ICF sample has been blotted and probed with a 1:1000 dilution of primary antibodies and a 1:15,000 dilution of secondary antibody.

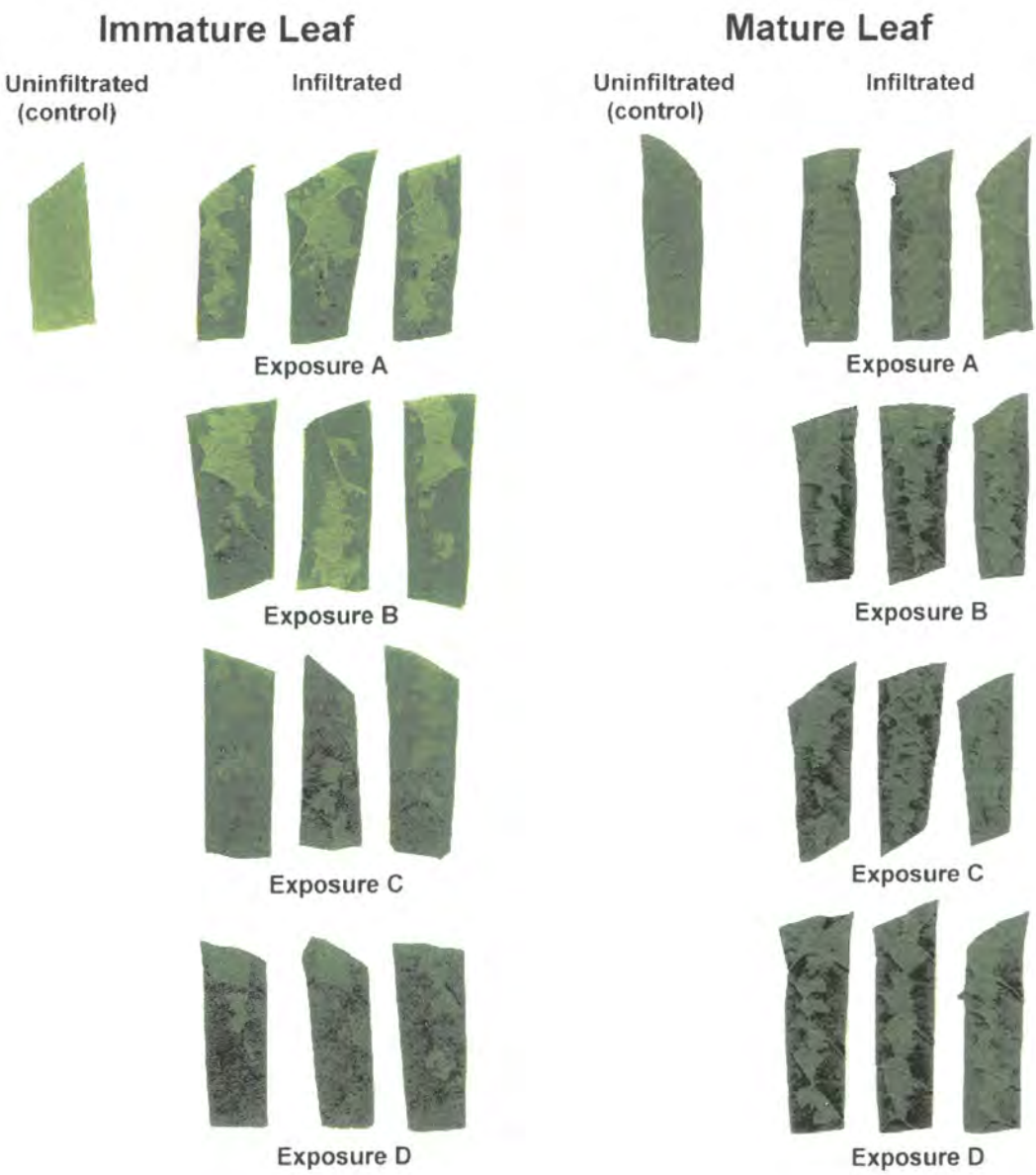

Figure 5.4

The effect of vacuum conditions on the infiltration of young and mature tobacco leaf tissue.

Several leaf strips were sectioned from immature and mature tobacco leaves and infiltrated with 100mM NaCl phosphate buffered to pH 7.5, vacuum conditions were: Exposure A = 15 sec. to evacuate ICF gas; 5 sec. agitation; 15 sec. repressurisation; Exposure B = 15 sec. to evacuate ICF gas; 15 sec. agitation; 15 sec. repressurisation; Exposure C = 15 sec. to evacuate ICF gas; 30 sec. agitation; 15 sec. repressurisation; Exposure D = 15 sec. to evacuate ICF gas; 60 sec. agitation; 15 sec. repressurisation; Control leaf strips are shown. Representative strips were scanned.

consequence of the inherently greater infiltration potential of immature tobacco leaf tissue it was used throughout this project, except where stated otherwise.

Two points were identified within the small scale VI technique that when optimised would maximise the yield of uncontaminated ICF: -

1. In order to infiltrate the leaf tissue any gas present in the intercellular spaces must be removed. During the exposure to the vacuum the leaf tissue is in a depressurised environment and consequently cellular leakage may occur. Minimisation of the duration the tissue is exposed to a vacuum will reduce the level of intracellular contamination of ICF.
2. The recovery of infiltrated buffer from the leaf tissue requires the exposure of the leaf tissue to a centrifugal force; an excessive centrifugal force would cause the leaf tissue to be crushed at the bottom of the tube, and would thus directly elevate levels of intracellular contamination of ICF.

Therefore, using immature tobacco leaf tissue, the effects of the duration of exposure to the vacuum and the relative centrifugal force (RCF) used to recover the infiltrated buffer were investigated. The resultant measurements of the volume of visually uncontaminated ICF recovered, its protein content and the relative MDH-activities are graphed (A-C) on figure 5.5.

The volumes of visually uncontaminated ICF recovered at centrifugal forces of 500 and 700 were very low and when the tissue strips were examined they still appeared to be 'water logged' with buffer, it is therefore probably that the force exerted was not sufficient to drain the apoplast of infiltrated buffer. At 900 and 1200 g the tissue strips did not have the 'water logged' appearance, however, at 1200 g it was evident that some of the tissue was getting crushed at the bottom of the tube thereby reducing the volume of visually uncontaminated ICF recovered (figure 5.5, graph A). Consequently the maximum volumes of visually uncontaminated ICF were recovered after a 30 or 60 second exposure to vacuum and at a centrifugal force of 900 g. Similarly, at 900 g the protein content of ICF was relatively high (~280μg/ml) and because of the greater volume of visually uncontaminated ICF recovered at a 60 second vacuum exposure the overall yield was better. The final measurement of uncontaminated ICF is displayed on graph C, and shows that at 900 the ICF recovered after a 60 second vacuum exposure has a relative MDH-activity of ~0.8%, this corresponded to no visible RUBISCO on an SDS-PAGE gel (data not shown but see figure 5.2 for an example). The final optimised small scale VI technique is presented in section 4.2.1.

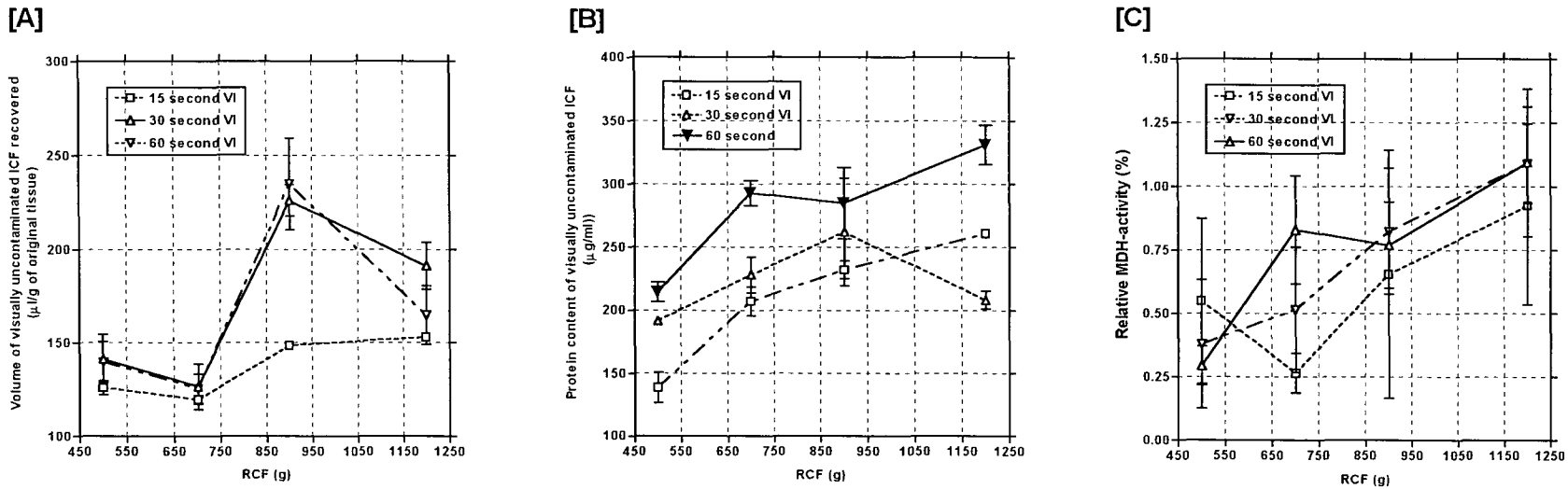

Figure 5.5

Assessment of ICF's recovered from tissue using different conditions.

Duplicate VI's were carried out as described in section 4.2.1, except that the period of time that the leaf strips spent under vacuum was adjusted and the recovery of the ICF was undertaken at differing RCF's. After recovery, any ICF's that were visually contaminated were discarded and uncontaminated ICF's were pooled and the volume measured, the data is presented on graph [A]. Graph [B] - the protein content of each uncontaminated ICF was estimated using the Bradford assay (section 4.3.2). Graph [C] - the relative MDH-activity for each uncontaminated ICF was calculated as described in section 4.3.1. Data are the means of ± SD of two measurements.

5.2.1.3 Buffer selection

A series of vacuum infiltrations were conducted to select the most appropriate buffer to maximise the extraction of apoplastic materials while minimising any intracellular contamination of ICF. The buffers were chosen based on their different properties and previous use to selectively extract cell wall proteins from cell suspensions cultures [Robertson *et al.* 1997]. The buffers and their properties are presented in table 2.1.

Table 2.1 – VI buffers and their properties [Robertson *et al.* 1997].

VI Buffer	Extraction properties
dH_2O	Water soluble components only.
50mM potassium phosphate, pH 7.5	Components that require low salt or neutral pH.
200mM sodium chloride, pH 7.5	Ionically bound components.
200mM calcium chloride	Previously utilised for the extraction of cell wall proteins.
50mM EDTA	Cation sequestered proteins/polypeptides.
50mM sodium borate, pH 7.5	Disruption of glycoprotein-polysaccharide interactions.

Each buffer had very noticeable and individual effects on both the tissue and the resultant ICF. When infiltrated into the leaf tissue the calcium chloride VI buffer induced the loss of tissue 'elasticity' which was not regained after recovery of the infiltrated liquid, sodium chloride had a similar but lesser effect, this presumably stems from the altered properties of the cell wall in the presence of these ions [Greringer *et al.* 1995; Tibbits *et al.* 1998]. ICF recovered from tobacco leaf tissue was usually colourless or occasionally had a slight pink tint, however, ICF recovered after infiltration with the EDTA buffer had a deep pink-red colouration, no explanation of what components generate such a colour has been found. The spectrophotometric scan in figure 5.7 illustrates that the different ICF's recovered using buffers with different properties also exhibited different spectral properties.

Figure 5.6, A, shows the concentration of protein in each ICF (left Y-axis) and the final total quantity of protein recovered (right Y-axis). The sodium and calcium chloride VI buffers extracted the most protein, however, the calcium chloride ICF had a relatively high MDH-activity (graph B; the other buffers used all recovered ICF with relative MDH-activities of <1%) that presumably arose because the tissue was very difficult to handle after infiltration because of the loss of 'elasticity'. The ICF's were subjected to SDS-PAGE analysis to assess if intracellular contamination had occurred and to view the profile of

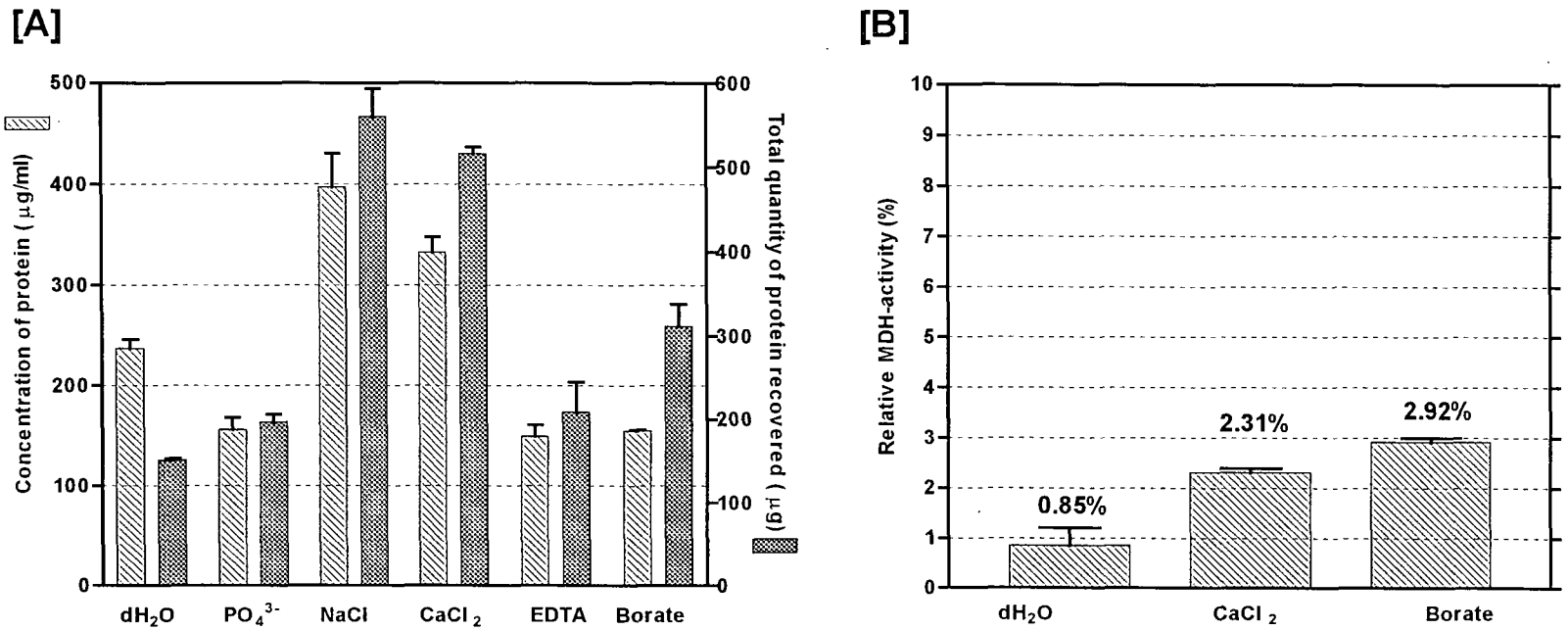

Figure 5.6

Small scale VI using infiltration buffers with different properties.

Duplicate VI's were carried out as described in section 4.2.1 except that different infiltration buffers were used. Graph [A] – the concentration of protein in each visually uncontaminated ICF was assessed as described in section 4.3.2, the data is displayed on the left Y-axis; the volume of uncontaminated ICF was also recorded and used to the calculate the total quantity of protein recovered (right Y-axis). Graph [B] – the relative MDH-activity of each ICF was calculated against the appropriate TE prepared with the same buffer (see sections 4.2.3 and 4.3.1). Data are the means of ± SD of two measurements.

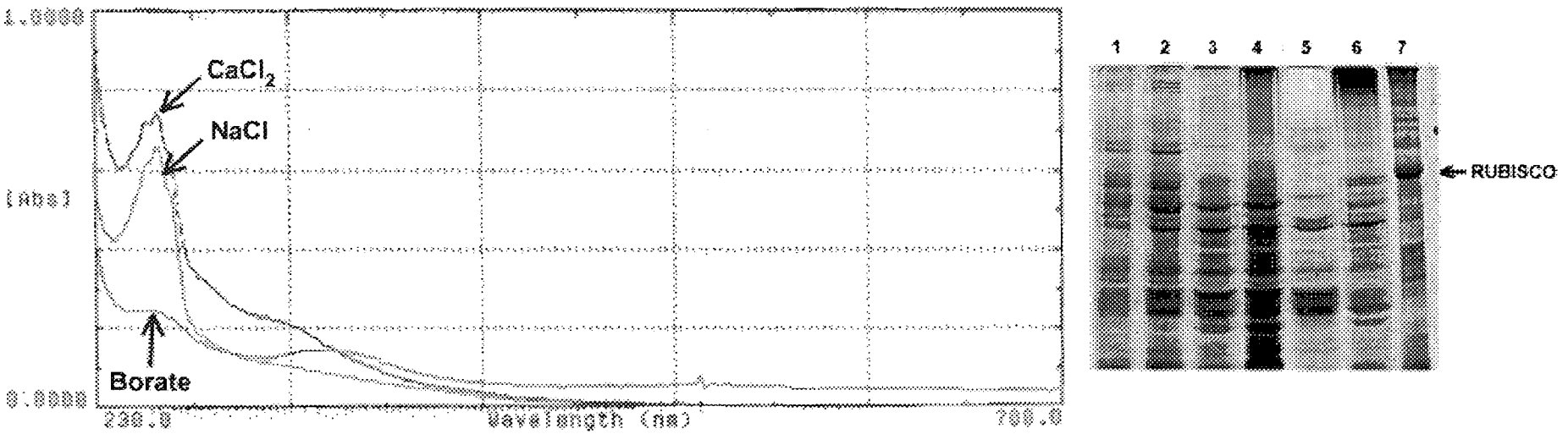

Figure 5.7

Analysis of ICF's extracted using infiltration buffers with differing extraction properties.

See section 5.1 for detailed information. Duplicate VI's were carried out as described in section 4.2.1 except that different infiltration buffers were used. The ICF's extracted with NaCl, $CaCl_2$ and borate infiltration buffers were spectrophotometrically scanned between 230 and 700nm against a water blank, the scan is shown on the left. Each of the ICF's was dialysed overnight and then subjected to protein quantification (section 4.3.2), aliquoted into volumes that contained 25μg of protein and then lyophilised (section 4.2.4). The lyophilised solid was reconstituted in 50μl of SDS-PAGE sample buffer and subjected to SDS-PAGE as described in section 4.4.1; each ICF lane was loaded with 10μg of protein. Key: 1=dH_2O ICF; 2=PO_4^{3-} ICF; 3=NaCl; 4=$CaCl_2$ ICF; 5=EDTA ICF; 6=Borate ICF; 7=10μg loading of NaCl TE (see section 4.2.3) The gel was silver stained (section 4.4.4).

extracted polypeptides. The gel image is displayed in figure 5.7. A low level of intracellular contamination (the RUBISCO polypeptide) is present in both the water and calcium chloride infiltrated ICF's, but is not present in the other samples. It is immediately obvious that the different buffers selectively extracted proteins and polypeptides from the apoplast. The 200mM sodium chloride buffer was chosen because of the combination of low intracellular contamination determined from the relative MDH-activity, the SDS-PAGE gel analysis, high total protein recovery and the similarity of banding patterns to the other VI buffers utilised (see section 4.2.1 for the full details of the final method).

5.2.1.4 Large scale VI

The small-scale VI method yielded relatively small volumes of ICF during a working day consequently a large scale VI technique was developed. The major difference was that bulk quantities of leaf tissue were rolled and therefore supported within a mesh during exposure to vacuum and centrifugation as a consequence the need to individually roll each tissue strip was removed. Therefore the time taken to VI comparable quantities of leaf tissue was greatly reduced and the volumes recovered greatly increased.

The technique was optimised in a similar manner to that of the small scale VI technique (see section 5.2.1.2). The data are not shown and described here because it is presented in a research paper that is currently undergoing submission to a peer reviewed journal. The paper is presented in appendix 1.

5.2.2 N-terminal sequence identification of ICF polypeptides

One of the main aims of this research project was to identify changes in the complement of apoplastic proteins. Therefore N-terminal sequence analysis was carried out on proteins present at different stages of leaf development (see section 5.2.2.1), during abiotic stress (see section 5.2.2.2) and finally, because of the substantial N-terminal blockage experienced, on as many polypeptides as could be clearly identified on a blot (see section 5.2.2.3).

5.2.2.1 N-terminal sequencing of ICF polypeptides during leaf development

Leaves were categorised as immature or mature as described in section 5.2.1.2, and then subjected to the fully optimised small scale VI technique (section 4.2.1). Similarly, age specific-TE's were prepared using immature and mature leaf tissues. All protein extracts were then subjected to SDS-PAGE separation. Gel lanes that contained marker proteins, ICF and TE were detached from each gel and Coomassie stained (see figure 5.8), the remainder of each gel was then electroblotted (section 4.4.11). The blots were

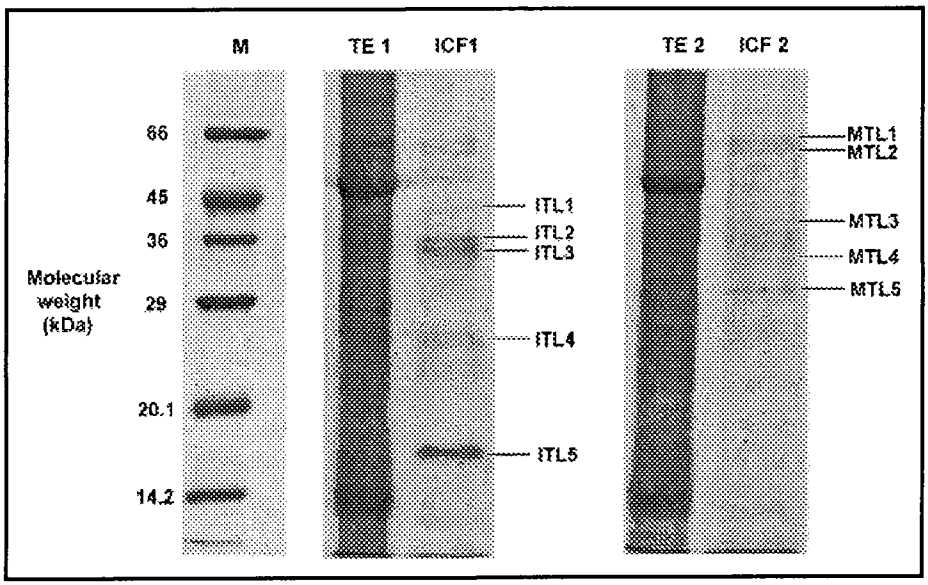

Band	M.W. (kDa)	Sequence	% homology	Description
ITL1	43.8	-	-	-
ITL2	33.9	-	-	-
ITL3	32.0	-	-	-
ITL4	26.0	ATFDIVNQDTYTVWA	86	thaumatin-like antifungal protein
ITL5	16.5	SVQDFCVADD	100	germin-like protein from arabidopsis
MTL1	63.8	-	-	-
MTL2	62.4	-	-	-
MTL3	35.2	-	-	-
MTL4	31.5	-	-	-
MTL5	30.5	-	-	-

Figure 5.8

N-terminal sequence analysis of immature and mature tobacco leaf polypeptides.

ICF was extracted from immature or mature tobacco leaf tissue as described in section 4.2.1. Proteins were loaded as follows; TE1=immature TE 35μg; TE2=mature TE 35μg; ICF1=immature 20μg; ICF2=immature 20μg. This gel was coomassie stained (section 4.4.3) and the duplicate was blotted (section 4.4.11) and selected polypeptide bands were then subjected to N-terminal sequencing. The table below the gel image details the results of sequence analysis and database searches for homology using BLAST (see section 4.4.12 for details of search criteria). Refer to the text for full information of the species and reference for each homology.

Coomassie stained and comparisons were made with the appropriate stained gel in order to select individual bands that appeared age-specific. Five immature (ITL) and five mature (MTL) polypeptide bands could be clearly identified on each respective blot and gel that appeared to be mutually exclusive of each developmental age, they were therefore subjected to N-terminal sequencing. The gel image and sequencing results are presented in figure 5.8 and the original BLAST search results are presented in appendix 2.

After several attempts using three different ICF preparations, sequencing revealed that 80% of the chosen polypeptides were seemingly either N-terminally blocked or composed of multiple bands. This level is high, but some studies have reported that in general plant proteins do tend to have a higher level of N-terminal blockage than other organisms. However, two of the ten polypeptides were successfully sequenced. A 29.2 kDa polypeptide which shared a significant (86%) homology with a 27 kDa thaumatin-like protein from Diospyros texana [Vu & Huynh 1994] and a 16.5 kDa polypeptide shared a 100% homology to germin-like protein from Arabidopsis thaliana.

5.2.2.2 N-terminal sequencing of ICF polypeptides during abiotic stress

There have been many reports of changes in the apoplastic protein complement in response to abiotic stress (see section 1.4.3.1 for an overview). Therefore tobacco plants were subjected to heat stress for 5 days at 40°C and drought stress was mimicked by restricting the water supply until all the leaves had wilted (~14 days) after which watering was resumed, the plants were then allowed to rehydrate over a 3 day period. Both sets of plants were then subjected to VI, SDS-PAGE and electroblotting.

A total of six polypeptide bands, which appeared to be induced by the imposed stress, were selected for N-terminal sequencing. Figure 5.9 displays the gel image and the selected bands. Several attempts were made but unfortunately, all of the selected polypeptides appeared to be N-terminally blocked or composed of multiple bands and therefore sequencing could not be carried out.

5.2.2.3 N-terminal sequencing of multiple ICF polypeptides from standard ICF

The consistent problem of N-terminal blockage of selected polypeptides had hindered the subsequent identification of apoplastic components. It was therefore decided that all of the bands that were clear, distinct and visible on a blot generated from standard ICF (see section 4.2.1) would be N-terminally sequenced. A total of 13 distinct polypeptide bands could be readily identified on the sequencing blot (SICF1-13) and the resultant gel image is presented in figure 5.10.

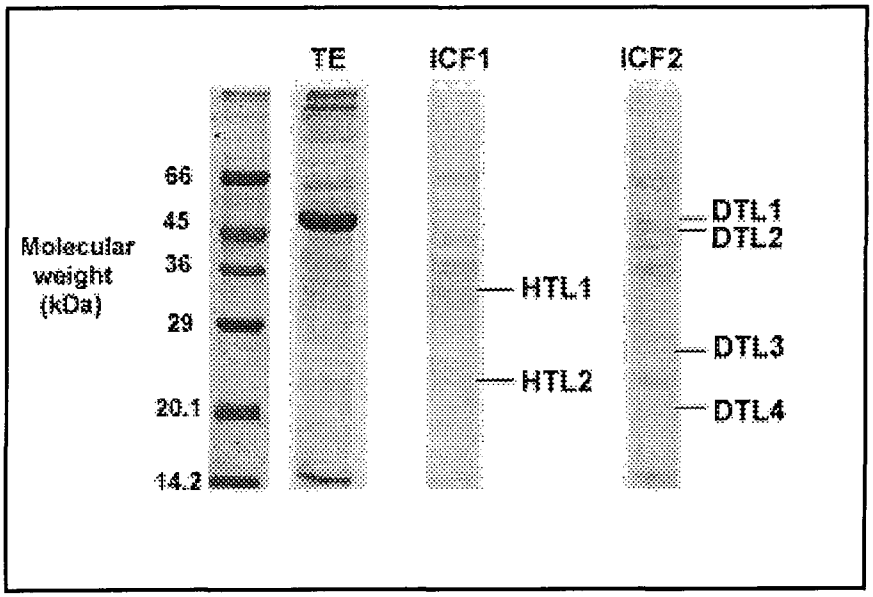

Band	M.W. (kDa)	Sequence	% homology	Description
HTL1	31.2	-	-	-
HTL2	22.9	-	-	-
DTL1	50.2	-	-	-
DTL2	45.0	-	-	-
DTL3	27.9	-	-	-
DTL4	19.4	-	-	-

Figure 5.9

N-terminal sequence analysis of polypeptides from abiotically stressed plants.

ICF was extracted from heat stressed or drought stressed plants as described in sections 4.2.1 and 5.2.2.2. Proteins were loaded as follows; TE=NaCl TE 20μg; ICF1=heat treated ICF 20μg; ICF2=drought treated ICF 20μg. This gel was coomassie stained (section 4.4.3) and the duplicate was blotted (section 4.4.11) and selected polypeptide bands were then subjected to N-terminal sequencing. The table below the gel image details the results of sequence analysis and database searches for homology using BLAST (see section 4.4.12 for details of search criteria). Refer to the text for full information of the species and reference for each homology.

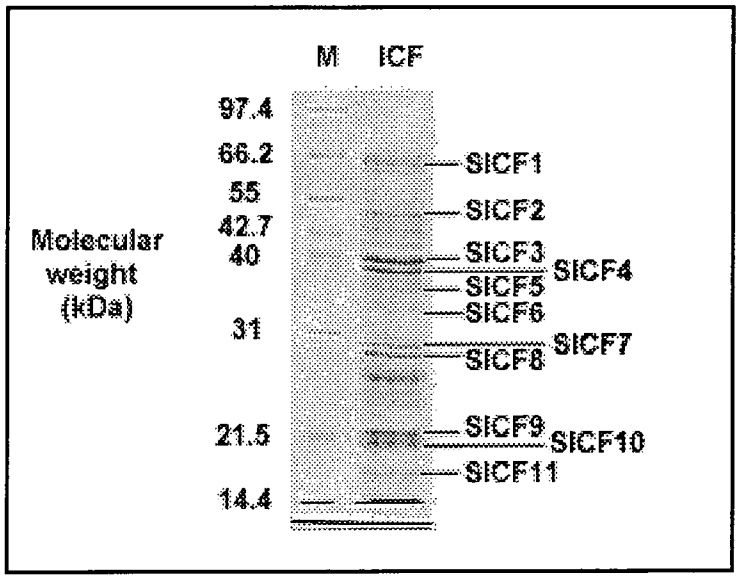

Band	M.W. (kDa)	Sequence	% homology	Description
SICF1	65.1	-	-	-
SICF2	46.9	MPVDITYLQSAVRKG RVPL	90	Putative pectinacetylesterase
SICF3	39.2	ASNGLGRTPQMGN	90	acetylgalactosaminidase
SICF4	38.2	-	-	-
SICF5	36	-	-	-
SICF6	34	-	-	-
SICF7	30.4	DDPD?T	-	-
SICF8	29.4	AVLDFCVGDLSVPDN PAG	77	Auxin-binding protein 20
SICF9	21.5	AVLDFC<	-	-
SICF10	20.3	-	-	-
SICF11	17.2	MPDP?PTFAE	0	No homology detected

Figure 5.10

N-terminal sequence analysis of ICF polypeptides.

ICF was extracted from young tobacco leaves as described in sections 4.2.1. 40μg of ICF proteins and polypeptides were loaded to 5 duplicate lanes 4 were blotted and 1 was coomassie stained (shown above). This gel was coomassie stained (section 4.4.3) and the other lanes were blotted (section 4.4.11) and then the selected bands were subjected to N-terminal sequencing. The table below the gel image details the results of sequence analysis and database searches for homology using BLAST (see section 4.4.12 for details of search criteria). Refer to the text for full information of the species and reference for each homology. Key: ?=undetermined amino acid residue; <=sequencing reaction stopped.

Five polypeptide bands did not yield sequence data (~46%) either because of insufficient quantity of the polypeptide, the presence of more than one polypeptide or N-terminal blockage. Of the remainder only five polypeptides generated enough amino acid sequence to ensure a useful search of the database (>6 residues). Two homologies were present with carbohydrate related enzymes (SICF2 and 3) and two with an intercellular signalling protein (SICF8 and 9). The latter was an auxin-binding protein (ABP) isolated from prunus persica [Ohmiya *et al.* 1998]; both of these polypeptide bands had the same initial series of residues hence SICF9 sequencing was terminated by the operator of the sequencer because of the similarity to SICF8.

5.2.3 Attempted isolation of auxin binding proteins from ICF

Two ICF polypeptide sequences (SICF8 and 9) both yielded high homologies to an auxin-binding protein (ABP) identified in Prunus persica [Ohmiya *et al.* 1998]. Consequently, because the putative site of ABP action is assumed to be the apoplast [Brown & Jones 1994], ICF may well contain a disproportionate quantity of ABP's. Therefore, an affinity chromatography method was established in order to isolate and characterise any auxin-binding proteins present in ICF extracts.

5.2.3.1 Coupling hydroxyphenylacetic acid to epoxy-sepharose 6B

Several investigators had utilised hydroxyphenylacetic acid (HPAA) attached to a sepharose as an effective affinity matrix for the isolation of ABP's [Reinard & Jacobsen 1995; Kim *et al.* 1998]. The preparation of the epoxy-sepharose and subsequent HPAA-ligand coupling was carried out with reference to the manufacturers data and instructions (Pharmacia, Uppsala, Sweden) and as described in section 4.6.2. The following process was used to calculate the necessary concentration of HPAA for ligand coupling:-

Pharmacia quote that the epoxy-sepharose contains:-

> 19-40μM of reactive oxirane groups per ml of drained sepharose, and,
> 6-ml of sepharose in total was required for coupling to HPAA, therefore,
> a maximum total of 240μM oxirane groups for reaction with HPAA,
> the reaction between the oxirane group and HPAA is molar, therefore,
> a 300μM HPAA solution would provide enough ligand for coupling.

The efficiency of the coupling of the HPAA ligand to the epoxy-sepharose was assessed by following the decrease in absorbance of HPAA in the reaction mixture (figure 5.11, [A]) and by following the increase in absorbance of the optically clear epoxy-sepharose (figure

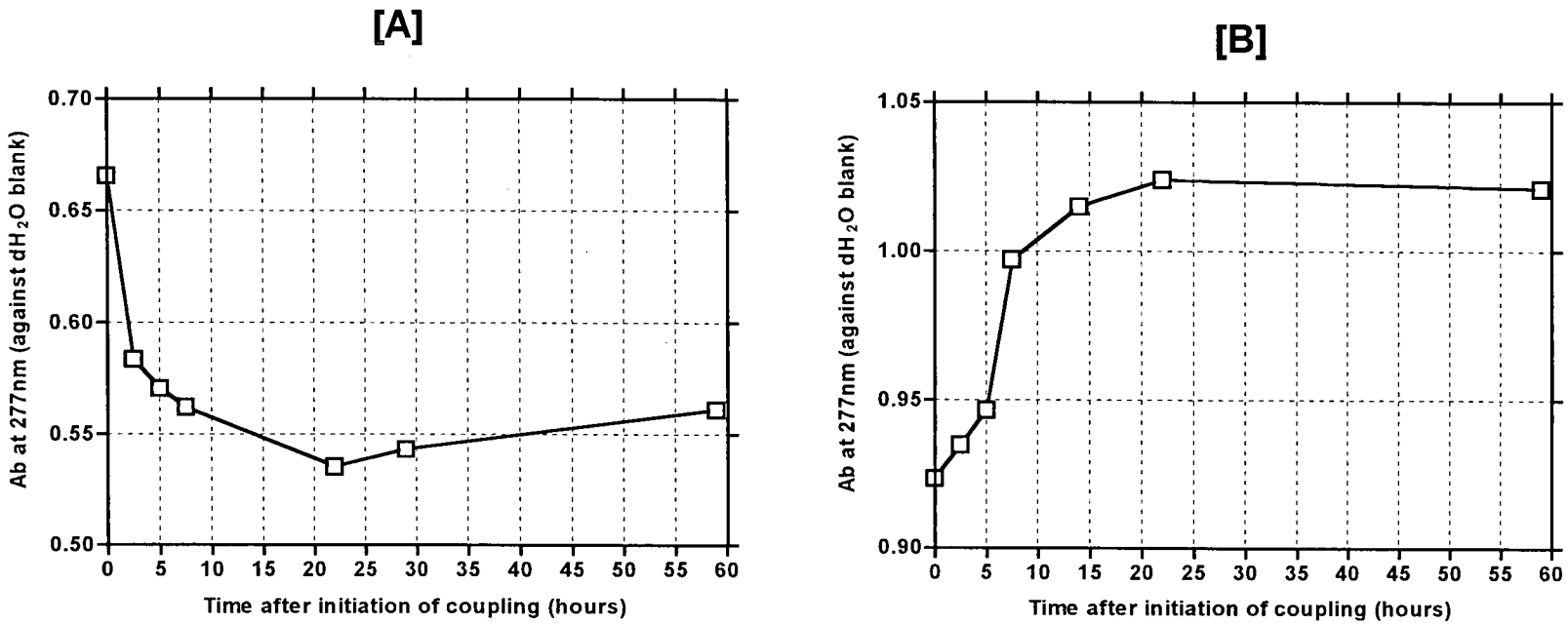

Figure 5.11

Auxin affinity column – graphs to show the progress and efficiency of the coupling of hydroxphenylacetic acid (HPAA) to epoxy-sepharose 6B.

The auxin affinity matrix was prepared as detailed in section 4.6.2. These are the measurements of the coupling reaction (see section 5.2.3). Graph [A] = absorbance of the coupling mixture supernatant at different time points at the λ_{max} for HPAA of 277nm against dH_2O. Graph [B] = absorbance of epoxy sepharose 6B at different time points at the λ_{max} for HPAA of 277nm against dH_2O. Data are individual measurements.

5.11, [B]). The data are presented in figure 5.11 and illustrates that the coupling reaction was complete after approximately 24 hours.

5.2.3.2 Affinity chromatography of ICF

Any ABP's present in the apoplast were likely to be present at very low levels [Brown & Jones 1994]. Previous work has illustrated this point because of the need for highly sensitive microscopy techniques to visualise ABP's in the apoplast [Jones & Herman 1993; Deikmann *et al.* 1995]. In order to maximise the chances of binding ABP's to the auxin affinity column large volumes of ICF (5-ml) were freshly prepared and loaded at 0.5ml/minute. The ICF eluent was recollected and re-circulated through the column a total of three times. Elution of bound material was achieved either in a 'general' manner by altering the pH and ionic strength or more, 'specifically' by the addition of an auxin. The eluting fractions were collected, dialysed, lyophilised and subjected to SDS-PAGE, see figure 5.12 (A and B).

Elution using a change of pH and ionic strength (i.e.: 'general' - see 4.6.3) revealed that fraction 3 contained 6 polypeptides which had bound to the auxin affinity matrix, these are arrowed on figure 5.12, gel A. Of particular interest was a 21 kDa polypeptide (band F) and two larger polypeptides of 61 and 57 kDa (bands A and B, respectively), these polypeptides also eluted (fractions 3-5) with an auxin, indicating that they can specifically bind auxins (figure 5.12, gel B). The remaining polypeptides (C-E) were assumed to have bound to the sepharose matrix in a non-specific manner.

5.3 Conclusions

Early in this research it was proven that VI yields preparations of apoplastic material that are not visually or enzymatically contaminated by intracellular components when assessed by any of the methods to minimise contamination described within this thesis. Consequently, these methods adequately guard against intracellular contamination of ICF and lead the author to the conclusion that ICF extracted as described here is at the very least, a highly purified apoplastic extract.

During the development and optimisation of VI it was shown that polypeptides can be selectively removed from the apoplast using buffers with specified properties in a similar manner to that shown by Robertson *et al.* [1997] using cell suspension cultures. It was also evident that the different buffers had differing effects upon the tissue, in particular calcium ions induced the loss of elasticity. Powell *et al.* [1982] and Tibbits *et al.* [1998] have both shown that calcium ions can affect PGA's and thus alter the physical properties of the pectin matrix and Greringer *et al.* [1995] have illustrated that calcium ions can

]

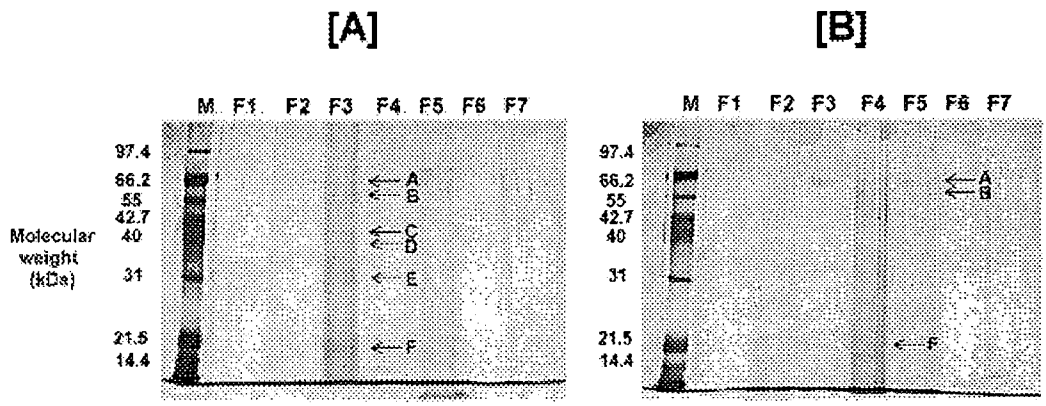

Figure 5.12

Analysis of bound fractions eluted from the auxin affinity column.

2x 5-ml volumes of ICF (see section 4.2.1) were recirculated through the auxin affinity column 3 times as described in section 4.6.3. Elution of bound material was achieved by changing the ionic concentration and buffer pH (gel A – elution method 1 in section 4.6.3) or specifically by supplementing the buffer with 10mM phenylacetic acid (gel B – elution method 2 in section 4.6.3). 1-ml fractions were collected, dialysed overnight against dH_2O and then lyophilised (see section 4.2.4). Lyophilised material was reconstituted with 10µl of SDS-PAGE sample buffer, subjected to SDS-PAGE (section 4.4.1) and the resultant gels were then silver stained (section 4.4.4) for polypeptide visualisation. The arrows indicate silver stained polypeptide bands.

disrupt electrostatic interactions between cell wall polysaccharides that ultimately alter the extensibility of the cell wall. The phenomenon observed here is presumably the gross, overall effect of these ions.

N-terminal sequencing of apoplastic polypeptides was very disappointing because of the low yield of sequence data generated. Three potential reasons could explain this low yield. Firstly, it was possible, in some cases, that there was simply not enough of the chosen polypeptide present in order to sequence. As a result, several attempts were made to overload ICF extracts and therefore elevate the quantity of material present on the subsequent sequencing blot, however, this did not appear to improve the sequencibility of any of the chosen polypeptides. The second possibility was that many of the polypeptides selected for sequencing were in fact composed of many polypeptides. Thus it would be impossible to obtain a sequence. To counter this various acrylamide gel compositions were tried in order to effect a better separation of the chosen polypeptides, unfortunately none of these appeared to improve the subsequent sequencing attempts. Therefore, N-terminal blockage appeared to be the only possible mechanism by which so many of these polypeptides were resistant to sequencing. Consequently, methods were adopted to minimise any N-terminal blockage caused during SDS-PAGE (see section 4.4.11); these also did not alter the subsequent sequencibility of the polypeptides. Therefore the conclusion was drawn that many VI extractable apoplastic proteins are N-terminally blocked.

However, from the successful sequencing runs that were undertaken some very interesting and significant results were obtained. Immature tobacco leaf tissue yielded an apoplastic polypeptide of 16.5 kDa with a 100% sequence homology to a germin-like protein found in arabidopsis. Germin is a known extracellular protein of barley [Lane 1988] that actively produces hydrogen peroxide in tight correlation with tissue growth and is essential for cell wall maturation [Lane *et al.* 1992]. It is possible that a similar process may occur in the expanding tobacco leaf. Interestingly, this sequence also shares a 100% homology with a 19 kDa ABP isolated from peach [Ohimya *et al.* 1998] and although the protein did not exhibit hydrogen peroxide generating activity, wheat germin is also known to contain an auxin-responsive element [Lane 1994]. This raises the possibility of an auxin-mediated control of cell wall elongation during growth in tobacco leaf.

Immature ICF also contained a polypeptide with a mass of 26 kDa and good homology (86%) to a 27 kDa thaumatin-like antifungal protein isolated from Diospyros texana [Vu & Huynh 1994]. The presence of this protein in immature tobacco leaf tissue is unknown.

Unfortunately, abiotically stressed plants yielded only polypeptides with N-terminal blockages, which may reflect the stress the plant has been subjected to, i.e.: oxidative

stress is a common phenomenon present in many types of stress (see section 1.5) and some oxidative species are known to induce the modification of the N-terminal region of animal proteins and polypeptides [Burcham & Kuham 1997] (see section 1.7). Coincidentally, the apoplast is also a known site of the production and release of oxidative species and this may explain why such a high level of N-terminal blockage was experienced during this study.

Standard ICF contained two polypeptides with polysaccharide and pectin related functioning, i.e.: they were extracellular matrix and cell wall related enzymes, not an unusual finding [Fry 1991]. Potential ABP's were again sequenced from ICF with molecular masses of 29.4 and 20.3 kDa; the latter corresponds to the molecular weight of an auxin-binding protein isolated from peach [Ohimya *et al.* 1998].

A surprising number of non-N-terminally-blocked proteins shared high homology with ABP's. Consequently, ICF preparations were subjected to chromatography through an auxin affinity matrix. Six proteins could be eluted from the affinity column with a simple change to the pH and ionic strength of the buffer. However, only three of these proteins were specifically eluted with an auxin supplemented washing buffer, thus indicating that these proteins were indeed *bona fide* ABP's. Unfortunately, there was not enough time to complete this study and obtain definite sequence confirmation that these proteins shared sequence homology with any known and characterised tobacco ABP's, but one of the putative ABP's was a 21 kDa polypeptide. A 20.3 kDa polypeptide was sequenced within this study (SICF9) that did share homology to an ABP, it is possible that these are true homologues of the same polypeptide and the slight difference in molecular mass can be accounted for by the day-to-day variation of the SDS-PAGE technique utilised in this study.

SECTION 6

THE DEVELOPMENT OF 2D ANALYSIS

6.1 Introduction

It was naively anticipated at the start of this part of the programme that 2-dimensional electrophoresis (2D) would be a relatively simple though highly resolving technique for the further separation of proteins and polypeptides observed on 1D gels (see section 5), in fact, the technique was deemed as an essential method of analysis primarily because it is the most powerful technique known for resolving complex protein mixtures [O'Farrell 1975; Ames & Nikaido 1976]. The resolution of a typical 2D-system is extremely high with the theoretical capability of separating individual polypeptides to homogeneity in one step, as a consequence small changes to the complement of the apoplast during stress and development could potentially be observed. For these reasons 2D analysis is rapidly becoming the method of choice for creating protein 'maps' or 'snapshots' of a particular tissue at a particular time point [Mollenkopf *et al.* 1999; Pardo *et al.* 1999; Yamaguchi & Pfeiffer 1999] and was therefore considered a useful tool for the study of the apoplast. A simple diagrammatic representation of a typical 2D-setup is presented in figure 6.1.

The most popular first dimension for 2D separations is polyacrylamide gel isoelectric focusing (PAG-IEF); this electrophoresis technique separates molecules based on their surface electrical charge. Two conditions must be met to effect an isoelectric separation of proteins and polypeptides: -

1. A pH gradient must be present in the gel, and,
2. The gel must not exhibit sieving properties.

The most common manner of establishing a pH gradient is the addition of 'carrier ampholytes' to a basic polyacrylamide gel mixture that contains no conducting species (i.e.: salts) and therefore has a very low ionic strength and poor ability to conduct current. Carrier ampholytes are comprised of hundreds of low molecular weight, polymeric and amphoteric species. When these compounds are exposed to an electrical field they migrate to their own isoelectric point (pI), at this position they are electrical neutral and therefore effectively do not migrate any further. Carrier ampholytes fulfil two crucial roles during isoelectric focusing, firstly they are very good conductors, and consequently are very effective at 'carrying' the current through the gel, secondly, they are very effective buffers, and thus they can establish a pH gradient once they have reached their isoelectric points.

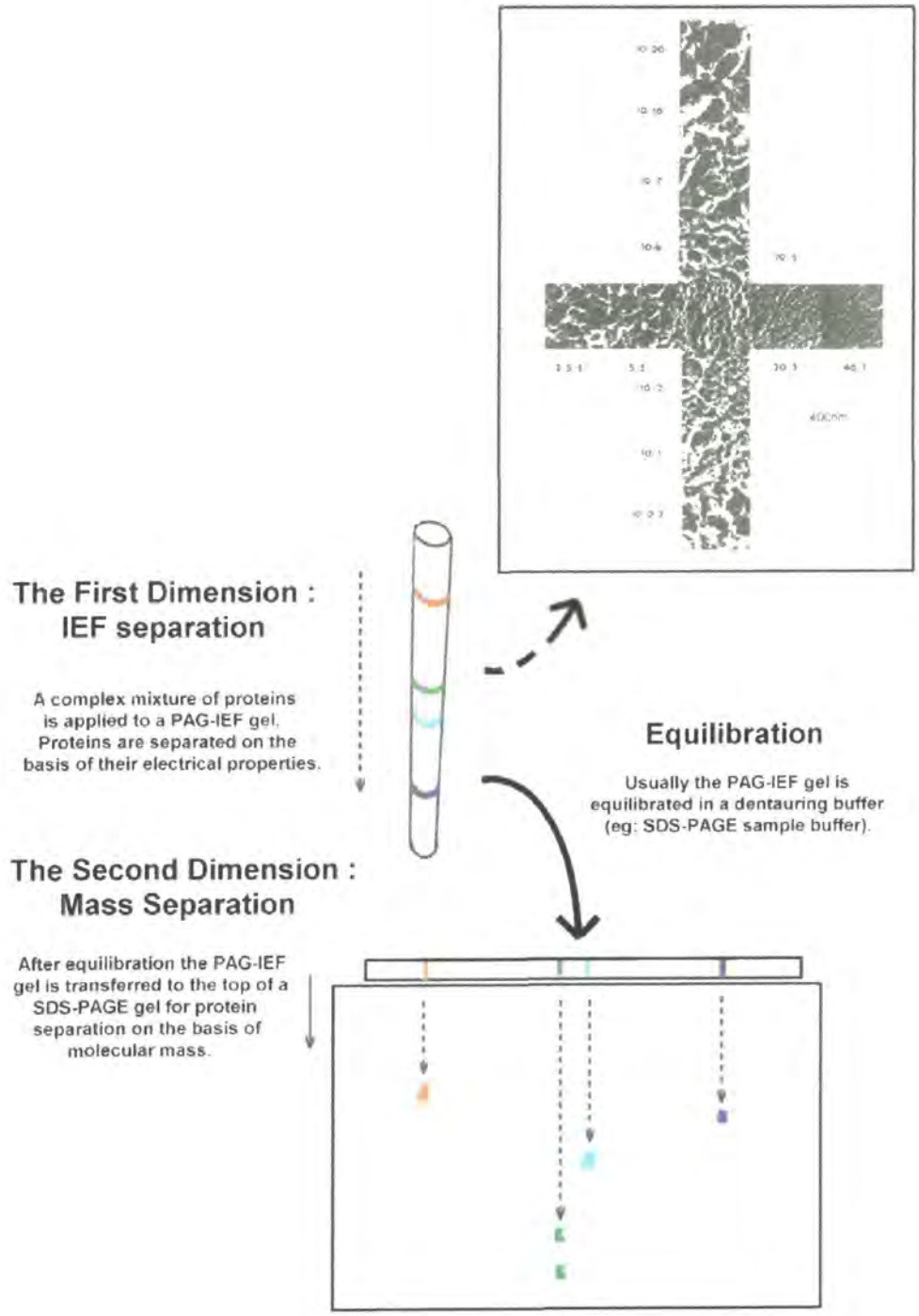

Figure 6.1

The principle of 2-dimensional electrophoresis.

See section 6.1 for details. Briefly, complex solutions of proteins and polypeptides are applied to an isoelectric focusing (IEF) gel and electrophoresed until the proteins have reached the pI's and they are stationary. The IEF gel is physically transferred to a denaturing SDS-PAGE gel and electrophoresed to further separate the proteins and polypeptides on the basis of their molecular mass. The inset image (top right) is derived from Rüchel *et al.* [1978] and illustrates the pore formation characteristics of varying combinations of T (total acrylamides)/C (cross-linker) in polyacrylamide gels.

The second major pre-requisite for effective PAG-IEF is a polyacrylamide gel that does not appreciably sieve proteins and consequently does not hinder the movement of proteins and polypeptides through the gel matrix. Polyacrylamide gels are typically composed of a bis-acrylamide crosslinker (C) and acrylamide that is catalytically polymerised to form a porous matrix, the ratio of crosslinker to total acrylamides (T) determines the pore forming characteristics of the resultant polymerised gel. The inset figure (6.1) shows a collage of electron microscope images of polyacrylamide gels. In the horizontal series, C remains constant and as T increases left to right, the gel exhibits decreasing pore size and hence increasing sieving properties. On the vertical bar, T remains constant but C is varied, a parabolic relationship is observed which reflects the known sieving properties of polyacrylamide gels [Rüchel and Brager 1975; Rüchel *et al.* 1978]. Polyacrylamide gels are therefore practically non-sieving when gels are either dilute, the lowest concentration possible is 2%T, 2.2%C, or contain high levels of cross-linker, (%C >25).

The combination of non-sieving polyacrylamide gel containing a carrier ampholyte based pH gradient will cause proteins or polypeptides to migrate unhindered through the pH gradient while they still have surface charge and cease migration when they reach electrical neutrality, i.e.: their pI. Ultimately, the stationary zone the protein or polypeptides occupy at their pI will represent a dynamic equilibrium between pI-directed electrophoretic migration and diffusion away from the focused zone. A common problem encountered during PAG-IEF is the isoelectric precipitation of proteins and polypeptides at or near their pI; that is caused because they have little or no electrical charge and are present in an environment almost bereft of ionic species. As a consequence, PAG-IEF can be performed under native or denaturing conditions, typically, native PAG-IEF (contains no denaturants or detergents) is used only with proteins that are highly soluble throughout an isoelectric focusing procedure. Denaturing PAG-IEF, is the more commonly employed version of PAG-IEF because most proteins have a tendency to precipitate at their pI; typically, non-ionic denaturants and detergents such as, urea and triton X-100, are utilised to maintain the solubility of these proteins and polypeptides during the isoelectric focusing run.

The diagrammatic outline of 2D presented in figure 6.1 illustrates that after PAG-IEF, the gel is equilibrated in a denaturing buffer, usually SDS-PAGE sample buffer. This incubation permits sodium dodecyl sulphate to penetrate the gel and bind to the separated proteins and polypeptides, and allows the reducing agent (i.e.: β-mercaptoethanol or dithiothreitol) to break any disulphide linkages. Commonly, denaturation was aided by pre-warming the SDS-PAGE buffer to 70-80°C prior to submerging the PAG-IEF. After equilibration the PAG-IEF was then loaded onto the top of

a SDS-PAGE and electrophoresed proteins and polypeptides that had been denatured in the equilibration step will now migrate into the SDS-PAGE gel and undergo separation based on their molecular mass. The highly resolving nature of this technique lies in the fact that proteins and polypeptides progress through two independent stages of separation; each stage separates based on completely different and individual physical properties of the proteins.

6.2 Results

6.2.1 Initial IEF trials

Effective use of 2D electrophoresis is highly dependent upon the reproducibility of banding patterns achieved during PAG-IEF, ultimately the spotting patterns observed on the resultant 2D 'protein map' must be superimposable between gels in order to accurately compare changes in the expression patterns of proteins. Consequently, a variety of PAG-IEF methods were evaluated early during this study to separate Pharmacia IEF marker proteins, test protein extracts, and ICF preparations. PAG-IEF gels of varying composition and formats were trailed, including, thin layer gels polymerised on microscope slides [Gorg *et al.* 1980], Pharmacia Multiphor immobilised pH gradient strips, a variety of horizontal and vertical slab and capillary tube systems [Tuszynski *et al.* 1979; Robertson *et al.* 1987; Baun *et al.* 1990]. All of these systems could effectively separate IEF markers and to some extent TE, but all invariably failed to effect an adequate separation of ICF's. One of the key problems experienced was that ICF's consistently formed a white precipitate after electrophoresis was started, which subsequently limited protein entry into the gel. This is a common phenomenon of certain protein mixtures (see sections 6.1 and 6.5) and has been traditionally circumvented by changing the sample preparation procedure prior to loading. Sample preparation procedures to remove contaminants that might induce precipitation [Granier 1988] and reduce IEF resolution were attempted but none succeeded effectively. Figure 6.2 shows the best PAG-IEF achieved during these trials; the technique used was an in-house adaptation of a vertical slab gel format system proposed by Robertson *et al.* [1987]. This gel was fairly representative of the PAG-IEF systems trialed, and indicated that ICF proteins do not enter the PAG-IEF; the poor entry of ICF-proteins and polypeptides in PAG-IEF gels was established as arising because of the rapid precipitation of ICF-proteins that was visually evident very soon after the current had been switched on (<10 minutes).

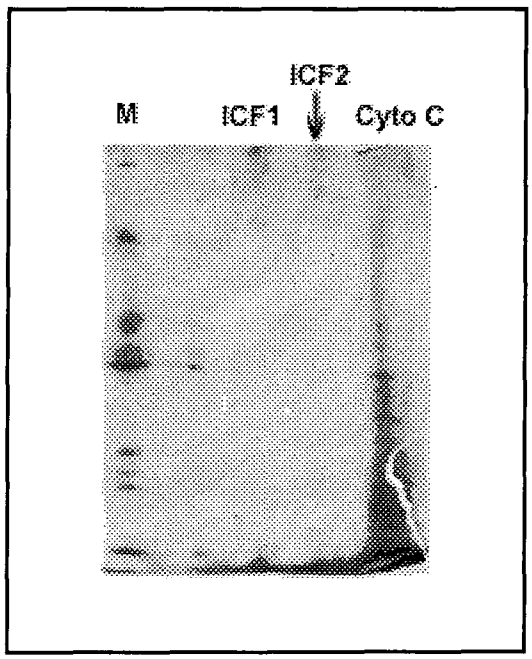

Figure 6.2

Typical example of an analysis of ICF using PAG-IEF in a slab format.

BioRad Mini-Protean vertical gel 8 x 7cm format was used. The gels were cast at a thickness of 0.75mm from the following mixture: 7ml deionised water (QH_2O), 2ml deionised acrylamide mixture (30%(w/v) acrylamide, 2% (w/v) bis-acrylamide), 2.4ml 50% glycerol and 0.6ml ampholytes (pH range 3-10). This mixture was degassed and polymerisation initiated by the addition of 50μl of 10% (w/v) ammonium persulphate and 20μl of TEMED, the gels were left to polymerise for 1 hour. The cathode solution was 25mM NaOH and the anode solution was 20mM acetic acid, both buffers were pre-chilled to 4°C prior to the electrophoresis. Samples and standards were prepared in a loading solution of final concentrations 30%(v/v) glycerol, 2%(v/v) ampholytes. Electrophoresis was conducted at a constant 200V for 1.5 hours followed by a further 1.5 hours at a constant 400V. After electrophoresis the gel was removed from the cassette and Coomassie stained (see section 4.4.3).

6.2.2 In-house adaptation of ESA Investigator™ 2D system

After several months of evaluation of many PAG-IEF systems without much success, the opportunity arose to visit the laboratory of ESA (Cambridge, UK), a commercial company specialising in 2D-electrophoresis systems. Separation of various age-related ICF's was achieved during this visit using the ESA-Investigator™ 2D system – the final 2D-protein 'maps' obtained are exhibited in figure 6.3. The ICF material was extracted (as described in section 4.2.1) from tobacco leaves that had been graded into the three distinct leaf 'ages'; young (number 1), mid (number 2) or old (number 3). It was immediately evident that at least some ICF proteins did actually enter the PAG-IEF gel and were successfully separated by this 2D-system furthermore, these 2D gels did illustrate the potential of this highly resolving technique to discern changes in apoplastic proteins and polypeptides, for example: -

1. Gp A, shows a triple spot pattern of proteins that does not seem to alter, at least qualitatively, as tobacco leaves age from young to old (figure 6.3 a-c).
2. B, illustrates a protein component that is either, lost or becomes unextractable from the apoplast as the tobacco leaf ages.
3. C, shows a new protein component apparently appearing during the mid-leaf age only.
4. A 'diffuse mass' that stains very heavily in the centre of all of the gels indicating that there is material in the sample that is present throughout leaf development that has heterogeneous charge spanning the pI range 5-8.
5. >60 polypeptide spots were visible in the youngest leaf tissue and this number drops to <30 in the oldest ICF extracts (figures 6.3 a-c)

However, even using this method it is evident that isoelectric focusing of many of the proteins and polypeptides had not reached the desired resolution; this was deduced because of the horizontal smearing present in the upper half of figure 6.3 (ICF 1) for example, and the general 'fuzzy' appearance of individual protein spots (see, 'B' or 'Gp A' on figure 6.3). This behaviour may be due to that fact that ICF material probably contains a range of glycoproteins with a wide degree of carbohydrate heterogeneity that would invariably lead to a wide degree of heterogeneity of isoelectric points as has been demonstrated previously for animal and plant derived glycoproteins [Dawes *et al.* 1994; Amoresano *et al.* 1999]. However, more disconcerting was that 400μg of ICF sample was required to produce each of the 2D gels presented in figure 6.3. The PAG-IEF sample preparation methodology used by ESA, included, acetone precipitation, denaturation with SDS and heat, and digestion of nucleic acids with nucleases (see section 4.5.2 for the full

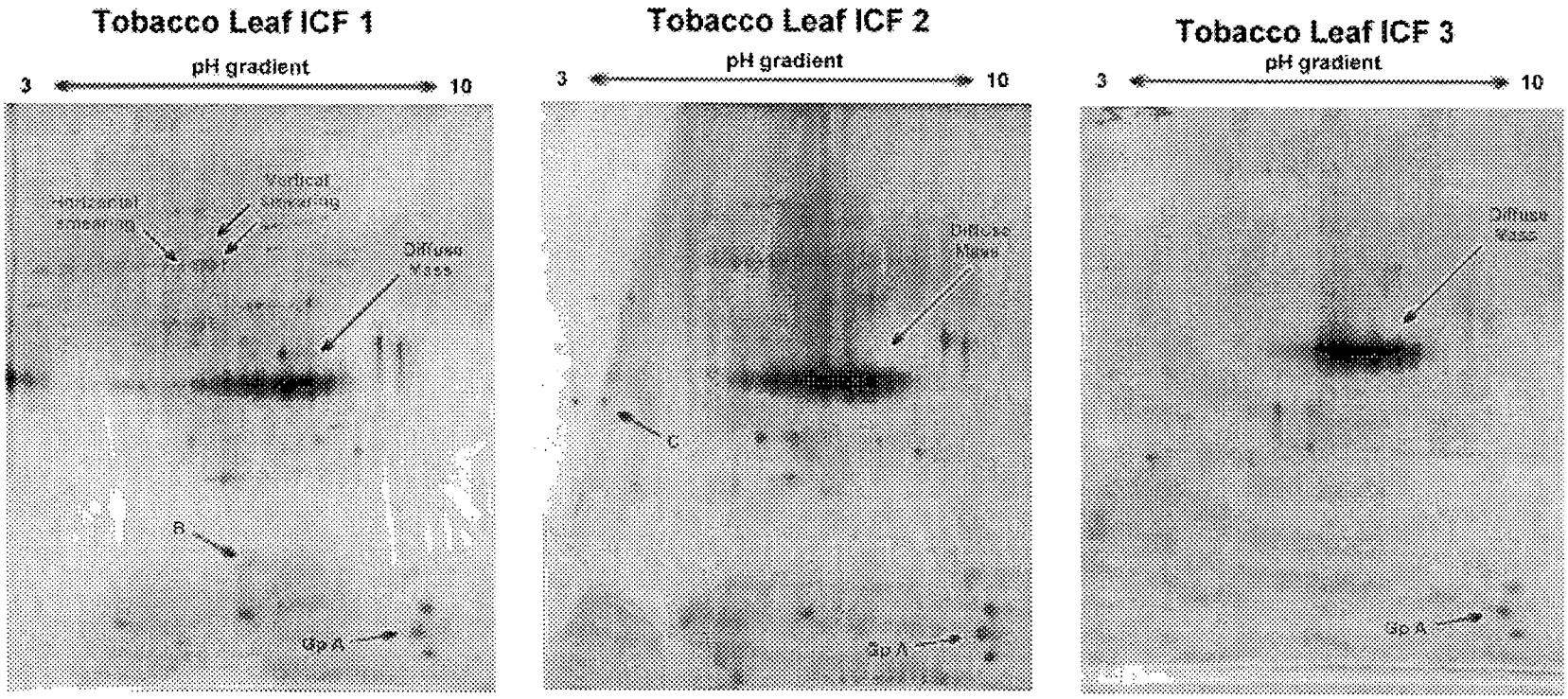

Figure 6.3

Analyses of ICF samples carried out in Cambridge using the ESA Investigator™ 2D electrophoresis system.

See section 6.3 for details. ICF's were recovered, dialysed and freeze-dried from leaves of different ages (see section 7.12 for details of leaf age determination). Briefly; 400μg of each ICF was reconstituted, processed and loaded onto an IEF pre-cast immobilised pH gradient gel; sample preparation was as described in section 4.5.2 except using ESA pre-prepared reagents. After IEF the gels were transferred to gradient pre-cast Duracryl SDS-PAGE gels and mass separated. All gels have been stained with the ESA pre-prepared silver staining kit; GpA = is a group of 3 proteins that are present in ICF throughout development; B= a protein that is apparently lost from ICF as leaves age; C= a new protein present as leaves age; Diffuse Mass = a dark staining area present throughout the leaf development series.

procedure) and despite this a considerable quantity of precipitation was still evident when the electrophoresis procedure was started. Presumably this material was proteinaecous in origin because it had undergone such a rigorous sample preparation procedure for the extraction of proteins for application to the isoelectric focusing gel. Furthermore, 400μg of protein and polypeptide material separated into individual polypeptide spots in the final 2D gel should have been easily visible with only Coomassie staining, however, in all cases silver staining had to be adopted and as can be seen in figure 6.3 some of the gels are relatively over developed. It was apparent therefore that only a very small percentage of the total polypeptide material present in the ICF extract had actually entered the PAG-IEF gel.

The ESA method provided by far the best 2D separations of ICF material and thus it was decided to adapt equipment and techniques at Durham to develop an in-house version of the ESA Investigator™ system. It was necessary to adapt equipment and techniques because the ESA Investigator™ system cost in excess of £6,500, and resources for such a purchase were not available. Unfortunately, equipment and consumables of identical specification were difficult to acquire and it took over 1 month before a suitable power pack, capillary tubing and tube gel electrophoresis kit could be gathered together. Wherever possible identical equipment and parameters were used but certain modifications had to be made from the original ESA set-up; some of the more obvious included: -

1. The dimensions of the capillary tubes used for PAG-IEF were different, consequently, voltage and current regimes had to be altered to effect similar separations.
2. PAG-IEF gels used by ESA were precast using an immobilised pH gradient, importantly at Durham the PAG-IEF gels were cast using mobile carrier ampholytes, therefore consideration had to be given to the possibility of cathodic drift and increased potential for isoelectric precipitation.
3. Differences in power pack supply settings had to be considered.

All of these factors and others ensured that the adaptation of the methodology was not a direct replication of the ESA system. This meant that a number of trials varying electrophoretic duration, voltage, and current regimes based on extrapolated voltage, current densities derived from the ESA methodology and a variety of gel compositions, and formats were necessary to achieve a comparable separation of proteins. In order to monitor the PAG-IEF Pharmacia IEF marker proteins and a control protein mixture derived from mitochondria (see section 4.5.4 for preparation details) were utilised to ensure that pH gradient formation was successful. The control protein mixture was used

in preference to ICF during the method development for a couple of reasons, primarily because there was an abundant supply of material and the extraction of ICF was extremely time consuming and labour intensive, and secondly because, the opportunity existed to separate this material for a publication. Typically, to speed up the method development marker proteins and the control protein mixture were only subjected to PAG-IEF, after which proteins were visualised by staining the PAG-IEF. Furthermore a trial to assess the relative PAG-IEF separations in a small-scale format (6.5 cm) and a large-scale format (15 cm) were also tested.

Figures 6.4 and 6.5 illustrate the isoelectric separation of the marker proteins and control protein mixture, respectively under optimised conditions (see section 4.5.6 for in-house optimised electrophoresis conditions). Concomitantly, both the large and small format PAG-IEF capillary tube gels were analysed. Both of these formats yielded very similar separation patterns for both the marker proteins and the major components of the control protein mixture. Switching to the small format PAG-IEF system had the added advantage of greatly reduced electrofocusing times thus enabling higher sample throughput, in this case focusing in the small format system was reduced by 10 hours. The graphs on each figure show the Rf of each marker component in either the small or the large format system, it is obvious that the two formats essentially effect the same protein separation patterns.

Figures 6.6 and 6.7 illustrate that the hardware and conditions used in the ESA Investigator™ system were successfully adapted using in-house equipment and altered methodology, in both large and small scale formats. The pattern of proteins was extremely reproducible in both the large and small format systems, as illustrated by the comparison of protein separation in each (figures 6.6 and 6.7). The large format system does afford much better resolution but takes over 25 hours (including staining time) to complete a single gel, whereas, the loss of resolution observed in the small format system was to an extent compensated for by the greatly reduced running time, <10 hours (including staining time) for these particular gels. These images and the resulting antibody probed blots were presented at an international conference [see Memorandum, page v; Bowler *et al.* 1998].

Once again however, precipitation soon after electrophoresis had started was observed when attempting to run ICF in this adapted ESA system. Consequently, several variations of sample preparation were trialed (see sections 4.5.1, 4.5.2 and 4.5.3 for 2D sample preparation protocols), unfortunately, none yielded results because of the recurrent problem of polypeptide precipitation. Figure 6.8 is exemplary of the small format 2D gels obtained from ICF using this in-house adapted ESA system. The gel was greatly over stained to illustrate that very little protein or polypeptide material is actually present in the

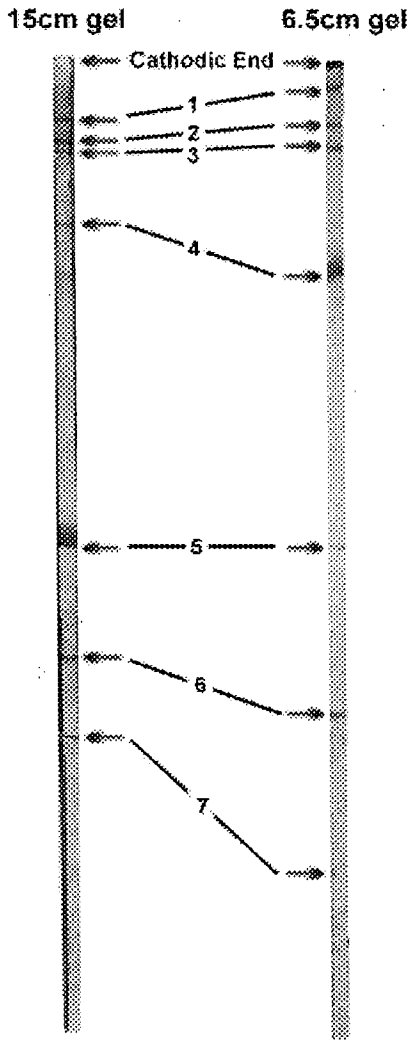

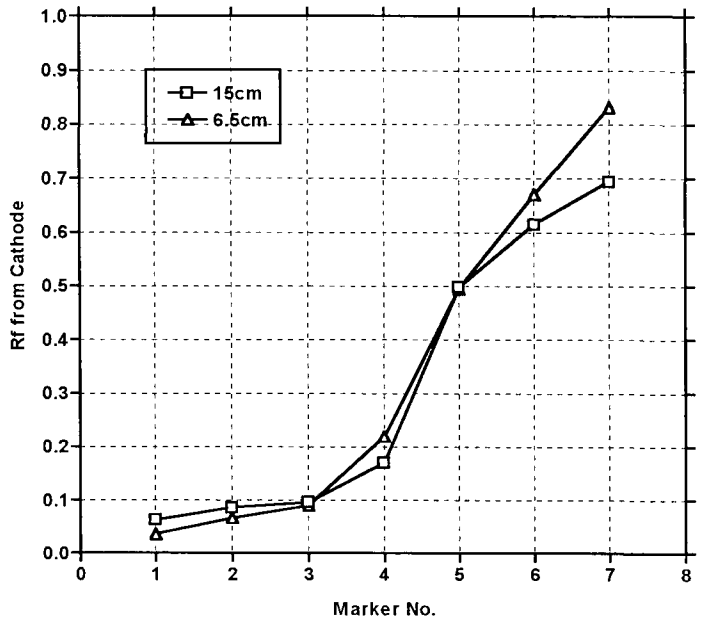

Figure 6.4

IEF using marker proteins.

1x 15cm and 1x 6.5cm capillary tube PAG-IEF gels (composition and electrofocusing conditions are detailed in section 4.5.6), were loaded with a 10μl aliquot of Pharmacia pI markers. After electrophoresis gels were extruded and stained with coomassie blue to visualise bands (see section 4.4.3). The relative mobility (Rf) was calculated for each protein and is plotted on the graph.

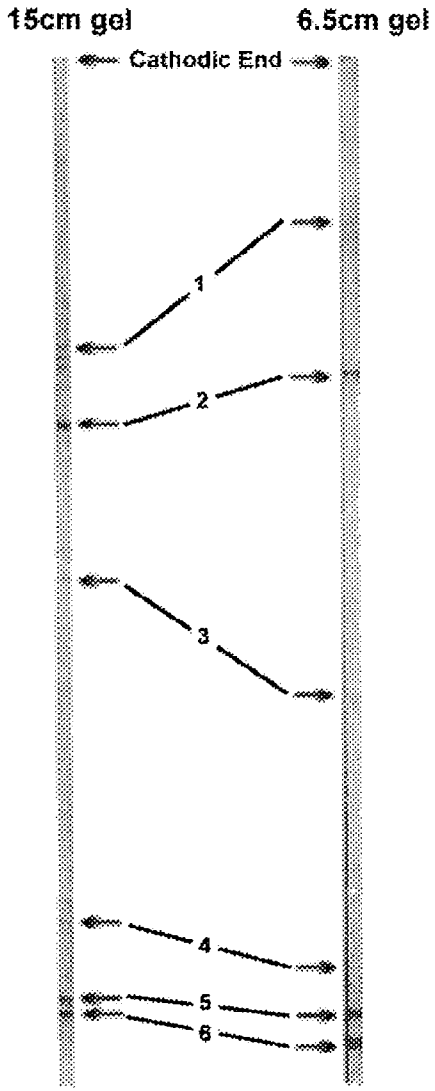

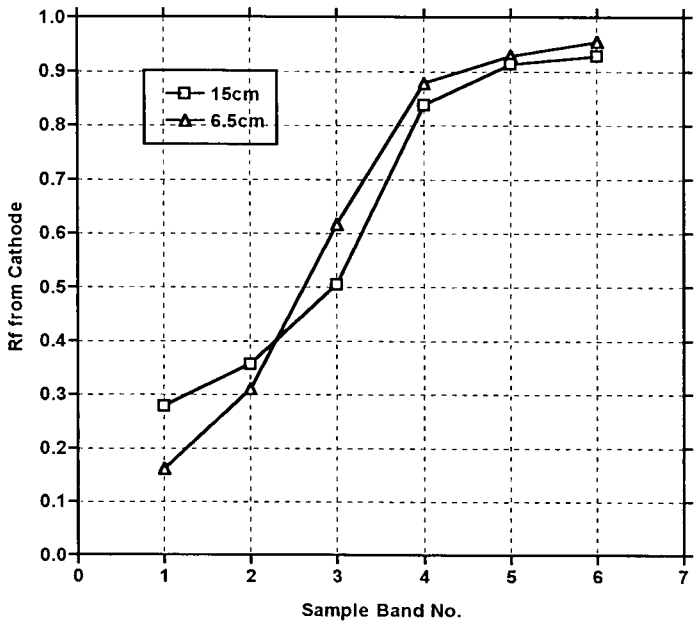

Figure 6.5

IEF using control mitochondrial proteins.

1x 15cm and 1x 6.5cm capillary tube PAG-IEF gels (composition and electrofocusing conditions are detailed in section 4.5.6), were loaded with a 50μl aliquot of control mitochondrial protein mixture (see section 4.5.4). After electrophoresis gels were extruded and stained with coomassie blue to visualise bands (see section 4.4.3). The relative mobility (Rf) was calculated for each major protein band and is plotted on the graph.

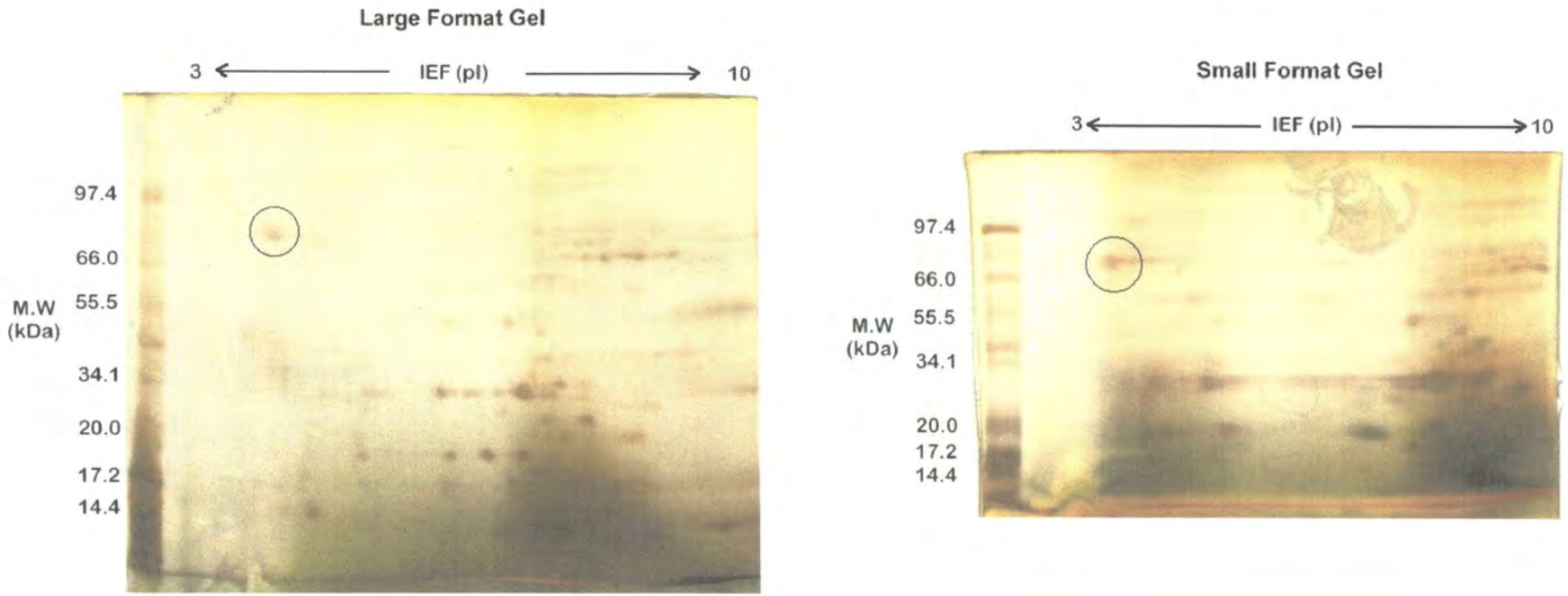

Figure 6.6

630µg loading of control mitochondrial proteins separated on large and small format 2D system.

100µl of a 42mg/ml solution of mitochondrial proteins (section 4.5.4) was prepared for IEF as described in section 4.5.2; the final pellet was resuspended in 100µl of IEF loading buffer. 15µl of this solution (630µg) was loaded onto a 15cm or a 6.5cm long IEF gel and focused for 17.5 and 7.5 hours, respectively (see section 4.5.6 for full protocol). After electrophoresis the IEF gels were extruded from their capillary tubes into SDS-PAGE sample buffer, equilibrated for 5 minutes and then loaded onto a large format SDS-PAGE gel (12%, 1.5mm thick) or a small format SDS-PAGE gel (12%, 1.5mm thick) and electrophoresed. After electrophoresis the gels were silver stained (section 4.4.4). Note: the circle on each image relates to the publication, Bowler *et al.* [1998].

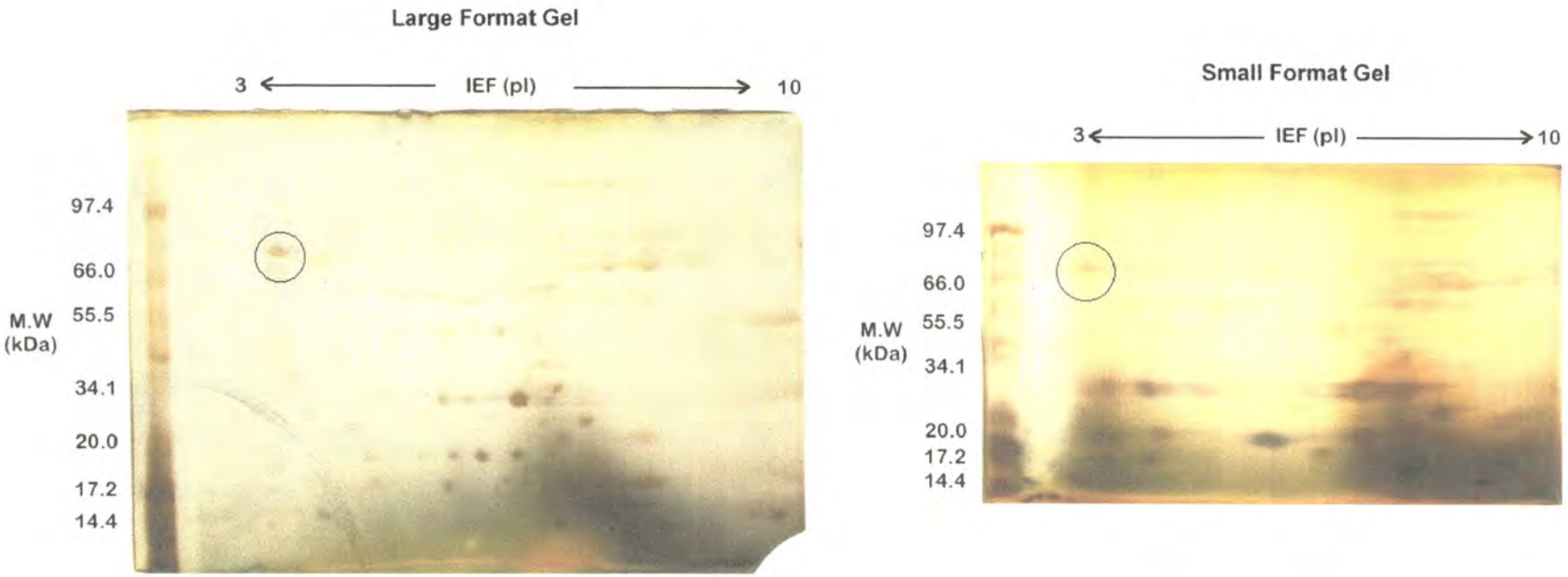

Figure 6.7

630µg loading of heat shocked mitochondrial proteins separated on small and large format 2D system.

100µl of a 42mg/ml solution of heat shocked mitochondrial proteins (see section 4.5.4) was prepared for IEF as described in section 4.5.2; the final pellet was resuspended in 100µl of IEF loading buffer. 15µl of this solution (630µg) was loaded onto a 15cm or a 6.5cm long IEF gel and focused for 17.5 and 7.5 hours, respectively (see section 4.5.6 for full protocol). After electrophoresis the IEF gels were extruded from their capillary tubes into SDS-PAGE sample buffer, equilibrated for 5 minutes and then loaded onto a large format SDS-PAGE gel (12%, 1.5mm thick) or a small format SDS-PAGE gel (12%, 1.5mm thick) and electrophoresed. After electrophoresis the gels were silver stained (section 4.4.4). Note: the circle on each image relates to the publication, Bowler *et al.* [1998].

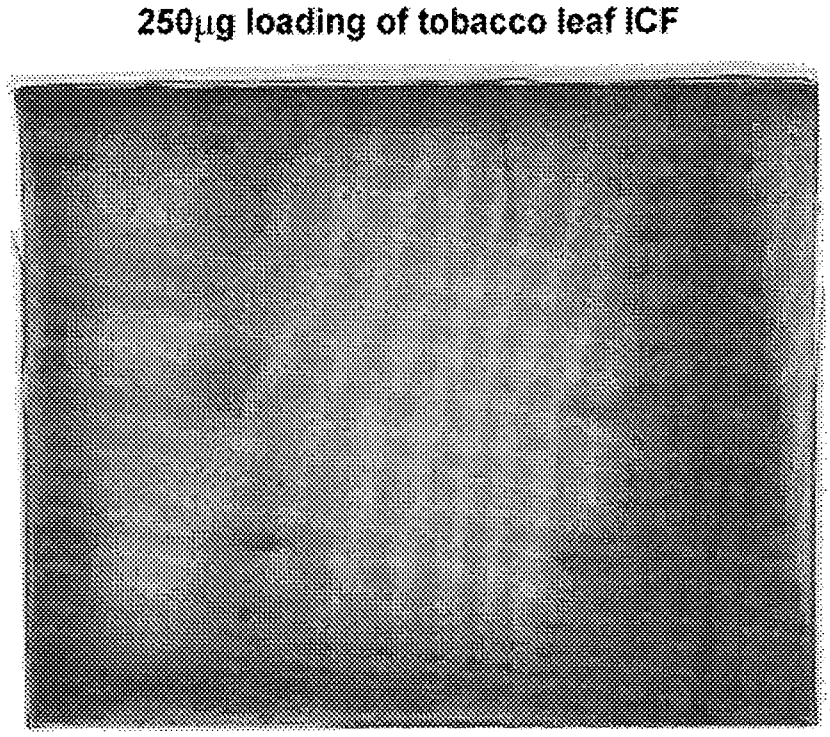

Figure 6.8

ICF proteins separated on a small format 2D system

250µg of freeze-dried ICF was reconstituted and processed according to ESA methodology (see section 4.5.2 and 6.3). The protein solution was applied to a 6.5cm long PAG-IEF gel in a 20µl volume of IEF loading buffer. Focusing was 'achieved' by applying the voltage/current regime detailed in section 4.5.6 for 7.5hours, after which the gel was extruded into SDS-PAGE sample loading buffer and equilibrated for 5 minutes. The IEF gel was then loaded onto the top of a small format SDS-PAGE gel (12%, 1.5mm thick), electrophoresed. After electrophoresis the gels were silver stained (section 4.4.4). (For information, the cathodic end IEF is on the left-hand side of the slab gel).

second dimension gel. After several abortive weeks this methodology was abandoned because of the lack of progress.

6.2.3 In-house adaptation of the Barent & Elthon 2D system

During a survey of the literature a report of a rapid, small format capillary tube PAG-IEF and SDS-PAGE 2D system was found [Barent & Elthon 1992], this technique was adapted to the equipment available at Durham. Simultaneously the use of more subtle ways to follow the formation and maintenance of the pH gradient during PAG-IEF were used. Mixtures of coloured markers were developed which consisted of a combination of methyl red (pI~3), myoglobin (pI~7) and cytochrome C (pI~9.5) (see section 4.5.5 for preparation details). Figure 6.9 illustrates the use of such coloured markers during the optimisation of the Barent & Elthon adapted PAG-IEF method. The markers were invaluable, as it was much easier to view the location of a coloured marker in a glass capillary tube and thus actually 'view' the gradient forming. To confirm the visual data, capillary gels were routinely extruded and divided into 9 x 0.5cm segments, in triplicate, and placed into deionised water and after a set incubation period direct pH readings were taken. Figure 6.10 shows the pH readings displayed above each of the exhibited capillary gels. Figure 6.10 shows the same data plotted against time and confirms that the pH gradient in the system is rapidly lost after the first hour. The use of these two methods to view and monitor the formation of the pH gradient greatly sped up the trials of ampholyte composition, alteration of the anodic and cathodic buffer systems and changes to the duration of isoelectric focusing undertaken to optimise the system.

Figure 6.11 illustrates pH data generated as described above in the final optimised system (see section 4.5.7 for details of the final optimised method). Alteration to the range and ratio of ampholytes greatly reduced the pH gradient breakdown and ensured that the pH gradient is fully established within 1 hour and is maintained until 3 hours. The final isoelectric focusing run time was set at 2 hours and an example of mitochondrial control protein mixture run under these conditions is illustrated in gel A, figure 6.13. Separation was good and reproducible as judged by comparison with gel B; the whole 2D technique was extremely rapid. The gels in figure 6.12 were completed in less than 4.5 hours, including the 1-hour polymerisation time for the PAG-IEF gel. Gel A also exhibited a problem found throughout the development of all 2D methods that utilised mobile carrier ampholytes, 'ampholyte smear'. This is caused by the migration and intense staining of ampholytes with pI's>7 into the SDS-PAGE gel. Barent & Elthon [1992] also detailed an efficient ampholyte-removal step that can be applied to either the PAG-IEF gel prior to loading onto the SDS-PAGE gel or, to the SDS-PAGE gel prior to staining. Gel B figure 6.12 illustrates how the ampholytes can be selectively removed from a SDS-PAGE gel with a simple 5-minute wash with an, 'ampholyte removal solution' (see section 4.5.8) -

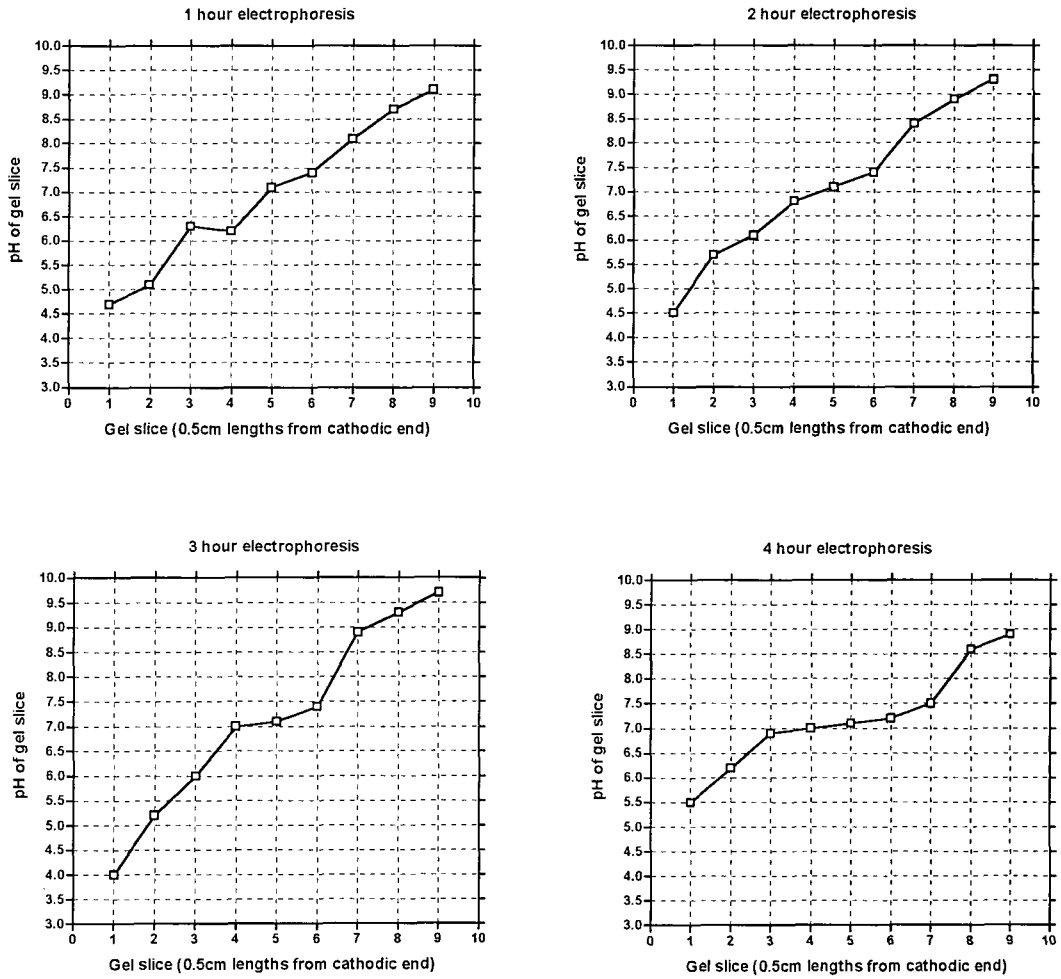

Figure 6.11

Alteration of the gel composition and ampholytes of the small format IEF and the effect on pH gradient formation.

Twelve 5cm IEF gels were loaded with 15μl volumes of a mixture of coloured pI markers, see section 4.5.5 for preparation details. IEF was conducted as described in the legend that accompanies figure 6.10, but the gel composition and buffer system were adjusted (see section 6.2.3 for details). At the specified time-point electrophoresis was stopped and each group of 3 gels were then extruded, scanned, divided into 9 pieces, each 0.55cm in length, placed into 1.5-ml of QH_2O and incubated for 2hours. After incubation the gel piece was removed and the pH of each of the resultant solutions was measured, the data is presented on the graphs above.

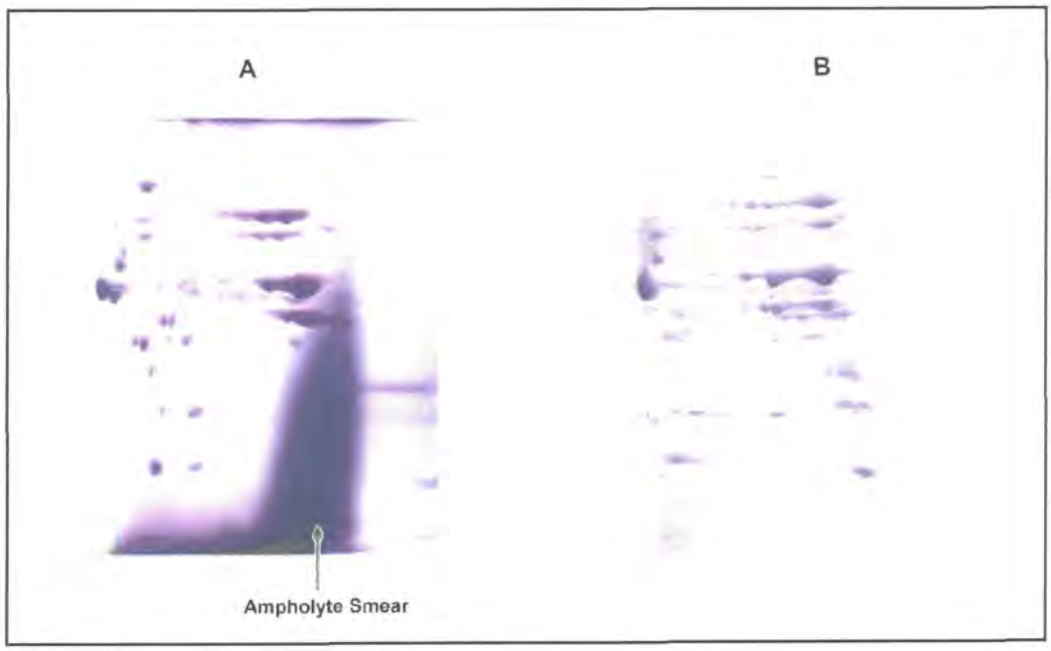

Figure 6.12

Removal of the ampholyte 'smear'.

Gel A = 300µg of control mitochondrial proteins was electrophoresed in the following sequence: 10minutes at 100V max.; 10minutes at 250V; 100minutes at 400V through a 5cm IEF gel using the altered electrode buffer system and gel composition (see section 6.4) and then subjected to small format SDS-PAGE (12%, 1.5mm thick). Gel B = 200µg of control mitochondrial proteins was electrophoresed in the following sequence: 10minutes at 100V max.; 10minutes at 250V; 100minutes at 400V through a 5cm IEF gel using the altered electrode buffer system and gel composition (see section 6.4) and then subjected to small format SDS-PAGE (12%, 1.5mm thick). Gel A was immediately Coomassie stained (section 4.4.3); Gel B was treated with the, 'ampholyte removal solution' (see section 4.5.8 and 6.4) and then Coomassie stained in the usual manner (see section 4.4.3).

the resultant stained gel of control mitochondrial protein mixture revealed an additional number of previously obscured proteins.

Several attempts were made to separate ICF using this methodology (section 4.5.7) preparing the sample using the intricate ESA acetone based sample preparation methodology that had given reasonable results in section 6.3 (see section 4.5.2). Unfortunately, precipitate was obvious and no 2-D pattern was produced, see figure 6.13, gel A. A variety of other sample preparation methods were attempted (see sections 4.5.1 and 4.5.3 for 2-D sample preparation protocols), but again all failed apparently due to excessive precipitation of proteins, figure 6.13, gels B & C show examples.

A new loading strategy was devised after consultation with the authors of the Barent & Elthon paper. The strategy was unusual in that the sample was incorporated directly in the gel mixture prior to polymerisation. This strategy worked exceptionally well for the control protein mixture and enabled the isoelectric focusing of up to 500μg of protein material. Also this strategy did yield a protein pattern for ICF, see figure 6.14 – but not what was expected. It was noticeable that ICF protein or other components loaded in this manner still precipitated out in the gel during electrophoresis and effectively turned the gel white.

6.3 Conclusions

A significant number of IEF systems were tried initially, but it was found to be extremely difficult to get a PAG-IEF system to work reproducible when separating ICF material. Throughout the method development of 2D undertaken during this research project the ability to effectively monitor the formation of the pH gradient during PAG-IEF had been the limiting step. Consequently, methods to directly monitor the gradient were devised and rapidly speeded up progress towards the eventual development of two 2D systems each with their own unique merits. The ESA adapted system yielded excellent 2D separations of mitochondrial proteins good enough to be presented at an international conference [see memordandum; Bowler *et al.* 1998]. Furthermore, scaling down the procedure proved useful for the development of a rapid throughput 2D system that could yield protein 'maps' within 1 day. The second 2D system that was developed was based upon a similar small scale system described by Barent & Elthon [1992] and after trials a unique in-gel loading strategy was undertaken that could separate upto 500μg of polypeptide material in a single gel (data not shown). This potentially opens up the possibility of traditional N-terminal sequencing from 2D blots.

Unfortunately, good reproducible separation of ICF material was never achieved within the time constraints of the project primarily because of the constant problems with

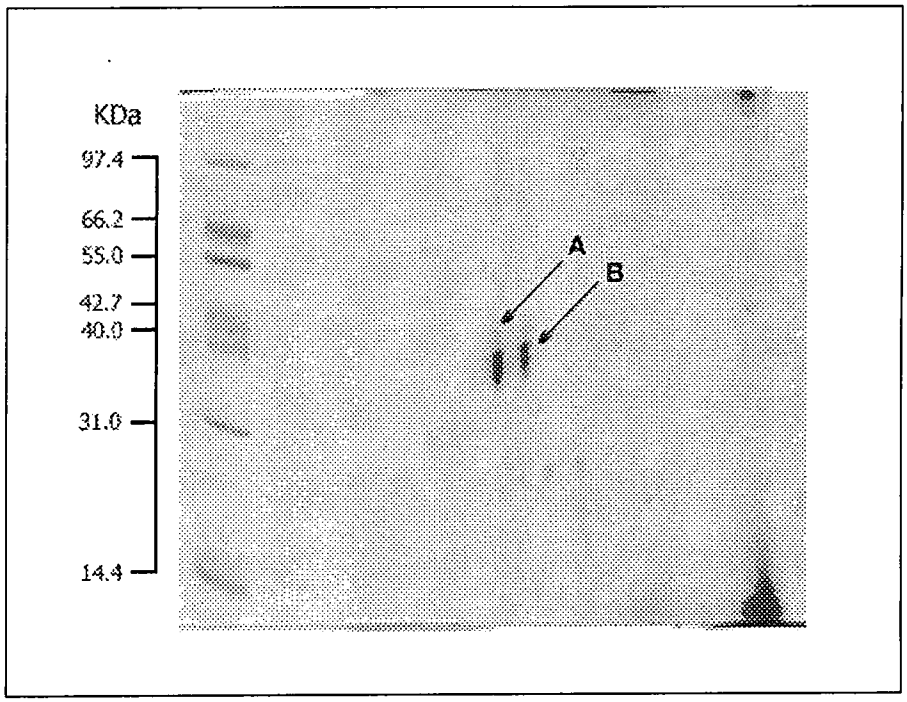

Figure 6.14

Separation of ICF using an in-gel loading strategy.

150μg of freeze-dried ICF was reconstituted in IEF gel mixture; the gel/sample mixture was briefly microfuged to pellet any precipitate and the supernatent collected. The gel was polymerised by the addition of ammonium persulphate. The normal 2-D separation protocol was followed (see sections 4.5.8 and 6.4) and the resulting gel was Coomassie stained (see section 4.4.3).

precipitation of ICF components. However, even the best separations achieved using the ESA Investigator™ 2D-system exhibited quite marked precipitation, horizontal smearing and 'fuzzy' protein spotting patterns, this can presumably be explained by the heterogeneous nature of the glycoprotein materials extracted from the apoplast and/or the presence of potentially heterogeneous contaminants such as phenolic compounds and carbohydrate material [Fry 1991; Dawes *et al.* 1994; Dietz *et al.* 1997]. The constant and rapid precipitation of ICF in an isoelectric focusing system is evidently a feature of plant apoplastic proteins and polypeptides and presumably belies the ionically rich environment that this material normal resides in, isolation into an *ionically poor* buffer coupled with huge heterogeneity in charge may go someway to explain the precipitous behaviour of these proteins during PAG-IEF.

SECTION 7

APOPLASTIC ANTI-AOS ENZYMES

7.1 Introduction

Active oxygen species (AOS) include the superoxide anion ($^{\cdot}O_2^-$), hydrogen peroxide (H_2O_2) and the hydroxyl radical ($^{\cdot}OH$). These molecules are the highly reactive and consequently very deleterious by-products of aerobic respiration and photosynthesis [Richter 1995]; see section 1.5 for more detail. The intracellular environment contains anti-AOS defences (see table 1.6) that can absorb the oxidative potential of AOS (ubiquinol, vitamin E, etc) and a range of enzymes that can catalytically convert AOS (superoxide dismutase, etc), these defences provide effective protection against intracellular AOS.

It may therefore be surprising to find, that AOS are also biologically useful molecules that are deliberately generated and released into the apoplast during particular developmental stages in order to oxidatively couple cell wall polymers and proteins [Canny 1995; Dietz 1997] and in response to pathogen attack because of their anti microbial activity [Chen *et al.* 1994; Bergmann *et al.* 1994; Broekaert *et al.* 1995; Brisson *et al.* 1994]. Surprisingly, abiotic stress such as, temperature [Marentes *et al.* 1993], wounding [Bradley *et al.* 1992; Bergmann *et al.* 1994], drought [Covarrubias *et al.* 1995], and toxic chemicals [Brune *et al.* 1994; Blinda *et al.* 1997] are all known to elevate the levels of AOS, a similar elevation has also been observed during ageing and senescence of plant tissue [Rogiers *et al.* 1998]. The exact mechanisms for abiotic- and age-related elevation of AOS have not yet been elucidated.

The observable presence of AOS in the leaf apoplast is proposed to occur via one or a combination of three independent processes (see figure 1.6 and section 1.5 for an overview): -

1. The action of an NADPH-oxidase complex regulated from the cytosol [Sutherland 1991; Vera-Estrella *et al.* 1992; Scheel 1998].
2. The action of apoplastic and cell wall peroxidases and oxidases [Lane 1994; Wojataszek *et al.* 1997; Fry *et al.* 1998; Schweikert *et al.* 2000].
3. A general age-related decline in anti-AOS defences that would ordinarily remove any AOS present [Rogiers *et al.* 1998].

In addition to being the site of AOS accumulation the apoplast also contains a range of anti-AOS defences presumably to manage levels of AOS; these include antioxidant compounds, such as, glutathione, ascorbate, polysaccharides and phenolic compounds and a suite of enzymes that can directly metabolise AOS's such as catalases, peroxidases and superoxide dismutases (see table 1.6 and section 1.5). Unfortunately, relatively little information is known about the occurrence and action of apoplastic anti-AOS enzymes and in fact until very recently many had been considered to be purely intracellular, for example, superoxide dismutase [McCord & Fridovich 1969; Vanacker *et al.* 1998]. As a consequence, of the scant literature concerning the anti-AOS enzymes present in the apoplast it was a relatively logical extension of this research project to further investigate these enzymes.

The superoxide dismutases (SOD's) are the only known enzymes that can dismutate the superoxide anion, therefore reducing the potential for the generation of the more deleterious, hydroxyl radical [McCord & Fridovich 1969]. All SOD's have been characterised into one of three groups depending upon which metal ion they co-ordinate. The most primitive form of SOD contains an iron ion (Fe-SOD) or a manganese ion (Mn-SOD), and are typically found in bacteria, algae, mitochondria and therefore, of course, in plant and animal cells. More recently evolved forms of SOD containing the metal ions, copper and zinc (CuZn-SOD) have been located to the chloroplast and cytosol [reviewed in Bannister *et al.* 1987]. SOD was, until relatively recently, considered to be purely an intracellular enzyme, until the discovery of its ubiquitous distribution in the animal extracellular matrix [Strålin *et al.* 1995] and the recent localisation of CuZn-SOD to the plant apoplast [Streller & Wingsle 1994]. This new information has lead to a re-evaluation of the roles of SOD's in both animals [Strålin *et al.* 1995] and plants [Streller & Wingsle 1994; Ogawa *et al.* 1996].

Peroxidases (POD's) are ubiquitous throughout the primary cell walls of all higher plants and are often expressed in a tissue-specific, developmental- and stress-related manner. Therefore, they are frequently implicated in differentiation, pathogen resistance and wound response [Rao *et al.* 1990; Cordewener *et al.* 1991]. POD enzymatic action is integral to apoplastic integrity, development and intercellular signalling [Mader 1980; Fry 1986]. It is also clear that apoplastic POD activity rises in response to virtually all abiotic and biotic stress [Dietz 1997] indicating major roles for POD in stress responses and anti-AOS defence. POD's can be classified as either cyanide-sensitive (Fe-POD's) or -insensitive (Se-POD's) depending upon their reaction to the cyanide ion [Rob *et al.* 1997].

The primary aim in this part of the study was to positively and unequivocally identify apoplastic SOD's, POD's and catalases, preferably by N-terminal sequencing and homology searching. A range of convenient, native-PAGE in-gel assays, specific for each of the anti-AOS enzyme groups of interest was utilised to locate bands with activity. These methods were a rapid way to partially purify and simultaneously identify components within relatively complex apoplastic extracts with anti-AOS enzyme activity. Once bands of activity had been identified, characterisation was attempted using SDS-PAGE, enzyme inhibition studies and N-terminal sequencing.

7.1.2 Notes on Experimental Design

Figures 7.1, 7.2 and 7.6 illustrate enzyme activity staining in native-PAGE gels for the enzymes catalase, peroxidase (POD) and superoxide dismutase (SOD), respectively. Materials for the gel analyses were prepared in native sample buffer and extracts applied to the wells of native-PAGE gels (see section 4.4.2), after which the gel was removed from the cassette and submerged in the appropriate staining solution until stained to the desired intensity (see sections 4.4.5-7). Gels were then scanned using a flat bed scanner attached to a PC. Initial trials with SOD and POD stains revealed that the two procedures could be applied to a single gel providing that the gel was washed for >3 minutes in pure water between staining procedures.

Three independent physical properties, electrical charge, overall mass, and the shape of the native protein dictate how they migrate in such an electrophoresis system. As such, it is difficult to assign unequivocally physical characteristics to individual bands separated in native-PAGE systems; however, it is possible to make broad and simplistic generalisations. Small proteins with high pI's will tend to migrate further down the gel towards the cathode, while on the other hand, larger proteins with more acidic pI's will either not enter the gel or will not progress very far.

In sections 7.8 and 7.9 attempts were made to assign molecular weights to components that had specific enzyme activities. A number of trial attempts were made to elucidate the most effective way of removing an enzymatically active band from a native-PAGE gel and to transfer it to denaturing system (data not shown) in order to perform SDS-PAGE and subsequent mass estimation. Eventually a similar method to that of 2-dimensional electrophoresis was chosen; bands were excised and incubated for 5 minutes in warmed denaturing SDS-PAGE sample buffer, loaded on the top of a denaturing separating gel, overlaid with more SDS-PAGE sample buffer and then electrophoresed.

Comparison of in gel POD and SOD enzyme assays of TE and ICF samples (i.e.: figures 7.2 and 7.5, but also throughout section 7), illustrated either a potential overlap between the anti-AOS enzymes present in the apoplast and the intracellular environment or a degree of contamination. Both are possible explanations, but it should be noted that VI is not a perfect separation technique for the isolation of pure and uncontaminated apoplastic protein material and it will always have the potential to contain some degree of intracellular contamination. What can be said is that VI, although not ideal, does selectively and preferentially concentrate apoplastic material in relation to intracellular contaminants. As such, subsequent in gel enzyme activity analysis should be viewed as a qualitative assessment of the existence of unique extracellular POD's and SOD's and quantitative judgement should only be made with great care.

7.2 Results

7.2.1 Attempted detection of apoplastic catalase

Figure 7.1 (gel A) illustrates that control enzyme (commercially available catalase - Sigma, UK) can be detected as a yellow to pale blue band on a dark blue background at the bottom of a native gel. Unfortunately, catalase from tobacco leaf TE's could not be identified on the same gel. This was assumed to be due to the extremely dark blue background staining that may have masked any pale blue to yellow bands of enzyme activity. Consequently, the concentration of the enzyme substrate, hydrogen peroxide, was reduced from 3% (v/v) to 0.3% (v/v) in order to decrease the level of dark blue background staining, the result is illustrated in figure 7.1, gel B.

Gel B shows that alteration of the concentration of the substrate did improve the overall clarity of the detection system, as indicated by the improved resolution of the control enzyme, but still no catalase could be readily identified in TE or ICF preparations. A number of possibilities can be thought of to explain this negative result; catalase may have never entered the gel; it is possible that catalase has strong ionic interactions with the plant cell wall and the infiltration buffer was not of sufficient ionic strength to break the interactions; it is also possible, that the sample preparation procedure of extensive dialysis and lyophilisation had inactivated any catalase enzyme present in the ICF. Therefore, this assay was not developed further within this study.

7.2.2 Detection and optimisation of separation of apoplastic POD's

Staining for POD enzymes capable of utilising the artificial POD substrate guaiacol was much more fruitful (see figure 7.2, gels A and B). The control enzyme (commercially

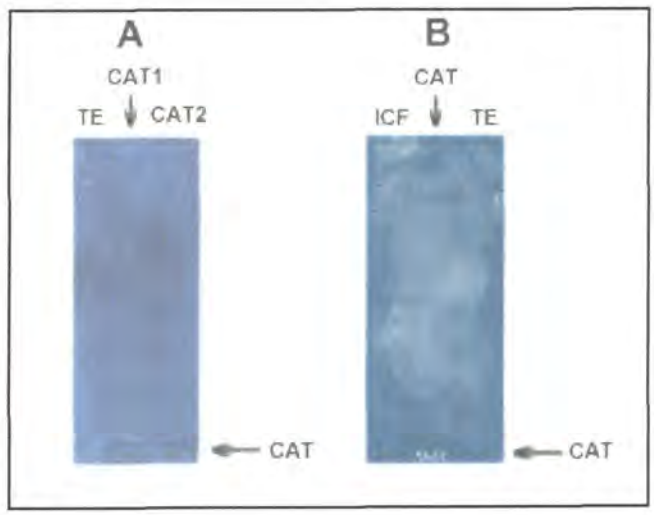

Figure 7.1

Assay of catalase enzyme activity of control catalase enzyme, TE and ICF in native-PAGE gels.

TE and ICF were prepared as described in sections 4.2.3 and 4.2.1, respectively. Both gels were 10% (w/v) native-PAGE gels and samples were prepared in native PAGE sample buffer (see section 4.4.2). The quantities quoted refer to either Bradford quantified protein concentration or quantities of protein/enzyme activity was derived from the information from the commercial supplier (control POD enzyme – Sigma, UK). Gel A was loaded as follows; TE = 35µg of total extract; CAT1 = 89.55 U (45µg) of control enzyme; CAT2 = 29.85 U (15µg) of control enzyme; and assayed at a substrate concentration of 3% (v/v). Gel B was loaded as follows; ICF = 35µg of sodium chloride extract ICF; CAT = 17.91 U (9µg) of control enzyme; TE = 35µg of total extract; and assayed at a substrate concentration of 0.3% (v/v). See section 4.4.5 for a detailed description of the catalase staining technique.

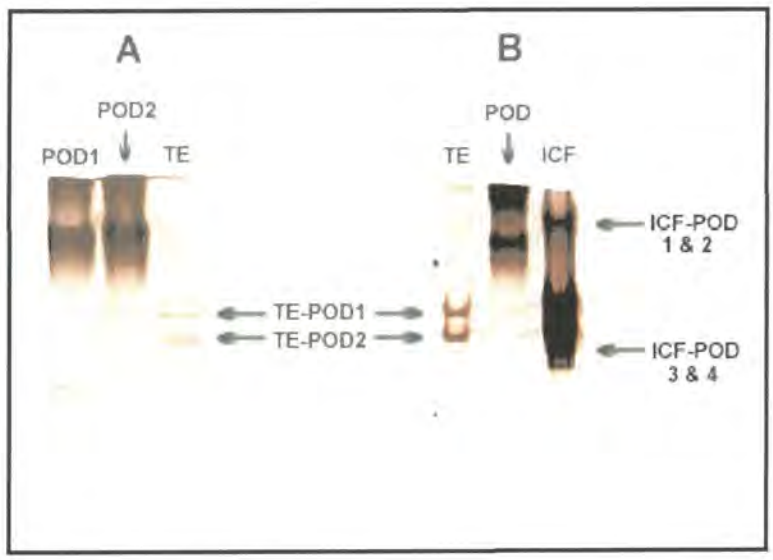

Figure 7.2

Assay of peroxidase enzyme activity of control peroxidase enzyme, TE and ICF in native-PAGE gels.

TE and ICF were prepared as described in sections 4.2.3 and 4.2.1, respectively. Both gels were 10% native PAGE gels and samples were prepared in native PAGE sample buffer (see section 4.4.2). The quantities quoted refer to either Bradford quantified protein concentration or quantity of protein/enzyme activity was derived from the information from the commercial suppliers (control POD enzyme – Sigma, UK). Gel A is loaded as follows; POD1 = 1.8 U (30µg) of control enzyme; POD2 = 5.4 U (90µg) of control enzyme; TE = 17.5µg of total extract. Gel B is loaded as follows; TE = 35µg of total extract; POD = 0.9 U (15µg) of control enzyme; ICF = 35µg of sodium chloride extract ICF. See section 4.4.6 for a detailed description of the POD staining technique.

available enzyme - Sigma, UK) migrated to the upper third of the gel and was easily visible as two red-brown densely staining bands on a clear background.

TE protein from tobacco leaf yielded two well-defined bands that migrated to the middle of the gel (TE-POD 1 & 2). The same loading of ICF protein also indicated that these enzymes were present in the apoplastic preparation, but in addition 4 further bands of POD enzyme activity were present, 2 above and 2 below what had been designated as TE-POD 1 & 2 (see figure 7.2, gel B). POD enzyme active bands located only in ICF were named ICF-POD 1-4 progressing from the top of the gel to the bottom.

In order to qualify the assumption that the four identified ICF-POD's were truly apoplastic the pattern of POD enzyme staining bands in TE was examined using a higher loading range (5-150μg) of protein, (see figure 7.3, gel A). Analysis of the TE-POD enzyme patterns illustrates that TE-POD's 1 and 2 appear to be the only peroxidase active bands in TE. Furthermore, even when 150μg of TE protein was loaded the unique POD enzyme bands, designated ICF-POD's 1-4 that have only been observed in ICF were not detected in TE preparations. It was concluded that ICF-POD's 1-4 are apoplastic in origin because they are unique to ICF samples as determined by POD activity staining.

Figure 7.3, gel B, illustrates a gel with increasing protein loadings of ICF and clearly shows that ICF-POD's 1 and 2 and ICF-POD's 3 and 4 are grouped into two pairs. In an attempt to achieve a better separation of these proteins and to reveal if the four bands of enzyme activity present in the ICF preparations were composed of more components, the same ICF preparation was subjected to native-PAGE electrophoresis in gels of varying acrylamide concentrations (see figure 7.4). The 10% (w/v) acrylamide native-PAGE gel clearly demonstrated that the upper ICF-POD's was definitely comprised of two distinct bands of POD enzyme of activity. ICF-POD's 3 and 4 did not separate as effectively but remained as two distinct bands of POD enzyme activity (see figure 7.4, 10% and 12.5% (w/v) gels).

7.2.3 Spectrophotometric assay of POD activity in excised bands

In order to re-confirm that ICF-PODs 1, 2, 3 and 4 actually contained POD enzyme activity, two groups of duplicate bands were carefully excised from a POD stained native gel and placed into eppendorfs. 750μl of 100mM phosphate buffer, pH 7.0 was added and the gel was macerated for >1 minute. The buffer and gel mixture was incubated for 24 hours at 4°C, after which the gel was pelleted in a microfuge and the supernatants collected and assayed for POD activity spectrophotometrically as described in section 4.3.4 (using a Beckman DU7500 spectrophotometer). The activity data derived from

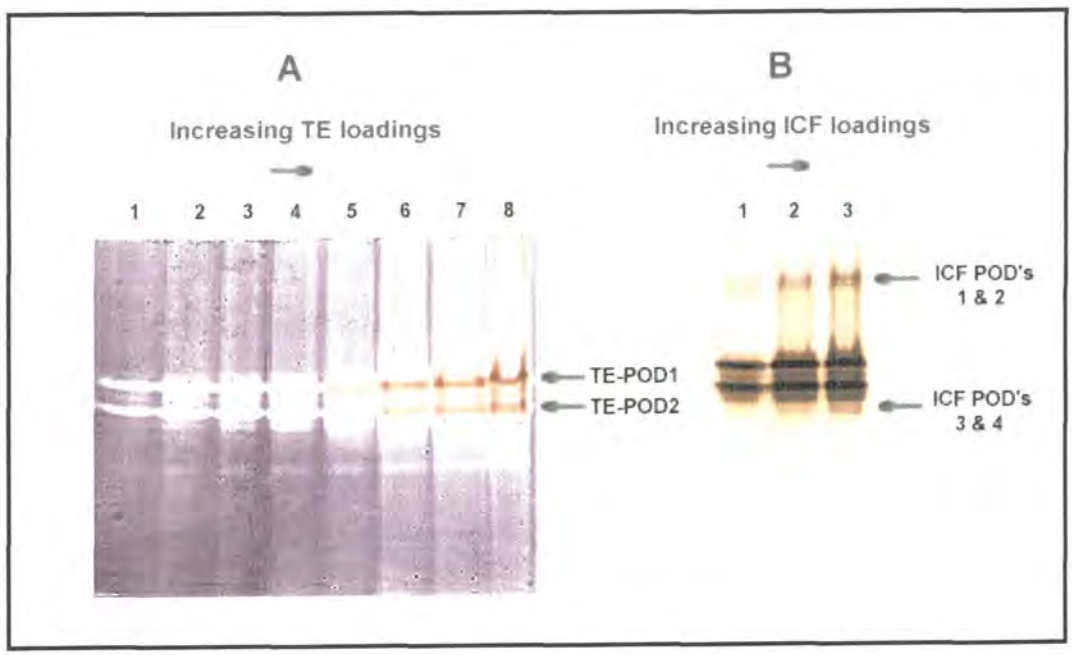

Figure 7.3

Assay of peroxidase activity in TE and ICF separated in native-PAGE gels.

TE and ICF were prepared as described in sections 4.2.3 and 4.2.1, respectively. Both gels were 10% native PAGE gels and samples were prepared in native PAGE sample buffer (see section 4.4.2). The quantities quoted refer to Bradford quantified protein concentration. See section 4.4.6 for a detailed description of the POD staining technique. Gel A has initially been stained for SOD activity and is loaded left to right, as follows; Lane 1 = 5µg TE; Lane 2 = 20µg TE; Lane 3 = 35µg TE; Lane 4 = 50µg TE; Lane 5 = 75µg TE; Lane 6 = 100µg TE; Lane 7 = 125µg TE; Lane 8 = 150µg TE. Gel B is loaded left to right, as follows; Lane 1 = 17.5µg ICF; Lane 2 = 35µg ICF; Lane 3 = 52.5µg ICF.

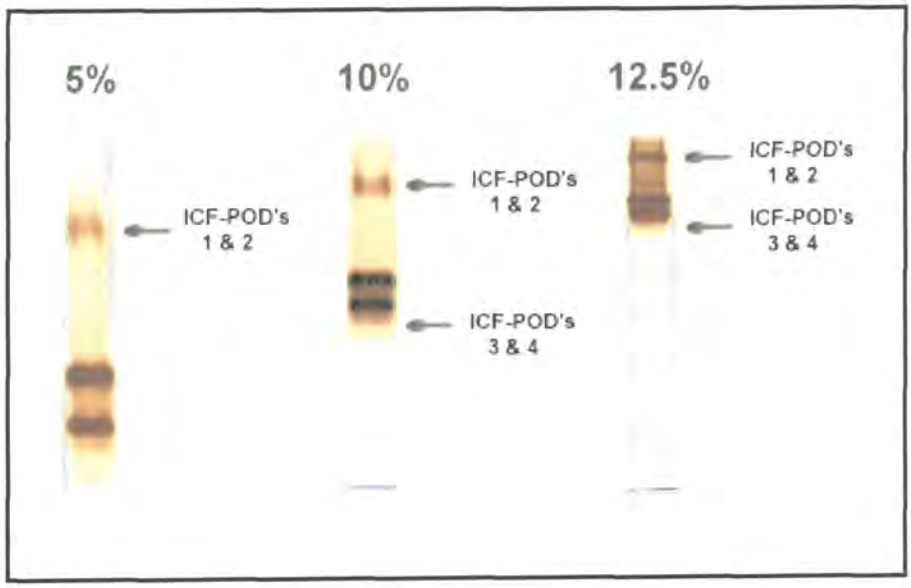

***Figure* 7.4**

Assay for peroxidase enzyme activity in ICF separated in native-PAGE gels of differing compositions.

All gels are native (see section 4.4.2) but of differing acrylamide ratios (the actual acrylamide percentage (w/v) of each gel is indicated above the gel image). All gels were loaded with 35µg of Bradford assay quantified protein from the same sodium chloride extracted ICF. All gels were initially stained for SOD enzyme activity and then counterstained for POD enzyme activity. See section 4.4.6 for detailed descriptions of the staining techniques.

duplicate measurements were expressed as percentages of the total POD activity present in the same quantity of protein. Unfortunately, measurement of the recovery of protein from the gel extract was not attempted, and the potential for enzyme inactivation had not been considered consequently, direct comparisons cannot be made. However, it appears that approximately 26% of the total POD enzyme activity present in ICF is contained within ICF-POD's 1-4 as separated by native-PAGE even after electrophoresis and a 24 hour incubation period (see figure 7.5).

7.2.4 Detection and optimisation of separation of apoplastic SOD's

Using a SOD-specific native in-gel staining assay (see section 4.4.7), it was possible to identify the SOD control enzyme (commercially available SOD – Sigma, UK) on native gels as a large clear zone on a dark blue background (see figure 7.6, lanes SOD1 and SOD2) in the top third of the gel.

TE extracted from tobacco leaf tissue exhibited 4 distinct bands of SOD enzyme activity in the middle section of the native gel, these bands were named TE-SOD's 1-4, see figure 7.6, gels A and B; it was also noticeable that TE exhibited a high background level of SOD enzyme activity that presented as a smeared area in the upper portion of the native gel. Unfortunately, this SOD enzyme component could not be directly attributed to one or more specific bands of activity thus revealing that some proteins are not resolving well in this native-PAGE system.

On a protein weight-for-weight basis gel B (figure 7.6) clearly shows that ICF also contains an area of high SOD activity on the upper portion of the gel, this area is much more active than observed in TE, and potentially indicated that vacuum infiltration has selectively enriched a true apoplastic SOD. ICF also exhibits 2 of the 4 bands of SOD activity present in TE (TE-SOD's 1 & 2) in the middle section of the native gel, this may arise because of some degree of intracellular contamination of ICF has occurred or because these particular enzymes are present in both compartments. In the lower half of the native gel distinct groupings of SOD-active bands are visible that are not present in TE.

In order to ensure that the bands that had stained enzymatically positive for ICF-SOD activity were not an artifact of a low TE loading, a range of 5μg to 150μg of TE was loaded and run through a 10% (w/v) native gel (see figure 7.7, gel A). A similar loading study was performed with ICF with a view to enhancing the distinct bands present in the lower portion of the native gel (see figure 7.7, gel B). A quick and direct visual comparison between the lane 8 of gel A (150μg of TE) and the lane 1 of gel B (17.5μg of

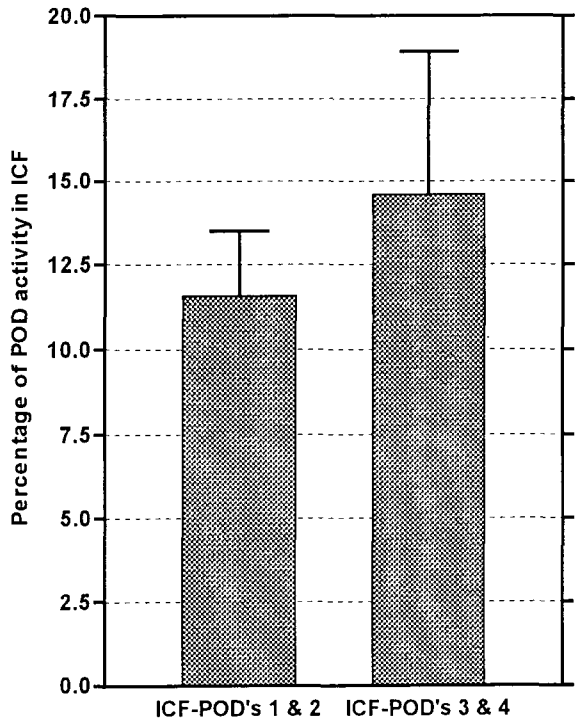

Figure 7.5

Estimation of relative ICF-POD activity in extracts from excised gel bands.

Duplicate groups of 2 lanes of ICF-POD's 1 & 2 and 3 & 4 pairs were excised from 10% (w/v) native-PAGE gels, and treated as described in section 7.5. Guaiacol peroxidase activity was assayed in each extract. The mean total POD activity present in ICF was calculated by assaying 35μg aliquots of freeze-dried ICF prepared in POD assay. All enzyme activities were calculated per g of fresh weight of original leaf material and the final values of extracts from bands were expressed as a percentage of the mean total POD activity in the ICF of 8.5U POD/g fresh weight (see section 4.3.4 for details of the POD assay). Data presented are the means and SD of duplicate measurements.

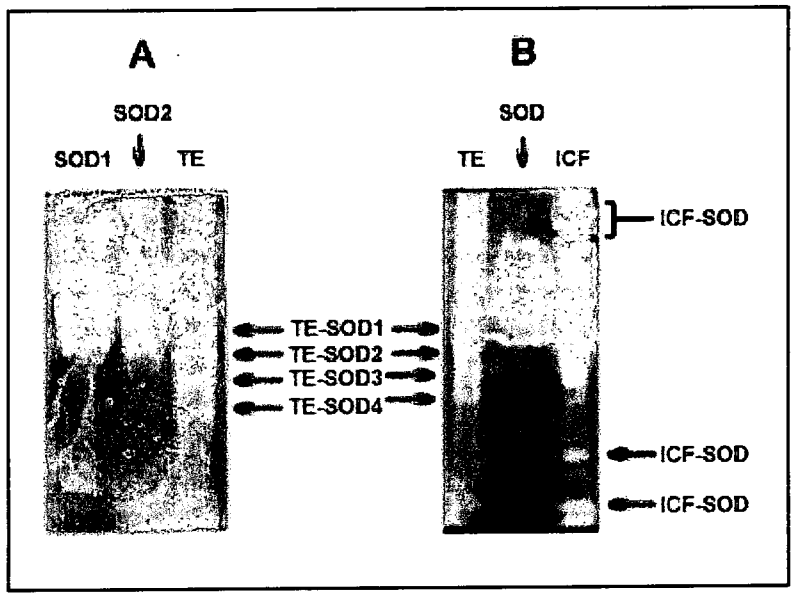

Figure 7.6

Assay for superoxide dismutase enzyme activity of control superoxide dismutase enzyme, TE and ICF in native-PAGE gels.

TE and ICF were prepared as described in sections 4.2.3 and 4.2.1, respectively. Both gels were 10% (w/v) native-PAGE gels and samples were prepared in native PAGE sample buffer (see section 4.4.2). The quantities quoted refer to either Bradford quantified protein concentration or the quantity of protein/enzyme activity was derived from the information of commercial suppliers (control SOD enzyme – Sigma, UK). Gel A is loaded as follows; SOD1 = 21 U (6μg) of control enzyme; SOD2 = 63 U (18μg) of control enzyme; TE = 35μg of total extract. Gel B is loaded as follows; TE = 35μg of total extract; SOD = 4.2 U (1.2μg) of control enzyme; ICF = 35μg of sodium chloride extract ICF. See section 4.4.7 for a detailed description of the SOD staining technique.

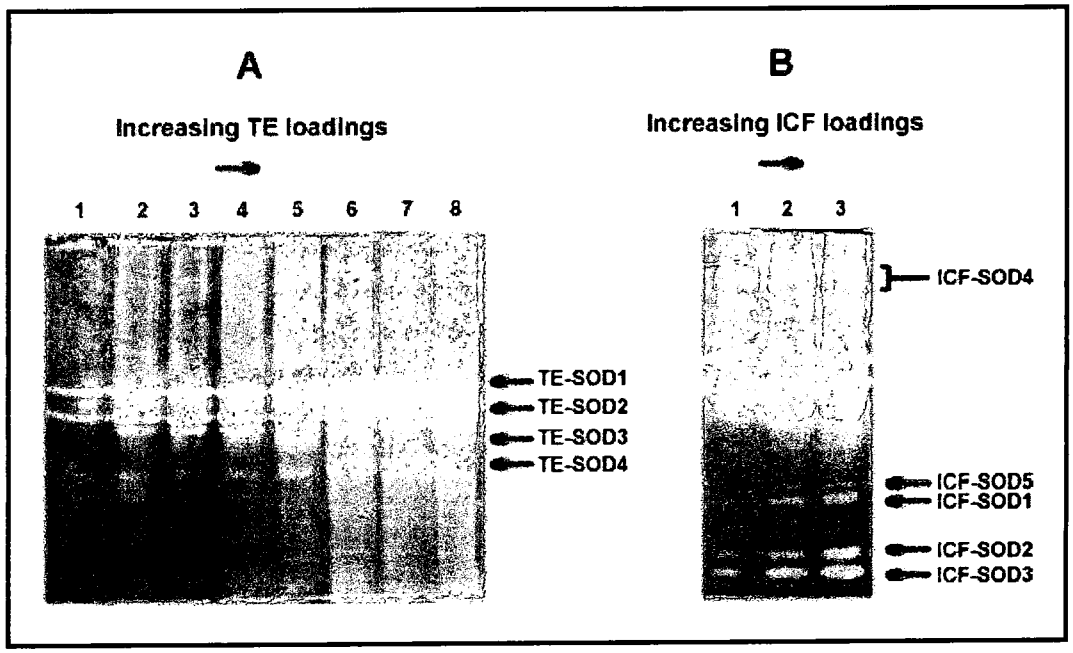

Figure 7.7

Assay of superoxide dismutase enzyme activity in TE and ICF native-PAGE gels.

TE and ICF were prepared as described in sections 4.2.3 and 4.2.1, respectively. Both gels were 10% (w/v) native-PAGE gels and samples were prepared in native PAGE sample buffer (see section 4.4.2). The quantities quoted refer to Bradford quantified protein concentration. See section 4.4.7 for a detailed description of the SOD staining technique. Gel A is loaded left to right, as follows; Lane 1 = 5µg TE; Lane 2 = 20µg TE; Lane 3 = 35µg TE; Lane 4 = 50µg TE; Lane 5 = 75µg TE; Lane 6 = 100µg TE; Lane 7 = 125µg TE; Lane 8 = 150µg TE. Gel B is loaded left to right, as follows; Lane 1 = 17.5µg ICF; Lane 2 = 35µg ICF; Lane 3 = 52.5µg ICF.

ICF) illustrated that even when 8.5 times more TE protein is loaded the distinctive bands of ICF-SOD enzyme activity observed in gel B (figure 7.7) are not present in TE. Thus, with a reasonable degree of certainty, it is highly probable that these SOD-active enzymes are apoplastic in origin.

The ICF loading study presented in figure 7.7 (gel B) clearly illustrated that when less protein is loaded it is possible to discern a distinct and reasonably well defined and very SOD active band in the upper part of the gel (best seen in lane 1), this band has been termed, ICF-SOD 4. In contrast, very distinct, well resolved and discrete bands are present in the lower half of the gel and may represent single proteins; they have been designated ICF-SOD's 1, 2, 3, and 5 (figure 7.7).

ICF's were subjected to electrophoresis through a range of acrylamide gels with decreasing pore size (figure 7.8) in an attempt to further resolve and therefore distinguish the individual ICF derived SOD-active components. It was hoped that the 5% (w/v) gel would result in better resolution of the ICF-SOD 4 band at the top of the gel. Unfortunately, it did not and the band simply broadened (figure 7.8, 5% gel). However, ICF-SOD's 1, 2, 3 and 5, were very well resolved in the 12.5% (w/v) gel (figure 7.8, 12.5% gel) and furthermore the broad region that contained ICF-SOD 4 became more discrete which made physical isolation easier for subsequent molecular weight analysis.

7.2.5 Spectrophotometric assay of SOD activity in excised bands

To re-confirm that ICF-SOD's 1-5 actual contained SOD activity a highly sensitive spectrophotometric enzyme assay was employed (see section 4.3.3). Briefly, ICF-SOD enzyme activity bands designated 1-5 were carefully excised from the main gel and treated as outlined in section 7.4.1, except that SOD assay buffer was used. The activity data derived from duplicate measurements were expressed as percentages of the total SOD activity present in the same quantity of protein. Similar shortcomings were evident, in that, measurement of the recovery of protein from the gel extract was not attempted, and the potential for enzyme inactivation had not been considered. Consequently, direct comparisons cannot be made, however, it appears that approximately 18% of the total SOD enzyme activity present in ICF is contained within ICF-SOD's 1-5 as separated by native-PAGE even after electrophoresis and a 24 hour incubation period (see figure 7.9).

7.2.6 Molecular mass estimation and sub-unit analysis of apoplastic POD's

The resolution of ICF-POD's 1, 2, 3 and 4 was deemed to be best for individual band excision and subsequent polypeptide molecular mass estimation on 10% (w/v) native

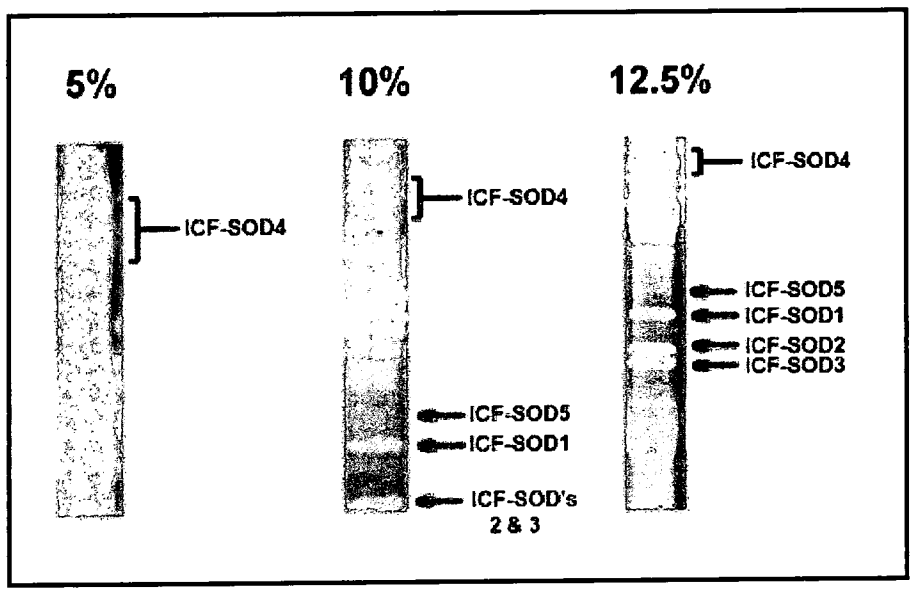

Figure 7.8

Assay for superoxide dismutase enzyme activity in ICF separated in native-PAGE gels of differing compositions.

All gels are native (see section 4.4.2) but of differing acrylamide ratios (the actual acrylamide percentage (w/v) of each gel is indicated above the gel image). All gels were loaded with 35µg of Bradford assay quantified protein from the same sodium chloride extracted ICF (protein concentration quantified from Bradford assay results). All gels were initially stained for SOD enzyme activity; see section 4.4.6 for a detailed description of the staining technique.

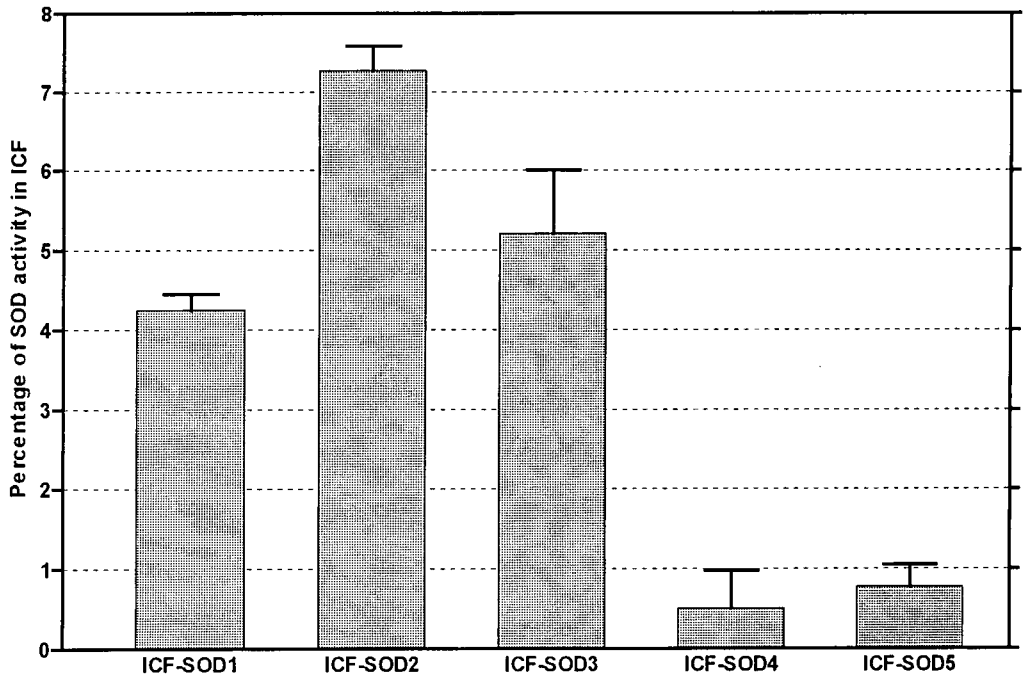

Figure 7.9

Estimation of relative ICF-SOD activity in extracts from excised gel bands.

Duplicate groups of 2 lanes of ICF-SOD1, 2, 3, 4 and 5 bands were excised from 12.5% (w/v) native gels, placed into eppendorf tubes and macerated. SOD activity was assayed in each extract. The mean total SOD activity present in ICF was calculated by assaying 35μg aliquots of freeze-dried ICF prepared in SOD assay. All enzyme activities were calculated per g of fresh weight of original leaf material and the final values of extracts from bands were expressed as a percentage of the mean total SOD activity in the ICF of 2.2U SOD/g fresh weight (see section 4.3.5 for details of the SOD assay). Data presented are the means and SD of duplicate measurements.

gels (see figure 7.4). The method used for the transfer of POD enzyme activity stained bands from the native gel to the SDS-PAGE gel for sub-unit separation is detailed in section 7.2.

Figure 7.10 illustrates a SDS-PAGE separation of ICF-POD's 1 & 2. ICF-POD 1 appeared to be composed of 2 polypeptide components (A and B) with molecular weights of 58.1 and 29.2 kDa, which readily stained with Coomassie. Interestingly, the large polypeptide is almost exactly twice the size of the small polypeptide, this firstly indicated that the denaturation process is not 100% efficient, and secondly that ICF-POD 1 may be a dimer. ICF-POD 1 migrated to the upper portion of a native-PAGE gel (figure 7.4) and consequently it can be assumed that it either had a relatively high molecular weight and/or is of neutral pI. It is also therefore possible that component A is undenatured ICF-POD 1. If this is correct, the dimer is probably held together by disulphide linkages because it had only been partially denatured before electrophoresis. Figure 7.10 also shows the molecular weight estimation of ICF-POD 2, it is composed of one component (A) with almost exactly the same molecular weight as component B from ICF-POD1. Salzer & Hager [1993] and Otter & Polle [1997] have both described a 'cell wall' peroxidase enzyme with a molecular mass of 29 kDa from Norway spruce. It was unfortunate that neither component could be satisfactorily subjected to N-terminal sequence analysis because of N-terminal blockage.

Figure 7.11 shows the same experiment for ICF-POD's 3 and 4, no bands could be seen when the gel had been Coomassie stained. Therefore, it was counter-stained with silver stain. The higher in gel enzyme activity (figure 7.4) and spectrophotometric enzyme activity (figure 7.5) present in a relatively small quantity of material that cannot be visualised with Coomassie staining indicated that the specific activity of these polypeptides for guaiacol is much higher than that of either ICF-POD's 1 or 2 (also see figure 7.5). Both ICF-POD's 3 and 4 exhibited essentially the same polypeptide pattern, 3 components were present in both excised enzyme activity bands, it cannot be determined if these components are related or are in fact an artifact.

7.2.7 Molecular mass estimation and sub-unit analysis of apoplastic SOD's

12.5% (w/v) native-PAGE gels were deemed to yield the best resolution for the excision of SOD enzyme activity bands (see figure 7.4) and were used throughout this section. Figure 7.12 illustrates the initial estimation of the molecular weights of ICF-SOD's 1 and 2. ICF-SOD 1 yielded a single major polypeptide band with an apparent molecular mass of 20.2 kDa, ICF-SOD 2 generated two denatured components, A and B, with molecular masses of 25.2 and 22.2 kDa, respectively. Figure 7.12, illustrated that a low quantity of

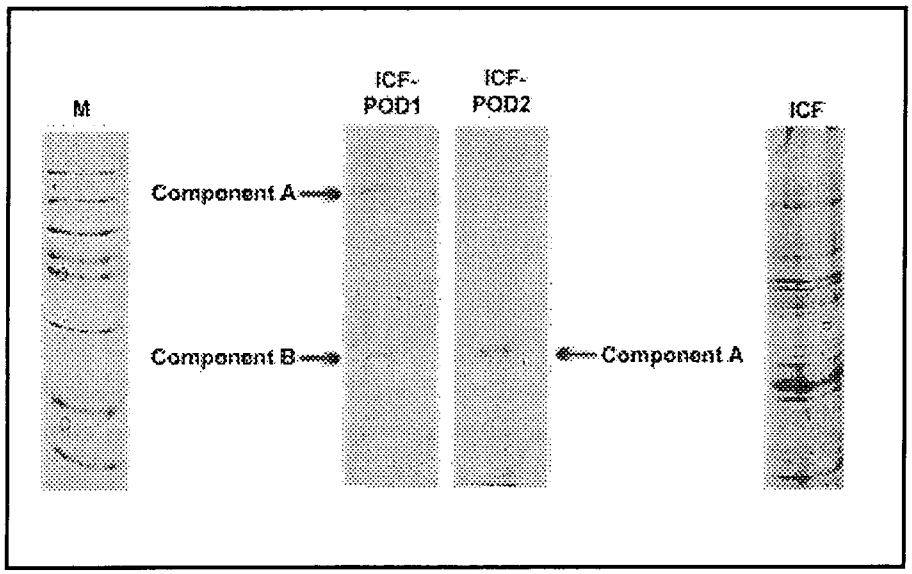

	Component	Rf	MW (kDa)
ICF-POD1	A	0.1944	**58.1**
	B	0.6500	**29.2**
ICF-POD2	A	0.6389	**29.9**

Figure 7.10

Molecular mass estimation of the sub-unit composition of ICF-POD 1 and 2.

All samples and standards were run on the same 12.5% (w/v) denaturing gel and coomassie blue stained (see sections 4.4.1 and 4.4.3, respectively). All quantities quoted refer to protein concentrations calculated using the Bradford assay (see section 4.3.2). Lane 'M' = 6μl of Promega Mid Range molecular weight marker proteins; Lane 'ICF-SOD1' = 4x ICF-POD1 bands excised from 10% (w/v) native-PAGE gel that had been activity stained; Lane 'ICF-POD2' = 4x ICF-POD2 bands excised from 10% (w/v) native-PAGE gel that had been activity stained; Lane 'ICF' = 35μg of ICF. Table was constructed from molecular weight calibration curve data (not shown). Refer to section 7.2 for details of loading strategy.

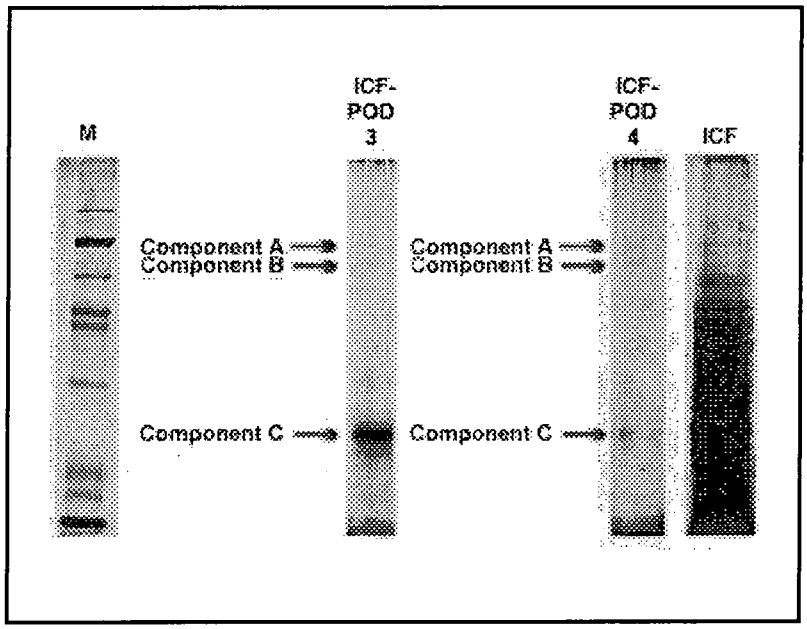

	Component	Rf	MW (kDa)
ICF-POD3	A	0.2553	**55.5**
	B	0.3032	**52.5**
	C	0.7447	**25.2**
ICF-POD4	A	0.2553	**55.5**
	B	0.3032	**52.5**
	C	0.7447	**25.2**

Figure 7.11

Molecular mass estimation of the sub-unit composition of ICF-POD 3 and 4.

All samples and standards were run on the same 12.5% (w/v) denaturing gel, initially coomassie blue stained and the silver stained (see sections 4.4.1, 4.4.3 and 4.4.4, respectively). All quantities quoted refer to protein concentrations calculated using the Bradford assay (see section 4.3.2). Lane 'M' = 3μl of Promega Mid Range molecular weight marker proteins; Lane 'ICF-POD3' = 1x ICF-POD3 bands excised from 10% (w/v) native-PAGE gel that had been activity stained; Lane 'ICF-POD4' = 1x ICF-POD4 bands excised from 10% (w/v) native-PAGE gel that had been activity stained; Lane 'ICF' = 11.7μg of ICF. Table was constructed from molecular weight calibration curve data (not shown). Refer to section 7.2 for details of loading strategy.

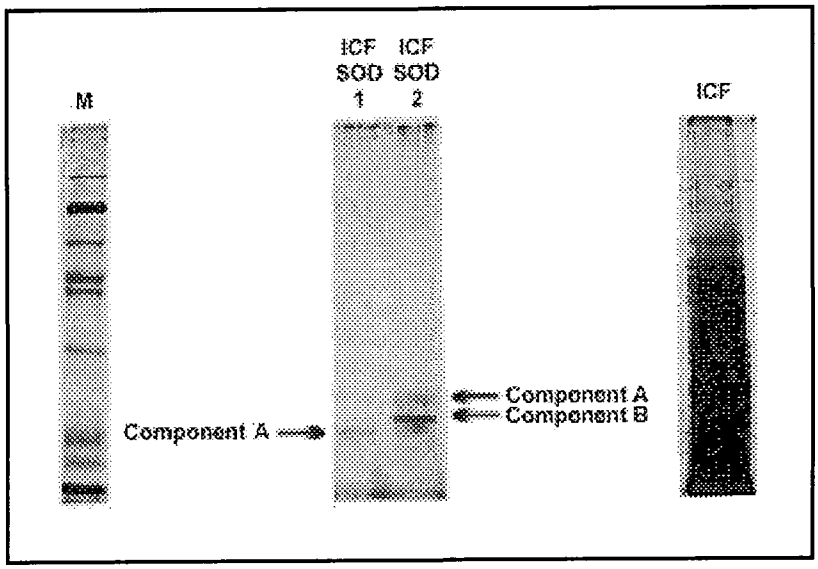

	Component	Rf	MW (kDa)
ICF-SOD1	A	0.8245	**20.2**
ICF-SOD2	A	0.7447	**25.2**
	B	0.7926	**22.2**

Figure 7.12

Molecular mass estimation of the sub-unit composition of ICF-SOD 1 and 2.

All samples and standards were run on the same 12.5% (w/v) denaturing gel, initially coomassie stained and then silver stained (see sections 4.4.1, 4.4.3 and 4.4.4, respectively). All quantities quoted refer to protein concentrations calculated using the Bradford assay (see section 4.3.2). Lane 'M' = 3μl of Promega Mid Range molecular weight marker proteins; Lane 'ICF-SOD1' = 1x ICF-SOD1 band excised from 12.5% (w/v) native-PAGE gel that had been activity stained; Lane 'ICF-SOD2' = 1x ICF-SOD2 band excised from 12.5% (w/v) native-PAGE gel that had been activity stained; Lane 'ICF' = 11.7μg of ICF. Table was constructed from molecular weight calibration curve data (not shown). Refer to section 7.2 for details of loading strategy.

protein was present in both ICF-SOD 1 and 2 enzyme activity stained bands because of the necessity to silver stain the SDS-PAGE gel, consequently, more native-PAGE gels were run and ICF-SOD's 1-3 re-isolated, the resultant SDS-PAGE molecular mass estimation is presented in figure 7.13. An increased loading of native-PAGE excised activity bands permitted the major polypeptides to be visualised utilising Coomassie staining only. ICF-SOD 1 and 2 were consistent and the banding patterns of polypeptides observed in figure 7.12 were successfully reproduced. A small degree of variation in the final determined molecular masses of each polypeptide was observed (~1 kDa) which presumably reflects the day-to-day variability of the system. ICF-SOD 3 produced a slightly 'wavy' single polypeptide band with an apparent molecular mass of ~22 kDa.

Scant information is available regarding plant apoplastic SOD's and the only reports that could be found detailed a Mn-SOD with a denatured molecular mass of 22 kDa from the moss, *Barbula unguiculata* [Yamahara *et al.* 1999] and a homogenous dimeric CuZn-SOD from *Pinus sylvestris* needles with a sub-unit molecular mass estimated to be around 17.8 kDa [Streller & Wingsle 1994]. Other reports of extracellular SOD's include a Fe-SOD from a cyanobacteria with a molecular mass of 21 kDa [Shirkey *et al.* 2000] and a CuZn-SOD from a nematode with a mass of 19.8 kDa [Liddell & Knox 1998]. The molecular masses reported within this thesis are of the same order as these reports even though a different species is under study thus reinforcing the native-gel and spectrophotometric assay data and confirming SOD enzyme activity.

ICF-SOD 4 was SOD-active and exhibited as a very broad band even when electrophoresed through a 12.5% (w/v) native-PAGE gel. Consequently, ICF-SOD 4 was isolated as a 3mm long piece of gel and divided into 3x 1mm pieces progressing from the top of the gel to the bottom and termed ICF-SOD4[i], [ii] and [iii], respectively. Figure 7.14 illustrates the molecular weight estimation for the polypeptides present in these gel pieces. What was immediately obvious and different from the other, highly discrete ICF-SOD's 1-3 (figure 7.13) was a diffuse low molecular weight material with apparent molecular weights of <21 kDa, that is present in all of the ICF-SOD 4 runs and that stained quite intensely. ICF-SOD 4 [i] did not exhibit a distinctive banding pattern and as such could not be analysed further, however, there was further diffuse protein material present at the top of the gel (>66 kDa) that was not present in ICF-SOD 4 [ii] or [iii] lanes. ICF-SOD's 4 [ii] and [iii] showed a doublet of bands of approximately the same mass, 44.7 kDa. The potentially multimeric, complex and diffuse nature of ICF-SOD 4 in the denaturing gel system prevented further isolation and analysis.

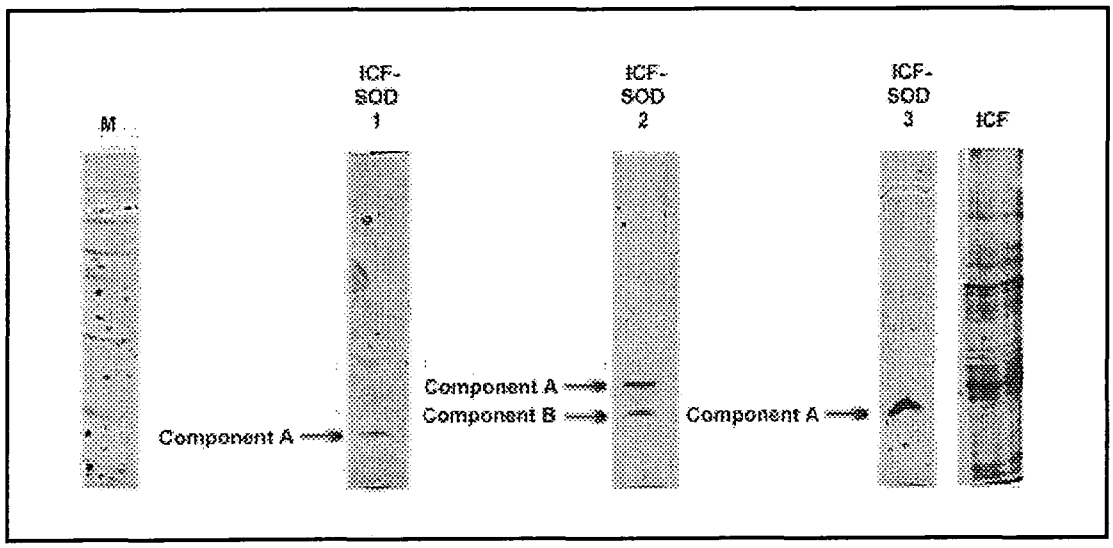

	Component	Rf	MW (kDa)
ICF-SOD1	A	0.8120	**19.0**
ICF-SOD2	A	0.6930	**26.5**
	B	0.7701	**21.7**
ICF-SOD3	A	0.7701 - 0.7594	**22 ± 0.3**

Figure 7.13

Molecular mass estimation of the sub-unit composition of ICF-SOD 1, 2 and 3.

All samples and standards were run on the same 12.5% (w/v) denaturing gel and coomassie stained (see sections 4.4.1 and 4.4.3, respectively). All quantities quoted refer to protein concentrations calculated using the Bradford assay (see section 4.3.2). Lane 'M' = 6μl of Promega Mid Range molecular weight marker proteins; Lane 'ICF-SOD1' = 4x ICF-SOD1 bands excised from 12.5% native PAGE gel that had been activity stained; Lane 'ICF-SOD2' = 4x ICF-SOD2 bands excised from 12.5% native PAGE gel that had been activity stained; Lane 'ICF-SOD3' = 4x ICF-SOD3 bands excised from 12.5% native PAGE gel that had been activity stained; Lane 'ICF' = 35μg of ICF. Table was constructed from molecular weight calibration curve data (not shown). Refer to section 7.2 for details of loading strategy.

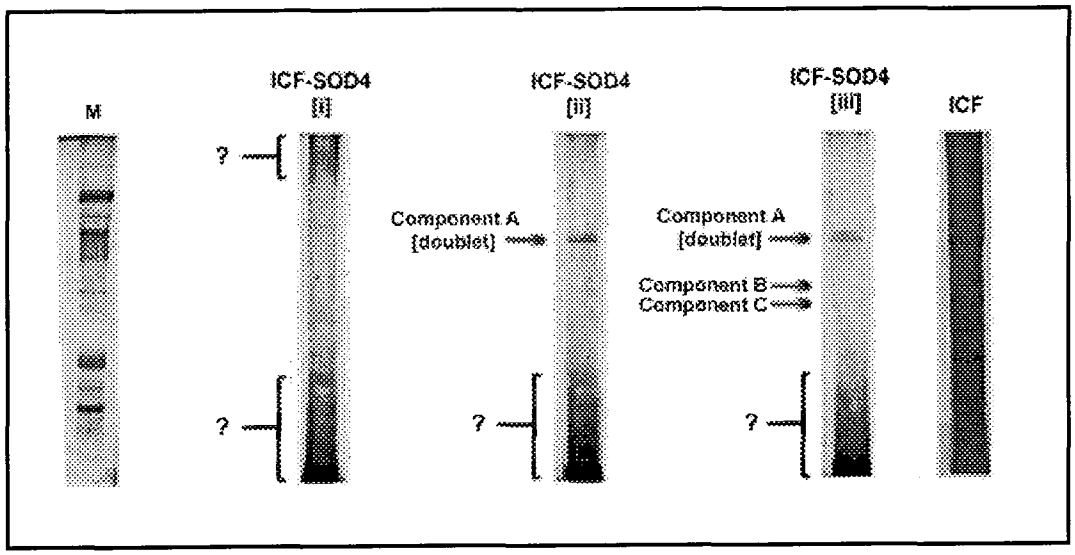

	Component	Rf	MW (KDa)
ICF-SOD4[i]	?	Wide range	>66KDa
	?	Wide range	<21KDa
ICF-SOD4[ii]	A [doublet]	0.3249	45.9
	?	Wide range	<21KDa
ICF-SOD4[iii]	A [doublet]	0.3401	44.7
	B	0.4721	34.7
	C	0.5228	30.8
	?	Wide range	<21KDa

Figure 7.14

Molecular mass estimation of sub-unit composition of ICF-SOD4.

All samples and standards were run on the same 12.5% (w/v) denaturing gel, initially coomassie blue stained and then silver stained (see sections 4.4.1, 4.4.3 and 4.4.4, respectively). All quantities quoted refer to protein concentrations calculated using the Bradford assay (see section 4.3.2). Lane 'M' = 3μl of Promega Mid Range molecular weight marker proteins; Lane 'ICF-SOD4[i]' = 4x ICF-SOD4[i] bands excised from 12.5% % native PAGE gel that had been activity stained; Lane 'ICF-SOD4[ii]' = 4x ICF-SOD4[ii] bands excised from 12.5% % native PAGE gel that had been activity stained; Lane 'ICF-SOD4[iii]' = 4x ICF-SOD4[iii] bands excised from 12.5% % native PAGE gel that had been activity stained; Lane 'ICF' = 5.85μg of ICF. Table was constructed from molecular weight calibration curve data (not shown). Refer to section 7.2 for details of loading strategy and section 7.9 for details of how ICF-SOD4 was sectioned.

7.2.8 Inhibition studies

Different types of SOD's and POD's can be broadly identified through their differential responses to inhibitors.

7.2.8.1 Inhibition of ICF-SOD's

The best way to distinguish between the various types of SOD's is by the characterisation of the metal ion present [Bannister *et al.* 1987], cyanide is known to inhibit CuZn-SOD's but not Mn-SOD's [Fridovich 1974]; hydrogen peroxide inactivates both the CuZn- and Fe- containing SOD's but not Mn-SOD [Symonyan & Nalbandyan 1972]. Three identical loadings of ICF were run through a 12.5% (w/v) native-PAGE gel and after electrophoresis each lane was excised and treated for 5 minutes in the dark in either, 50mM phosphate buffer, pH 7.5 (control), 50mM phosphate buffer, pH 7.5 containing 1mM potassium cyanide or 50mM phosphate buffer, pH 7.5 containing 10mM hydrogen peroxide. After each treatment, the lanes were subjected to SOD enzyme activity staining. Figure 7.15 shows the result of the SOD staining, ICF-SOD's 1 and 5 were both inactivated by 1mM cyanide and by 10mM hydrogen peroxide indicating that these are probably CuZn-SOD enzymes. The activity of ICF-SOD's 2 and 3 is inhibited by treatment with hydrogen peroxide but not cyanide indicating that these are probably Fe-SOD's. Completely unaffected by either treatment was ICF-SOD 4 which was therefore assigned as a Mn-SOD. Ogawa *et al.* [1996] and Schinkel *et al.* [1998] have both isolated apoplastic CuZn-SOD's from plants, but no reports of apoplastic Fe- or Mn-SOD's could be found. However, extracellular Fe- and Mn-containing SOD's have been described in cyanobacteria [Shirkey *et al.* 2000] and moss [Yamahara *et al.* 1999], respectively.

7.2.8.2 Inhibition of ICF-POD's

The results of the above SOD stained inhibition study were re-confirmed in a repeat experiment using 10% (w/v) native-PAGE gels. It was decided to counter-stain these gels for ICF-POD enzyme activity to assess if any inhibition had taken place. POD's can be classified as selenium-dependent and cyanide insensitive [Paes & Oliveira 1999] or Fe-containing and cyanide sensitive [Rob *et al.* 1997]. Figure 7.16 illustrates the results of the ICF-POD inhibition study; treatment with 1mM potassium cyanide had completely inactivated all ICF-POD's, they were therefore determined to be cyanide sensitive and therefore probably were Fe-containing POD's. It is noteworthy that the TE-POD's are cyanide insensitive, marking a clear distinction between apoplastic and intracellular POD's.

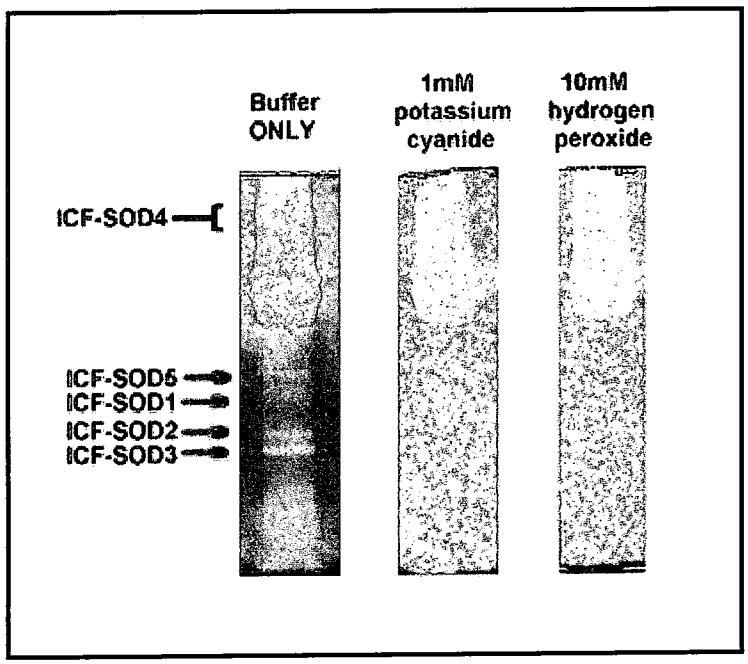

Figure 7.15

Inhibition of individual ICF-SOD enzymes.

3x lanes of 35μg (Bradford quantified protein) loadings of the same ICF preparation were run through a 12.5% (w/v) native-PAGE gel (section 4.4.2); each lane was excised and treated individually before staining for SOD activity; buffer (control) = 50mM phosphate buffer, pH 7.5; potassium cyanide= 50mM phosphate buffer, pH 7.5 containing 1mM potassium cyanide; hydrogen peroxide = 50mM phosphate buffer, pH 7.5 containing 10mM hydrogen peroxide; each was then washed extensively for >3minutes and then SOD stained according to section 4.4.7.

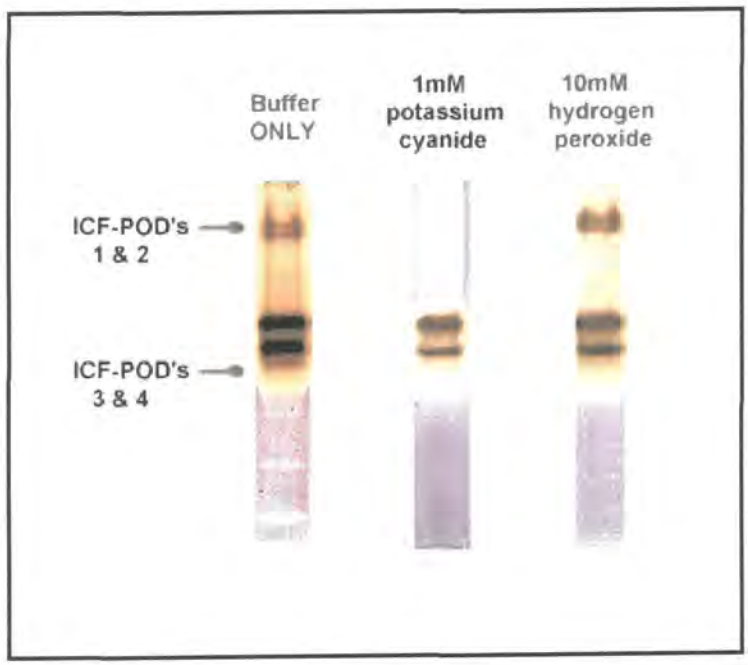

Figure 7.16

Inhibition of individual ICF-POD enzymes.

3x lanes of 35µg (Bradford quantified protein) loadings of the same ICF preparation were run through a 10% (w/v) native-PAGE gel; each lane was excised and treated individually before staining for POD activity; buffer (control) = 5 minutes in 50mM phosphate buffer, pH 7.5 in the dark; potassium cyanide= 5 minutes in 50mM phosphate buffer, pH 7.5 containing 1mM potassium cyanide in the dark; hydrogen peroxide = 5 minutes in 50mM phosphate buffer, pH 7.5 containing 10mM hydrogen peroxide in the dark; each was then washed extensively for >3minutes and then POD stained according to section 4.4.6.

7.2.9 Changes in the anti-AOS status of the leaf apoplast

The activities of anti-AOS enzymes are known to alter during abiotic stress [Yahraus *et al.* 1995; Luwe 1996; O'Kane *et al.* 1996] and during development [Rogiers *et al.* 1998; Takahama *et al.* 1999]. The activities of the apoplastic forms of these enzymes were therefore assessed during abiotic stress and through development.

7.2.9.1 The effect of abiotic stress on ICF-SOD and POD activities

Tobacco plants were subjected to a range of abiotic conditions typically found to induce environmental stress: -

1. Drought was mimicked by restricting the water supply until all the leaves had wilted (~14 days) after which watering was resumed, the plants were allowed to rehydrate over a 3 day period and were then subjected to VI.
2. Leaves were mechanically stressed by cutting off the top fifth of one leaf from 10 tobacco plants. After 48 hours the injured leaves were collected and subjected to VI.
3. Temperature stress was achieved by incubating tobacco plants at 40°C in a growth chamber for 5 days, after which the leaves were subjected to VI.

Leaf ICF from each set of stressed plants was subjected to electrophoresis side-by-side and on a 10% (w/v) native-PAGE gel, and then subjected to SOD and POD enzyme activity staining, the results are displayed in figure 7.17. Although figure 7.17 provides only a visual assessment of the relative activities of each ICF-SOD and ICF-POD active band, it does illustrate that the anti-AOS enzymes present in the apoplast are differentially responsive to differing stresses.

Drought stress did not appear to have any effect on the profile or the activity of ICF-SOD's or ICF-POD's, see figure 7.17, control and drought gels. However, mechanical stress reduced enzyme activity of ICF-SOD's 1, 2 and 3 while it enhanced the enzyme activity of ICF-POD's 1 and 2. Yahraus *et al.* [1995] have observed a similar enhancement of apoplast POD activity during pathogen interaction, that may share a common signal transduction route with mechanical (wounding) stress [Jongsma *et al.* 1994; Baron & Zambryski 1995]. Elevated temperature similarly reduced the detectable enzyme activity of ICF-SOD's 1, 2 and 3, but no concurrent or dissimilar data could be

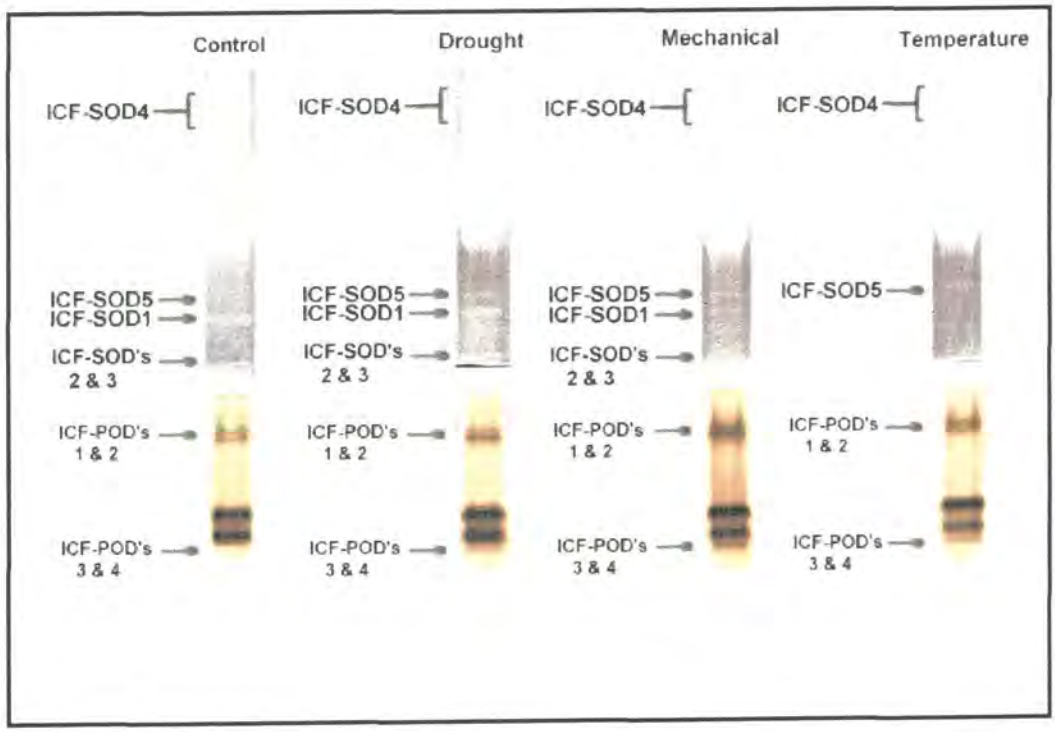

Figure 7.17

ICF-SOD and ICF-POD patterns during abiotic stress.

All samples were run on the same 10% (w/v) native gel (see section 4.4.2) and initially stained for SOD activity and then counterstained for POD activity (see sections 4.4.7 and 4.4.6, respectively). All quantities quoted refer to protein concentrations calculated using the Bradford assay (see section 4.3.2). Lane 'Control' = 35µg of ICF VI from untreated plants; Lane 'Drought' = 35µg of ICF VI from drought stressed plants; lane 'Mechanical' = 35µg of ICF VI from mechanically stressed plants; lane 'Temperature' = 35µg of ICF VI from temperature stressed plants.

found in the literature because of the lack of studies investigating the effects of elevated temperatures.

7.2.9.2 The effect of leaf developmental age on ICF-SOD and POD activities

Leaves were categorised into four sets according to their relative developmental age. Care was taken to ensure that all plant material was of the same initial age by monitoring germination. 10-week old plants (post-germination) were brought together and their leaves categorised. The definitions of the different ages were as follows: -

Age #1 - defined as 'young'; excised the upper quarter of the stem.
Age #2 - defined as 'mid'; excised the next quarter of the stem.
Age #3 - defined as 'old'; excised the next quarter of the stem.
Age #4 - defined as 'senescing'; excised the bottom quarter of the stem.

Each category was excised from the stem and subjected to VI (section 4.2.2) in order to recover ICF from each leaf developmental age. ICF preparations from each leaf developmental age were prepared and loaded onto a 12.5% (w/v) native-PAGE gel, on a protein weight-for-weight basis and subjected to electrophoresis. Afterwards SOD enzyme activity staining followed by POD enzyme activity staining was undertaken, the results are presented in figures 7.18 and 7.19, gel images labelled A.

The SOD enzyme activity stained gel (figure 7.18, gel A) exhibited a general loss of SOD activity and an altered profile of ICF-SOD's as the leaves progressed through the developmental ages. This is very evident for the better separated ICF-SOD's (1, 2, 3 and 5) in the lower part of the gel, but is also evident as a general decline in ICF-SOD 4 enzyme activity in the upper part of the gel. The observable profile of ICF-SOD's using native-PAGE and in-gel enzyme activity staining, shows a rapid loss of ICF-SOD's 1 and 5 as the leaves age, until there is no detectable activity in senescing leaves (see figure 7.18, gel A, lanes 1-4). In order to quantitatively confirm the loss of ICF-SOD enzyme activity a sensitive spectrophotometric assay was utilised (section 4.3.3); the data are shown on the graph in figure 7.18 (B). The ICF-SOD enzyme activity remains stable during developmental ages 1 and 2, but rapidly drops to less than 40% of this value by the time the leaves are undergoing senescence.

Similarly, to detect if ICF-POD enzyme activities had altered the native-PAGE gel was counter stained for POD enzyme activity, see figure 7.19 (A). The gel image shows that during early development (lane 1) and into maturity (lane 3) there was very little discernible difference between the ICF-POD enzyme profile and apparent activity using

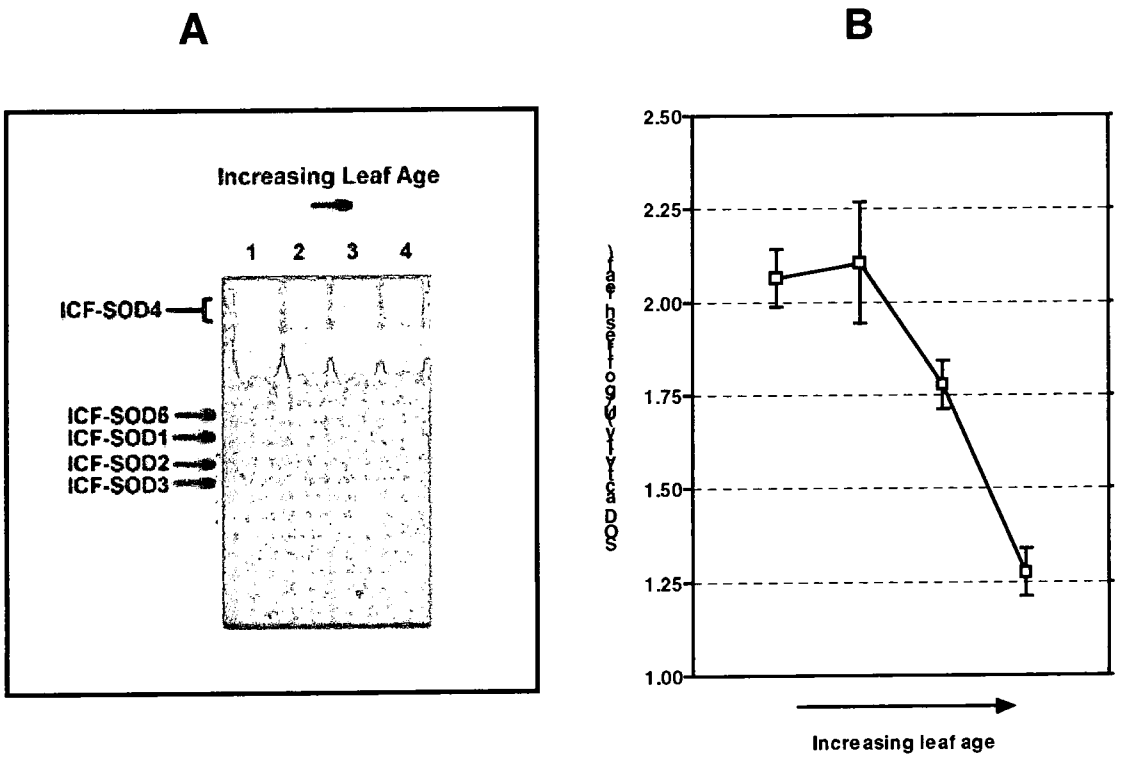

Figure 7.18

Quantitative analysis of ICF-SOD enzyme activity during leaf development.

A = All samples were run on the same 12.5% (w/v) native gel (see section 4.4.2) and initially stained for SOD activity (see section 4.4.7). All lanes were loaded with 35µg of ICF protein as calculated from Bradford assay results (section 4.3.2). Refer to section 7.12 for details of how leaf age was determined. ICF was prepared from leaves of differing developmental stages as described in section 4.2.1.

B = Refer to section 7.12 for details of how leaf age was determined. ICF was prepared from leaves of differing developmental stages as described in section 4.2.1. Duplicate lyophilised solid equivalent to 35µg of protein from each developmental stage was reconstituted in SOD assay buffer (50mM phosphate, pH 8.2) and assayed as per section 4.3.5. Units of activity were scaled back to reflect the quantity of tissue the ICF had been sampled from.

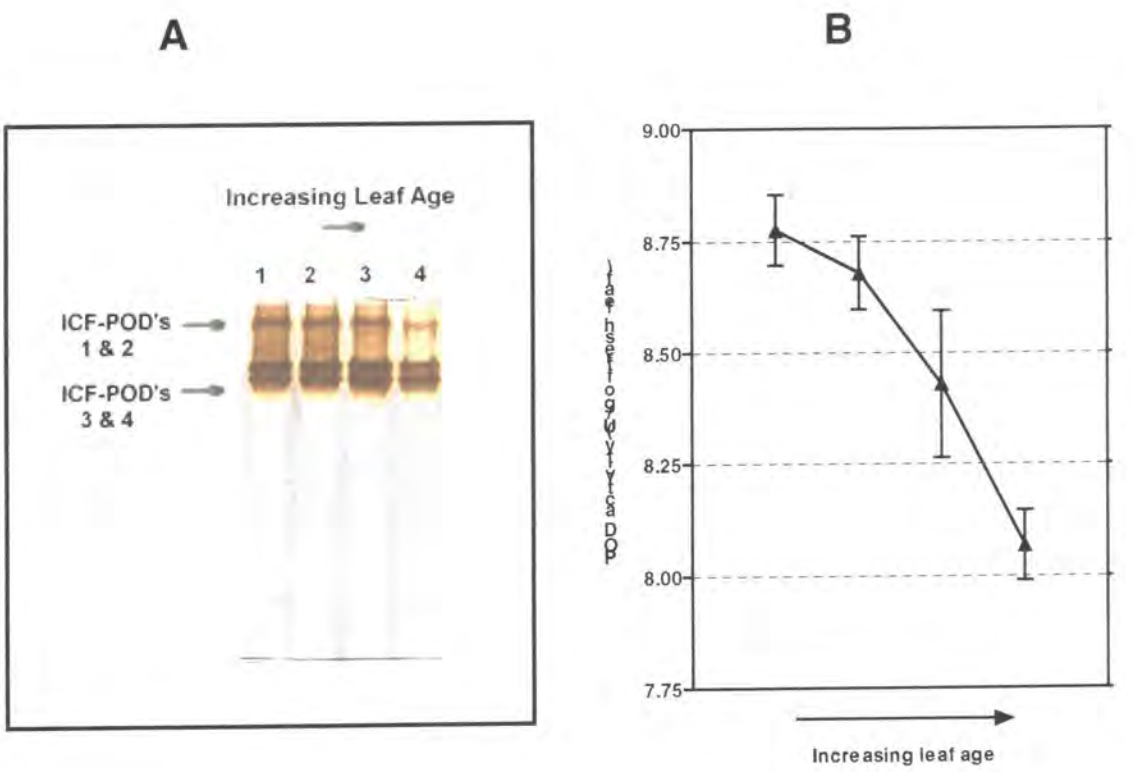

Figure 7.19

Quantitative analysis of ICF-POD enzyme activity during leaf development.

A = All samples were run on the same 12.5% (w/v) native gel (see section 4.4.2) and initially stained for POD activity (see section 4.4.6). All lanes were loaded with 35µg of ICF protein as calculated from Bradford assay results (section 4.3.2). Refer to section 7.12 for details of how leaf age was determined. ICF was prepared from leaves of differing developmental stages as described in section 4.2.1.

B = Refer to section 7.12 for details of how leaf age was determined. ICF was prepared from leaves of differing developmental stages as described in section 4.2.1. Duplicate lyophilised solid equivalent to 35µg of protein from each developmental stage was reconstituted in POD assay buffer (100mM phosphate, pH 7.0) and assayed as per section 4.3.4. Units of activity were scaled back to reflect the quantity of tissue the ICF had been sampled from.

native-PAGE and in gel enzyme activity staining. However, contradictory data are displayed on the graph (figure 7.19, B), that shows a constant decrease in total ICF-POD enzyme activity as the leaf tissue progresses through each of the developmental ages. It is therefore possible that the gel (A) had been over-stained for POD activity. What is obvious from both the gel image (A) and the spectrophotometric assay (B) is that total ICF-POD activity is greatly reduced when the leaves are undergoing senescence.

A similar age-related decrease in enzymatic anti-AOS capacity has been observed previously [Rogiers *et al.* 1998; Takahama *et al.* 1999] and will be expanded upon in the conclusions (section 7.9).

7.2.9.3 The effect of leaf developmental age on the level of apoplastic oxidative protein modification.

In the introduction to this thesis (section 1.5) it had been outlined that the apoplast has a number of important anti-AOS strategies, broadly they can be classified into one of two depending upon their mode of action, i/ AOS-scavengers, or, ii/ anti-AOS enzymes. (see table 1.5). The above data had revealed that the activities of the anti-AOS enzymes ICF-SOD's and ICF-POD's declined as leaves aged, consequently it was inferred that the level of AOS present would gradually increase in an age-dependent manner.

In order to test this assumption the degree of oxidative modification to proteins and polypeptides (one of the major targets of AOS) can be assessed using an antibody based assay specific for the oxidative modification of proteins induced by the oxidative action of the hydroxyl radical. This is the 'oxyblot kit' described in section 4.4.10.

Equal quantities of ICF Bradford assay quantified (section 4.3.2) protein from the differing leaf developmental ages were therefore analysed for oxidative protein modification and the data are presented in figure 7.20. A general increase in the level of oxidative protein modification, which is specific for AOS, can be seen in the apoplastic extracts as the leaf material progresses through the developmental ages. These data follow the trend of decreasing ICF-SOD and ICF-POD activities observed in figures 7.18 and 7.19 and it is thought that the decreased capacity to detoxify AOS directly elevates the number of oxidative protein modifications.

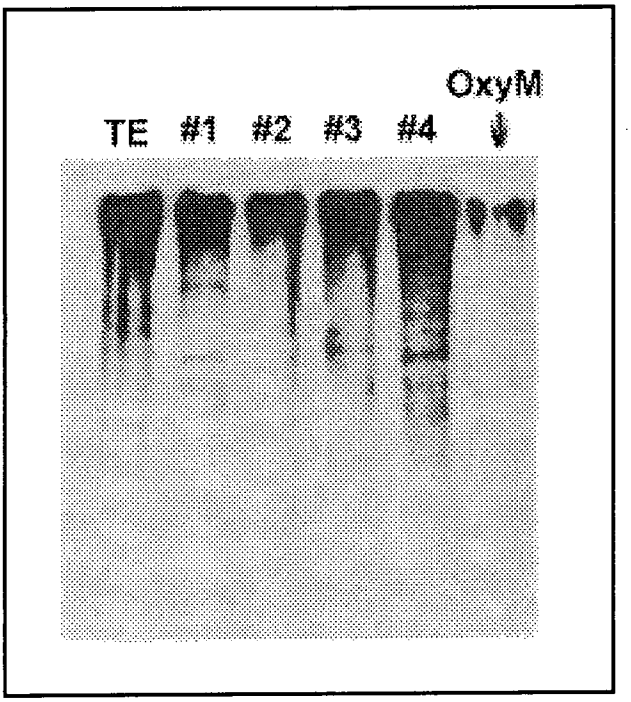

Figure 7.20

Oxidative modification of ICF proteins during leaf development.

ICF's were prepared from leaves at different stages of development as described in section 7.12. Samples and standards were derivatised and run through a 10% (w/v) SDS-PAGE gel (section 4.4.1), blotted to nitrocellulose membrane (section 4.4.9) and antibody probed for oxidative modification to proteins using a commercial kit (Oncor, France; see section 4.4.10); a horseradish peroxidase conjugated secondary antibody was used for detection. Samples are labeled on the oxyblot as progressing from the youngest leaves (#1) through to the senescing (#4). All leaf ICF samples were at 11.7μg of protein and the remainder of the lanes were loaded as follows; Lane 'TE' = 11.7μg; Lane 'OxyM' = 5μl of oxidatively modified marker proteins. All quoted sample concentrations have been

7.4 Conclusions

Utilising native-PAGE, in gel enzyme activity assays and more specific spectrophotometric enzyme assays this part of the study has identified that the tobacco leaf apoplast contains POD's and SOD's that cannot be found inside the cell.

Four distinct guaiacol POD utilising enzyme active bands, which display unique separation patterns in native gels indicating that they have differing properties were visible and clearly not present in TE preparations. Molecular mass estimation revealed that ICF-POD 1 was potentially a disulphide linked dimer composed of two sub-units with identical molecular mass of ~29 kDa, both Salzer & Hager [1993] and Otter & Polle [1997] have reported the isolation of a basic cell wall 'bound' POD enzyme with the same molecular mass as the sub-unit of ICF-POD 1. All of the four identified ICF-POD's were designated as Fe-containing POD's rather than selenium dependent because of their sensitivity to the cyanide ion [Rob *et al.* 1997] and the activity of each was observed to reduce in an age-dependent manner. Very interestingly ICF-POD's 1 & 2 co-migrated in the native-PAGE system with a broad SOD-active band, ICF-SOD 4, and although in an entirely unrelated system, a recent report from Johansson *et al.* [1999] details a cell surface POD that can ionically interact with an extracellular SOD that can only be extracted from cells when treated with a salt solution. It is postulated that the POD-SOD interaction will enhance the efficiency of AOS breakdown via closer proximity of the POD to its substrate. A similar arrangement of anti-AOS enzymes at the plasma-membrane would be beneficial in preventing inadvertent membrane damage from apoplastic AOS.

Five distinct apoplastic SOD active bands were identified, which display unique separation patterns in native gels indicating that they have differing properties. As stated in section 7.2, it is impossible to assign distinct physical characteristics to proteins in native separation systems, but generalisations can be made. ICF-SODs 1, 2, 3 all migrated far into the gel indicating that they are probably small proteins with relatively high pI's. ICF-SOD's 1, 2 and 3 were indeed shown to be composed of small polypeptides ranging between 19 and 25 kDa. Furthermore, ICF-SOD 1 was designated as a CuZn-SOD based on its sensitivity to both cyanide and hydrogen peroxide, Streller *et al.* [1994] and Schinkel *et al.* [1998] have similarly identified apoplastic SOD's from Scots pine needles that have approximately the same molecular mass, are CuZn-SOD's and that have high isoelectric points, it seems likely that ICF-SOD 1 is a very similar tobacco enzyme. The inhibition study also indicated that ICF-SOD 4 is probably a Mn-SOD and that ICF-SOD's 2 and 3 are probably are Fe-containing SOD's. The first plant extracellular Mn-SOD was only identified within the last year [Yamahara *et al.* 1999] and to the authors knowledge the presumed Fe-containing apoplastic SOD's (ICF-SOD's 2 &

3) are the first to be described in plants. An extracellular Fe-SOD has very recently been discovered in bacteria [Shirkey *et al.* 2000] but not in higher organisms and interestingly, it has almost the same molecular mass as ICF-SOD 3. The overall ICF-SOD activity was observed to reduce in an age-dependent manner and the rapid and specific loss of the CuZn-SOD's (ICF-SOD's 1 and 5) was very evident.

The study presented here shows a distinct decline in the activity of SOD and POD extracted from the apoplast, thus indicating that the overall antioxidant capacity of the apoplast also declines in a similar manner to that of the intracellular environment during aging. It was proposed a number of years ago [Thompson 1984] and more recently established [Ferrie *et al.* 1994; Rogiers *et al.* 1998] that the maturation and ripening of fruit is accompanied by a general decline in the ability to cope with AOS. A very recent, and more relevant study by Takahama *et al.* [1999] has detailed a general decrease in leaf tobacco apoplastic anti-AOS compounds, such as ascorbate, depending upon the position of the leaf on the plant (i.e.: the age of the leaf). Surprisingly though, some of the ICF-SOD and ICF-POD activities measured by Takahama *et al.* [1999] predominantly increased as the leaves aged, and then dropped rapidly during senescence. The discrepancy between Takahama *et al.* [1999] and the results displayed herein may be artifactual and arise because of the different methods used for grouping leaves into a particular developmental age. An oxyblot analysis confirmed that an age-dependent loss of apoplastic anti-AOS enzymes results in an age-dependent increase in the levels of hydroxyl radical mediated protein modification, similar results have been obtained for lipid peroxidation [Thompson 1984].

SECTION 8

RADICAL RESPONSES TO STRESS IN THE APOPLAST

8.1 Introduction

The production of active oxygen species (AOS) in the apoplast during plant-pathogen interactions has been well documented [see Mehdy 1994; Wojtaszek 1997 for reviews, section 1.5 and figure 1.5]. In addition to biotic stress, chemical [Kangasjarvl *et al.* 1994], temperature [Fadzillah *et al.* 1996; O'Kane *et al.* 1996], osmotic [Cazalé *et al.* 1998] and mechanical stresses [Jaffe *et al.* 1985; Legendre *et al.* 1993; Yahraus *et al.* 1995] can all induce the production of AOS (see section 1.5 and figure 1.6) although the mode of production is still under investigation. Typically, these studies have quantified the production of hydrogen peroxide from cell suspension cultures as an indicator of the presence of the other AOS. Unfortunately, the use of cell suspension cultures reduces the physiological relevance of the data and the measurement of hydrogen peroxide rather than the 'precursor' molecule, the superoxide anion ($^{\cdot}O_2^-$), is not stress-specific (see figure 1.6). The direct quantification of $^{\cdot}O_2^-$ in leaves during exposure to ozone has been documented [Runeckles & Vaartnou 1997] but required the use of an expensive electron paramagnetic resonance spectrometer and highly specialised knowledge for the interpretation of the resultant data.

Nitric oxide (NO) is an integral component of the inflammatory signalling pathway leading to apoptosis in animals [Kooy *et al.* 1995] and it has recently been postulated that the cell death observed during the hypersensitive response of plants to pathogens is essentially the same mechanism [see Douglas 2000, for an overview]. The first report of nitric oxide involvement in plant defence responses came after Noritake *et al.* [1996] illustrated that NO can induce phytoalexin accumulation in potato. In 1998 Delledonne *et al.* and Durner *et al.* both independently established that the production and release of NO and AOS was integral to hypersensitive cell death during plant-pathogen interactions. Interestingly it is the interplay between NO and $^{\cdot}O_2^-$ to generate the peroxynitrite radical that is proposed to mediate programmed cell death [Sadoval *et al.* 1997], exert direct anti-microbial effects [Mayer & Hemmens 1997] and modulate the activity of a range of other proteins [Ischiropoulos *et al.* 1992; Jiamrong *et al.* 1997; So *et al.* 1998; Souza & Radi 1998]. A more detailed description is provided in section 1.5.4.

The apoplast is central to the interaction of NO and AOS due to the fact that it is one of the primary sites for the generation of AOS [Mehdy 1994; Wojtaszek 1997; Scheel 1998]

and because many of the potential effects of NO and the resultant peroxynitrite radical are postulated to occur in the extracellular environment [Delledonne *et al.* 1998; Durner *et al.* 1998; see section 1.5]. As a consequence, investigation of the apoplastic presence of NO and O_2^- during stress was undertaken.

Throughout this project VI had been utilised as an effective method for selectively sampling proteins and polypeptides from the leaf apoplastic environment. However, the technique was not applied to the study of apoplastic NO and the superoxide anion primarily because apoplastic fluid from tobacco leaf tissue typically had a pink colouration that would have directly interfered with the chosen assay systems and secondly because the lag period between infiltration and recovery was deemed to be too variable. A series of experiments utilising oxyblot analysis (section 4.4.10) had been carried out by S. Johnson [Croy *et al.* 1998; and personal communications with S. Johnson] at the University of Durham. These experiments had inferred that impact stressed potato tuber tissue generated AOS from a small, well defined sub-epidermal site directly below the point of impact. The tuber-impact experimental system offered several important advantages for the study of apoplastic O_2^- and NO in comparison with the standard leaf VI model:-

1. It was important to know that this system had the potential to yield positive results; Croy *et al.* [1998] had already indirectly shown that AOS were present.
2. Because AOS generation in response to impact stress was limited to a very small site it is technically easier to measure AOS/NO generation furthermore, it was possible to excise control tissue from the same tuber and thus reduce any potential variability that may be present between tubers.
3. Providing that the AOS generating site was carefully excised and extensively washed (in a similar manner to leaf pieces during the VI method), it could be assumed with a reasonable degree of certainty that AOS/NO were being produced and/or released in the apoplast in the intact tuber.
4. The reagent used for the quantification of the superoxide anion is expensive; using the tuber-impact system would greatly reduce the costs because relatively small volumes of reagent would be needed.

Consequently, the tuber-impact model system was utilised during this research for the study of apoplastic O_2^- and NO.

The initial work describing the design and optimisation of assays for the detection of the superoxide anion and nitric oxide were originally designed for use with mechanically stressed cell suspension cultures and were carried out solely by the author. Subsequently the assays were applied to a more biologically relavent system, namely the response of potato tubers to impact stress. This latter experimental project was jointly developed with PhD student colleague (Mr. S. Johnson). The effort in this part of the work was equal and has subsequently been submitted as a joint publication to Planta (see appendix 1).

8.1.2 Notes on experimental design

An impact stress of 0.7 joules was applied to one end of the tuber by dropping a bolt of defined weight from a pre-determined standard height. The impact time was designated as time zero and the impact site was marked with a felt-tipped pen. The tuber was either used immediately (zero time point) or incubated for a required period. After incubation the tuber was halved through the impact site with a sharp knife and duplicate half cores (9mm long by 2.5mm radius) were taken from each half of the tuber. Duplicate control cores were excised at the 2 and 10 o'clock positions with respect to the impact site cores (see figure 8.1). Each core was cut into 3x 3mm long sections with a sharp blade and washed extensively for >5 minutes with at least 3 changes of dH_2O to remove any leaked intracellular components. See figure 8.1 for a diagrammatic overview. Tuber pieces were then thoroughly dried with paper towel, placed into individual eppendorf tubes and submerged under 200µl of the radical detection reagents. The tubes were placed in the dark for the 20 minute assay period since both of the radical detection systems have light sensitive components. After 20 minutes the tuber pieces were removed and discarded, and the assay reagents were centrifuged for 5 minutes in a benchtop microfuge (13000g) and the optical density of the supernatants measured against the appropriate reagent blank (see sections 8.2.1 and 8.2.2 for details of each assay system).

8.2 Results

8.2.1 Assay development

In order to quantify the generation of the superoxide anion and nitric oxide from potato tuber tissue assays for the quantitative detection of each molecule were developed.

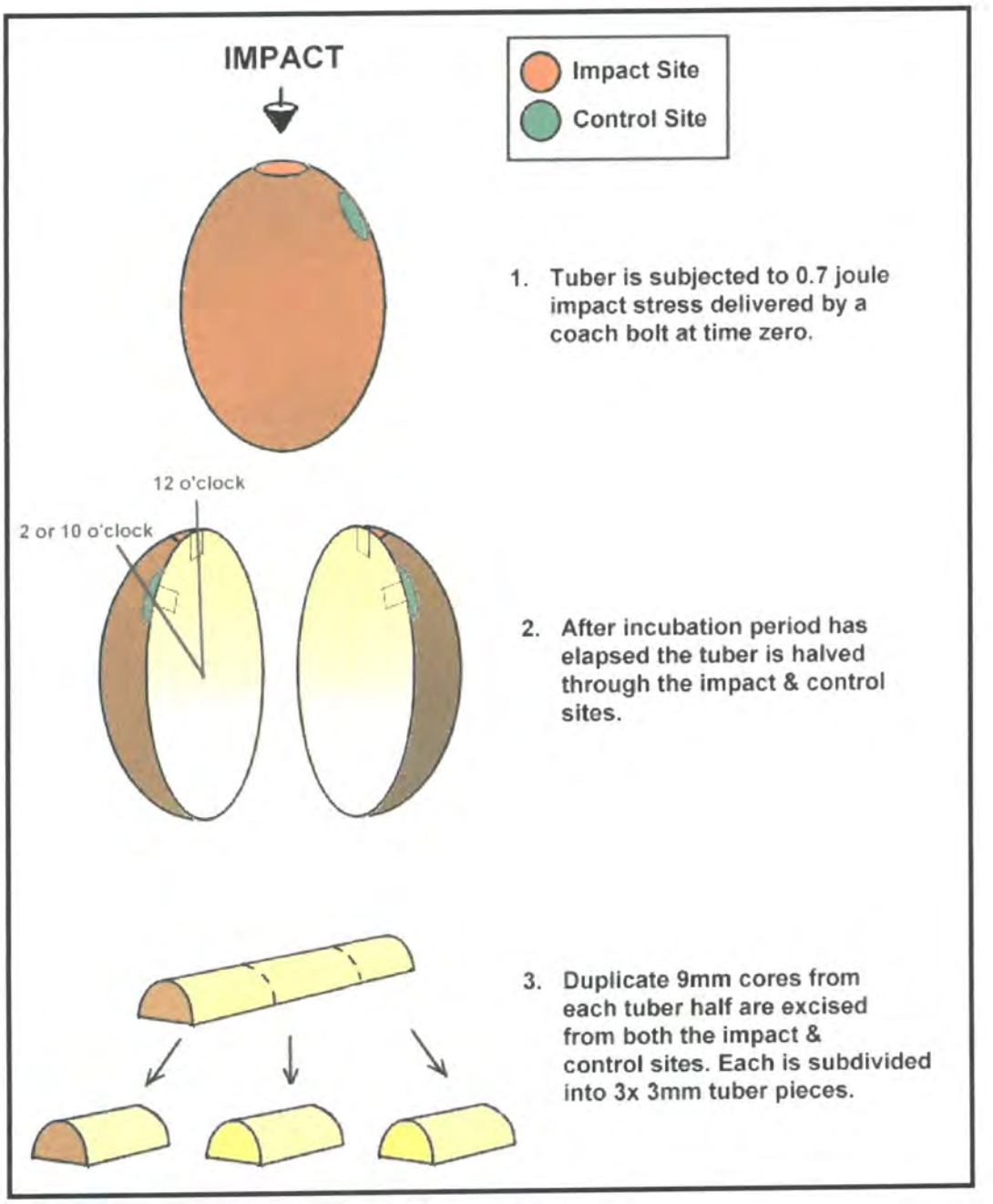

Figure 8.1

Experimental Outline : Impact stress and sample collection.

Image compiled for this thesis; see section 8.1.2 for a detailed explanation.

8.2.1.1 Development of an assay system for the detection of the superoxide anion ($^{\cdot}O_2^-$)

The superoxide anion can be measured directly because of its distinctive physical characteristics; an unpaired electron generates a diagnostic electron paramagnetic resonance spectrum, and unique UV absorption [Marklund 1976]. Unfortunately, neither of these methods is suitable for routine quantification of the superoxide anion in biological systems. The redox protein, cytochrome C has been utilised for superoxide quantification previously, but was not chosen for this study because it has a molecular weight of 12.5 kDa which would hinder efficient diffusion through cell walls to the proposed site of superoxide production, the outer face of plasma-membrane. The hydroperoxyl/superoxide anion acid-base pair ($^{\cdot}O_2H/^{\cdot}O_2^-$ - see section 1.5.1 for details of the chemistry of AOS) selectively reduce tetrazolium compounds producing formazan dyes that can be readily quantified.

Tetrazolium Salt + $^{\cdot}O_2^-$ ⟶ Formazan dye (λ_{max})

Nitroblue tetrazolium has been utilised for the colourimetric detection of the $^{\cdot}O_2H/^{\cdot}O_2^-$ pair, unfortunately, the resulting formazan is relatively insoluble in aqueous solutions, a highly desirable quality for histochemical localisation studies, but less suitable for kinetic or simple quantification studies. Relatively recently a new tetrazolium compound, XTT (2,3-bis-[2-Methoxy-4-nitro-5-sulphophenyl]-2H-tetrazolium-5-carboxanilide) had been utilised successfully for the measurement of $^{\cdot}O_2H/^{\cdot}O_2^-$ in cell suspension cultures during the pathogen-induced oxidative burst [Sutherland *et al.* 1998]. The reduced form of XTT is fully soluble in aqueous solutions thereby obviating the insolubility problems associated with nitroblue tetrazolium, it is also relatively small compared with cytochrome C and consequently will not encounter any diffusion barriers.

The vast majority of AOS-measurement studies have been limited to the quantification of hydrogen peroxide as an indicator of the $^{\cdot}O_2H/^{\cdot}O_2^-$ radical pair, even though hydrogen peroxide is a relatively ubiquitous substrate and by-product of many intracellular and apoplastic processes [Willekens *et al.* 1995; Schopfer 1996]. XTT has been proposed to react selectively with the $^{\cdot}O_2H/^{\cdot}O_2^-$ radical pair [Ewing & Janero 1997] therefore any inadvertent H_2O_2-mediated reduction of XTT (i.e.: cross-reactivity) would elevate the estimated concentration of $^{\cdot}O_2H/^{\cdot}O_2^-$, effectively increasing the level of false positive error in any measurements. Consequently, the cross reactivity of H_2O_2 was assessed by spectrophotometrically following XTT reduction in the presence of H_2O_2 only. Figure 8.2 depicts the data; as can be seen, there was no significant change in optical density at

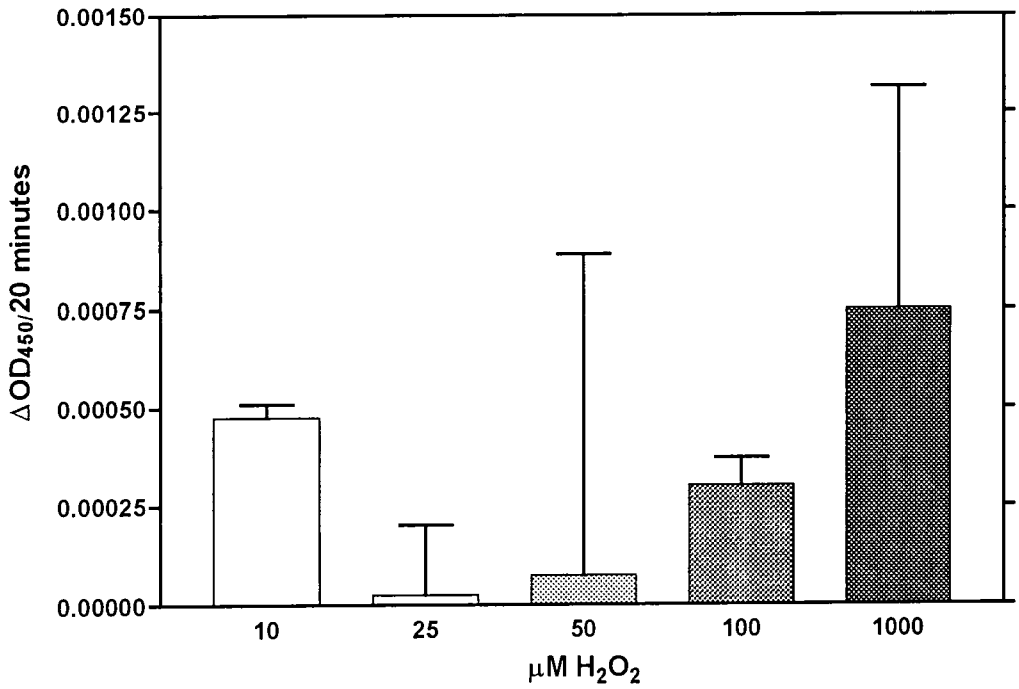

Figure 8.2

Hydrogen peroxide reaction with XTT.

200μl of 50mM phosphate buffer, pH 7.8 containing, 100μM XTT was pipetted into the wells of a microtitre plate. Stock hydrogen peroxide was diluted to form a calibration series of hydrogen peroxide concentration at 0.2, 0.5, 1, 2 and 20mM/ml; a 50μl aliquot of each was added to the XTT solution at time zero and the microtitre plate was then stored in a light proof container until OD_{450} (optical density) was measured after 20 minutes against an XTT control lacking H_2O_2. The final concentration of hydrogen peroxide per mixture is show on the abiscca. Data are the means of ± SD of four measurements.

λ_{max} for the reduced formazan over a 20-minute period, thereby indicating that hydrogen peroxide and XTT do not cross-react.

In order to verify the efficacy of the $^{\cdot}O_2H/^{\cdot}O_2^-$-induced reduction of XTT, a method to artificially generate $^{\cdot}O_2^-$ radicals was employed. Commonly, superoxide generating systems utilise the enzyme xanthine oxidase however, xanthine oxidase alone can also induce reduction of related tetrazolium compounds (e.g.: nitroblue tetrazolium) [Beauchamp & Fridovich 1971] thus causing an increase in false positive error, consequently it was not chosen for this study. Instead a non-enzymatic system of superoxide anion production was adopted utilising aerobic mixtures of NADH and phenazine methosulphate (PMS) [Ewing & Janero 1997].

$$_{[red]}PMS + O_2 + NADH \longrightarrow {}_{[ox]}PMS + {}^{\cdot}O_2^- + NAD^+ + H^+$$

It is known that the superoxide anion generated from either biological material or chemically via the PMS-NADH system dismutates to hydrogen peroxide and oxygen with increasing rapidity from basic through to acidic pH [Oberly & Spitz 1996]. In order to ensure accurate assay of the superoxide generated from either biological material or chemically via the PMS-NADH system, the pH was adjusted to ensure the longevity of the $^{\cdot}O_2H/^{\cdot}O_2^-$ pair and therefore to maximise the chance of XTT reduction. Figure 8.3 depicts the results of this experiment. At the pH extremes measured (<7.5 and >8.7), XTT reduction dropped markedly indicating that the $^{\cdot}O_2H/^{\cdot}O_2^-$ pair were dismutating at a faster rate or that the PMS-NADH system was not producing as much superoxide at these pHs. XTT reduction was maximal between pH 7.5 and 8.7 indicating that there was a stable concentration of the $^{\cdot}O_2H/^{\cdot}O_2^-$ pair in the reaction mixture and that the reduction of XTT was occurring at a relatively constant rate. A proportion of the superoxide may be dismutating into hydrogen peroxide and oxygen, but a 'fixed' quantity is reacting with XTT. The remainder of the experiments for setting up the superoxide detection assay and those described later with sample material were carried out at pH 8.2 to ensure maximal reaction rate between superoxide and XTT.

When attempting to quantify the $^{\cdot}O_2H/^{\cdot}O_2^-$ from intact biological samples it was essential to ensure that the concentration of XTT (i.e.: the radical scavenger) was saturated. In this state the reduction of XTT and hence colour formation by the superoxide anion is maximal. Reacting varying concentrations of the radical scavenger, XTT with the standard PMS-NADH-superoxide generating system assessed this, figure 8.4 shows the data. The reaction rate between superoxide and XTT, as determined by optical density change per minute, was shown to be greatest at XTT concentrations of ≥120μM, illustrating that the reaction was proceeding at a maximal rate. XTT in the PMS-NADH-

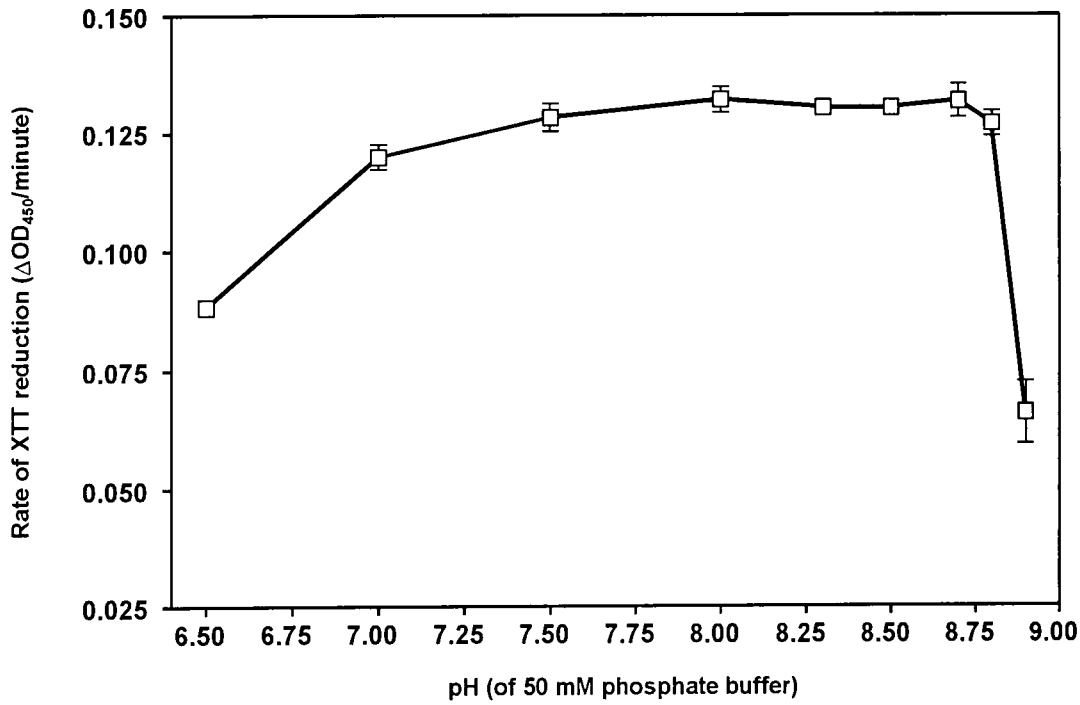

Figure 8.3

The reaction between XTT and superoxide with varying pH.

200μl of 50mM phosphate buffer, pH in the range 6.5-8.9, containing, 0.1mM EDTA, 100μM XTT and 98μM NADH were pipetted into the wells of a microtitre plate. Superoxide radical production was initiated with 50μl of 14μM PMS in 50mM phosphate buffer, pH in the range 6.5-8.9. OD_{450} was measured every 30 seconds over 3 minutes from which ΔOD_{450}/minute was calculated. Then data are the means of ± SD of four measurements.

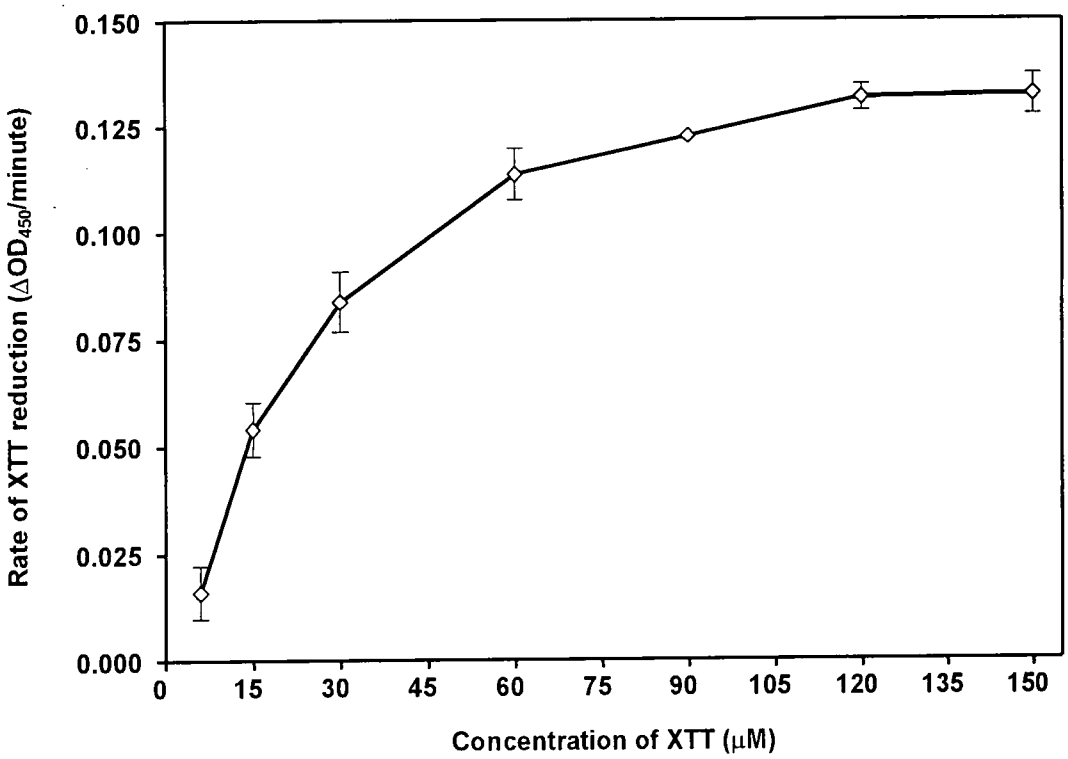

Figure 8.4

Determination of optimal XTT concentration for superoxide detection.

50mM phosphate buffer, pH 8.2 containing, 80μM EDTA, 78.4μM NADH and 6-150μM XTT. The reaction was initiated with a final PMS concentration of 2.8μM. The optical density was read at 2 minutes from which ΔOD_{450}/minute was calculated. The final concentration of XTT/assay is displayed on the abscissa. Data are means of ± SD of four measurements.

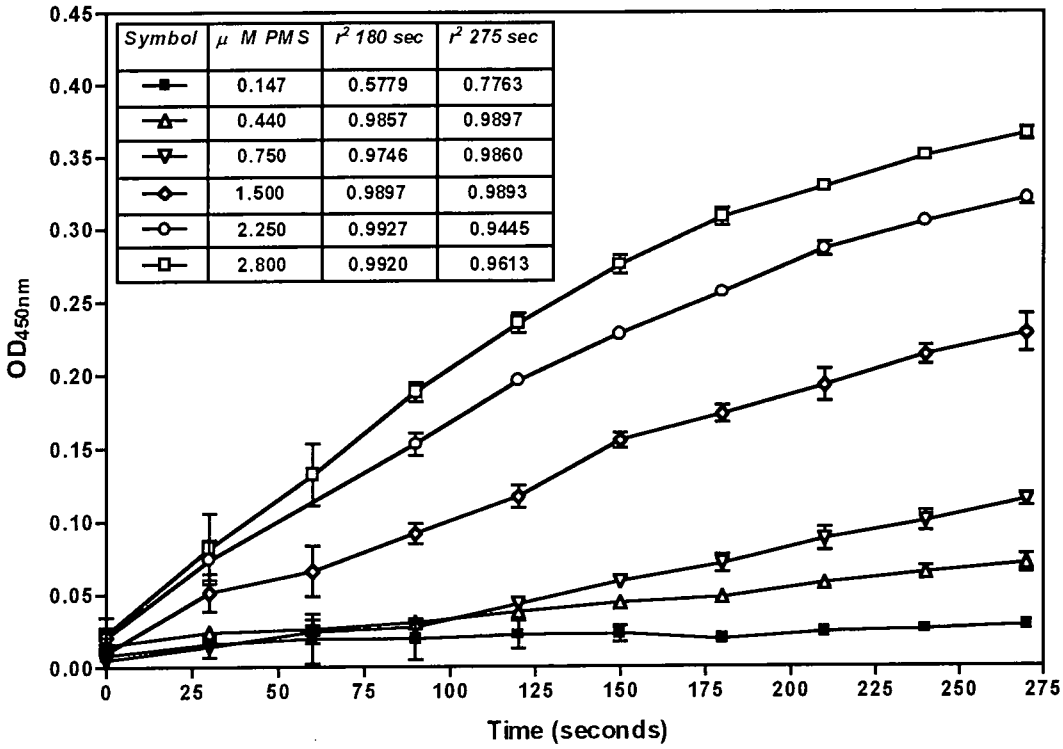

Figure 8.5

Progress of radical generation by the PMS-NADH system.

200μl of 50mM phosphate buffer, pH 8.2 containing, 0.1mM EDTA, 150μM XTT and 98μM NADH were pipetted into the wells of a microtitre plate. Superoxide radical production was initiated with 50μl of varying concentrations of PMS in 50mM phosphate buffer, pH 8.2. OD_{450} was measured every 30 seconds over 4.5 minutes. The key for the symbols, the final concentration of PMS/assay and the resultant correlation coefficients (r^2) for 180 and 275 second measurements is displayed in the box on the graph. The data are the means of ± SD of four measurements

superoxide generating system at concentrations ≥120μM is effectively saturated with respect to its reaction with superoxide and consequently it is acting as an efficient radical scavenger.

Preliminary investigations using mechanically stressed tuber tissue indicated that in order to obtain a reasonably measurable optical density change (set at ~0.1 ΔOD U) tuber tissue needed to be incubated for approximately 20 minutes (data not shown). During this assay period it was necessary to ensure that the concentration of XTT did not fall below the saturation concentration of 120μM. Figure 8.5 illustrates the concentration-dependent superoxide production by the PMS-NADH system that is ultimately dependent upon the electron donor, PMS. At a PMS concentration of 2.8μM linearity of XTT reduction is evident for the first 3 minutes of the reaction (r^2=0.9920, p<0.0001), illustrating that during this period there is enough XTT to react with the radicals at a maximal rate. Beyond 3 minutes linearity is lost (r^2=0.9613, p<0.0001) indicating that either the generation of the superoxide anion has decreased or that the XTT concentration has dropped below the saturation level of 120μM. Adding additional XTT to the reaction mixture results in a resumption of optical density increase showing that it is not superoxide generation that has slowed but XTT reduction (data not shown). Using the published extinction coefficient for XTT at λ_{max} of 2.16 x 10^4 M^{-1} cm^{-1} [Sutherland & Learmonth 1997] and the change in optical density reading of 0.125 Δ_{450}/min it can be calculated that 4.34 nMoles of $^{\cdot}O_2H/^{\cdot}O_2^-$ reacted with XTT before its concentration drops below the saturation threshold of 120μM. Providing the biological system under study does not produce more than 4.34 nMoles in the 20 minute assay period an XTT saturation state will be maintained. Able *et al.* [1998] quantified $^{\cdot}O_2H/^{\cdot}O_2^-$ generation from tobacco cell suspension cultures using XTT, and calculated that 0.6 nMoles of $^{\cdot}O_2H/^{\cdot}O_2^-$/g fresh weight/min, scaling to 20 minutes gives, 12 nMoles $^{\cdot}O_2H/^{\cdot}O_2^-$/g fresh weight. This is greatly exceeds the saturation range of XTT calculated within this work, but it should be noted that the tissue pieces used within these experiments were much smaller than one gram and weighed of the order 30-35mg. Consequently reducing the XTT concentration below the saturation level should not occur providing a 35mg piece of tuber tissue does not generate >4.34 nMoles $^{\cdot}O_2H/^{\cdot}O_2^-$ over a 20 minute assay period, this effectively equates to ~124 nMoles $^{\cdot}O_2H/^{\cdot}O_2^-$/g/20 minutes, a very large quantity of superoxide ! The final assay set-up is concisely described in section 4.3.5.

8.2.1.2 Development of an assay system for the detection of the nitric oxide (NO)

A number of colourimetric, fluorometric and chemiluminescent assays for quantification of nitric oxide (NO) released from S-nitrothiol compounds (see section 1.5.4) have been

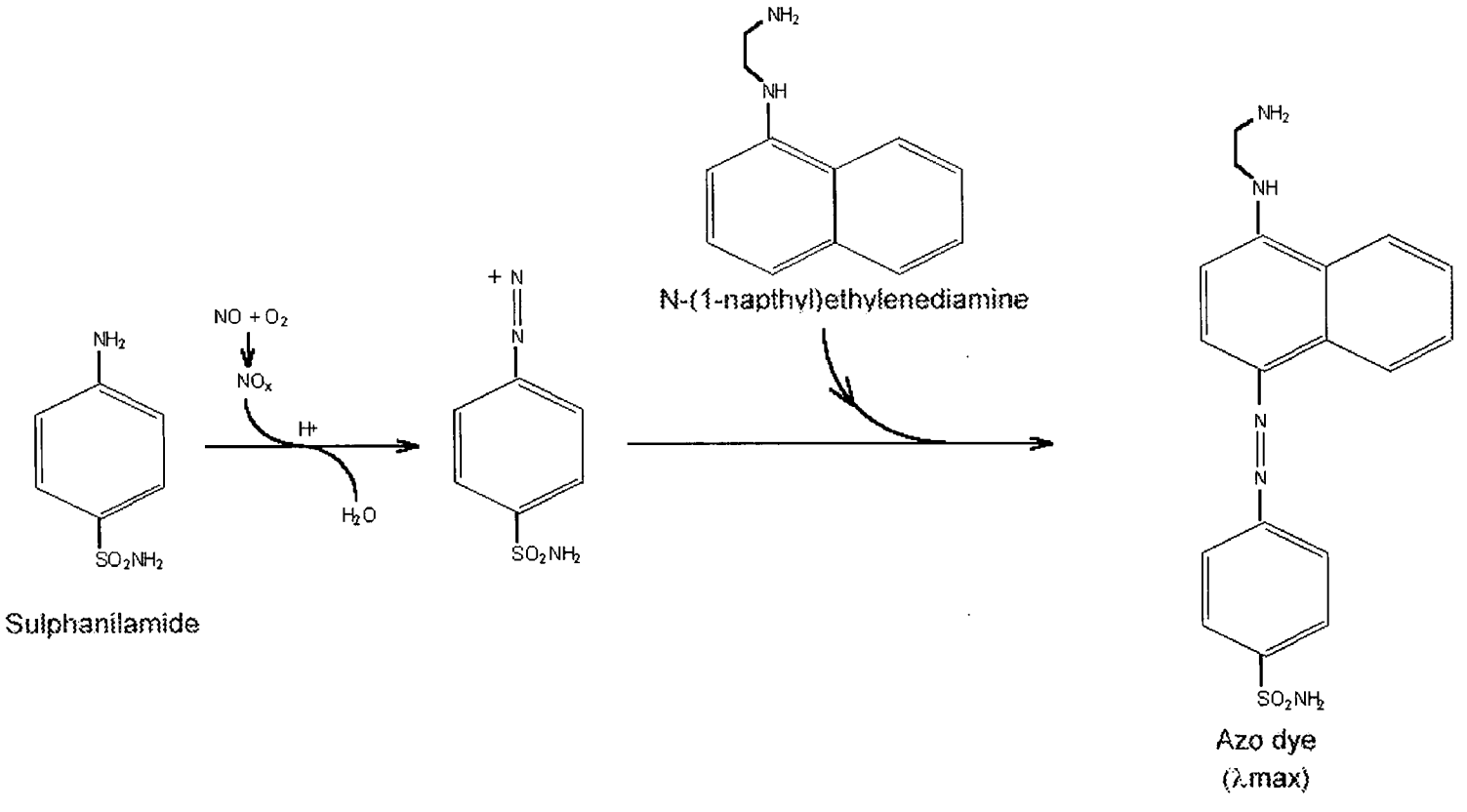

Figure 8.6 **The reaction of the Neutral Griess reagent with ·NO.**
Adapted from Cook *et al.* 1996.

described previously [Cook *et al.* 1996]. The method chosen relies upon the spontaneous reaction of NO and molecular oxygen to form nitrite compounds (NO_x) which react with the neutral Griess reagent (composed of sulphanilamide (SULF) and N-(1-napthyl)ethylenediamine dihydrochloride (NEDD)) to form an azo dye [Nims *et al.* 1995]. A simplified reaction scheme is presented in figure 8.6. Utilising this reaction has several distinct advantages over other methods of quantification, importantly no extremely toxic or hazardous chemicals are used, the reaction occurs maximally at neutral pH (±1 pH unit) and finally, no major alterations to the experimental set-up described in section 8.1.2 are required. Consequently, because measurements for both NO and the $O_2^{\cdot}$ are taken in exactly the same manner they will be directly comparable and error introduced by altering the experimental system to accommodate a different type of measurement will be greatly reduced.

A major consideration when considering the independent measurements of the superoxide anion and nitric oxide was whether the independent assay systems would cross-react. Figure 8.7 confirms that superoxide anions generated by the PMS-NADH system do not cross-react with the SULF-NEDD NO detection system thereby illustrating that azo dye formation and consequent colour change will reflect NO concentration only.

In order to verify the efficacy of NO detection using the SULF-NEDD assay a chemical means of NO production was employed. Sodium nitroprusside (SNP) releases NO when exposed to a reducing agent such as dithiolthreitol (DTT) [Delledonne *et al.* 1998]. Figure 8.8 depicts the production profiles of NO from varying concentrations of SNP by 10mM DTT utilising the SULF-NEDD assay system over a 20-minute period. After an 18-minute period absorbance plateaued at all SNP concentrations, effectively all the NO had been released and had reacted with the SULF-NEDD reagent. This can be illustrated by the addition of more SNP - the optical density increase is effectively resumed (data not shown). Taking these data and plotting them as a 20-minute end point optical density at λ_{max} (figure 8.9) it is immediately obvious that the reaction is linear, with respect to NO chemically released from SNP (r^2=0.9975; $p<0.001$), the reaction is therefore maximal and the assay is quantitative. Using the published extinction coefficient for the SULF-NEDD reagent of 12,500 M^{-1} cm^{-1} [Nims *et al.* 1995] the 400μM and 100μM SNP concentrations are releasing approximately 3.5 nMoles and 0.4 nMoles of NO over the 20 minute period respectively, these figures are in approximate concordance with published concentrations of NO produced by plant systems [Delledonne *et al.* 1998]. The final assay set-up is concisely described in section 4.3.6.

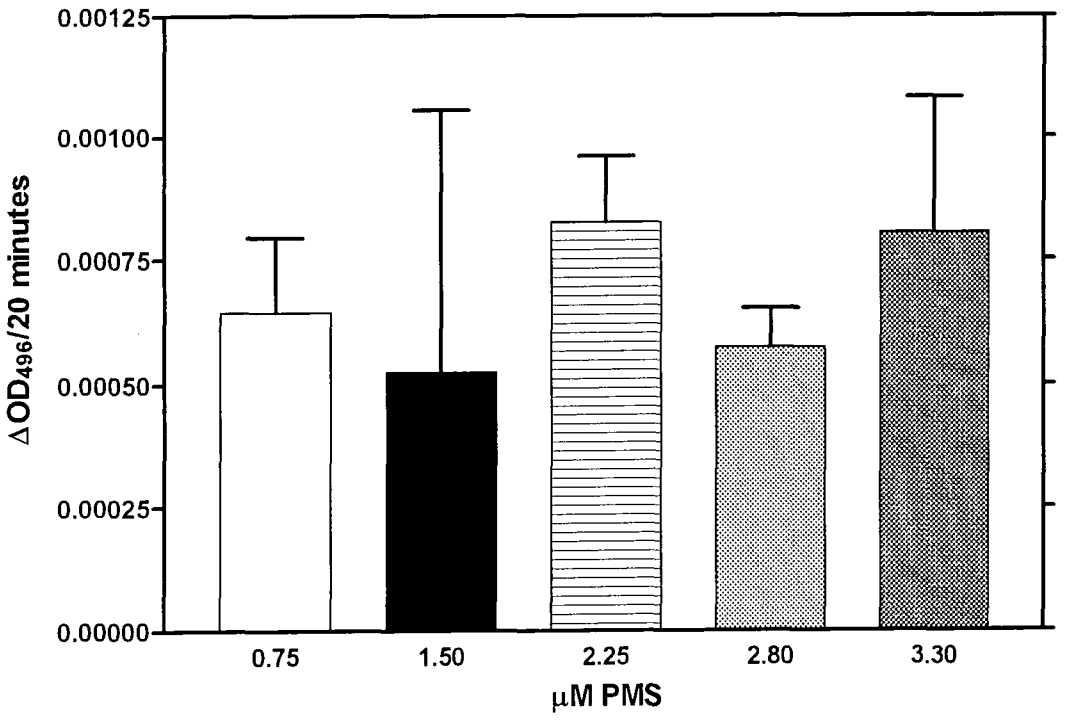

Figure 8.7

Superoxide anion cross-reaction with the SULF-NEDD reagent.

100μl of 50mM phosphate buffer, pH 7.8 containing 114mM SULF and 2.4mM NEDD were pipetted into the wells of a microtitre plate, to each a further 100μl of 50mM phosphate buffer, pH 7.8 containing 0.2μM EDTA and 196μM NADH were added. At time zero a 50μl aliquot of varying concentrations of PMS dissolved in 50mM phosphate buffer, pH 7.8 was added to each well in order to initiate superoxide anion generation. The microtitre plate was then stored in a light proof container until OD_{496} was measured at time 20 minutes against a blank in which PMS was replaced was buffer. The final concentration of PMS per mixture is show on the abiscca. The data are the means of ± SD of four measurements

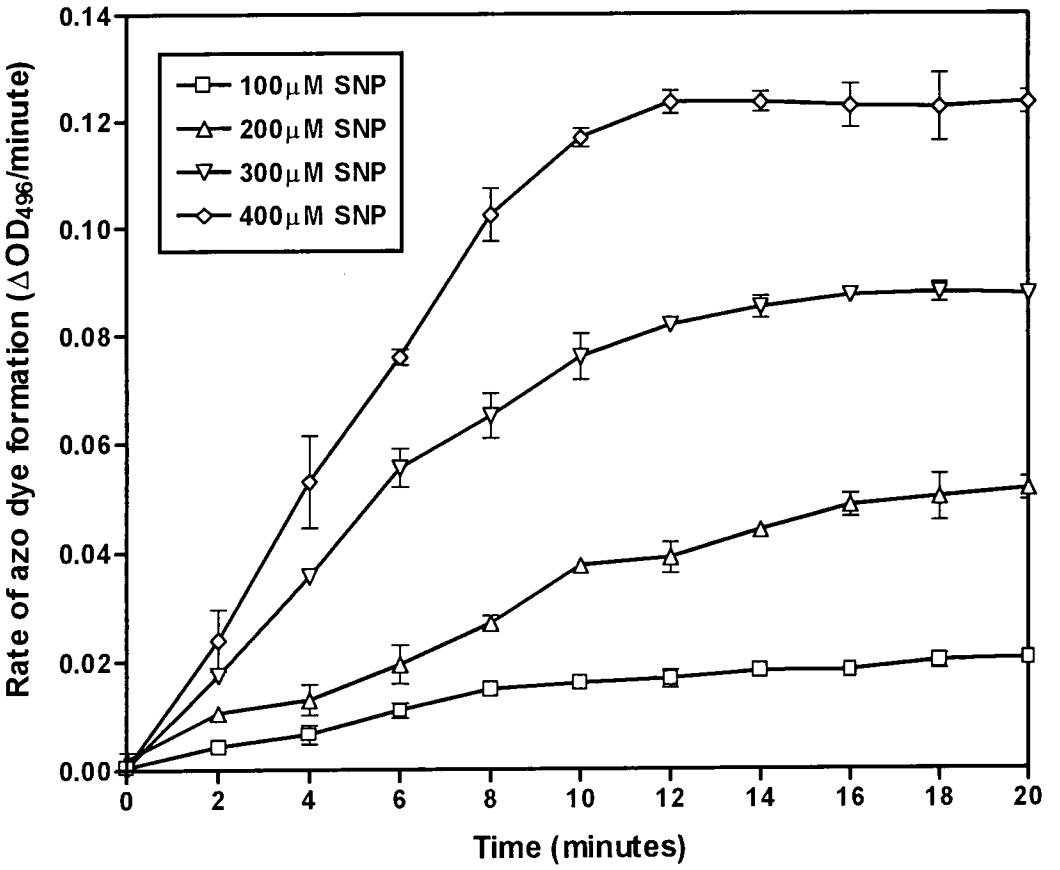

Figure 8.8

Azo dye formation produced by NO liberated from SNP.

100μl of 50mM phosphate buffer, pH 7.8 containing 114mM SULF and 2.4mM NEDD were pipetted into the wells of a microtitre plate, to each a further 100μl of 50mM phosphate buffer, pH 7.8 containing varying concentrations of SNP was added and mixed. At time zero a 50μl aliquot of 50mM phosphate buffer, pH 7.8 containing 50mM DTT was added to each well in order to initiate NO liberation from SNP. OD readings at 490nm were taken every 2 minutes over a 20 minute period versus a buffer control (lacking DTT), between readings the microtitre plate was stored in a light proof container. The final concentration of SNP in each mixture is shown in the box. The data are the means of ± SD of four independent measurements.

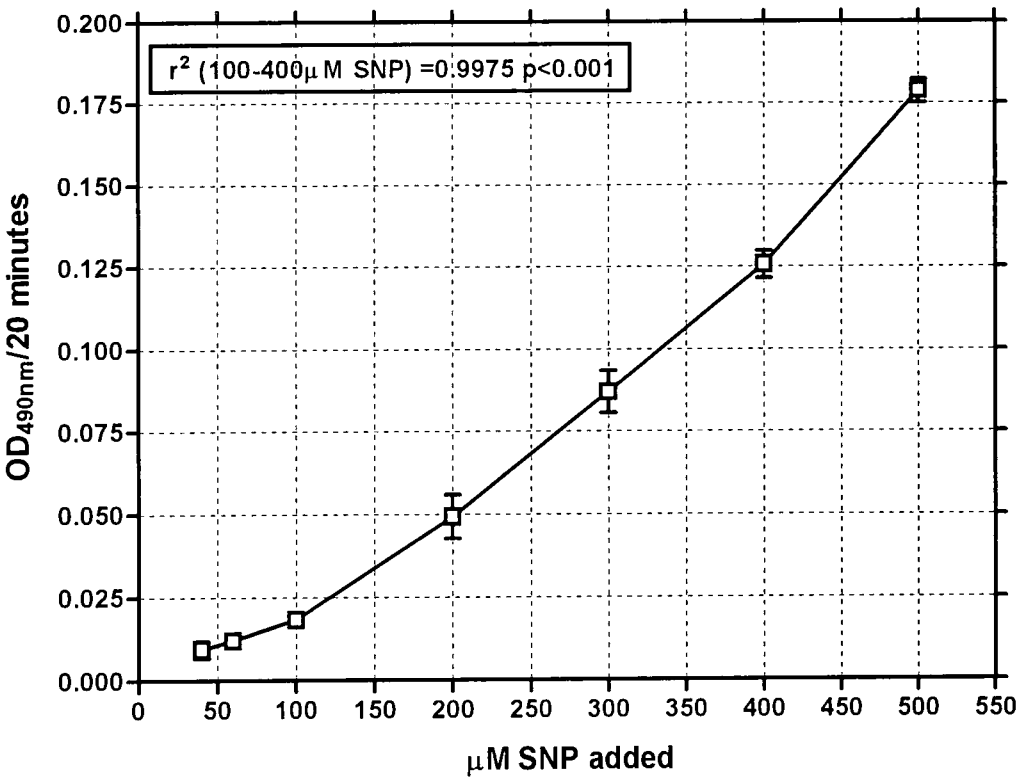

Figure 8.9

Detection of reaction between SULF-NEDD and NO liberated from SNP at different concentrations.

100μl of 50mM phosphate buffer, pH 7.8 containing 114mM SULF and 2.4mM NEDD were pipetted into the wells of a microtitre plate, to each a further 100μl of 50mM phosphate buffer, pH 7.8 containing varying concentrations of SNP was added and mixed. At time zero a 50μl aliquot of 50mM phosphate buffer, pH 7.8 containing 50mM DTT was added to each well in order to initiate NO liberation from SNP. OD was measured at 490nm after 20 minutes versus a control (lacking DTT); the microtitre plate was stored in a light proof container until read. The final concentration of SNP in each mixture is shown in the box. The data between 100 and 400μm of SNP have been subjected to linear regression, the data is presented in the box on the graph. The data are the means of ± SD of four independent measurements.

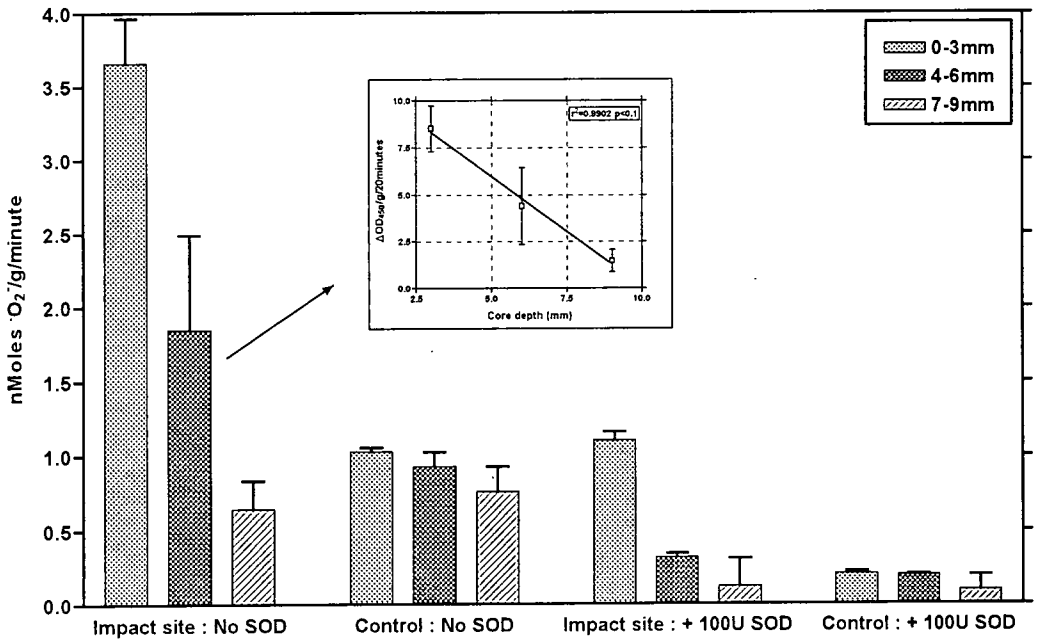

Figure 8.10

Measurement of the superoxide anion produced by impact stressed tuber tissue.

Experimental design described in section 8.1.2 and the final assay is presented in section 4.3.5. Briefly, the tuber was subjected to impact, the impact site was then marked and the potato incubated for 4 hours at room temperature. Duplicates cores were taken from both the impact site and a control site and incubated in the 50mM phosphate buffer, pH 8.2, 150μM XTT; in the presence or absence of 100U of SOD (Sigma, UK), at ambient temperature in the dark. Tuber tissue was removed from the reagents after 20 minutes and discarded, the reagents were then centrifuged for 5 minutes and the OD of the supernatant at 450nm measured. The data are the means of ± SD of 4 measurements. The inset graph illustrates the decreasing linear response of superoxide production from tuber tissue as cores are taken deeper into the impact stressed tuber; the data was derived from 'Impact site: No SOD' data presented on the main graph. The key (top right) indicates depth of core into the tuber.

8.2.2 Superoxide anion quantification from tuber tissue

Mechanical stress has been stated as a trigger for the generation of AOS in plants [Jaffe *et al.* 1985; Legendre *et al.* 1993; Yahraus *et al.* 1995] and specifically potato [Croy *et al.* 1998]. A preliminary study was carried out to test the superoxide assay developed in this study using mechanically stressed tuber tissue (c.v. King Edward), figure 8.10 depicts the data. Superoxide anion production was shown to be approximately four times as great at the impact site at 4 hours post impact stress when compared with the control site. This can be reduced to level of the control site by the addition of 100U of the anti-AOS enzyme superoxide dismutase (see section 1.5.3). This therefore confirms that it is the superoxide anion that is causing the optical density change. The control site manifests approximately 25% of the superoxide generation that the impact site exhibits. It is assumed that this high background level of superoxide anion generation is induced by the general trauma and mechanical stress imposed upon the tuber in order to recover the core for quantitative superoxide measurement. This background level of superoxide anion generation can effectively be reduced to zero by incubation with 100U of superoxide dismutase.

These data effectively illustrate that we have a largely localised and specific generation of the superoxide anion at the impact site that is preferentially confined to the outer 3mm of the tuber (see figure 8.10). Progressing a few millimetres more into the tuber and the production of superoxide tails off indicating a spatial regulation of superoxide generation. The inset graph on figure 8.10 illustrates that this constant reduction of superoxide generation bears a linear relationship with depth into the tuber core (r^2=0.9902; $p<0.1$). Consequently, in order to maximise and standardise all subsequent superoxide measurements they were conducted using only the outer 3mm of tuber tissue.

Figure 8.11 depicts the data derived from a preliminary time course experiment using c.v. King Edward potatoes and shows that between 4 and 6 hours the impact site generates upto 4 times more superoxide than the control site. During this period the difference in superoxide generation between the impact and control sites is statistically significant ($p<0.05$) and clearly illustrates that the generation of the superoxide anion is regulated with respect time.

Even though subsequent repeats of this experiment re-confirmed the general trend of greater superoxide anion generation from the impact site (data not shown), the data were generally more variable. It is well documented that the nutrient supply during growth, tuber age, storage temperature [see Peters 1996 for a review] and previous impact status [S. Johnson, personal communication] all have a profound effect upon the ability of tuber material to respond to impact stress. The tuber material utilised for these trial experiments

Figure 8.11

Preliminary time course of superoxide anion production from impact stressed tuber tissue.

Experimental design described in section 8.1.2 and the final assay is presented in section 4.3.5. The experiment was carried out using shop bought King Edward potatoes and the data is presented on the graph. The data from the control site and the impact site were statistically assessed (using GraphPad Prism software) to evaluate if there was any significant difference between the two data sets; this is shown below the graph. P-value summary key; ns=no significant difference; *=significant difference ; **=very significant difference.

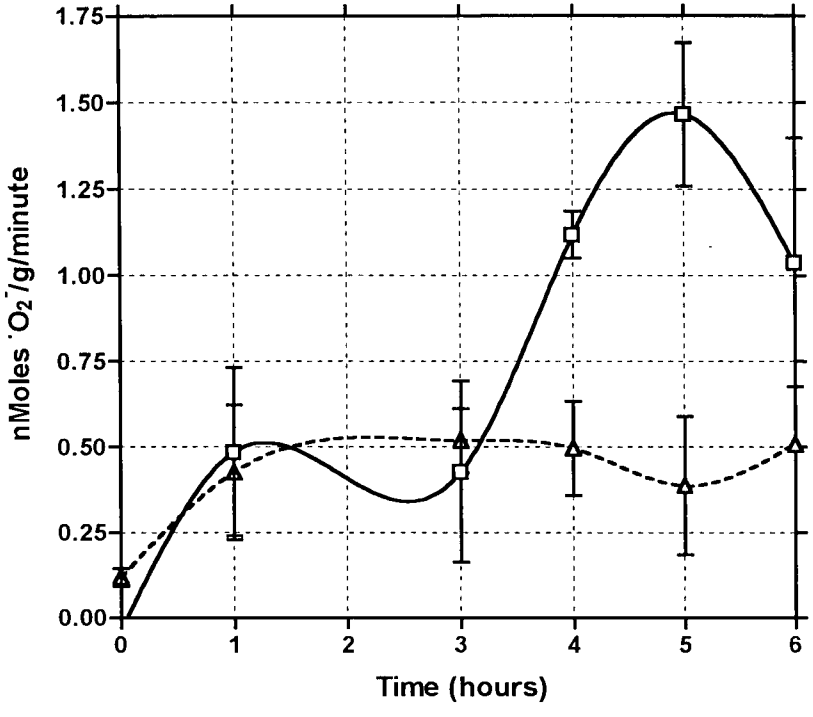

Parameter	Value
P value	0.0730
P value summary	ns
Are means signif. different? (P < 0.05)	No
One- or two-tailed P value?	One-tailed
t, df	t=1.721 df=5
Number of pairs	6

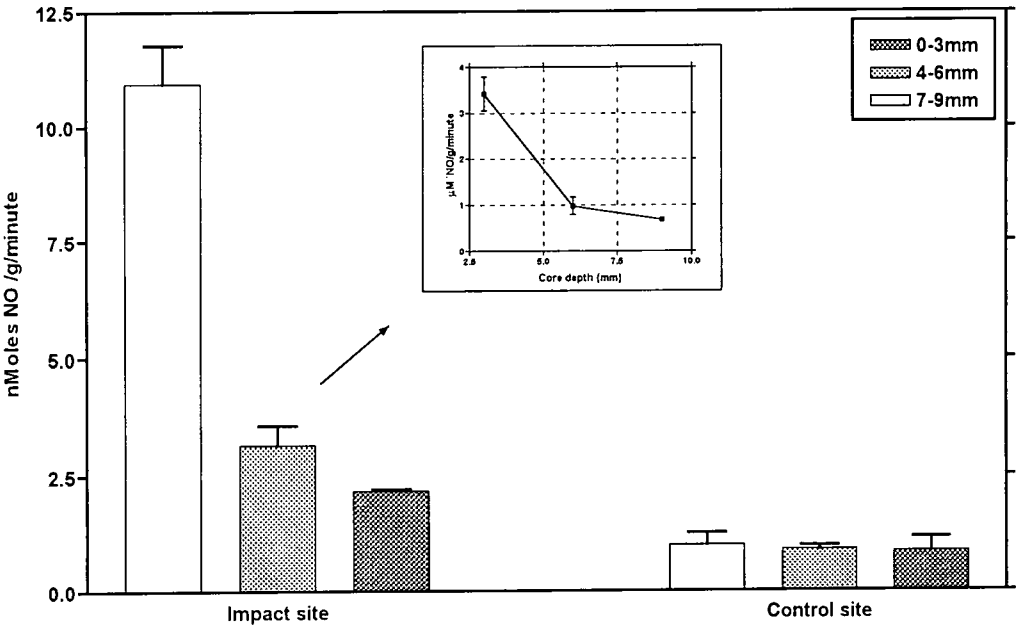

Figure 8.12

Nitric oxide production from impact stressed tuber tissue.

Experimental design described in section 8.1.2 was used and the final assay is presented in section 4.3.6. Briefly, the tuber was subjected to impact, the impact site was then marked and the potato incubated for 4 hours at room temperature. Duplicates cores were taken from both the bruise site and a control site and incubated in the 50mM phosphate buffer, pH 7.8, containing 114mM SULF and 2.4mM NEDD in the dark. Tuber tissue was removed from the reagents after 20 minutes and discarded, the reagents were then centrifuged for 5 minutes and the OD of the supernatant at 496nm measured. The data are the means of ± SD of 4 measurements. The inset graph illustrates the decreasing production of nitric oxide production from tuber tissue as cores are taken deeper into the impact stressed tuber; the data was derived from 'Impact site: No SOD' data presented on the main graph. The key (top right) indicates depth of core into the tuber.

had been bought from a local supermarket outlet and consequently were not of known history.

8.2.3 Nitric oxide quantification from tuber tissue

A preliminary experiment to establish if NO generation and consequent quantification could be achieved in intact tuber tissue (c.v. King Edward) and to indicate the degree and type of spatial regulation of nitric oxide generation was undertaken in the same manner as for superoxide anion detection (section 8.2.2). Figure 8.12 depicts the data. In a broadly similar way to superoxide anion generation observed in figure 8.10, NO appears to be spatially regulated, with higher quantities found locally at the impact site when compared with the control site. Furthermore, the quantity of NO generated drops off markedly as the core depth increases, though the actual spatial kinetics of generation do not bear the linear relationship that superoxide appears to (see inset graph, figure 8.12).

These data illustrate a number of points, firstly, impact stressed potato tuber tissue generates NO, secondly this impact stress induced NO generation is highly localised to the outer 3 mm of the tuber, at the impact site, and finally, as the experimental core is excised from deeper into the tuber the production of NO rapidly tails off indicating a very tight spatial regulation of NO generation. In order to maximise and standardise all subsequent nitric oxide measurements only the outer 3mm of tuber tissue was utilised.

Repeated nitric oxide determination with supermarket tuber material proved just as variable as described in the superoxide quantification experiments (section 8.2.2). It was assumed that the inconsistency stemmed from the same problems – variation in tuber age and potential pre-laboratory impact damage.

8.2.4 $^{\cdot}O_2^-$ and NO generation in different potato varieties

As stated in sections 8.2.3 and 8.2.4, repeated time course experiments produced variable and less consistent superoxide anion and nitric oxide generation profiles. Likely probable causes of this inconsistency included, tuber age and impact damage prior to arriving at the laboratory. Consequently, it was deemed necessary to acquire potatoes from a more consistent source. The potato research council out-station at Sutton Bridge, Lincolnshire were able to supply a variety of hand collected potatoes that had a known history. Each of these potato varieties were known to have differing degrees of susceptibility to impact damage and consequently provided an excellent opportunity to investigate superoxide and nitric oxide production from impact and control sites within

tubers with varying susceptibility to impact damage. S. Johnson had tested a number of potato varieties for their susceptibility to impact damage, the data are presented below. The arrow diagram below graphically depicts a linear scale of impact susceptibilty calculated by the propensity of a tuber to form a bruise (depth of colour and size) in response to impact stress. This index of impact susceptibilty was carried out by S. Johnson at the University of Durham.

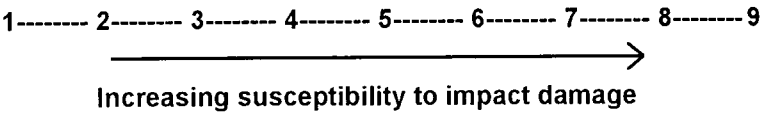

Tuber variety	Susceptibility Index
Maris Piper	2
King Edward	4
Saturna	8
Russet Burbank	9

Each of these varieties was tested independently for the generation of the superoxide anion (see figures 8.13 graphs A-D) and the nitric oxide molecule (see figure 8.14 A and B) over the six hours after an impact stress had been imposed (see section 8.1.1 for experimental design).

Comparisons of the four superoxide time courses reveal that the overall duplicate measurements of superoxide generation were more stable and less variable using tubers with a known history (compare error bars between figures 8.12 and 8.13 A-D). These data are presumably reflect the greater consistency in growth conditions, storage and impact status of the potatoes from Sutton Bridge. Note also the consistency of superoxide generation at the control sites during all four time courses, generation remained relatively stable over the whole assay period, regardless of which potato variety is being tested (<1.5 nMoles O_2^-/g/minute). It was concluded from these observations that the control site is in fact generating a 'background' level of the superoxide anion, that is assumed to be produced as a response to the stress of excising the core for analysis.

Figure 8.13 (A and B) graphically presents the time course experiments for the impact resistant varieties (King Edward and Maris Piper). They both exhibited very little difference between the control and impact sites; and in fact, if we discount the King Edward four hour time point, the impact sites of both varieties stay below the control site superoxide level found in all varieties of <1.5 nMoles O_2^-/g/minute. Overall, no statistically

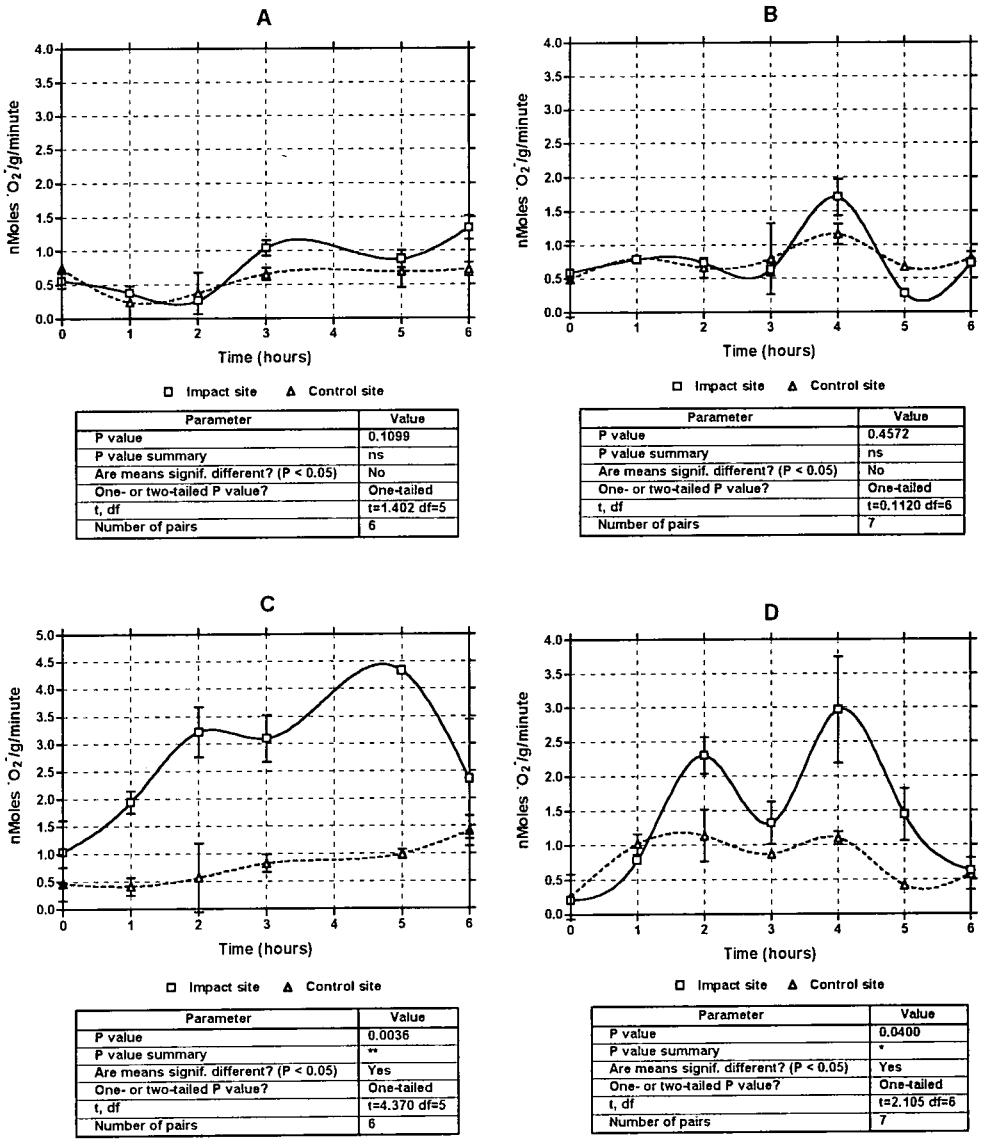

Parameter	Value
P value	0.1099
P value summary	ns
Are means signif. different? (P < 0.05)	No
One- or two-tailed P value?	One-tailed
t, df	t=1.402 df=5
Number of pairs	6

Parameter	Value
P value	0.4572
P value summary	ns
Are means signif. different? (P < 0.05)	No
One- or two-tailed P value?	One-tailed
t, df	t=0.1120 df=6
Number of pairs	7

Parameter	Value
P value	0.0036
P value summary	**
Are means signif. different? (P < 0.05)	Yes
One- or two-tailed P value?	One-tailed
t, df	t=4.370 df=5
Number of pairs	6

Parameter	Value
P value	0.0400
P value summary	*
Are means signif. different? (P < 0.05)	Yes
One- or two-tailed P value?	One-tailed
t, df	t=2.105 df=6
Number of pairs	7

Figure 8.13

Time course of superoxide anion production from impact stressed tuber tissue of different varieties.

Experimental design is described in section 8.2.1.1 and the final assay is presented in section 4.3.5. The experiments were carried out with Maris Piper (graph A), King Edwards (graph B), Russet Burbank (graph C) and Saturna (graph D) potato varieties. The data from the control site and the impact site were statistically assessed (using GraphPad Prism software) to evaluate if there was any significant difference between the two data sets; this is shown below each graph. P-value summary key; ns=no significant difference; *=significant difference; **=very significant difference

significant difference was found between the impact and control sites in either King Edward or Maris Piper impact resistant potato varieties.

The impact susceptible varieties exhibited a very different superoxide generation response than the impact resistant varieties. Figure 8.13 (C) graphically depicts the data for superoxide anion generation over a 6 hour period, post impact damage at the impact and control sites for the impact susceptible potato variety, Russet Burbank. It is immediately obvious that superoxide generation levels at the control site are generally low and relatively stable over the six-hour period, they could be possibly described as, 'basal' and probably arise because of tissue damage caused during core excision (see above and section 8.2.2). However, the impact site exhibits a massive and concerted increase in the production and liberation of the superoxide anion into the extracellular medium, peaking at 5 times the quantity produced at the control site after approximately 4.5 hours. Statistically the production of the superoxide anion at the impact site is significantly different from production of the superoxide anion at the control site, thus reflecting the spatial regulation of superoxide production. Similarly, the other impact susceptible variety, Saturna (figure 8.13, graph D) exhibited a statistically significant difference in superoxide anion generation between the control and impact sites. Most interestingly, the superoxide generation response in both impact susceptible varieties exhibited a distinct biphasic nature, with a peak in generation at approximately 2 hours followed later by a greater generation of the superoxide anion at approximately 4-5 hours, this phenomenon can be seen very clearly in figure 8.13, graph D.

Nitric oxide measurements were generally more variable, even using tubers with a known history. Figure 8.14, graph A, shows the data for a NO time course of the impact resistant Maris Piper potato variety. The control site showed a relatively stable 'background' level of nitric oxide generation that was attributed to the stress of core excision (<0.6 nMoles NO/g/minute). The NO generated at the impact site was significantly greater than the control site, thereby re-confirming that in different areas of the tuber nitric oxide is generated at different rates (i.e.: spatial regulation). Furthermore the production of NO by the impact site appears broadly biphasic peaking initially at approximately 1.5-hours and again at 4-hours. No significant difference was found between the control and impact sites of the impact susceptible variety, Russet Burbank, in fact inspection of the data (figure 8.14, B) reveals that the control site appears to match the NO generation profile observed at the impact site.

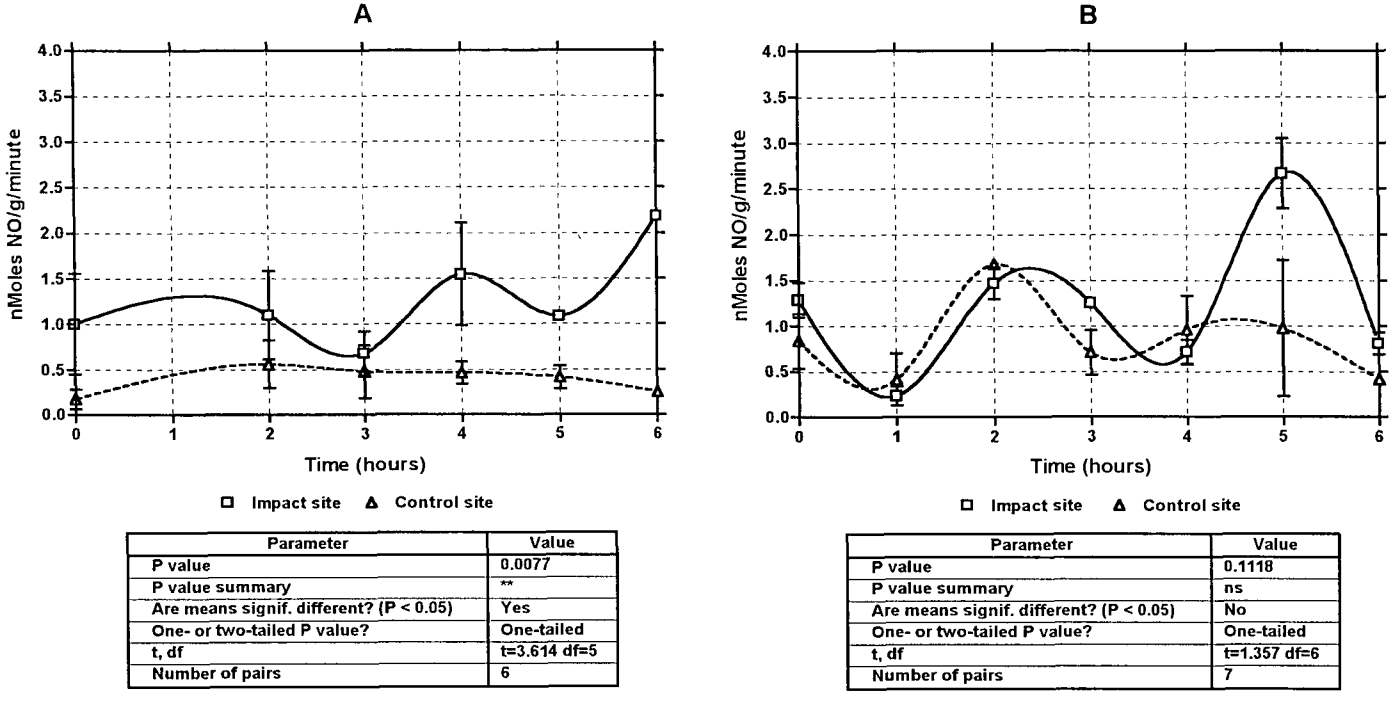

Parameter	Value
P value	0.0077
P value summary	**
Are means signif. different? (P < 0.05)	Yes
One- or two-tailed P value?	One-tailed
t, df	t=3.614 df=5
Number of pairs	6

Parameter	Value
P value	0.1118
P value summary	ns
Are means signif. different? (P < 0.05)	No
One- or two-tailed P value?	One-tailed
t, df	t=1.357 df=6
Number of pairs	7

Figure 8.14

Time course of nitric oxide production from impact stressed tuber tissue of different varieties.

Experimental design is described in section 8.1.2 and the final assay is presented in section 4.3.6. The experiments were carried out with Maris Piper (graph A) and Russet Burbank (graph B) potato varieties. The data from the control site and the impact sites were statistically assessed (using GraphPad Prism software) to evaluate if there was any significant difference between the two data sets; this is shown below the graph. P-value summary key; ns=no significant difference; *=significant difference; **=very significant difference.

8.3 Conclusions

The detection and quantification of the superoxide anion and nitric oxide molecule in the extracellular environment and generated by impact stressed tuber tissue using the assay systems and experimental design described here have been successfully confirmed. Although both assay systems were originally designed with the intention of measuring $^{\cdot}O_2^-$ and NO generated from stressed cell suspension cultures they have proved robust and readily adaptable to the direct quantification of these molecules from more physiologically relevant material.

Previous reports have identified mechanical stress as a trigger for the production of AOS, invariably all of these reports have indirectly measured AOS, using the relatively ubiquitous H_2O_2 [Jaffe *et al.* 1985; Legendre *et al.* 1993; Yahraus *et al.* 1995]. Work at the University of Durham using an tuber-impact model had inferred the participation of the hydroxyl radical during the potato response to impact stress [Croy *et al.* 1998]. The study presented here is the first direct confirmation of the production of the $^{\cdot}O_2H/^{\cdot}O_2^-$ radical pair in response to impact stress. Similarly, nitric oxide has very recently been implicated in the biotic stress response [Delledonne *et al.* 1998; Durner *et al.* 1998] this is the first direct confirmation of the production of NO from potato tuber tissue.

It was obvious that the impact site of impact susceptible varieties generated much more superoxide than impact resistant varieties, for instance superoxide production from the Russet Burbank variety peaked at >4 nMoles $^{\cdot}O_2^-$/g/minute, whereas the impact resistant varieties did not rise above 1.75 nMoles $^{\cdot}O_2^-$/g/minute. The greater generation of superoxide by impact susceptible potato varieties was in agreement with data generated from oxyblot analysis carried out by Croy *et al.* [1998]. Impact resistant varieties showed a distinctly different response with little or no discernible generation of superoxide. It seems highly probable that the impact susceptibility (i.e.: the propensity to bruise) is directly linked to the production of AOS.

Another distinctive feature of the superoxide generation from impact susceptible varieties was a distinct biphasic generation starting with an early burst (1-2 hours) followed by a later and greater production (4-5 hours). Interestingly this biphasic generation of the superoxide anion has essentially the same kinetics of AOS generated by plant cells in response to a bacterial pathogen [Wojtaszek 1997]. The initial production is thought to be a non-specific and general stress response, the latter production is considered specific to incompatible interactions [Levine *et al.* 1994]. This opens up the intriguing possibility that the impact susceptible tuber is responding to impact stress in essentially the same manner as it would a pathogen and asks the question; do the two disparate stresses

share the same recognition pathway? Similar theories of shared signal transduction pathways have been aired previously [Jongsma *et al.* 1994; Baron & Zambryski 1995].

Unfortunately measurements of nitric oxide generation were not as consistent as would have been hoped and compared to the superoxide assay much more variability was evident. However, significantly elevated levels of NO were seen at the impact site of an impact resistant variety. Many reports concerning the actions of NO, detail the synergistic interplay of the superoxide anion and the nitric oxide molecule to form the peroxynitrite radical ($^{\cdot}OONO^{-}$) [Delledonne *et al.* 1998; Durner *et al.* 1998]. However, it was not possible to directly measure $^{\cdot}OONO^{-}$ generation in this research, but its formation is presumed to occur because both reactants are present in the extracellular environment. The exact roles that NO and $^{\cdot}ONOO^{-}$ actual play is not yet clear though this series of experiments will provide a good starting point for further investigation.

SECTION 9

DISCUSSION & FURTHER WORK

Vacuum infiltration was successfully utilised to selectively extract apoplastic polypeptides without contamination from the intracellular environment. Many previous workers [e.g.: Ilett 1998] have utilised VI to investigate individual apoplastic components, but to the authors' knowledge, none have utilised the technique in such a wide-ranging and diverse study of the apoplast.

Direct N-terminal sequencing of SDS-PAGE separated apoplastic polypeptides did provide some sequence data but overall the vast majority of apoplastic polypeptides that underwent sequencing appeared to be N-terminally blocked. Interestingly, in animal systems proteins that are exposed to AOS can undergo modification to their N-termini that ultimately results in blockage [Burcham & Kuham 1997] and in plants the apoplast is a proposed site of AOS generation and release during stress and growth [Lane *et al.* 1992; Wojtaszek 1997; Fry 1998]. The constant exposure of apoplastic proteins to AOS may explain the unusually high level of N-terminal blockage experienced and if correct would also explain why all of the attempted sequencing of apoplastic polypeptides from abiotically stressed plants failed. Several methods do exist for the deblocking of N-terminally blocked polypeptides and may be of use for the sequencing of apoplastic polypeptides in the future [Hirano *et al.* 1992], but were not utilised in this study.

However, some polypeptides did generate sequence data, which could be utilised for homology searching. Two apoplastic polypeptides (SICF2 and SICF3) were shown to exhibit a degree of homology with cell wall/carbohydrate related enzymes already known to be present in the apoplast [see Fry 1991] and a 27 kDa thaumatin-like protein from Diospyros texana [Vu & Huynh 1994] had some homology to an apoplastic polypeptide of ~26 kDa. Most strikingly however were the number of potential ABP's that were successfully sequenced, high homologies were found to germin-like proteins and ABP's (ITL5, SICF8 and 9) from peach [Ohimya *et al.* 1998].

The putative site of auxin action is thought to be the apoplast [Brown & Jones 1994] although the vast majority of the most well characterised ABP, ABP1 from maize, is resident in the endoplasmic recticulm [Campos *et al.* 1995]. However, recently, circumstantial evidence has accumulated that ABP's are indeed apoplastic, for instance, Tsurusaki *et al.* [1997] have shown that the concentration of endogenous auxin is higher in the apoplast than the symplast and Jones & Herman [1993] and Deikmann *et al.* [1995] have both provided microscopy evidence. Consequently, ICF was subjected to

auxin affinity chromatography. Three potential auxin binding polypeptides were identified by SDS-PAGE analysis and one of these polypeptides may have been sequenced earlier and proved to be a putative ABP (SICF9 ~20.3 kDa). Recently, Shimomura *et al.* [1999] have identified a 19.6 kDa homologue of maize ABP1 that is secreted from tobacco leaf discs into the surrounding medium, this polypeptide and SICF9 may be the same. With two independent pieces of evidence localising a tobacco leaf ABP of ~20 ±1 kDa, to the apoplast a strong suggestion that the active site of ABP's is indeed the apoplast can be proffered.

ITL5 was a 16.5 kDa apoplastic polypeptide that shared 100% homologies with an ABP and a germin-like protein. Some germin-like proteins have been identified as containing auxin responsive elements [Lane *et al.* 1992] and have been tightly linked with cell wall elongation [Lane *et al.* 1992; Ohimya *et al.* 1993]. ITL5 was present only in the immature tobacco leaf tissue and may therefore play roles in cell wall elongation during leaf growth.

The approach of utilising VI to recover ABP's present in the apoplast circumvents a major problem associated with the more commonly employed whole tissue studies, that invariably suffer from the problem that >99% of ABP's are typically present in the endoplasmic reticulum [Campos *et al.* 1995]. The use of VI in the study of ABP's is therefore very important precisely because such low quantities of ABP present in the apoplast are difficult to distinguish from ABP resident in the intracellular environment. Thus, this approach of sampling only the compartment in which ABP's are proposed to be active is extremely novel and worthy of further work.

Early in the project it was identified that 2D electrophoresis would be a useful technique to improve the separation of apoplastic polypeptides extracted using VI. The hope was that smaller changes to the apoplastic complement of polypeptides could be visualised. All the methods detailed within this thesis failed primarily because of the nature of the material. The ionic environment apoplastic proteins and polypeptides inhabit is ionically rich and unfortunately the first dimension of 2D electrophoresis requires that proteins and polypeptides were present in a buffer and gel that has an extremely low ionic strength. This change in the ionic environment coupled with the exposure of the polypeptides to a strong electrical field is assumed to have contributed greatly to the observed and consistent electro-precipitation. A further potential complication associated with ICF samples is varied and heterogeneous nature of other components that are unwittingly extracted alongside apoplastic proteins and polypeptides during VI. Molecules and compounds with the potential to be problematic include highly heterogeneous carbohydrates, phenolic and polyphenolic compounds [Fry 1991; Dawes *et al.* 1994; Dietz *et al.* 1997]. Additionally, the glycoprotein modifications present on all apoplastic

proteins and polypeptides also show evidence of charge heterogeneity [Dawes *et al.* 1994; Amoresano *et al.* 1999] which may explain the smearing of 2D separated polypeptides observed in the ESA Investigator™ gels. Due to these problems 2D electrophoresis of ICF that attained a suitable standard could not be achieved during this project.

The apoplast has been determined to be a site of production and release of AOS in response to stress and growth [Lane *et al.* 1992; Wojtaszek 1997; Fry 1998]. A range of anti-AOS defences that include the enzymes peroxidase and superoxide dismutase, are known to be present in the apoplast [Fry 1991; Schinkel *et al.* 1998] and are presumed to control the formation of apoplastic AOS.

Native-PAGE in gel enzyme activity staining was successfully utilised to analyse ICF extracted using VI. These techniques revealed 4 ICF-POD's and 5 ICF-SOD's. All of the ICF-POD's separated using native-PAGE contained the metal ion, iron; this was distinct from their intracellular counterparts, all of which appeared to contain the selenium ion. ICF-POD 1 was potentially identified as a dimer with a sub-unit mass of ~29 kDa, a similar sized basic polypeptide with POD enzyme activity has been isolated from the apoplast of pine needles by Slazer & Hager [1993] and Otter & Polle [1997].

ICF-SOD 1 was 20.2 kDa CuZn-SOD with a high isoelectric point, an apoplastic SOD enzyme with a similar mass and isoelectric point has been characterised recently from pine needles [Schinkel *et al.* 1998]. A putative Mn-SOD (ICF-SOD 4) was identified in the tobacco leaf apoplast and potentially is only the second apoplastic plant Mn-SOD ever identified [Yamahara *et al.* 1999]. The remaining ICF-SOD's were Fe-containing SOD's (ICF-SOD's 2 and 3) and to the authors knowledge they are the first apoplastic iron containing SOD's described in plants. An extracellular Fe-SOD has very recently been discovered in bacteria [Shirkey *et al.* 2000] but none have been currently located to the apoplast/extracellular matrix in higher organisms. Coincidentally, the extracellular Fe-SOD from bacteria has almost the same molecular mass as the apoplastic Fe-SOD, ICF-SOD 3 identified within this study.

Very interestingly native-PAGE revealed that ICF-POD's 1 and 2 co-migrated with ICF-SOD 4 which indicated two possibilities, either, these proteins have both SOD and POD enzyme activities, or alternatively they may be independent enzymes with similar separation characteristics in this native-PAGE system. The final explanation proffered for the co-migration in the native-PAGE system is that they were in fact linked in some manner. Johansson *et al.* [1999] has described such an interaction of POD and SOD enzymes via carbohydrate moieties in the extracellular matrix of animals. An interaction

between these two enzymes may potentially streamline the process of AOS detoxification in the apoplast.

In the study of the complement of apoplastic, POD's and SOD's VI appears to have yielded unique results. It is possible that the novelty of application of VI coupled with native-PAGE separation and in gel assays to identify individual proteins and polypeptides that are SOD or POD active has yielded such new observations. A similar approach by Schinkel *et al.* [1998] using pine needles has also generated unique insights into apoplastic anti-AOS enzymes. The more commonly employed experimental procedure of extraction of the particular cellular compartment of interest followed by the use of a spectrophotometric assay of all the active components within that compartment, does not yield information on the activities of individual components. Obviously, this approach is worthy of greater investigation, perhaps to the study of other stress related apoplastic enzymes.

Investigation of the generation and release of apoplastic AOS was technically difficult with the leaf-VI system used throughout this research. Consequently, a tuber-impact stress system already in use in Durham was adopted. The system had the distinct advantage that direct quantification of the superoxide anion and nitric oxide molecule in response to a defined stress was possible.

Preliminary studies revealed that superoxide anion production in response to impact stress was spatially regulated. This result concurs with oxyblot data generated by Croy *et al.* [1998]. More detailed impact studies using potatoes with a well known history revealed a distinct difference between impact susceptible and resistant varieties, based upon their propensity to form a bruise in response to the impact stress. Impact resistant varieties did not exhibit superoxide anion production greater than that observed at control sites within the same tuber. Impact susceptible varieties exhibited a distinct biphasic production of the superoxide anion that was extremely reminiscent of the well documented pathogen induced oxidative burst [Wojtaszek 1997; Levine *et al.* 1994]. There is the possibility that both 'stresses' induce a similar oxidative burst in the apoplast [Jongsma *et al.* 1994; Baron & Zambryski 1995].

The presence of apoplastic NO was shown, however, 'bursts' and 'phases' of production in response to impact stress were not as distinct as the measurements of the superoxide anion. Commonly nitric oxide and AOS act synergistically to produce a biological effect [Delledonne *et al.* 1998; Durner *et al.* 1998], via the formation of peroxynitrite from the superoxide anion and nitric oxide. The combination of superoxide and nitric oxide at the site of impact stress would generate the peroxynitrite radical; this radical is an effective anti-microbial agent because of its strong oxidising properties [Mayer & Hemmens 1997].

Thus impact stress and pathogen attack may in fact share the same signalling pathway highlighted by the presence of anti-microbial peroxynitrite [Mayer & Hemmens 1997; Durner *et al.* 1998].

The impact site of impact susceptible potato tubers can be typified by the formation of a bruise and localised cell death [Peters 1996]. Peroxynitrite is involved in the process of apoptosis in animal systems via protein modification to kinases and caspases [So *et al.* 1998; Jianrong *et al.* 1997] and may be playing a similar fundamental biological role in plants. Much more study is required before firm roles can be attributed to peroxynitrite in plants, although both Delledonne *et al.* [1998] and Durner *et al.* [1998] have implicated peroxynitrite in the plant hypersensitive response to pathogen attack.

A potential avenue for further research, which may yield very rapid results, is the investigation of the protein modifications induced by peroxynitrite. The adoption of a 'nitroblot', based on exactly the same principle as the 'oxyblot' [Gow *et al.* 1996] would be a suitable approach for this work. Such an approach would make it possible to investigate which proteins are being modified at the time stress, and ultimately to determine the consequences of modification.

As an adjunct; it is noteworthy that phenolic compounds are intimately involved in the response of potato tubers to impact stress at the impact site, and in particular tyrosine and melanins [Croy *et al.* 1998] essentially form the colouration distinctive of a bruise. These compounds are known antioxidants that are effective against peroxynitrite and AOS [Sandova *et al.* 1997] and furthermore they are extremely indigestible to enzymatic action [Matern *et al.* 1995]. The exact role of phenolic compounds at the impact site is not known, though they would presumably limit pathogen ingress.

SECTION 10

REFERENCES

Able, A. J., Guest, D. I., and Sutherland, M. W. (1998)
Use of a new tetrazolium-based assay to study the production of superoxide radicals by tobacco cell cultures challenged with avirulent zoospores of Phytophthora parasitica var nicotianae.
***Plant Physiology* 117**-2 491-499

Akiyama, Y., Mori, M., and Kato, K. (1980)
***Agricultural and Biological Chemistry* 44** 2487-2489

Albersheim, P., Darvill, A., Augur, C., Cheong, J. J., Eberhard, S., Hahn, M. G., Marfa, V, Mohnen, D., Oneill, M. A., Spiro, M. D., and York, W. S. (1992)
Oligosaccharins - oligosaccharide regulatory molecules.
***Accounts Of Chemical Research* 25** 77-83

Alexander, D. (1995)
Extracellular polypeptides of *Brassica napus* leaves.
University of Durham, Final Year MBB BSc project report.

Altus, D. P. and Canny, M. J. (1985)
Water pathways in wheat leaves .1. The division of fluxes between different vein types.
***Australian Journal Of Plant Physiology* 12** 173-181

Amoresano, A., Brancaccio, A., Andolfo, A., Perduca, M., Monaco, H. L., and Marino, G. (1999)
The carbohydrates of the isoforms of three avian riboflavin- binding proteins.
***European Journal Of Biochemistry* 263**-3 849-858

Ananyev, G., Renger, G., Wacker, U., and Klimov, V (1994)
The photoproduction of superoxide radicals and the superoxide- dismutase activity of photosystem-ii - the possible involvement of cytochrome b559.
***Photosynthesis Research* 41** 327-338

Apostol, I, Heinstein, P. F., and Low, P. S. (1989)
Rapid stimulation of an oxidative burst during elicitation of cultured plant-cells - role in defense and signal transduction.
***Plant Physiology* 90** 109-116

Arroyo, A., Navarro, F., Navas, P., and Villalba, J. M. (1998)
Ubiquinol regeneration by plasma-membrane ubiquinone reductase.
***Protoplasma* 205** 107-113

Ashford, D., Desai, N. N., Allen, A. K., Neuberger, A., Oneill, M. A., and Selvendran, R. R. (1982)
Structural studies of the carbohydrate moieties of lectins from potato (Solanum-tuberosum) Tubers and thornapple (Datura-stramonium) Seeds.
***Biochemical Journal* 201** 199-208

AZCONBIETO, J., FARQUHAR, G. D., and CABALLERO, A. (1981)
EFFECTS OF TEMPERATURE, OXYGEN CONCENTRATION, LEAF AGE AND SEASONAL-VARIATIONS ON THE CO2 COMPENSATION POINT OF LOLIUM-PERENNE L - COMPARISON WITH A MATHEMATICAL-MODEL INCLUDING NON-PHOTORESPIRATORY CO2 PRODUCTION IN THE LIGHT.
***Planta* 152**-6 497-504

Bacic, A., Gell, A. C., and Clarke, A. E. (1988)
Arabinogalactan proteins from stigmas of nicotiana-alata.
***Phytochemistry* 27** 679-684

BANNISTER, J. V., BANNISTER, W. H., and ROTILIO, G. (1987)
ASPECTS OF THE STRUCTURE, FUNCTION, AND APPLICATIONS OF SUPEROXIDE-DISMUTASE.
***Crc Critical Reviews In Biochemistry* 22**-2 111-180

Barent, R. L. and Elthon, T. E. (1992)
Two-dimensional gels: An easy method for large quantities of proteins.
***Plant Molecular Biology Reporter* 10** 338-344

Baron, C. and Zambryski, P. C. (1995)
Notes from the underground - highlights from plant-microbe interactions.
***Trends In Biotechnology* 13** 356-362

Beauchamp, C. O. and Fridovich, I. (1971)
Superoxide dismutase: improved assays and an assay applicable to acrylamide gels.
***Analytical Biochemistry* 44** 276-287

Beckman, J. S., Chen, J., Ischiropoulos, H., and Crow, J. P. (1994)
Oxidative chemistry of peroxynitrite.
***Methods In Enzymology* 233** 229-240

Bergmann, C. W., Ito, Y., Singer, D., Albersheim, P., Darvill, A. G., Benhamou, N., Nuss, L., Salvi, G., Cervone, F., and Delorenzo, G. (1994)
Polygalacturonase-inhibiting protein accumulates in phaseolus- vulgaris l in response to wounding, elicitors and fungal infection.
***Plant Journal* 5** 625-634

Betz, M., Martinoia, E., Hincha, D. K., Schmitt, J. M., and Dietz, K. J. (1992)
Purification and compartmentation of alpha-mannosidase isoenzymes of barley leaves.
***Phytochemistry* 31** 433-440

Bi, Y. M., Kenton, P., Mur, L., Darby, R., and Draper, J. (1995)
Hydrogen-peroxide does not function downstream of salicylic-acid in the induction of pr protein expression.
***Plant Journal* 8** 235-245

Bilang, J., Macdonald, H., King, P. J., and Sturm, A. (1993)
A soluble auxin-binding protein from hyoscyamus-muticus is a glutathione-s-transferase.
***Plant Physiology* 102** 29-34

Biro, R. L., Daye, S., Serlin, B. S., Terry, M. E. , Datta, N., Sopory, S. K., and Roux, S. J. (1984)
Characterization of oat calmodulin and radioimmunoassay of its subcellular-distribution.
***Plant Physiology* 75** 382-386

Bishop, J. E., Johnson, J. D., and Berman, M. C. (1984)
Transient kinetic-analysis of turnover-dependent fluorescence of 2',3'-o-(2,4,6-Trinitrophenyl)-Atp bound to ca-2+-atpase of sarcoplasmic-reticulum.
***Journal Of Biological Chemistry* 259** 5163-5171

Blinda, A., Koch, B., Ramanjulu, S., and Dietz, K. J. (1997)
De novo synthesis and accumulation of apoplastic proteins in leaves of heavy metal-exposed barley seedlings [Full text delivery].
***Plant Cell And Environment* 20** 969-981

Bohlmann, H. and Apel, K. (1991)
Thionins.
***Annual Review Of Plant Physiology And Plant Molecular Biology* 42** 227-240

Bowler, C., Neuhaus, G., Yamagata, H., and Chua, N. H. (1994)
Cyclic-gmp and calcium mediate phytochrome phototransduction.
***Cell* 77** 73-81

Braam, J. (1999)
If walls could talk - Commentary.
***Current Opinion In Plant Biology* 2** 521- 524

Bradford, M. M. (1976)
A rapid and sensitive method for quantification of microgram quantities of protein utilising the principle of protein-dye binding.
***Analytical Biochemistry* 72** 248-254

Bradley, D. J., Kjellbom, P., and Lamb, C. J. (1992)
Elicitor-induced and wound-induced oxidative cross-linking of a proline-rich plant-cell wall protein - a novel, rapid defense response.
***Cell* 70** 21-30

Brett, C. T. (2000)
Cellulose microfibrils in plants: Biosynthesis, deposition, and integration into the cell wall.
***International Review Of Cytology - A Survey Of Cell Biology, Vol 199* 199** 161-199

Briggs.G.E. (1957)
Apparent free space.
***Annual Review Of Plant Physiology* 8** 11-30

Brisson, L. F., Tenhaken, R., and Lamb, C. (1994)
Function of oxidative cross-linking of cell-wall structural proteins in plant-disease resistance.
***Plant Cell* 6** 1703-1712

Broekaert, W. F., Terras, F. R. G., Cammue, B. P. A., and Osborn, R. W. (1995)
Plant defensins - novel antimicrobial peptides as components of the host-defense system.
***Plant Physiology* 108** 1353-1358

Brown, E. G. and Newton, R. P. (1992)
Analytical procedures for cyclic-nucleotides and their associated enzymes in plant-tissues.
***Phytochemical Analysis* 3** 1-13

Brown, J. C. and Jones, A. M. (1994)
Mapping the auxin-binding site of auxin-binding protein-1.
***Journal Of Biological Chemistry* 269** 21136- 21140

Brune, A. and Dietz, K. J. (1995)
A comparative-analysis of element composition of roots and leaves of barley seedlings grown in the presence of toxic cadmium, molybdenum, nickel, and zinc concentrations.
***Journal Of Plant Nutrition* 18** 853-868

Brune, A., Urbach, W., and Dietz, K. J. (1994)
Zinc stress induces changes in apoplasmic protein-content and polypeptide composition of barley primary leaves.
***Journal Of Experimental Botany* 45** 1189-1196

Brune, B., Sandau, K., and vonKnethen, A. (1998)
Apoptotic cell death and nitric oxide: Activating and antagonistic transducing pathways.
***Biochemistry-Moscow* 63** 817-825

Brzobohaty, B., Moore, I, Kristoffersen, P., Bako, L., Campos, N., Schell, J., and Palme, K. (1993)
Release of active cytokinin by a beta-glucosidase localized to the maize root-meristem.
***Science* 262** 1051-1054

Burcham, P. C. and Kuhan, Y. T. (1997)
Diminished susceptibility to proteolysis after protein modification by the lipid peroxidation product malondialdehyde: Inhibitory role for crosslinked and noncrosslinked adducted proteins.
***Archives Of Biochemistry And Biophysics* 340**-2 331-337

Caelles, C., Delseny, M., and Puigdomenech, P. (1992)
The hydroxyproline-rich glycoprotein gene from oryza-sativa.
***Plant Molecular Biology* 18** 617-619

Campos, N., Schell, J., and Palme, K. (1994)
In-vitro uptake and processing of maize auxin-binding proteins by er- derived microsomes.
***Plant And Cell Physiology* 35** 153-161

Canny, M. J. (1995)
Apoplastic water and solute movement - new rules for an old space.
***Annual Review Of Plant Physiology And Plant Molecular Biology* 46** 215-236

Canny, M. J. (1987)
LOCATING ACTIVE PROTON EXTRUSION PUMPS IN LEAVES.
***Plant Cell And Environment* 10**-3 271-274

Carpenter, C. D., Kreps, J. A., and Simon, A. E. (1994)
Genes encoding glycine-rich arabidopsis-thaliana proteins with rna- binding motifs are influenced by cold treatment and an endogenous circadian-rhythm.
***Plant Physiology* 104** 1015-1025

Carpita, N. C. and Gibeaut, D. M. (1993)
Structural models of primary-cell walls in flowering plants - consistency of molecular-structure with the physical-properties of the walls during growth.
***Plant Journal* 3** 1-30

Cassab, G. I. and Varner, J. E. (1988)
Cell-wall proteins.
***Annual Review Of Plant Physiology And Plant Molecular Biology* 39** 321-353

Castro, L., Rodriguez, M., and Radi, R. (1994)
Aconitase is readily inactivated by peroxynitrite, but not by its precursor, nitric-oxide.
***Journal Of Biological Chemistry* 269** 29409-29415

Cazale, A. C., Rouet-Mayer, M. A., Barbier-Brygoo, H., Mathieu, Y., and Lauriere, C. (1998)
Oxidative burst and hypoosmotic stress in tobacco cell suspensions.
***Plant Physiology* 116**-2 659-669

Chameides, W. L., Kasibhatla, P. S., Yienger, J., and Levy, H. (1994)
Growth of continental-scale metro-agro-plexes, regional ozone pollution, and world food-production.
***Science* 264** 74-77

Chen, J. and Varner, J. E. (1985)
An extracellular-matrix protein in plants - characterization of a genomic clone for carrot extensin.
***Embo Journal* 4** 2145 -2151

Chen, R. D., Yu, L. X., Greer, A. F., Cheriti, H., and Tabaeizadeh, Z. (1994)
Isolation of an osmotic stress-induced and abscisic-acid-induced gene encoding an acidic endochitinase from lycopersicon-chilense.
***Molecular & General Genetics* 245** 195-202

Chen, Z. L., Warren, C. R. , and Adams, M. A. (2000)
Separation of rubisco in extracts of plant leaves by capillary electrophoresis with sieving polymers.
***Analytical Letters* 33**-4 579-587

Chrispeels, M. J. (1991)
Sorting of proteins in the secretory system.
***Annual Review Of Plant Physiology And Plant Molecular Biology* 42** 21-53

Cohen, J. D. and Bandurski, R. S. (1982)
Chemistry and physiology of the bound auxins.
***Annual Review Of Plant Physiology And Plant Molecular Biology* 33** 403-430

Condit, C. M. and Meagher, R. B. (1986)
A gene encoding a novel glycine-rich structural protein of petunia.
***Nature* 323** 178-181

Condit, C. M., Mclean, B. G., and Meagher, R. B. (1990)
Characterization of the expression of the petunia glycine-rich protein-1 gene-product.
Plant Physiology **93** 596-602

Constabel, C. P. and Brisson, N. (1995)
Stigma-specific and vascular-specific expression of the pr-10a gene of potato - a novel pattern of expression of a pathogenesis-related gene.
Molecular Plant-Microbe Interactions **8** 104-113

Cook, J. A., Kim, S. Y., Teague, D., Krishna, M. C., Pacelli, R., Mitchell, J. B., Vodovotz, Y., Nims, R. W., Christodoulou, D., Miles, A. M., Grisham, M. B., and Wink, D. A. (1996)
Convenient colorimetric and fluorometric assays for S- nitrosothiols.
Analytical Biochemistry **238**-2 150-158

Cordewener, J., Booij, H., Vanderzandt, H., Vanengelen, F., Vankammen, A., and Devries, S. (1991)
Tunicamycin-inhibited carrot somatic embryogenesis can be restored by secreted cationic peroxidase isoenzymes.
Planta **184** 478-486

Covarrubias, A. A., Ayala, J. W., Reyes, J. L., Hernandez, M., and Garciarrubio, A. (1995)
Cell-wall proteins induced by water-deficit in bean (Phaseolus- vulgaris l) Seedlings.
Plant Physiology **107** 1119-1128

Craig, A. L., Morrison, I, Baird, E., Waugh, R., Coleman, M., Davie, P., and Powell, W. (1994)
Expression of reducing sugar accumulation in interspecific somatic hybrids of potato .
Plant Cell Reports **13** 401-405

Cretin, C. and Puigdomenech, P. (1990)
Glycine-rich rna-binding proteins from sorghum-vulgare.
Plant Molecular Biology **15** 783-785

Croy, R.R.D., Baxter, R., Deakin, W., Edwards, R., Gatehouse, J.A., Gates, P., Harris, N., Hole, C., Johnson, S.J. and Raemaekers, R. (1998)
Blackspot bruising in potatoes: structural and molecular approaches to the identification of factors associated with tuber bruising susceptibility.
Aspects of applied biology **52** 207-214

Cueto, M., HernandezPerera, O., Martin, R., Bentura, M. L., Rodrigo, J., Lamas, S., and Golvano, M. P. (1996)
Presence of nitric oxide synthase activity in roots and nodules of Lupinus albus.
Febs Letters **398** 159-164

Darvill, A. G. and Albersheim, P. (1984)
Phytoalexins and their elicitors - a defense against microbial infection in plants.
Annual Review Of Plant Physiology And Plant Molecular Biology **35** 243-275

Datta, K., Schmidt, A., and Marcus, A. (1989)
Characterization of 2 soybean repetitive proline-rich proteins and a cognate cdna from germinated axes.
Plant Cell **1** 945-952

Davis, D. A., Tsao, D., Seo, J. H., Emery, A., Low, P. S., and Heinstein, P. (1992)
Enhancement of phytoalexin accumulation in cultured plant-cells by oxalate.
Phytochemistry **31** 1603-1607

DAWES, H., Boyes, S., KEENE, J., and Heatherbell, D. (1994)
Protein instability of wines - influence of protein isoelectric points.
American Journal of Enology and Viticulture **45** 319-326

Deikman, J., Coupe, S., Xu, R. L., and Kim, K. N. (1995)
Regulation of gene-transcription by ethylene during tomato fruit ripening.
Plant Physiology **108** 28-

Delledonne, M., Xia, Y. J. , Dixon, R. A., and Lamb, C. (1998)
Nitric oxide functions as a signal in plant disease resistance.
***Nature* 394**-6693 585-588

Delmer, D. P., Read, S. M. , and Cooper, G. (1987)
Identification of a receptor protein in cotton fibers for the herbicide 2,6-dichlorobenzonitrile.
***Plant Physiology* 84** 415-420

Delmer, D. P., Shedleztky, E., Shmuel, M., Trainin, T., Amor, Y., Andrawis, A., Benziman, M., Mayer, R., Solomon, M., and Gonen, L. (1991)
The plant-cell wall - structure, function and biosynthesis.
***Biological Chemistry Hoppe-Seyler* 372** 643-644

Dempsey, D. A., Shah, J., and Klessig, D. F. (1999)
Salicylic acid and disease resistance in plants.
***Critical Reviews In Plant Sciences* 18** 547-575

Didierjean, L., Frendo, P. , and Burkard, G. (1992)
Stress responses in maize - sequence-analysis of cdnas encoding glycine-rich proteins.
***Plant Molecular Biology* 18** 847-849

Dietz, K. J., Schramm, M., Betz, M., Busch, H., Durr, C., and Martinoia, E. (1992)
Characterization of the epidermis from barley primary leaves .1. Isolation of epidermal protoplasts.
***Planta* 187** 425-430

Dietz, K. J. (1997)
Functions and Responses of the LEaf Apoplast under stress.
***Progress in Botany* 58** 221-254

Douglas, A. (2000)
Roots of Immunity.
***New Scientist* Article** 47-49

Driouich, A., Faye, L., and Staehelin, L. A. (1993)
The plant golgi-apparatus - a factory for complex polysaccharides and glycoproteins.
***Trends In Biochemical Sciences* 18** 210-214

Durner, J., Gow, A. J., Stamler, J. S., and Glazebrook, J. (1999)
Ancient origins of nitric oxide signaling in biological systems.
***Proceedings Of The National Academy Of Sciences Of The United States Of America* 96** 14206-14207

Durner, J., Wendehenne, D. , and Klessig, D. F. (1998)
Defense gene induction in tobacco by nitric oxide, cyclic GMP, and cyclic ADP-ribose.
***Proceedings Of The National Academy Of Sciences Of The United States Of America* 95** 10328-10333

Ebel, J. and Cosio, E. G. (1994)
Elicitors of plant defense responses.
***International Review Of Cytology-A Survey Of Cell Biology* 148** 1-36

Edwards, M. C., Smith, G. N., and Bowling, D. J. F. (1988)
Guard-cells extrude protons prior to stomatal opening - a study using fluorescence microscopy and ph micro-electrodes.
***Journal Of Experimental Botany* 39** 1541-1547

Edwards, R. and Dixon, R. A. (1991)
Glutathione s-cinnamoyl transferases in plants.
***Phytochemistry* 30** 79-84

Elwadawi, R. and Bowler, K. (1995)
The development of thermotolerance protects blowfly flight muscle mitochondrial function from heat damage.
***Journal Of Experimental Biology* 11** 2413-2412

Epstein, L. and Lamport, D. T. A. (1984)
An intramolecular linkage involving isodityrosine in extensin.
***Phytochemistry* 23** 1241-1246

Evans, I. M., Gatehouse, L. N., Gatehouse, J. A., Yarwood, J. N., Boulter, D., and Croy, R. R. D. (1990)
The extensin gene family in oilseed rape (Brassica-napus I) - Characterization of sequences of representative members of the family.
***Molecular & General Genetics* 223** 273-287

Ewald, R., Heese, P., and Klein, U. (1991)
***Journal of Chromatography* 542** 239-245

Ewing, J. F. and Janero, D. R. (1995)
Microplate superoxide dismutase assay employing a nonenzymatic superoxide generator.
***Analytical Biochemistry* 232**-2 243-248

Fadzillah, N. M., Gill, V, Finch, R. P., and Burdon, R. H. (1996)
Chilling, oxidative stress and antioxidant responses in shoot cultures of rice.
***Planta* 199**-4 552-556

Feldwisch, J., Vente, A., Zettl, R., Bako, L., Campos, N., and Palme, K. (1994)
Characterization of 2 membrane-associated beta-glucosidases from maize (Zea-mays I) Coleoptiles.
***Biochemical Journal* 302** 15-21

Ferrer, M. A. and Barcelo, A. R. (1999)
Differential effects of nitric oxide on peroxidase and H2O2 production by the xylem of Zinnia elegans [Full text delivery].
***Plant Cell And Environment* 22** 891-897

FERRIE, B. J., BEAUDOIN, N., BURKHART, W., BOWSHER, C. G., and ROTHSTEIN, S. J. (1994)
THE CLONING OF 2 TOMATO LIPOXYGENASE GENES AND THEIR DIFFERENTIAL EXPRESSION DURING FRUIT RIPENING.
***Plant Physiology* 106**-1 109-118

Ferte, N., Moustacas, A. M., Nari, J., Teissere, M., Borel, M., Thiebart, I, and Noat, G. (1993)
Characterization and kinetic-properties of a soybean cell-wall phosphatase.
***European Journal Of Biochemistry* 211** 297-304

Fincher, G. B., Stone, B. A., and Clarke, A. E. (1983)
Arabinogalactan-proteins - structure, biosynthesis, and function.
***Annual Review Of Plant Physiology And Plant Molecular Biology* 34** 47- 70

Fleming, T. M., Mccarthy, D. A., White, R. F., Antoniw, J. F., and Mikkelsen, J. D. (1991)
Induction and characterization of some of the pathogenesis-related proteins in sugar-beet.
***Physiological And Molecular Plant Pathology* 39** 147-160

Fowler, D. B., Dvorak, J., and Gusta, L. V. (1977)
Comparative cold hardiness of several *Triticum* species and *Secale cereale* L.
***Crop science* 17** 941-943

Franssen, H. J., Nap, J. P., Gloudemans, T., Stiekema, W., Vandam, H., Govers, F., Louwerse, J., Vankammen, A., and Bisseling, T. (1987)
Characterization of cdna for nodulin-75 of soybean - a gene-product involved in early stages of root nodule development.
***Proceedings Of The National Academy Of Sciences Of The United States Of America* 84** 4495-4499

Freshour, G., Clay, R. P., Fuller, M. S., Albersheim, P., Darvill, A. G., and Hahn, M. G. (1996)
Developmental and tissue-specific structural alterations of the cell- wall polysaccharides of Arabidopsis thaliana roots.
***Plant Physiology* 110** 1413-1429

Fridovich, I. (1974)
Superoxide dismutases.
***Advanced Enzymology* 41** 35-44

Fry, S. C. (1991)
Cell wall bound proteins.
***Methods in Plant Biochemistry* 5** 307-331

Fry, S. C. (1986)
Cross-linking of matrix polymers in the growing cell-walls of angiosperms.
***Annual Review Of Plant Physiology And Plant Molecular Biology* 37** 165-186

Fry, S. C. (1986)
Invivo formation of xyloglucan nonasaccharide - a possible biologically-active cell-wall fragment.
***Planta* 169** 443-453

Fry, S. C. (1998)
Oxidative scission of plant cell wall polysaccharides by ascorbate- induced hydroxyl radicals.
***Biochemical Journal* 332** 507-515

Gatti, R. M., Radi, R., and Augusto, O. (1994)
Peroxynitrite-mediated oxidation of albumin to the protein-thiyl free-radical.
***Febs Letters* 348** 287-290

Gibeaut, D. M. and Carpita, N. C. (1994)
Biosynthesis of plant-cell wall polysaccharides.
***Faseb Journal* 8** 904-915

Gieringer, R., Steinert, P., Buttersack, C., and Buchholz, K. (1995)
Anisotropic swelling of cell walls of sugar beet tissue - influence of ion exchange and sucrose.
***Jounral of the scicence of food and agriculture* 68** 439-449

Gillet, C., Cambier, P., and Liners, F. (1992)
Release of small polyuronides from nitella cell-walls during ionic exchange.
***Plant Physiology* 100** 846-852

Gleeson, P. A., Mcnamara, M., Wettenhall, R. E. H., Stone, B. A., and Fincher, G. B. (1989)
Characterization of the hydroxyproline-rich protein core of an arabinogalactan-protein secreted from suspension-cultured lolium- multiflorum (Italian ryegrass) Endosperm cells.
***Biochemical Journal* 264** 857-862

Govers, F., Harmsen, H., Heidstra, R., Michielsen, P., Prins, M., Vankammen, A., and Bisseling, T. (1991)
Characterization of the pea enod12b gene and expression analyses of the 2 enod12 genes in nodule, stem and flower tissue.
***Molecular & General Genetics* 228** 160-166

Gow, A. J., Duran, D., Malcolm, S., and Ischiropoulos, H. (1996)
Effects of peroxynitrite-induced protein modifications on tyrosine phosphorylation and degradation.
***Febs Letters* 385** 63-66

Graham, J. S., Hall, G., Pearce, G., and Ryan, C. A. (1986)
Regulation of synthesis of proteinase inhibitors I and II mRNA's in leaves of wounded tomato plants.
***Planta* 169** 399-405

GRANIER, A. (1987)
EVALUATION OF TRANSPIRATION IN A DOUGLAS-FIR STAND BY MEANS OF SAP FLOW MEASUREMENTS.
***Tree Physiology* 3**-4 309-319

Griffith, M., Ala, P., Yang, D. S. C., Hon, W. C., and Moffatt, B. A. (1992)
Antifreeze protein produced endogenously in winter rye leaves.
***Plant Physiology* 100** 593-596

Hajibagheri, M. A., Harvey, D. M. R., and Flowers, T. J. (1984)
Photosynthetic oxygen evolution in relation to ion contents in the chloroplasts of suaeda-maritima.
***Plant Science Letters* 34** 353-362

Halliwell, G. (1965)
Catalytic decomposition of cellulose under biological conditions.
***Biochemical Journal* 95** 35-40

Hammond-Kosack, K. E. (1992)
Preparation and analysis of intercellular fluid in Molecular Plant Pathology : A Practical Approach II.
Edited by SJ Gurr, MJ McPherson & DJ Bowles, 15-21

Hartung, W., Radin, J. W., and HENDRIX, D. L. (1988)
ABSCISIC-ACID MOVEMENT INTO THE APOPLASTIC SOLUTION OF WATER-STRESSED COTTON LEAVES - ROLE OF APOPLASTIC PH.
***Plant Physiology* 86**-3 908-913

Hartung, W., Weiler, E. W. , and Radin, J. W. (1992)
Auxin and cytokinins in the apoplastic solution of dehydrated cotton leaves.
***Journal Of Plant Physiology* 140** 324-327

Hartung, W., Weiler, E. W. , and VOLK, O. H. (1987)
IMMUNOCHEMICAL EVIDENCE THAT ABSCISIC-ACID IS PRODUCED BY SEVERAL SPECIES OF ANTHOCEROTAE AND MARCHANTIALES.
***Bryologist* 90**-4 393-400

Hatfield, R. D. and Nevins, D. J. (1987)
Hydrolytic activity and substrate-specificity of an endoglucanase from zea-mays seedling cell-walls.
***Plant Physiology* 83** 203-207

Hayashi, T. (1989)
Xyloglucans in the primary cell wall.
***Annual review of plant molecular biolog* 40** 139 -168

Heath, R. L. (1994)
Possible mechanisms for the inhibition of photosynthesis by ozone.
***Photosynthesis Research* 39** 439-451

Hejgaard, J., Jacobsen, S. , Bjorn, S. E., and Kragh, K. M. (1992)
Antifungal activity of chitin-binding pr-4 type proteins from barley- grain and stressed leaf.
***Febs Letters* 307** 389-392

Hildmann, T., Ebneth, M., Penacortes, H., Sanchezserrano, J. J., Willmitzer, L., and Prat, S. (1992)
General roles of abscisic and jasmonic acids in gene activation as a result of mechanical wounding.
***Plant Cell* 4** 1157-1170

Hirose, T., Sugita, M., and Sugiura, M. (1994)
Characterization of a cdna-encoding a novel type of rna-binding protein in tobacco - its expression and nucleic acid-binding properties.
***Molecular & General Genetics* 244** 360-366

Hoj, P. B. and Fincher, G. B. (1995)
Molecular evolution of plant beta-glucan endohydrolases.
***Plant Journal* 7** 367-379

Hong, J. C., Nagao, R. T., and Key, J. L. (1990)
Characterization of a proline-rich cell-wall protein gene family of soybean - a comparative-analysis.
***Journal Of Biological Chemistry* 265** 2470-2475

Hong, J. C., Nagao, R. T., and Key, J. L. (1989)
Developmentally regulated expression of soybean proline-rich cell- wall protein genes.
***Plant Cell* 1** 937-943

Horemans, N., Asard, H., and Caubergs, R. J. (1994)
The role of ascorbate free-radical as an electron-acceptor to cytochrome b-mediated trans-plasma membrane electron-transport in higher-plants.
***Plant Physiology* 104** 1455-1458

Horn, M. A., Heinstein, P. F., and Low, P. S. (1989)
Receptor-mediated endocytosis in plant-cells.
***Plant Cell* 1** 1003-1009

Hufton, C. A., Besford, R. T., and Wellburn, A. R. (1996)
Effects of NO (+NO2) pollution on growth, nitrate reductase activities and associated protein contents in glasshouse lettuce grown hydroponically in winter with CO2 enrichment.
***New Phytologist* 133**-3 495-501

Ilett, C. (1998)
Barley oxalate oxidase.
University of Durham PhD thesis.

Inui, T., Ochi, Y., Hachiya, T., Kajita, Y., Ishida, M., Nakajima, Y., and Nagamune, T. (1990)
The inhibition by calmodulin of thyroid-stimulating hormone binding to epididymal fat, testis and thyroid membranes in the guinea-pig.
***Journal Of Endocrinology* 125** 103-107

Ischiropoulos, H. and Almehdi, A. B. (1995)
Peroxynitrite-mediated oxidative protein modifications.
***Febs Letters* 364** 279-282

JAFFE, M. J., HUBERMAN, M. , JOHNSON, J., and TELEWSKI, F. W. (1985)
THIGMOMORPHOGENESIS - THE INDUCTION OF CALLOSE FORMATION AND ETHYLENE EVOLUTION BY MECHANICAL PERTURBATION IN BEAN STEMS.
***Physiologia Plantarum* 64**-2 271-279

Jaikaran, A. S. I., Kennedy, T. D., Dratewkakos, E., and Lane, B. G. (1990)
Covalently bonded and adventitious glycans in germin.
***Journal Of Biological Chemistry* 265** 12503-12512

Jakob, U. and Buchner, J. (1994)
Assisting spontaneity - the role of hsp90 and small hsps as molecular chaperones.
***Trends In Biochemical Sciences* 19** 205-211

Jarvis, M. C., Logan, A. S., and Duncan, H. J. (1984)
Tensile characteristics of collenchyma cell-walls at different calcium contents.
***Physiologia Plantarum* 61** 81-86

Jeschke, W. D. and Pate, J. S. (1991)
Ionic interactions of petiole and lamina during the life of a leaf of castor bean (Ricinus-communis l) Under moderately saline conditions.
***Journal Of Experimental Botany* 42** 1051-1064

Jia, L., Bonaventura, C., Bonaventura, J., and Stamler, J. S. (1996)
S-nitrosohaemoglobin: A dynamic activity of blood involved in vascular control.
***Nature* 380** 221-226

Johansson, M. W., Holmblad, T., Thornqvist, P. O., Cammarata, M., Parrinello, N., and Soderhall, K. (1999)
A cell-surface superoxide dismutase is a binding protein for peroxinectin, a cell-adhesive peroxidase in crayfish.
***Journal Of Cell Science* 112** 917-925

Jones, A. M. and Herman, E. M. (1993)
Kdel-containing auxin-binding protein is secreted to the plasma- membrane and cell-wall.
***Plant Physiology* 101** 595 -606

Jongsma, M. A., Bakker, P. L., Visser, B., and Stiekema, W. J. (1994)
Trypsin-inhibitor activity in mature tobacco and tomato plants is mainly induced locally in response to insect attack, wounding and virus-infection.
***Planta* 195** 29-35

Jun, T., Shupin, W., Juan, B., and Daye, S. (1996)
Extracellular camodulin-binding proteins in plants : purification of a 21-kDa calmodulin-binding protein.
***Planta* 198** 510-516

Kakimoto, T. and Shibaoka, H. (1992)
Synthesis of polysaccharides in phragmoplasts isolated from tobacco by-2 cells.
***Plant And Cell Physiology* 33** 353-361

KANGASJARVI, J., TALVINEN, J., UTRIAINEN, M., and KARJALAINEN, R. (1994)
PLANT DEFENSE SYSTEMS INDUCED BY OZONE.
***Plant Cell And Environment* 17**-7 783-794

Keller, B., Sauer, N., and Lamb, C. J. (1988)
Glycine-rich cell-wall proteins in bean - gene structure and association of the protein with the vascular system.
***Embo Journal* 7** 3625-3633

Kieliszewski, M., Dezacks, R., Leykam, J. F., and Lamport, D. T. A. (1992)
A repetitive proline-rich protein from the gymnosperm douglas-fir is a hydroxyproline-rich glycoprotein.
***Plant Physiology* 98** 919-926

Kieliszewski, M. J., Kamyab, A., Leykam, J. F., and Lamport, D. T. A. (1992)
A histidine-rich extensin from zea-mays is an arabinogalactan protein.
***Plant Physiology* 99** 538-547

Kim, Y. S., Kim, D. H., and Jung, J. (1998)
Isolation of a novel auxin receptor from soluble fractions of rice (Oryza sativa L.) shoots.
***Febs Letters* 438** 241-244

Klimov, S. V., Astakhova, N. V., and Trunova, T. I. (1993)
Structural and functional adaptation of photosynthetic apparatus of winter-wheat to low-temperature.
***Zhurnal Obshchei Biologii* 54** 30- 44

Knox, J. P. (1991)
Developmentally regulated epitopes of cell surface arabinogalactan proteins.
***Plant Journal* 1** 317-326

Kong, S. K., Yim, M. B., Stadtman, E. R., and Chock, P. B. (1995)
Peroxynitrite disables the tyrosine phosphorylation regulatory mechanism by nitrating the tyrosine residue - tyrosine kinase fails to phosphorylate nitrated tyrosine.
***Faseb Journal* 9** A1303-

KOOY, N. W., ROYALL, J. A. , YE, Y. Z., KELLY, D. R., and Beckman, J. S. (1995)
EVIDENCE FOR IN-VIVO PEROXYNITRITE PRODUCTION IN HUMAN ACUTE LUNG INJURY.
***American Journal Of Respiratory And Critical Care Medicine* 151**-4 1250-1254

Laemmli, U. K. (1970)
Cleavage of structural proteins during the assembly of the head of bacteriophage T4.
***Nature* 277** 680-685

Laisk, A., Kull, O., and Moldau, H. (1989)
Ozone concentration in leaf intercellular air spaces is close to zero.
***Plant Physiology* 90** 1163-1167

Lamb, C. J., Lawton, M. A. , Dron, M., and Dixon, R. A. (1989)
Signals and transduction mechanisms for activation of plant defenses against microbial attack.
***Cell* 56** 215-224

Lamport, D. T. A., Katona, L., and Roerig, S. (1973)
***Biochemistry Journal* 133** 125-131

Lane, B., Grzelczak, Z., Kennedy, T., Hew, C., and Joshi, S. (1987)
Preparation and analysis of mass amounts of germin - demonstration that the protein which signals the onset of growth in germinating wheat is a glycoprotein.
***Biochemistry And Cell Biology-Biochimie Et Biologie Cellulaire* 65** 354-362

Lane, B. G., Cuming, A. C. , Fregeau, J., Carpita, N. C., Hurkman, W. J., Bernier, F., Dratewkakos, E., and Kennedy, T. D. (1992)
Germin isoforms are discrete temporal markers of wheat development - pseudogermin is a uniquely thermostable water-soluble oligomeric protein in ungerminated embryos and like germin in germinated embryos, it is incorporated into cell-walls.
***European Journal Of Biochemistry* 209** 961-969

Lane, B. G., Dunwell, J. M., Ray, J. A., Schmitt, M. R., and Cuming, A. C. (1993)
Germin, a protein marker of early plant development, is an oxalate oxidase.
***Journal Of Biological Chemistry* 268** 12239-12242

Lane, B. G. (1994)
Oxalate, germin, and the extracellular-matrix of higher-plants.
***Faseb Journal* 8** 294 -301

Leah, R., Tommerup, H., Svendsen, I, and Mundy, J. (1991)
Biochemical and molecular characterization of 3 barley seed proteins with antifungal properties.
***Journal Of Biological Chemistry* 266** 1564-1573

Legendre, L., YUEH, Y. G., CRAIN, R., HADDOCK, N., Heinstein, P. F., and Low, P. S. (1993)
PHOSPHOLIPASE-C ACTIVATION DURING ELICITATION OF THE OXIDATIVE BURST IN CULTURED PLANT-CELLS.
***Journal Of Biological Chemistry* 268**-33 24559-24563

Levine, A., Tenhaken, R., Dixon, R., and Lamb, C. (1994)
H2o2 from the oxidative burst orchestrates the plant hypersensitive disease resistance response.
***Cell* 79** 583-593

Levy, S. (1991)
2 Separate zones of helicoidally orientated microfibrils are present in the walls of nitella internodes during growth.
***Protoplasma* 163** 145-155

Li, J., Billiar, T. R., Talanian, R. V., and Kim, Y. M. (1997)
Nitric oxide reversibly inhibits seven members of the caspase family via S-nitrosylation.
***Biochemical And Biophysical Research Communications* 240** 419-424

Liddell, S. and Knox, D. P. (1998)
Extracellular and cytoplasmic Cu/Zn superoxide dismutases from Haemonchus contortus.
***Parasitology* 116** 383-394

Lin, A., Krockmalnic, G., and Penman, S. (1990)
Imaging cytoskeleton mitochondrial-membrane attachments by embedment- free electron-microscopy of saponin-extracted cells.
Proceedings Of The National Academy Of Sciences Of The United States Of America **87** 8565-8569

Lin, X. Y., Hwang, G. J. H., and Zimmerman, J. L. (1996)
Isolation and characterization of a diverse set of genes from carrot somatic embryos.
Plant Physiology **112** 1365-1374

Lobler, M. and Klambt, D. (1985)
Auxin-binding protein from coleoptile membranes of corn (Zea-mays-l) .1. Purification by immunological methods and characterization.
Journal Of Biological Chemistry **260** 9848-9853

Lobler, M. and Klambt, D. (1985)
Auxin-binding protein from coleoptile membranes of corn (Zea-mays-l) .2. Localization of a putative auxin receptor.
Journal Of Biological Chemistry **260** 9854-9859

Lohaus, G., Winter, H., Riens, B, and Heldt, H. W. (1995)
Botanica Acta **108** 270-275

Long, J. M. and Widders, I. E. (1990)
Quantification of apoplastic potassium content by elution analysis of leaf lamina tissue from pea (Pisum-sativum l cv argenteum).
Plant Physiology **94** 1040-1047

Luwe, M. (1996)
Antioxidants in the apoplast and symplast of beech (Fagus sylvatica L) leaves: Seasonal variations and responses to changing ozone concentrations in air.
Plant Cell And Environment **19** 321-328

Luwe, M. and Heber, U. (1995)
Ozone detoxification in the apoplasm and symplasm of spinach, broad bean and beech leaves at ambient and elevated concentrations of ozone in air.
Planta **197** 448-455

Luwe, M. (1994)
Zur Entgiftung von Ozon im Blatt durch Antioxidantien unter besonderer Berucksichtigung des Apoplasten.
University of Wurzberg PhD thesis.

Luwe, M. W. F., Takahama, U., and Heber, U. (1993)
Role of ascorbate in detoxifying ozone in the apoplast of spinach (Spinacia-oleracea l) Leaves.
Plant Physiology **101** 969-976

Macdonald, H., Jones, A. M., and King, P. J. (1991)
Photoaffinity-labeling of soluble auxin-binding proteins.
Journal Of Biological Chemistry **266** 7393-7399

Macneil, S., Dawson, R. A. , Crocker, G., Barton, C. H., Hanford, L., Metcalfe, R., Mcgurk, M., and Munro, D. S. (1988)
Extracellular calmodulin and its association with epidermal growth- factor in normal human-body fluids.
Journal Of Endocrinology **118** 501-

Maltby, D., Carpita, N. C. , Montezinos, D., Kulow, C., and Delmer, D. P. l. (1979)
β-1,3-glucan in developing cotton fibres. Structure, localization and relationship of synthesis to that of secondary wall cellulose.
Plant Physiology **63** 1158-1164

Marcus, A., Greenberg, J., and Averyhartfullard, V (1991)
Repetitive proline-rich proteins in the extracellular-matrix of the plant-cell.
***Physiologia Plantarum* 81** 273-279

Marentes, E., Griffith, M. , Mlynarz, A., and Brush, R. A. (1993)
Proteins accumulate in the apoplast of winter rye leaves during cold- acclimation.
***Physiologia Plantarum* 87** 499-507

Marklund, S. L. (1976)
Spectrophotometric study of spontaneous disproportionation of superoxide anion radical and sensitive direct assay for superoxide dismutase.
***Journal Of Biological Chemistry* 251** 7504-7508

Matsumoto, I, Jimbo, A., Mizuno, Y., Seno, N., and Jeanloz, R. W. (1983)
Purification and characterization of potato lectin.
***Journal Of Biological Chemistry* 258** 2886-2891

Mäder, M. (1980)
Origin of the heterogeneity of peroxidase isoenzymes group G1 from *Nicotiana tabacum.*
***Pflanzenzphysiologia* 96** 283-296

Mccann, M. C. and Roberts, K. (1994)
CHANGES IN CELL-WALL ARCHITECTURE DURING CELL ELONGATION.
***Journal Of Experimental Botany* 45**-280 1683-1691

Mccann, M. C., Wells, B., and Roberts, K. (1992)
Complexity in the spatial localization and length distribution of plant cell-wall matrix polysaccharides.
***Journal Of Microscopy-Oxford* 166** 123-136

Mccann, M. C., Wells, B., and Roberts, K. (1990)
Direct visualization of cross-links in the primary plant-cell wall.
***Journal Of Cell Science* 96** 323-334

McCord, J. M. and Fridovich, I. (1969)
Superoxide dismutase: an enzymic function for erythrocurein (hemocuperin).
***Journal Of Biological Chemistry* 244** 6049-6055

McCord, J. M. (2000)
The evolution of free radicals and oxidative stress.
***American Journal Of Medicine* 108**-8 652-659

Mcdonald, L. J. and Moss, J. (1994)
Nitric-oxide and nad-dependent protein modification.
***Molecular And Cellular Biochemistry* 138** 201-206

Mcgurl, B., Pearce, G., Orozcocardenas, M., and Ryan, C. A. (1992)
Structure, expression, and antisense inhibition of the systemin precursor gene.
***Science* 255** 1570-1573

Mcgurl, B. and Ryan, C. A. (1992)
The organization of the prosystemin gene.
***Plant Molecular Biology* 20** 405-409

McNair, M. R. (1993)
***New Phytologist* 124** 541-559

Mcqueenmason, S. and Cosgrove, D. J. (1994)
Disruption of hydrogen-bonding between plant-cell wall polymers by proteins that induce wall extension.
***Proceedings Of The National Academy Of Sciences Of The United States Of America* 91** 6574-6578

Mcqueenmason, S. J. and Cosgrove, D. J. (1995)
Expansin mode of action on cell-walls - analysis of wall hydrolysis, stress-relaxation, and binding.
***Plant Physiology* 107** 87-100

Mehdy, M. C. (1994)
Active oxygen species in plant defense against pathogens.
***Plant Physiology* 105** 467 -472

Memelink, J., Devries, S. C., Schilperoort, R. A., and Hoge, J. H. C. (1988)
Changes in the tissue-specific prevalence of translatable messenger- rnas in transgenic tobacco shoots containing the t-dna cytokinin gene.
***Plant Molecular Biology* 11** 625-631

Memelink, J., Swords, K. M. M., Dekam, R. J., Schilperoort, R. A., Hoge, J. H. C., and Staehelin, L. A. (1993)
Structure and regulation of tobacco extensin.
***Plant Journal* 4** 1011-1022

Miller, A. R. (1986)
Oxidation of cell wall polysaccharides by hydrogen peroxide: a potential mechanism for cell wall breakdown in plants.
***Biochemical And Biophysical Research Communications* 141** 238-244

Millner, P. A. (1995)
The auxin signal.
***Current Opinion In Cell Biology* 7** 224-231

MIMURA, T., SAKANO, K., and TAZAWA, M. (1990)
CHANGES IN THE SUBCELLULAR-DISTRIBUTION OF FREE AMINO-ACIDS IN RELATION TO LIGHT CONDITIONS IN CELLS OF CHARA-CORALLINA.
***Botanica Acta* 103**-1 42-47

Moberg, L., Karlberg, K., Blomqvist, S., and Larsson, U. (2000)
Comparison between a new application of multivariate regression and current spectroscopy methods for the determination of chlorophylls and their corresponding pheopigments.
***Analytica Chimica Acta* 411**-1-2 137-143

MOLINA, M. A., AVILES, F. X., and QUEROL, E. (1992)
EXPRESSION OF A SYNTHETIC GENE ENCODING POTATO CARBOXYPEPTIDASE INHIBITOR USING A BACTERIAL SECRETION VECTOR.
***Gene* 116**-2 129-138

Mollenkopf, H. J., Jungblut, P. R., and Raupach, B. (1999)
A dynamic two-dimensional PAGE database.
***Electrophoresis* 20** 2172 -2180

MUHLING, K. H., PLIETH, C. , HANSEN, U. P., and SATTELMACHER, B. (1995)
APOPLASTIC PH OF INTACT LEAVES OF VICIA-FABA AS INFLUENCED BY LIGHT.
***Journal Of Experimental Botany* 46**-285 377-382

Munch, E. (1930)
Die Stoffbewegungen in der Pflanze.
Jeana: Fischer 73-

Mundy, J. and Chua, N. H. (1988)
Abscisic-acid and water-stress induce the expression of a novel rice gene.
***Embo Journal* 7** 2279-2286

Murray, R. H. A. and Northcote, D. H. (1978)
***Phytochemistry* 17** 623-629

Nakajima, N., Morikawa, H. , Igarashi, S., and Senda, M. (1981)
Differential effect of calcium and magnesium on mechanical properties of pea stem cell

walls.
Plant cell physiology **22** 1305-1315

Napier, R. M., Fowke, L. C., Hawes, C., Lewis, M. , and Pelham, H. R. B. (1992)
Immunological evidence that plants use both hdel and kdel for targeting proteins to the endoplasmic-reticulum.
Journal Of Cell Science **102** 261-271

Niderman, T., Genetet, I, Bruyere, T., Gees, R., Stintzi, A., Legrand, M., Fritig, B., and Mosinger, E. (1995)
Pathogenesis-related pr-1 proteins are antifungal - isolation and characterization of 3 14-kilodalton proteins of tomato and of a basic pr-1 of tobacco with inhibitory activity against phytophthora- infestans.
Plant Physiology **108** 17-27

Ninnemann, H. and Maier, J. (1996)
Indications for the occurrence of nitric oxide synthases in fungi and plants and the involvement in photoconidiation of Neurospora crassa.
Photochemistry And Photobiology **64** 393-398

NIU, X. M., Bressan, R. A. , Hasegawa, P. M., and PARDO, J. M. (1995)
ION HOMEOSTASIS IN NACL STRESS ENVIRONMENTS.
Plant Physiology **109**-3 735-742

Nobel, P. S. (1983)
Nutrient levels in cacti - relation to nocturnal acid accumulation and growth.
American Journal Of Botany **70** 1244-1253

Noritake, T., Kawakita, K. , and Doke, N. (1996)
Nitric oxide induces phytoalexin accumulation in potato tuber tissues.
Plant And Cell Physiology **37**-1 113-116

O'Farrell, P. H. (1975)
High resolution two-dimensional electrophoresis of proteins.
Journal Of Biological Chemistry **250** 4007-4021

Ogawa, K., Kanematsu, S., and Asada, K. (1996)
Intra- and extra-cellular localization of "cytosolic" CuZn- superoxide dismutase in spinach leaf and hypocotyl.
Plant And Cell Physiology **37** 790-799

Ohmiya, A., Tanaka, Y., Kadowaki, K., and Hayashi, T. (1998)
Cloning of genes encoding auxin-binding proteins (ABP19/20) from peach: Significant peptide sequence similarity with germin-like proteins.
Plant And Cell Physiology **39**-5 492-499

Okane, D., Gill, V, Boyd, P., and Burdon, B. (1996)
Chilling, oxidative stress and antioxidant responses in Arabidopsis thaliana callus.
Planta **198** 371-377

Otter, T. and Polle, A. (1997)
Characterisation of acidic and basic apoplastic peroxidases from needles of Norway spruce (Picea abies, L, Karsten) with respect to lignifying substrates.
Plant And Cell Physiology **38** 595-602

Paes, M. C. and Oliveira, P. L. (1999)
Extracellular glutathione peroxidase from the blood-sucking bug, Rhodnius prolixus.
Archives Of Insect Biochemistry And Physiology **41** 171-177

Palme, K. and Galweiler, L. (1999)
PIN-pointing the molecular basis of auxin transport.
Current Opinion In Plant Biology **2** 375-381

Pardo, M., Monteoliva, L., Pla, J., Sanchez, M., Gil, C., and Nombela, C. (1999)
Two-dimensional analysis of proteins secreted by Saccharomyces cerevisiae regenerating protoplasts: A novel approach to study the cell wall.
***Yeast* 15**-6 459-472

Parsell, D. A. and Lindquist, S. (1993)
The function of heat-shock proteins in stress tolerance - degradation and reactivation of damaged proteins.
***Annual Review Of Genetics* 27** 437-496

Parsons, B. L. and Mattoo, A. K. (1994)
A wound-repressible glycine-rich protein transcript is enriched in vascular bundles of tomato fruit and stem.
***Plant And Cell Physiology* 35** 27-35

Pennell, R. I., Knox, J. P., Scofield, G. N., Selvendran, R. R., and Roberts, K. (1989)
A family of abundant plasma-membrane associated glycoproteins related to the arabinogalactan proteins is unique to flowering plants.
***Journal Of Cell Biology* 108** 1967-1977

Pennell, R. I. and Roberts, K. (1990)
Sexual development in the pea is presaged by altered expression of arabinogalactan protein.
***Nature* 344** 547-549

Peters, R. (1996)
Damage to potato tubers, a review.
***Potato Research* 39** 479-484

Pfanz, H. and Heber, U. (1989)
***In modern methods of plant analysis* Springer, Berlin.** 322-343

Pfanz, H. and Dietz, K. J. (1987)
A fluorescence method for the determination of the apoplastic proton concentration in intact leaf tissues.
***Journal Of Plant Physiology* 129** 41-48

Pfeiffer, S., Janistyn, B. , Jessner, G., Pichorner, H., and Ebermann, R. (1994)
Gaseous nitric-oxide stimulates guanosine-3',5'-cyclic monophosphate (Cgmp) Formation in spruce needles.
***Phytochemistry* 36** 259-262

Pfeiffer, S., Leopold, E., Hemmens, B., Schmidt, K., Werner, E. R., and Mayer, B. (1997)
Interference of carboxy-PTIO with nitric oxide- and peroxynitrite-mediated reactions.
***Free Radical Biology And Medicine* 22**-5 787-794

Pinedo, M. L., Segarra, C. , and Conde, R. D. (1993)
Occurrence of 2 endoproteinases in wheat leaf intercellular washing fluid.
***Physiologia Plantarum* 88** 287-293

Polle, A., CHAKRABARTI, K. , SCHURMANN, W., and Rennenberg, H. (1990)
COMPOSITION AND PROPERTIES OF HYDROGEN-PEROXIDE DECOMPOSING SYSTEMS IN EXTRACELLULAR AND TOTAL EXTRACTS FROM NEEDLES OF NORWAY SPRUCE (PICEA-ABIES L, KARST).
***Plant Physiology* 94**-1 312-319

Polle, A., Krings, B., and Rennenberg, H. (1989)
Factors modulating superoxide-dismutase activity in needles of spruce trees (Picea-abies l).
***Annales Des Sciences Forestieres* 46** S807-S810

Poulos, T. L., Raman, C., and Li, H. Y. (1998)
NO news is good news.
***Structure* 6**-3 255-258

Powell, D. A., Morris, E. R., Gidley, M. J., and Rees, D. A. (1982)
Conformations and interactions of pectins II. Influence of residue sequence on chain association in calcium pectate gels.
***Journal of molecular biology* 155** 517-531

Purvis, A. C., Shewfelt, R. L., and Gegogeine, J. W. (1995)
Superoxide production by mitochondria isolated from green bell pepper fruit.
***Physiologia Plantarum* 94** 743-749

Quigley, F., Villiot, M. L., and Mache, R. (1991)
Nucleotide-sequence and expression of a novel glycine-rich protein gene from arabidopsis-thaliana.
***Plant Molecular Biology* 17** 949-952

Quinn, P. J., Tsvetkova, N. M., and Genchov, B. G. (1988)
How trehalose affects the lipid phase-behavior of model membranes.
***Cryobiology* 25** 521-

Radi, R., Beckman, J. S., Bush, K. M., and Freeman, B. A. (1991)
Peroxynitrite oxidation of sulfhydryls - the cytotoxic potential of superoxide and nitric-oxide.
***Journal Of Biological Chemistry* 266** 4244-4250

Rao, D. N. R., Fischer, V, and Mason, R. P. (1990)
Glutathione and ascorbate reduction of the acetaminophen radical formed by peroxidase - detection of the glutathione disulfide radical-anion and the ascorbyl radical.
***Journal Of Biological Chemistry* 265** 844-847

Rasmussen, U., Giese, H., and Mikkelsen, J. D. (1992)
Induction and purification of chitinase in brassica-napus l ssp oleifera infected with phoma-lingam.
***Planta* 187** 328-334

Rautenkranz, A. A. F., Li, L. J., Machler, F., Martinoia, E., and Oertli, J. J. (1994)
Transport of ascorbic and dehydroascorbic acids across protoplast and vacuole membranes isolated from barley (Hordeum-vulgare l cv gerbel) Leaves.
***Plant Physiology* 106** 187-193

Rees, D. A. (1977)
Polysaccharide shapes.
London: Chapman and Hall

Reinard, T. and Jacobsen, H. J. (1995)
A soluble high-affinity auxin-binding protein from pea apex.
***Journal Of Plant Physiology* 147** 132-138

Richter, C., Gogvadze, V, Laffranchi, R., Schlapbach, R., Schweizer, M., Suter, M., Walter, P., and Yaffee, M. (1995)
Oxidants in mitochondria - from physiology to diseases.
***Biochimica Et Biophysica Acta-Molecular Basis Of Disease* 1271** 67-74

Rob, A., Hernandez, M., Ball, A. S., Tuncer, M., Arias, M. E., and Wilson, M. T. (1997)
Production and partial characterization of extracellular peroxidases produced by Streptomyces avermitilis UAH30.
***Applied Biochemistry And Biotechnology* 62** 159-174

ROBERTS, A. W. and HAIGLER, C. H. (1990)
TRACHEARY-ELEMENT DIFFERENTIATION IN SUSPENSION-CULTURED CELLS OF ZINNIA REQUIRES UPTAKE OF EXTRACELLULAR CA-2+ - EXPERIMENTS WITH CALCIUM-CHANNEL BLOCKERS AND CALMODULIN INHIBITORS.
***Planta* 180**-4 502-509

Robertson, D., Mitchell, G. P., Gilroy, J. S., Gerrish, C., Bolwell, G. P., and Slabas, A. R. (1997)
Differential extraction and protein sequencing reveals major differences in patterns of primary cell wall proteins from plants.
***Journal Of Biological Chemistry* 272** 15841-15848

Rogiers, S. Y., Kumar, G. N. M., and Knowles, N. R. (1998)
Maturation and ripening of fruit of Amelanchier alnifolia Nutt. are accompanied by increasing oxidative stress [Full text delivery].
Annals Of Botany **81** 203-211

Rohringer, R., Ebrahimnesbat, F., and Wolf, G. (1983)
Proteins in intercellular washing fluids from leaves of barley (Hordeum-vulgare-l).
Journal Of Experimental Botany **34** 1589-1605

Runeckles, V. C. and Vaartnou, M. (1997)
EPR evidence for superoxide anion formation in leaves during exposure to low levels of ozone.
Plant Cell And Environment **20**-3 306-314

Sadava, D., Walker, F., and Chrispeels, M. J. (1973)
Hydroxyproline-rich cell wall protein (extensin): biosynthesis and accumulation in growing pea epicotyls.
Developmental biology **30** 42-48

SALZER, P. and HAGER, A. (1993)
CHARACTERIZATION OF WALL-BOUND INVERTASE ISOFORMS OF PICEA- ABIES CELLS AND REGULATION BY ECTOMYCORRHIZAL FUNGI.
Physiologia Plantarum **88**-1 52-59

SALZER, P. and HAGER, A. (1993)
EFFECT OF AUXINS AND ECTOMYCORRHIZAL ELICITORS ON WALL-BOUND PROTEINS AND ENZYMES OF SPRUCE [PICEA-ABIES (L) KARST] CELLS.
Trees-Structure And Function **8**-1 49-55

Sanchez, O. J., Pan, A., Nicolas, G., and Labrador, E. (1989)
Relation of cell-wall peroxidase-activity with growth in epicotyls of cicer-arietinum - effects of calmodulin inhibitors.
Physiologia Plantarum **75** 275-279

Sawicka, T. and Kacperska, A. (1995)
Soluble and cell wall-associated beta-galactosidases from cold-grown winter rape (Brassica-napus l, var oleifera l) Leaves.
Journal Of Plant Physiology **145** 357-362

Scheel, D. (1998)
Resistance response physiology and signal transduction.
Current Opinion In Plant Biology **1** 305-310

Schinkel, H., Streller, S. , and Wingsle, G. (1998)
Multiple forms of extracellular superoxide dismutase in needles, stem tissues and seedlings of Scots pine.
Journal Of Experimental Botany **49** 931-936

Schopfer, P. (1996)
Hydrogen peroxide-mediated cell-wall stiffening in vitro in maize coleoptiles.
Planta **199**-1 43-49

Schuchmann, M. N. and von Sonntag, C. (1978)
International Journal of Radiation Biology **34** 397-400

Schweikert, C., Liszkay, A., and Schopfer, P. (2000)
Scission of polysaccharides by peroxidase-generated hydroxyl radicals.
Phytochemistry **53** 565-570

Serpe, M. D. and Matthews, M. A. (1992)
Rapid changes in cell-wall yielding of elongating begonia-argenteo- guttata l leaves in response to changes in plant water status.
Plant Physiology **100** 1852-1857

Shedtetzky, E., Shumel, M. , Delmer, D. P., and Lamport, D. T. A. (1990)
Adaptation and growth of tomato cells on the herbicide 2,6-dichlorobenzonitrile (DCB) leads to production of cell walls virtually lacking a cellulose-xyloglucan network.
***Plant Physiology* 94** 980-987

Shimizi, Y., Hayashi, T., Kawada, T., and Sakuno, T. (1997)
Promotion of pea stem elongation by the fragements of plant cell wall polysaccharides.
***Mokuzai Gakkaishi* 43** 121-127

Shimomura, S., Watanabe, S., and Ichikawa, H. (1999)
Characterization of auxin-binding protein 1 from tobacco: content, localization and anxin-binding activity.
***Planta* 209** 118-125

Shimomura, S., Inohara, N. , Fukui, T., and Futai, M. (1988)
Different properties of 2 types of auxin-binding sites in membranes from maize coleoptiles.
***Planta* 175** 558-566

Showalter, A. M. (1993)
Structure and function of plant-cell wall proteins.
***Plant Cell* 5** 9-23

Simon, D. I., Mullins, M. E., Jia, L., Gaston, B., Singel, D. J., and Stamler, J. S. (1996)
Polynitrosylated proteins: Characterization, bioactivity, and functional consequences.
***Proceedings Of The National Academy Of Sciences Of The United States Of America* 93** 4736-4741

Singh, N. K., Bracker, C. A., Hasegawa, P. M., Handa, A. K., Buckel, S., Hermodson, M. A., Pfankoch, E., Regnier, F. E., and Bressan, R. A. (1987)
Characterization of osmotin - a thaumatin-like protein associated with osmotic adaptation in plant-cells.
***Plant Physiology* 85** 529-536

Smith, J. A. C. and Nobel, P. S. (1986)
Water-movement and storage in a desert succulent - anatomy and rehydration kinetics for leaves of agave-deserti.
***Journal Of Experimental Botany* 37** 1044-1053

Smith, J. J., Muldoon, E. P., and Lamport, D. T. A. (1984)
Isolation of extensin precursors by direct elution of intact tomato cell-suspension cultures.
***Phytochemistry* 23** 1233-1239

Smith, J. J., Muldoon, E. P., Willard, J. J., and Lamport, D. T. A. (1986)
Tomato extensin precursors p1 and p2 are highly periodic structures.
***Phytochemistry* 25** 1021-1030

So, H. S., Park, R. K., Kim, M. S., Lee, S. R., Jung, B. H., Chung, S. Y., Ju, C. D., and Chung, H. T. (1998)
Nitric oxide inhibits c-Jun N-terminal kinase 2 (JNK2) via S- nitrosylation [Full text delivery].
***Biochemical And Biophysical Research Communications* 247** 809-813

Souza, J. M. and Radi, R. (1998)
Glyceraldehyde-3-phosphate dehydrogenase inactivation by peroxynitrite.
***Archives Of Biochemistry And Biophysics* 360**-2 187-194

Spector, T. (1978)
Refinement of Coomassie blue method of protein quantitation.
***Analytical Biochemistry* 86** 142-145

Speer, M. and Kaiser, W. M. (1991)
Ion relations of symplastic and apoplastic space in leaves from spinacia-oleracea l and pisum-sativum l under salinity.
***Plant Physiology* 97** 990-997

Speer, M. and Kaiser, W. M. (1994)
Replacement of nitrate by ammonium as the nitrogen-source increases the salt sensitivity of pea-plants .2. Intercellular and intracellular solute compartmentation in leaflets.
Plant Cell And Environment **17** 1223-1231

Stacey, N. J., Roberts, K. , and Knox, J. P. (1990)
Patterns of expression of the jim4 arabinogalactan-protein epitope in cell-cultures and during somatic embryogenesis in daucus-carota l.
Planta **180** 285-292

Stamler, J. S., Singel, D. J., and Loscalzo, J. (1992)
Biochemistry of nitric-oxide and its redox-activated forms.
Science **258** 1898-1902

Stiefel, V, Perezgrau, L., Albericio, F., Giralt, E., Ruizavila, L., Ludevid, M. D., and Puigdomenech, P. (1988)
Molecular-cloning of cdnas encoding a putative cell-wall protein from zea-mays and immunological identification of related polypeptides.
Plant Molecular Biology **11** 483-493

Stintzi, A., Heitz, T., Prasad, V, Wiedemannmerdinoglu, S., Kauffmann, S., Geoffroy, P., Legrand, M., and Fritig, B. (1993)
Plant pathogenesis-related proteins and their role in defense against pathogens.
Biochimie **75** 687-706

Strahm, A., Amado, R., and Neukom, H. (1981)
Hydroxyproline-galactoside as a protein-polysaccharide linkage in a water-soluble arabinogalactan-peptide from wheat endosperm.
Phytochemistry **20** 1061-1063

Stralin, P., Karlsson, K., Johansson, B. O., and Marklund, S. L. (1995)
The interstitium of the human arterial-wall contains very large amounts of extracellular-superoxide dismutase.
Arteriosclerosis Thrombosis And Vascular Biology ASCULAR 2032-2036

Streller, S. and Wingsle, G. (1994)
Pinus-sylvestris l needles contain extracellular cuzn superoxide- dismutase.
Planta **192** 195-201

Sturm, A. (1992)
A wound-inducible glycine-rich protein from daucus-carota with homology to single-stranded nucleic acid-binding proteins.
Plant Physiology **99** 1689-1692

Sturm, A. and Chrispeels, M. J. (1990)
Cdna cloning of carrot extracellular beta-fructosidase and its expression in response to wounding and bacterial-infection.
Plant Cell **2** 1107-1119

Sun, D. Y., BIAN, Y. Q., ZHAO, B. H., ZHAO, L. Y., YU, X. M., and SHENGJUN, D. (1995)
THE EFFECTS OF EXTRACELLULAR CALMODULIN ON CELL-WALL REGENERATION OF PROTOPLASTS AND CELL-DIVISION.
Plant And Cell Physiology **36**-1 133-138

Sutherland, M. W. (1991)
The generation of oxygen radicals during host plant-responses to infection.
Physiological And Molecular Plant Pathology **39** 79-93

Sutherland, M. W. and Learmonth, B. A. (1997)
The tetrazolium dyes MTS and XTT provide new quantitative assays for superoxide and superoxide dismutase.
Free Radical Research **27**-3 283-289

Symonan, M. A. and Nalbandyan, R. M. (1972)
Interaction of hydrogen peroxide with superoxide dismutase from erythrocytes.
***Febs Letters* 28** 22- 29

Taiz, L. (1984)
Plant-cell expansion - regulation of cell-wall mechanical-properties.
***Annual Review Of Plant Physiology And Plant Molecular Biology* 35** 585-657

Takahama, U., Hirotsu, M., and Oniki, T. (1999)
Age-dependent changes in levels of ascorbic acid and chlorogenic acid, and activities of peroxidase and superoxide dismutase in the apoplast of tobacco leaves: Mechanism of the oxidation of chlorogenic acid in the apoplast.
***Plant And Cell Physiology* 40** 716-724

Takahama, U. and Oniki, T. (1992)
Regulation of peroxidase-dependent oxidation of phenolics in the apoplast of spinach leaves by ascorbate.
***Plant And Cell Physiology* 33** 379-387

Tang, X. W., Ruffner, H. P., Scholes, J. D., and Rolfe, S. A. (1996)
Purification and characterisation of soluble invertases from leaves of Arabidopsis thaliana.
***Planta* 198** 17-23

Tenhaken, R., Levine, A., Brisson, L. F., Dixon, R. A., and Lamb, C. (1995)
Function of the oxidative burst in hypersensitive disease resistance.
***Proceedings Of The National Academy Of Sciences Of The United States Of America* 92** 4158-4163

Terry, M. E., Jones, R. L. , and Bonner, B. A. (1981)
Soluble cell-wall polysaccharides released from pea stems by centrifugation .1. Effect of auxin.
***Plant Physiology* 68** 531-537

Tetlow, I. J. and Farrar, J. F. (1993)
Apoplastic sugar concentration and ph in barley leaves infected with brown rust.
***Journal Of Experimental Botany* 44** 929-936

Thompson, J. E. (1984)
Physical changes in the membranes of senescing and environmentally stressed plant tissues.
In Physiology of membrane fluidity **Boca Rota: CRC Press**

Tibbits, C. W., MacDougall, A. J., and Ring, S. G. (1998)
Calcium binding and swelling behaviour of a high methoxyl pectin gel.
***Carbohydrate Research* 310**-1-2 101-107

Tierney, M. L., Wiechert, J., and Pluymers, D. (1988)
Analysis of the expression of extensin and p33-related cell-wall proteins in carrot and soybean.
***Molecular & General Genetics* 211** 393-399

Trewavas, A. and Gilroy, S. (1991)
Signal transduction in plant-cells.
***Trends In Genetics* 7** 356-361

Tsurusaki, K., Masuda, Y., and Sakurai, N. (1997)
Distribution of indole-3-acetic acid in the apoplast and symplast of squash (Cucurbita maxima) hypocotyls.
***Plant And Cell Physiology* 38**-3 352-356

Vanacker, H., Harbinson, J., Ruisch, J., Carver, T. L. W., and Foyer, C. H. (1998)
Antioxidant defences of the apoplast.
***Protoplasma* 205** 129-140

Vanacker, H., Foyer, C. H. , and Carver, T. L. W. (1999)
Changes in apoplastic antioxidants induced by powdery mildew attack in oat genotypes with race non-specific resistance.
***Planta* 208** 444-452

Vandervliet, A., Smith, D. , Oneill, C. A., Kaur, H., Darleyusmar, V, Cross, C. E., and Halliwell, B. (1994)
Interactions of peroxynitrite with human plasma and its constituents - oxidative damage and antioxidant depletion.
***Biochemical Journal* 303** 295-301

Vanholst, G. J. and Fincher, G. B. (1984)
Polyproline-ii confirmation in the protein-component of arabinogalactan-protein from lolium-multiflorum.
***Plant Physiology* 75** 1163-1164

Vanholst, G. J. and Varner, J. E. (1984)
Reinforced polyproline-ii conformation in a hydroxyproline-rich cell- wall glycoprotein from carrot root.
***Plant Physiology* 74** 247-251

Venis, M. A. and Napier, R. M. (1995)
Auxin receptors and auxin-binding proteins.
***Critical Reviews In Plant Sciences* 14** 27-47

Veraestrella, R., Blumwald, E., and Higgins, V. J. (1992)
Effect of specific elicitors of cladosporium-fulvum on tomato suspension cells - evidence for the involvement of active oxygen species.
***Plant Physiology* 99** 1208-1215

Vigers, A. J., Roberts, W. K., and Selitrennikoff, C. P. (1991)
A new family of plant antifungal proteins.
***Molecular Plant-Microbe Interactions* 4** 315-323

VU, L. and HUYNH, Q. K. (1994)
ISOLATION AND CHARACTERIZATION OF A 27-KDA ANTIFUNGAL PROTEIN FROM THE FRUITS OF DIOSPYROS-TEXANA.
***Biochemical And Biophysical Research Communications* 202**-2 666-672

Walkinshaw, M. D. and Arnott, S. (1981)
Conformations and interactions of pectins. II. Models for junction zones in pectinic acid and calcium pectate gels.
***Journal of molecular biology* 153** 1075-1085

Watt, D. K., Brasch, D. J. , Larsen, D. S., and Melton, L. D. (1999)
Isolation, characterisation, and NMR study of xyloglucan from enzymatically depectinised and non-depectinised apple pomace.
***Carbohydrate Polymers* 39** 165-180

Willekens, H., Inze, D., Vanmontagu, M., and Vancamp, W. (1995)
Catalases in plants.
***Molecular Breeding* 1** 207-228

Wingsle, G., Gardestrom, P., Hallgren, J. E., and Karpinski, S. (1991)
Isolation, purification, and subcellular-localization of isozymes of superoxide-dismutase from scots pine (Pinus-sylvestris l) Needles.
***Plant Physiology* 95** 21-28

Wink, D. A. (1998)
The chemical mechanisms in regulatory, cytotoxic, and cytoprotective roles of nitric oxide.
***Abstracts Of Papers Of The American Chemical Society* 215** 640-CHED

Winter, H., Robinson, D. G., and Heldt, H. W. (1993)
Subcellular volumes and metabolite concentrations in barley leaves.
***Planta* 191** 180-190

Winter, H., Robinson, D. G., and Heldt, H. W. (1994)
Subcellular volumes and metabolite concentrations in spinach leaves.
***Planta* 193** 530-535

Wojtaszek, P. (2000)
Nitric oxide in plants - To NO or not to NO.
***Phytochemistry* 54** 1-4

Wojtaszek, P. (1997)
Oxidative burst: An early plant response to pathogen infection.
***Biochemical Journal* 322** 681-692

Woolhouse, H. W. (1983)
Radioecological techniques - schultz,v, whicker,fw.
***Journal Of Ecology* 71** 662-663

Wyatt, R. E., Nagao, R. T. , and Key, J. L. (1992)
Patterns of soybean proline-rich protein gene-expression.
***Plant Cell* 4** 99-110

Wyatt, S. E. and Carpita, N. C. (1993)
New location for some plant glycine-rich proteins.
***Plant Physiology* 102** 91-

Yahraus, T., Chandra, S., Legendre, L., and Low, P. S. (1995)
Evidence for a mechanically induced oxidative burst.
***Plant Physiology* 109** 1259-1266

Yamaguchi, Y. and Pfeiffer, S. E. (1999)
Highly basic myelin and oligodendrocyte proteins analyzed by NEPHGE-two-dimensional gel electrophoresis: Recognition of novel developmentally regulated proteins.
***Journal Of Neuroscience Research* 56**-2 199-205

Yamaguchi, Y., Okabe, K., Masumura, F., Akizuki, E., Matsuda, T., Ohshiro, H., Liang, J., Yamada, S., Mori, K., and Ogawa, M. (1999)
Peroxynitrite formation during rat hepatic allograft rejection.
***Hepatology* 29** 777-784

Yamahara, T., Shiono, T., Suzuki, T., Tanaka, K., Takio, S., Sato, K., Yamazaki, S., and Satoh, T. (1999)
Isolation of a germin-like protein with manganese superoxide dismutase activity from cells of a moss, Barbula unguiculata.
***Journal Of Biological Chemistry* 274** 33274-33278

Yamasaki, H., Takahashi, S., and Heshiki, R. (1999)
The tropical fig Ficus microcarpa L. f. cv. golden leaves lacks heat- stable dehydroascorbate reductase activity.
***Plant And Cell Physiology* 40** 640-646

Ye, Z. H., Sun, D. Y., and Guo, J. F. (1989)
Preliminary-study on wheat cell-wall calmodulin.
***Chinese Science Bulletin* 34** 158-161

Ye, Z. H. and Varner, J. E. (1991)
Tissue-specific expression of cell-wall proteins in developing soybean tissues.
***Plant Cell* 3** 23-37

Zhu, B. L., Chen, T. H. H. , and Li, P. H. (1995)
Activation of 2 osmotin-like protein genes by abiotic stimuli and fungal pathogen in transgenic potato plants.
***Plant Physiology* 108** 929-937

Zhu, G. L. and Boyer, J. S. (1992)
Enlargement in chara studied with a turgor clamp - growth-rate is not determined by turgor.
***Plant Physiology* 100** 2071-2080

Zhu, J. K., Shi, J., Singh, U., Wyatt, S. E., Bressan, R. A., Hasegawa, P. M., and Carpita, N. C. (1993)
Enrichment of vitronectin-like and fibronectin-like proteins in nacl- adapted plant-cells and evidence for their involvement in plasma- membrane cell-wall adhesion.
Plant Journal **3** 637-646

APPENDIX 1

Submitted papers and papers in preparation

Doherty, S. & Croy, R.R.D.
Tobacco leaf apoplastic superoxide dismutases and peroxidases.
Plant, Cell and Environment
Submitted September 2000.

Johnson, S.M., Doherty, S. & Croy, R.R.D.
Superoxide radical production in potato tubers: a novel biphasic response to mechanical stress.
Planta
Submitted August 2000.

Doherty, S. & Croy, R.R.D.
A simple and rapid microtitre plate spectrophotometric assay for superoxide dismutase.
Pre-submission manuscript.

Planta (2000)

Planta

Superoxide radical production in potato tubers: a novel biphasic response to mechanical stress

Steven M Johnson, Sean J Doherty and Ronald R D Croy[1]

Crop Protection Group, Department of Biological Sciences, University of Durham, South Road, Durham, DH1 3LE, UK

Submitted : 26 August 2000

Abstract. Potato (*Solanum tuberosum* L.) cultivars differ quantitatively in their ability to produce blue-black melanin pigments in tubers following mechanical stress. Investigations into the events following mechanical stress exerted by direct impact on tuber tissues have shown that an early cellular response is a significant and rapid synthesis of superoxide radicals. Distinctively this burst of radical production displays a reproducible biphasic pattern over time with peaks of accumulation at 2 hours and 5 hours. A concomitant consequence of the generation of these free radicals is elevated levels of oxidatively modified tuber proteins. Both radical generation and protein modification vary between cultivars but both are directly proportional to the amount of melanin pigments produced.

Key words: blackspot bruising - mechanical stress - oxidative burst - potato tubers - superoxide radicals

Abbreviations: DNPH = 2,4-Dinitrophenylhydrazine; DOPA = 3,4-dihydroxyphenylalanine; PPO = Polyphenol Oxidase; AOS = Active Oxygen Species; XTT = 2,3-bis[2-Methoxy-4-nitro-5-sulfophenyl]-2H-tetrazolium-5-carboxanilide

Correspondance to: Ronald Croy

Introduction

Mechanical stress is imposed on plant cells by a variety of stimuli and lead to a range of responses. Early studies on mechanical stress used simple physical contact with bean stem tissues to examine responses in cell growth (thigmomorphogenesis), callose deposition and ethylene sythesis (Jaffe 1973, Jaffe et al. 1985). More recently Legendre et al. (1993), Yahraus et al. (1995) and Cazale et al. (1998) exposed soybean and tobacco cells to mechanical stress by agitation of suspension cultures or by exposing the cells to hypo-osmotic medium to increase cell turgor. Using these systems they were able to demonstrate short term generation of hydrogen peroxide. Yahraus et al. (1995) exerted direct pressure on soybean cells on a microscope slide and were able to show peroxide generation histochemically. Other than these examples few studies have been undertaken to investigate the primary biochemical responses to mechanical stress. Potato (*Solanum tuberosum*) tubers that undergo a physical impact produce melanin-based pigments, leading to a blue-black discoloration of subdermal tissues known as blackspot

bruising. Much of blackspot bruising occurs during harvesting, transport and storage and is a serious problem for potato growers leading to significant levels of rejection of tuber harvests (Rastovski 1987; Kleinschmidt and Thornton 1991; Anonymous 1994). The melanin synthesis pathway in tubers is catalysed in part by the enzyme polyphenol oxidase (PPO) (EC 1.14.18.1). Cellular disruption following mechanical stress leads to decompartmentalisation of the amyloplast-located PPO which then mixes with monophenolic substrates such as tyrosine. A series of oxygen-dependent reactions produce initially red-brown DOPA intermediates and ultimately lead to the formation of blue-black melanin pigments which can polymerise to water-insoluble complexes (Corsini et al. 1992; Stevens and Davelaar 1996; Friedman 1997). Recent evidence points to the involvement of covalently cross-linked protein in these complexes (Stevens and Davelaar 1996, 1997). The synthesis of melanin is thought to be a defence mechanism in which the polymerised, insoluble complexes form a resistant barrier sealing tuber tissues against the entry and spread of pathogens. The predisposition of tubers to melanin synthesis depends on the growing and storage conditions and exhibits a wide range of genetic variation (O'Leary and Iritani 1969; Hudson 1975; Skrobacki et al. 1989; Dixon 1992; British Potato Council 2000). Transgenic plants expressing anti-PPO gene constructs now form the basis of novel potato varieties highly resistant to bruising and confirm a catalytic involvement of PPO enzymes in this process (Bachem et al. 1994; Krohn et al. 1998).

The oxidative burst, a rapid production of highly active oxygen species (AOS) which include various oxygen free radicals and hydrogen peroxide, is a well characterised response of plant cells to pathogen challenge (Bolwell and Wojtaszek 1997; Lamb and Dixon 1997; Wojtaszek 1997). The generation of superoxide radicals is the first step in the production of AOS. Addition of a single electron to molecular oxygen generates the superoxide anion:

$$O_2 + e^{-1} > O_2^{\cdot}$$

and is believed to be catalysed by a plasma-membrane enzyme complex, NADPH-dependent oxidase (Doke 1995), although the possible involvement of an alternative pathway involving a pH-activated cell wall peroxidase has also been suggested (Bolwell et al. 1995). Under normal cellular conditions superoxide radicals are rapidly converted to hydrogen peroxide and oxygen by the enzyme superoxide dismutase. However, during an oxidative burst a vast excess of AOS are produced, which, due to their high reactivity with proteins, lipids and nucleic acids have been proposed as potent local inhibitors of pathogen spread (Tenhaken et al. 1995, Mehdy et al. 1996). AOS have also been implicated in signalling roles and in cross-linking of cell wall components (Brisson et al. 1994; Low and Merida, 1996) and it is likely that they also influence a wide range of metabolic events.

We have used an XTT-based assay to measure directly superoxide radical production in tissues from mechanically stressed potato tubers. The results show that levels of superoxide synthesis vary between potato cultivars which also exhibit differing susceptibilities to blackspot bruising. This synthesis is biphasic with two peaks of superoxide accumulation over a 6 hour period. We have also examined changes in the level of protein modification in mechanically stressed tubers and show a similar correlation with susceptibilities to blackspot bruising. We discuss the possible correlations between superoxide production, protein modification and the synthesis of melanin bruise pigments.

Materials and methods

Plant materials. Tubers from selected potato cultivars, specifically grown and carefully harvested to avoid any mechanical stress, were kindly supplied by Dr Adrian Briddon (Sutton Bridge Experimental Unit, Sutton Bridge, Lincolnshire, UK). Other tuber materials were purchased locally from commercial outlets. Five potato cultivars were used - *Cara*, *King Edward*, *Maris Piper*, *Russet Burbank* and *Saturna*. All tubers were stored in the dark at 10°C to inhibit greening and sprouting.

Tuber mechanical stress. Tubers were incubated for 48h at 4°C in the dark and then impacted at the

stolon end using a standard falling weight of 240g and a 300mm drop height imparting a force of 0.7J. Impacted and control tubers were incubated for 48h at 26°C to allow maximal synthesis of bruise pigments. Tubers were then cut in quarters at the impact site and the volume of affected tissue measured as well as a visual estimation of the intensity of pigmentation on a scale of 0 (no discoloration) to 3 (deep blue-black coloration). 30 tubers for each of the five cultivars were used and a mean bruise index calculated based on bruise extent and intensity.

Assay of superoxide radical generation in tuber tissues: Tubers of each cultivar were exposed to the standard mechanical stress and incubated in the dark at 26°C for various periods of time prior to assay for superoxide generation. $5mm^3$ slices of tuber tissue, excised from the centre of impact sites and from distal control sites were washed thoroughly with distilled water, blotted dry and then incubated at 16°C for 20 minutes in 200µl 0.6mM XTT in 50mM phosphate buffer, pH 8.2 (Able et al. 1998). The tissue pieces were removed and the assay solution centrifuged (13000g) for 5 minutes. The A_{450} of the supernatant was taken and converted to µmol superoxide generated using the molar extinction coefficient for the XTT formazan of 23,600 M^{-1} cm^{-1} (Sutherland and Learmonth, 1997; Sutherland M, personal communication). Superoxide estimations were carried out in duplicate and all assays were replicated.

Estimation of protein modification in tuber tissues: The carbonyl content of oxidatively modified tuber proteins was quantified by the spectrophotometric assay method of Levine et al (1994). Tubers were exposed to standard mechanical stress and incubated for 48h. Tuber proteins were extracted from 150mg of control and impacted tubers in 3ml of 50mM phosphate buffer, pH7.4. The carbonyl groups on extracted proteins were reacted with DNPH and the resulting hydrazone derivatives estimated from the peak absorbance at 355-390nm using a molar extinction coefficient of 22,000 M^{-1} cm^{-1}. Protein contents of duplicate samples were estimated from the A_{280}. Values were expressed as nmol carbonyl mg^{-1} tuber protein.

Results

Table 1. Bruise indices representing the relative susceptibility of different cultivars to mechanical stress leading to melanin pigment synthesis. The higher the bruise index indicates a higher susceptibility to mechanical stress. The values for the bruise indices are the mean values for 30 independent estimations for each of the five cultivars.

Cultivar	Bruise Index
Russet Burbank	9.2
Saturna	7.9
Cara	5.5
King Edward	4.0
Maris Piper	3.1

Bruise index estimation of potato cultivars: Table 1 lists the values estimated for the bruise susceptibilities for each of the five experimental cultivars. The cultivars used exhibited a wide range of susceptibilities to bruise development from highly susceptible (cv *Russet Burbank*) to highly resistant (cv *Maris Piper*). Our estimates of bruise indices for the cultivars used here are largely comparable with published values using similar methods (Dixon, 1992; British Potato Council, 2000).

Figure 1: Time course (hours post-impact) and levels of superoxide (nmol g^{-1} min^{-1}) generated in tubers exposed to mechanical stress. The five cultivars tested were A) *Russet Burbank*, B) *Saturna*; C) *Cara*; D) *King Edward*; E) *Maris Piper*. (■ — ■ mechanically stressed tissue, ▲ — ▲ control tissue). The results shown are the mean values for two independent estimates.

Superoxide production in mechanically stressed tuber tissue: Figures 1A-E show the time course of superoxide generation in tuber tissue slices. All cultivars showed some degree of superoxide production in response to impact. Very significant levels were produced by cv. *Russet Burbank* and cv. *Saturna* (Fig. 1A-B) while cv. *Maris Piper* (Fig. 1E) displayed only slightly elevated levels compared with the control values. Most striking was the biphasic nature of the superoxide generation pattern over time with an initial peak response at 1-2 hours post-impact followed by a larger response at 4-5 hours. This pattern was reproducible and apparent in all five cultivars although most obvious in cv. *Russet Burbank*, cv. *Saturna*, and cv. *Cara* (Fig. 1A-C) which also showed the highest bruise indices. The peak values for superoxide generation were plotted against bruise index for the five cultivars to illustrate the relationship between oxidative burst and melanin pigment synthesis (Fig. 2B).

Table 2. Tuber protein modification levels of the five potato cultivars following mechanical stress. Results shown are protein carbonyl levels expressed in nmol mg^{-1} tuber protein and are the mean values for two estimations corrected for background levels.

Cultivar	Carbonyl Content
Russet Burbank	10.1
Saturna	7.4
Cara	3.3
King Edward	2.9
Maris Piper	2.0

Figure 2: Histogram comparisons of cultivar bruise indices (Table 1), levels of protein modification (Table 2) and maximum levels of superoxide generated following mechanical stress (Fig. 1). Results shown are the mean values for two independent estimates corrected for control levels and provides a visual representation of the correlations between A) bruise index (solid bars) and protein modification (cross hatched bars) and B) bruise index (solid bars) and superoxide production (cross hatched bars). Cultivar abbreviations: RB=*Russet Burbank*, SA=*Saturna*, CA=*Cara*, KE=*King Edward*, MP=*Maris piper*.

Protein modification in mechanically stressed tuber tissue: Table 2 shows the results of assays for oxidatively modified tuber proteins 48h post-impact as indicated by the carbonyl content of extracted tuber proteins. It is immediately obvious that these values (Fig. 2A) closely mirror those for the levels of superoxide generation (Fig. 2B) in that cv. *Russet Burbank* showed the highest level of modified protein while cv. *Maris Piper* had the lowest. Furthermore comparison of the bruise indices for the cultivars (Table 1) with levels of protein modification (Fig.2A) and with superoxide generation (Fig.2B) show that there is a direct relationship between these variables. Thus high superoxide generation leads to high protein modification and both are linked to high bruise susceptibility.

Figure 3: Correlation plots between bruise index values, protein modification and levels of superoxide generation. Graph shows the near straight line relationships between the levels of melanin pigment synthesis (bruise index) and both superoxide generation and protein modification. (■ — ■ protein modification, ▲ — ▲ superoxide generation).

Discussion

Our observations show that cells in tuber tissues exposed to mechanical stress respond with a rapid production of superoxide radical anions. This oxidative burst is genetically highly variable since different potato cultivars show diverse reponses and quantities of superoxide generated (Figs. 1, 2). The use of nitroblue tetrazolium as a histochemical stain for superoxide radicals indicates that the tuber oxidative burst is restricted to the vicinity of the impact zone in a similar region to melanin pigment synthesis (data not presented). Synthesis of AOS such as hydrogen peroxide and superoxide is a primary response of plant cells to a pathogen attack or to treatment with chemical elicitors but few reports have described this response to a mechanical stimulus. Yahraus et al. (1995) simulated mechanical stress in soybean cell suspension cultures by hypo-osmotic media and demonstrated hydrogen peroxide synthesis within minutes. They also imposed direct mechanical stress by exerting physical pressure on the cells under a microscope slide and were able to demonstrate peroxide production histochemically after 3 minutes. Legendre et al. (1993) and Cazalé et al. (1998, 1999) used mixing of cell suspensions to impose mechanical stress and showed an oxidative burst of peroxide synthesis. In contrast to these studies, we have demonstrated over a much longer time-scale, the direct generation of superoxide radicals in differentiated plant tissues as a response to mechanical stress. This was most evident in *Russet Burbank*, *Saturna* and *Cara* the cultivars which also exhibited the highest susceptibility to mechanical stress ie. the highest bruise indices (Table 1, Fig. 2B). A unique feature of this superoxide synthesis was the biphasic pattern of generation with peak levels detectable at 1-2 hours and 4-5 hours post-impact. This pattern is reminiscent of the biphasic oxidative burst reported by Baker and Orlandi (1995) in which cultured cells treated with elicitor displayed two peaks of hydrogen peroxide generation over a period of 6-8 hours. Phase 1 was suggested to be a non-specific biological

response to stress while phase 2 was determined to be a specific interaction between the pathogen *hrp* complex and the plant receptors leading to hypersensitive cell death. In the present tuber system we see an initial peak which probably corresponds to the non-specific response. However, our second peak is potentially of much greater interest. The observation that a second burst arises in mechanically stressed tissues in the absence of elicitors or pathogens suggests the possible role of a cell receptor for detecting mechanical stimuli and an activation process. This is the first demonstration of what may be a specific response to mechanical stress and while its nature remains unclear it perhaps reflects transcriptional activation or initiation of signalling pathways by an unidentified mechanoreceptor as proposed by Cazalé et al. (1999). Jaffe et al. (1985) in a study of thigmomorphogenesis in bean stems, reported a minor transient deposition of callose 1.5 hours after mechanical stress in the form of gentle abrasion, followed by a major peak of callose deposition after 6 hours. Interestingly the time course for this response is nearly identical to the superoxide generation response reported here and both studies investigate responses in differentiated plant tissues to mechanical stress and it is tempting to speculate that both phenomena are initiated through similar mechanical receptors and signalling pathways.

The observation that the cultivars generating a large oxidative burst were also those exhibiting high melanin synthesis posed the question as to the relationship between the two processes (Fig. 2B). The correlation plot shown in figure 3 shows that there is a direct quantitative relationship. The near straight line obtained between superoxide generated and bruise indices provides direct quantitative proof of this relationship. Whether this is simply a fortuitous relationship or if there is an interaction between the two processes is an unresolved question. Direct involvement of oxygen free radicals in the enhancement of the melanin synthetic pathway or the PPO reactions has not yet been demonstrated. However melanin and related complexes are known to be free radical scavengers and melanin radicals have been demonstrated in animal pigments under conditions which elevate free radicals (Qu et al. 2000), so it seems plausible that radical production and melanin synthesis may be causally related.

One of the consequences of radical production is the oxidative modification of proteins in which carbonyl groups are introduced through modification of lysine, proline and arginine residues (Stadtman 1993). Such protein modifications are well documented in animal systems but this report is the first demonstration of the effect occurring as an outcome of mechanical stress in plants. Since oxidative modification of tuber proteins arises through interaction with the oxygen free radicals it is not unexpected that levels of protein modification produced a similar straight line relationship with bruise indices (Fig.3). Clearly the level of protein modification is directly proportional to levels of superoxide generated and therefore provides independent corroboration of the levels of radical production.

We present here some novel observations on the responses of plant tissues to mechanical stress based on a convenient experimental system. Further work is needed with this system to confirm and elucidate a causal relationship between radical production and melanin synthesis. Additionally questions remain as to how radicals, which are generated extracellularly, gain access to the largely intracellular tuber proteins in order to effect modification. The nature and function of the detection system for the mechanical stress remains to be elucidated.

The authors acknowledge the financial assistance of the British Potato Council, the Yorkshire Agricultural Society and the University of Durham. SMJ is a recipient of a Ministry of Agriculture, Fisheries and Food CASE Studentship in partnership with the British Potato Council. SJD is a recipient of a Special Studentship from the Biological and Biotechnology Research Council. We thank Dr Adrian Briddon for the supply of potato tubers.

References

Able AJ, Guest DI, Sutherland, MW (1998) Use of a new tetrazolium-based assay to study the production of superoxide radicals by tobacco cell cultures challenged with avirulent zoospores of *Phytophthora parasitica* var *nicotianae*. Plant Physiol 117: 491–499

Anonymous (1994) Factsheet 1. Potato Marketing Board, Cowley, UK

Bachem CWB, Speckmann G-J, van der Linde PCG, Verheggen FTM, Hunt MD, Steffens JC, Zabeau M (1994) Antisense expression of polyphenol oxidase genes inhibits enzymatic browning in potato tubers. Bio-Tech 12: 1101-1105

Baker GJ, Orlandi EW (1995) Active oxygen in plant pathogenesis. Annu Rev Phytopathol 33: 299-321

Bolwell GP, Butt VS, Davies DR, Zimmerlin A (1995) The origin of the oxidative burst in plants. Free Rad Res 23: 517-532

Bolwell GP, Wojtaszek P (1997) Mechanisms for the generation of reactive oxygen species in plant defence – a broad perspective. Physiol Mol Plant Pathol 51: 347-366

Brisson LF, Tenhaken R, Lamb C (1994) Function of oxidative cross-linking of cell wall structural proteins in plant disease resistance. Plant Cell 6: 1703-1712

British Potato Council (2000) in The British Seed Potato Variety Handbook pp172-174. British Potato Council.

Cazalé AC, Rouet-Mayer MA, Heberle-Bors H, Barbier-Brygoo, Mathieu Y, Laurière C (1998) Oxidative burst and hypoosmotic stress in tobacco cell suspensions Plant Physiol 116: 659-669

Cazalé AC, Droillard MJ, Wilson C, Heberle-Bors E, Barbier-Brygoo H, Laurière C (1999) MAP kinase activation by hypoosmotic stress of tobacco cell suspensions: towards the oxidative burst response? Plant J 19: 297-307

Corsini DL, Pavek JJ, Dean B (1992) Differences in free and protein-bound tyrosine among potato genotypes and the relationship to internal blackspot resistance. Am Pot J 69: 423–435

Croy RRD, Baxter R, Deakin W, Edwards R, Gatehouse JA, Gates P, Harris N, Hole C, Johnson SM, Raemaekers R (1998) Blackspot bruising in potatoes: structural and molecular approaches to the identification of factors associated with tuber bruising susceptibility. Asp App Biol 52: 207-214

Dixon TJ (1992) in Potato Varieties, published by Potato Marketing Board and National Institute of Agricultural Botany, Wooster P (Ed), (ISBN 0903623307), Performance Characters, 156-163

Doke N (1995) NADPH-dependent O_2^- generation in membrane fractions isolated from wounded potato tubers inoculated with *Phytophthora infestans*. Physiol Plant Pathol 27: 311-322

Friedman M (1997) Chemistry, biochemistry, and dietary role of potato polyphenols. A review. J Agric Food Chem 45: 1523-1540

Hudson DE (1975) The relationship of cell size, intercellular space, and specific gravity to bruise depth in potatoes. Am Pot J 52: 9-14

Jaffe MJ (1973) Thigmomorphogenesis: the response of plant growth and development to mechanical stimulation. Planta 114: 143-157

Jaffe MJ, Huberman M, Johnson J, Telewski FW (1985) Thigmomorphogenesis: the induction of callose formation and ethylene by mechanical perturbation in bean stems. Physiol Plant 64: 271-279

Kleinschmidt G, Thornton M (1991) Bulletin 725, University of Idaho Cooperative Extension System, Moscow, USA

Krohn BM, Hollier AA, Darchuk S, Stark DM (1998) Improving potato varieties through biotechnology. Asp App Biol 52: 239-254

Lamb C, Dixon RA (1997) The oxidative burst in plant disease resistance. Annu Rev Plant Physiol Plant Mol Biol 48: 251-275

Legendre L, Rueter S, Heinstein PF, Low PS (1993) Characterisation of the oligogalacturonide-induced oxidative burst in cultured soybean (*Glycine max*) cell. Plant Physiol 102: 233-240

Levine RL, Williams JA, Stadtman ER, Shacter E (1994) Carbonyl assays for determination of oxidatively modified proteins. Methods Enzymol 233: 346-357

Low PS, Merida JR (1996) The oxidative burst in plant defense: Function and signal transduction. Physiol Plant 96: 533-542

Mehdy MC, Sharma YK, Sathasivan K, Bays NW (1996) The role of activated oxygen species in plant disease resistance. Physiol Plant 98: 365-374

O'Leary AG, Iritani WM (1969) Potato bruise detection. Am Pot J 46: 352-354

Qu X, Kirschenbaum LJ, and Borish ET (2000) Hydroxyterephthalate as a fluorescent probe for hydroxyl radicals: application to hair melanin. Photochem Photobiol. 71: 307-313

Rastovski AA van es. (1987) Storage of potatoes: Post-harvest behaviour, store, design, storage practice, handling. Pudoc, Wageningen, Netherlands pp163-170

Skrobacki A, Halderson JL, Pavek JJ, Corsini DL (1989) Determining potato tuber resistance to impact damage. Am Pot J 66: 401–415

Stadtman ER (1993) Oxidation of free amino acids and amino acid residues in proteins by radiolysis and by metal-catalysed reactions. Annu Rev Biochem 62: 797-821

Stevens LH, Davelaar E (1996) Isolation and characterization of blackspot pigments from potato tubers. Phytochemistry 42: 941-947

Stevens LH, Davelaar E (1997) Biochemical potential of potato tubers to synthesize blackspot pigments in relation to their actual blackspot susceptibility. J Agric Food Chem 45: 4221–4226

Sutherland MW, Learmonth BA (1997) The tetrazolium dyes MTS and XTT provide new quantitative assays for superoxide and superoxide dismutase. Free Rad Res 27: 283-289

A simple and rapid microtitre plate spectrophotometric assay for superoxide dismutase

S. Doherty & R.R.D. Croy[1]

Department of Biological Sciences, University of Durham, South Road, Durham, DH1 3LE, UK.
[1]Author for correspondence

Direct assays for superoxide dismutase activity are time consuming, necessitate expensive equipment and high levels of expertise. In contrast, indirect assays are simple, speedy and inexpensive. Most indirect assays are two stage, with an initial generation of the superoxide anion and subsequent reduction of an indicator substance by the anion. Superoxide dismutase in such a system suppresses the reduction of the indicator thereby permitting measurement of activity. Commonly, an enzymatic superoxide generating system is utilised, such as the widely employed xanthine oxidase system. However, it has been noted that this system suffers not only from instability caused by rapid loss of xanthine oxidase activity but also limitations because of enzyme-indicator auto-reduction. Often a convenient indicator is nitroblue tetrazolium, but this too can introduce more acute problems; its reduction is not $O_2^{\cdot-}$-specific and the resulting mono- and di-formazan dyes are sparingly soluble in aqueous solutions. Consequently, optical density measurements are less than perfect. We have developed an assay utilising a stable non-enzymatic $O_2^{\cdot-}$-generating system based on the NADH-dependent oxidation of PMS with concurrent production of $O_2^{\cdot-}$ which reduces a new tetrazolium compound, XTT, to form a soluble dye with an absorbance maxima of approximately 450nm.

Superoxide dismutase ($O_2^{\cdot-}:O_2^{\cdot-}$ oxidoreducatse, E.C. 1.15.1.1.) (SOD)[2] catalyses the dismutation of the superoxide anion (SOA) into molecular oxygen and hydrogen peroxide (1). SOA's can originate from a multitude of biological processes, for instance, redox reactions in mitochondria and chloroplast organelles (2, 3), the auto-oxidation of flavins (4), hydroquinones (5) and catecholamines (6), the enzymatic actions of xanthine oxidase, aldehyde oxidase, flavin dehydrogenases (7) or dioxygenases (8). Furthermore, SOA's are produced in a controlled manner by neutrophils and macrophage during phagocytosis (9) and in plant-pathogen interactions which ultimately produce the characteristic hypersensitive response (10). The SOA has a relatively low toxicity primarily due to its very short half-life (2). However, molecular interaction with hydrogen peroxide, especially in the presence of trace metals (eg: Fe^{2+}), can lead to the formation of the relatively long-lived and highly toxic hydroxyl radical ($^{\cdot}OH$). Consequently, SOD has been frequently implicated in playing a primary defensive role against oxidative injury.

Direct assays of SOA and thus consequent measurement of SOD activity typically require high levels of expertise and expensive equipment. They rely on two distinguishing physical characteristics of the SOA, electron paramagnetic resonance (EPR) and UV absorption (11). The latter method necessitates time consuming and extensive sample cleanup prior to analysis, because of the inherently high UV absorbance typical of biological samples. EPR permits direct monitoring of SOA's because the molecule contains one unpaired electron (12). Unfortunately, the resonance frequency can only be distinguished from high background values at extremely low temperatures (4). Consequently, it is unsuitable for routine analysis.

A number of indirect SOD assays have been developed all of which detect reduction of an indicator by artificially generated SOA's. One of the most common ways to artificially produce SOA's utilises the enzyme xanthine oxidase (XO). XO-SOA generation can then be coupled to indicators such as ferricytochrome c or nitroblue tetrazolium (NBT) (13). The XO-SOA generating system suffers from several drawbacks. XO rapidly loses activity after preparation, consequently, later measurements in an assay series have lower SOA formation with a concurrent increase in the level of error. In addition, XO alone can cause indicator reduction when using either cytochrome c (14) or NBT (15) as the indicator, this process does not require the SOA and thus increases false positive error. Futhermore using NBT as an indicator also has inherent problems, the reduced forms of NBT, mono- and di-formazan dyes are sparingly soluble in water, an unfavorable property for accurate optical density measurements (15).

A non-enzymatic system of SOA production utilising aerobic mixtures of NADH and phenazine methosulphate (PMS) has been reported (16). This system when tested with NBT removes the inherent problems associated with XO-based SOA generation but still ultimately produces insoluble products. XTT (2,3-bis-[2-Methoxy-4-nitro-5-sulphophenyl]-2H-tetrazolium-5-carboxanilide) has been employed as a more promising indicator of SOA production and consequently SOD activity (17). We describe here the development of a SOD assay that combines these two very desirable features. The assay has been designed for rapidity of sample throughput utilising a 96 well microtitre plate format. SOA production is achieved using the PMS-NADH system thereby obviating the

[1] Telephone :+44(0)191-374-2433; Fax: +44(0)191-374-2417; e-mail R.R.D.Croy@durham.ac.uk

[2] Abbreviations used; EPR, Electron paramagnetic resonance; $^{\cdot}OH$ hydroxyl radical; NBT, nitroblue tetrazolium; PMS, phenazine methosulphate; $SOA/O_2^{\cdot-}$, superoxide anion; SOD, superoxide dismutase; XO, xanthine oxidase; XTT, (2,3-bis-[2-Methoxy-4-nitro-5-sulphophenyl]-2H-tetrazolium-5-carboxanilide) sodium salt.

problems associated with the enzyme XO. The resulting coloured dye has an absorption maxima of 450 nm and is highly stable, soluble and permits measurements to be taken at any point from 2 minutes to 18 hours after addition of sample.

MATERIALS AND METHODS

Chemicals

SOD (E.C. 1.15.1.1.; 3500 units/mg from bovine erythrocytes), β-NADH, NBT, XTT, EDTA, and PMS were purchased from Sigma Chemical Company (St. Louis, MO, USA) and were of analytical grade. All aqueous solutions were prepared with 18 Mohm/cm ultrapure water from an Elgastat UHQPs system (USF Elga Ltd., High Wycombe, UK).

XTT-SOD microtitre plate assay

For design and optimisation of the assay, 200µl of 50mM phosphate buffer, pH 7.8 containing, 0.1mM EDTA, 30µM XTT and 98µM NADH was pipetted into the wells of a microtitre plate. 25µl SOD containing a specified number of units in 50mM phosphate buffer, pH 7.8 or 50mM phosphate buffer pH 7.8 (buffer blank) was added. The reaction was initiated by the addition of 25µl of 33µM PMS. The microtitre plate was agitated for 5 seconds. The optical densities of each well were read at 450nm at 30 second intervals for 10 minutes and at 18 hours after initiation, using a Dynatech MR-5000 plate reader (Dynatech Laboratories, UK).

Preparation of blowfly muscle mitochondria

Control flies were grown at a constant 24°C. Flies were heat-shocked by incubating batches at 37°C for 40 minutes. After heat treatment they were returned to a constant 24°C chamber for 4 hours to permit the heat-shock responses to develop. Blowfly muscle mitochondria were isolated as described previously (18). Briefly, thoraces were collected and flight muscles removed and disrupted using a mortar and pestle. Mitochondria were centrifuged at 3,600 rpm (RCF = 1500g) in a Beckman Avanti 30 (F2402 rotor). The mitochondrial pellet was resuspended in 0.15M KCl, 1mM EDTA, 10mM Tris and stored frozen at –80°C.

Protein Assays

The protein contents of mitochondrial and other samples were determined by the Bradford assay using serial dilutions of standard bovine serum albumin (Bradford, 1976).

Data Analysis

GraphPad Prism® software version 2.1 (GraphPad Inc.) was used to produce standard curves, perform the regression analysis, quantify SOD levels, and calculate standard deviations (SD).

RESULTS & DISCUSSION

Principle of the assay

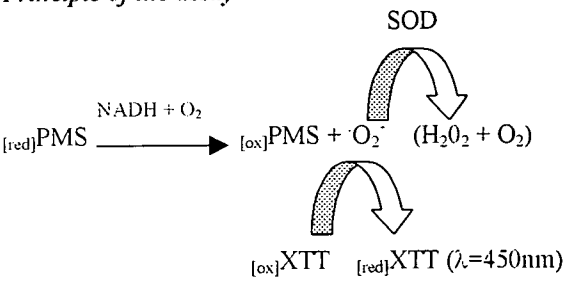

Optimising $O_2^{\cdot-}$ generation & assay duration

The addition of PMS to the reaction mixture initiates the generation of SOA's and consequently XTT reduction and coloured product generation. To establish the efficacy of XTT reduction by $O_2^{\cdot-}$ generated by the PMS-NADH system and to ascertain a suitable assay duration a series of PMS concentrations were kinetically assayed at 450nm against a buffer blank lacking PMS. Figure 1 illustrates the principle of the assay in which XTT is reduced in a PMS concentration dependent manner. At all PMS concentrations tested absorbance change was linear over a 3 minute assay period (>0.9965 ($p<0.0001$)). However, continued monitoring beyond 3 minutes for 3.2µM PMS and beyond 4 minutes for 2.8µM PMS, showed that the absorbance change quickly levelled out, indicating that the XTT concentration had been diminished below the level required to react with the constant stream of $O_2^{\cdot-}$ ions produced from the PMS-NADH generating system. Endpoint measurements beyond 4 minutes and up to 18 hours illustrated that the dye formed during the first 4 minutes remains stable because readings are virtually identical (*data not shown*).

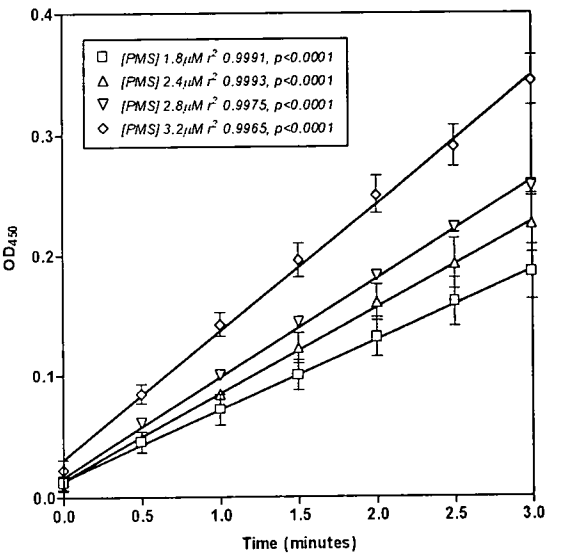

Figure 1 : The effect of PMS concentration on XTT reduction. Assay conditions were the same as described in Materials & Methods except that the PMS concentration/assay was adjusted. The reaction was initiated with 50µl of varying concentrations of PMS in 50mM phosphate buffer, pH 7.8. OD_{450} was measured every 30 seconds over 3 minutes. The final concentration of PMS/assay is displayed in the box. Data are means of ± SD of four measurements.

As would be expected maximal absorbance change occurs at the highest PMS concentration, 3.2μM. Unfortunately at this concentration the reaction is extremely rapid and it is difficult to attain an accurate initial 'zero time' value (see figure 1). At 2.8μM PMS, XTT reduction produced an average absorbance change per minute of approximately 0.1 OD_{450} units.

The concentration of PMS was therefore standardised to 2.8μM/assay with absorbance readings taken every 60 seconds over a 10 minute period and again at 18 hours. These conditions were used throughout all optimisation experiments. After 5 minutes optical density measurements did not alter over an 18-hour period. Consequently, XTT reduction by O_2^- generated by the non-enzymatic PMS-NADH system under these conditions is extremely stable and reproducible.

Optimising the XTT concentration

Reduction of all of the O_2^- ions generated by the optimised PMS-NADH system is a necessary pre-requisite for accurate measurement of the activity of SOD to dismutate SOA's. XTT concentration is therefore critical to kinetic measurements and requires standardisation to ensure that an XTT-saturation state is achieved during the assay period. This was assessed by performing the assay over a range of XTT concentrations; figure 2 depicts this data.

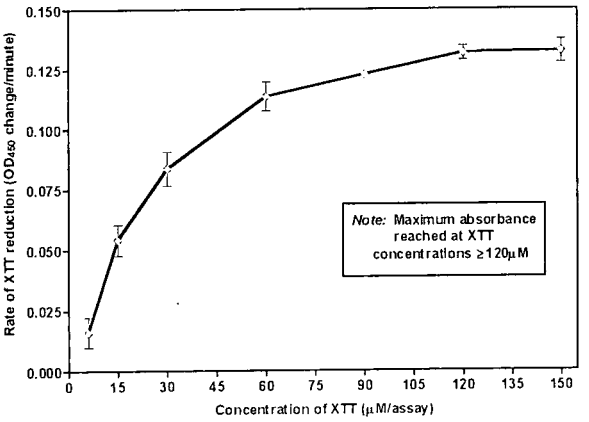

Figure 2 : Effect of XTT concentration on the reaction rate (OD_{450} change/minute). Assay conditions; 50mM phosphate buffer, pH 7.8 containing, 80μM EDTA, 78.4μM NADH and 6-150μM XTT (final assay concentrations). The reaction was initiated with a final PMS concentration of 2.8μM/assay. An endpoint OD_{450} was taken at 2 minutes from which OD change/minute was calculated. The final concentration of XTT/assay is displayed on the abscissa. Data are means of ± SD of four measurements.

Absorbance change per minute continuously increased with higher concentrations of XTT up to 120μM/assay. At this concentration and above, XTT reduction levelled off. In effect, at this concentration, all of the O_2^- ions produced by the PMS-NADH system were instantaneously reducing the XTT producing a maximal absorbance change. When the PMS concentration was set at 2.8μM/assay and the XTT concentration at 120μM/assay, the absorbance change at 450nm over 2 minutes was linear (r^2 = 0.9980, $p<0.0001$) and therefore was optimal for accurate kinetic measurements of SOD activity.

Defining optimal assay pH

It has been noted that the PMS-NADH system has a tendency to produce hydrogen peroxide at acidic pH and to preferentially generate O_2^- ions at more alkaline pH (20). We therefore assessed how pH influenced the PMS-NADH SOA-driven reduction of XTT. Figure 3 illustrates that XTT reduction is in fact pH-dependent, the reaction rate rises sharply from <0.09 OD_{450} change/minute at pH 6.5 to >0.12 OD_{450} change/minute in the pH range 7.5-8.7. The lower optical density readings exhibited below pH 8.0 are probably attributable to the PMS-NADH system producing a variable mixture of hydrogen peroxide and SOA species. Between pH 7.5 and 8.7, SOA production is much more consistent as evidenced by the relatively stable readings depicted in figure 3. At pH >8.7 XTT reduction drops markedly (<0.07 OD_{450} change/minute). This may arise because the PMS-NADH system cannot effectively produce O_2^- ions at pH values >8.7, or because XTT is not effectively reduced at this pH. Therefore, for routine analyses we standardised the assay buffer to pH 8.2, although any point within the pH range 7.5-8.7 is suitable.

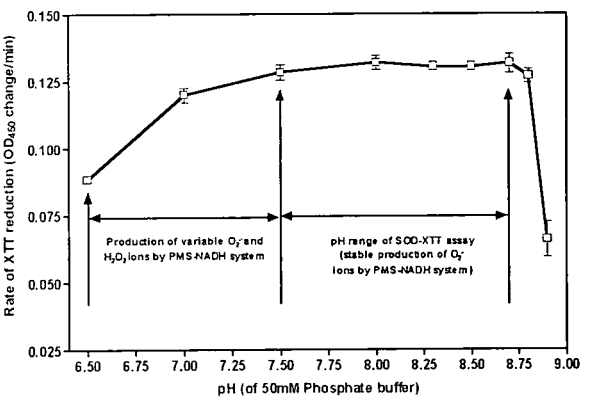

Figure 3 : pH-dependence of XTT reduction. Assay conditions; 50mM phosphate buffer, pH in the range 6.5-8.9, containing, 80μM EDTA, 78.4μM NADH and 120μM XTT (final assay concentrations). The reaction was initiated with a final PMS concentration of 2.8μM/assay. An endpoint OD_{450} was taken at 2 minutes from which the OD change/minute was calculated. Data are means of ± SD of four measurements.

Optimised SOD assay conditons

The final optimised assay conditions used for both the preparation of the SOD standard curve and for routine sample analysis were: 200μl of 50mM phosphate buffer, pH 8.2, containing 0.1mM EDTA, 98μM NADH, 150μM XTT. 25μl of SOD solution or sample were added and the assay initiated with 25μl of 28μM PMS in 50mM phosphate buffer, pH 8.2. This mixture had final concentrations of 80μM EDTA, 78.4μM NADH, 120μM XTT and 2.8μM PMS. If a microtitre plate reader is not available volumes can simply be scaled up by a factor of four and the measurements made using a spectrophotometer and

standard 1-ml plastic cuvettes. Mixing of the reactants can be achieved as with an ordinary cuvette-based assay using parafilm and rapid inversion of the cuvette.

Production of a SOD standard curve and analysis of unknown SOD samples

A commercial preparation of SOD from bovine erythrocytes, dissolved in 50mM phosphate buffer, pH 8.2 was used to prepare the standard curve. SOD was added to the reaction mixture in a 25µl aliquot in the range 0.01U (2.875 ng) to 100U (28.75 µg). Figure 4 illustrates the standard curve. Optical density readings were taken kinetically early after the addition of PMS (<5 minutes), or as endpoint readings (>7 minutes and up to 18 hours). Providing measurements are taken at a standardised time after the addition of PMS any point between 2 minutes and 18 hours provides highly reproducible data and permits inter-assay comparisons to be drawn.

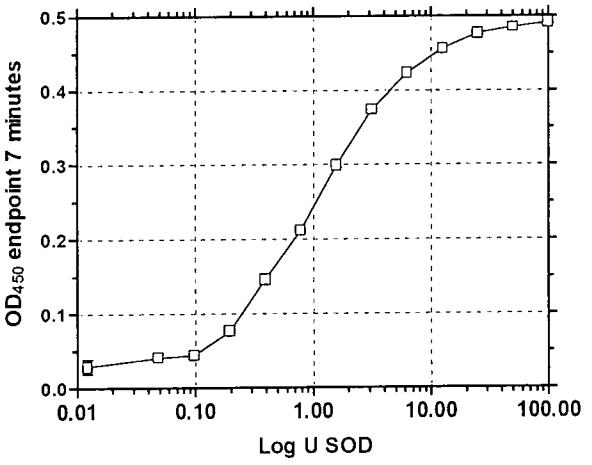

Figure 4 : SOD inhibition of XTT reduction - standard assay
The figure illustrates the final optimised assay as described in the text. OD_{450} readings at 7 minutes minus positive control are plotted against the Log. of the units of SOD in the reactions. Data are the means of ± SD of three measurements.

We have tested the utility of this assay using control and mitochondria from heat-shocked blow flies. Flight muscle mitochondria were isolated from flies as described previously (20), grown at a control temperature (24°C) and from those undergoing heat shock (36°C) treatment. Heat-shock as with many stresses increases oxidative metabolism, SOD is the only known enzyme that can dismutate $O_2^{\cdot-}$ radicals before they react with other components to form more reactive and deleterious molecules such as the $^{\cdot}OH$, hydroxyl radical. The activity of mitochondrial SOD is known to be elevated in response to stress (21, 22 & 23). These samples were assayed and the data is presented in Figure 5. As expected the mitochondria isolated from heat-shocked flies showed considerably higher levels of SOD activity confirming the results presented in the literature (21, 22 & 23).

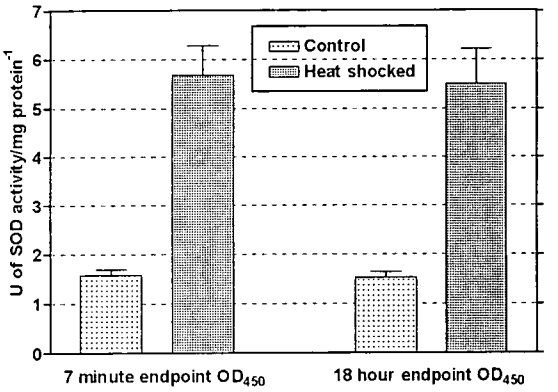

Figure 5 : Assay for SOD in unknown samples
Analysis of unknown mitochondrial samples (see text for details of assay) with endpoint measurements taken at 7 minutes and 18 hours. Data are means of ± SD of three measurements.

Optical density readings were taken at 7 minutes and at 18-hours after the addition of PMS to the reaction mixture. There was almost no change in the absorbance readings between the two times, illustrating the stability and longevity of the reduced form of XTT.

The assay described has significant advantages over previously described versions: i) it is large-scale and can accommodate up to 96 samples in a convenient microtitre plate format allowing multiple replicates; ii) it is rapid and simple to setup; iii) it does not suffer from the instability observed in the enzymatic SOA-generating system; iv) it does not suffer from interference from a sparingly soluble dye product; v) it has the added attraction of an extremely stable dye product formation which permits the user to read the assay results anytime between 2 minutes and 18 hours after reaction initiation. This allows rapid reaction rate (kinetic) measurements and reaction endpoint readings to be taken.

ACKNOWLEDGMENTS

The authors acknowledge the financial support of the biotechnology and biological sciences research council, U.K. SD is the recipient of a BBSRC special studentship. Thanks also to Judith Chambers, University of Durham, UK for the preparation of blow fly flight muscle mitochondria.

REFERENCES

1. Weisiger, R.A. & Fridovich, I. (1973) *J. Biol. Chem.* 248, 3582-3592.
2. Loschen, G. Azzi, A., Richter, C. & Flohe, L. (1974) *FEBS Lett.* 42, 68-71.
3. Halliwell, B. (1975) *Eur. J. Biochem.* 55, 355-361.
4. Ballou, D. Palmer, G. & Massey, V. (1969) *Biochem. Biophys. Res. Commun.* 36, 898-903.
5. Misra, H.P. & Fridovich, I. (1972) *Biol. Chem.* 247, 188-194.
6. Cohen, G. & Heikkila, R.E. (1974) *J. Biol. Chem.* 249, 2447-2450.
7. Fridovich, I. (1975) *Ann. Rev. Biochem.* 44, 147-156.
8. Hirata, F. & Hayaishi, O. (1975) *J. Biol. Chem.* 250, 5960-5965.
9. Bannister, J.V. & Bannister, W.H. (1985) *Environ. Health Perspect.* 104, 37-41.
10. Heath, M.C. (1998) *New Phyto.* 138, 251-263.
11. Marklund, S. (1976) *J. Biol. Chem.* 251. 7504-7507.
12. Knowles, P.I., Gibson, J.F., Pick, F.M. & Bray, R.C. (1969) *Biochem. J.* 11, 53-58.
13. Auclair, C., Torres, M. & Hakim, J. (1978) *FEBS Lett.* 89, 26-29.
14. Beauchamp, C. & Fridovich, I. (1972) *Arch. Biochem.* 44, 276-287.
15. Nishikimi, M. (1975) *Arch. Biochem. Biophys.* 166, 273-278.
16. Ewing, J.F. & Janero, D.R. (1995) *Ana. Biochem.* 232, 243-248.
17. Ukeda, H., Maeda, S., Ishii, T. & Sawamura, M. (1997) *Ana. Biochem.* 251, 206-209.
18. Elwadawi, R. & Bowler, K. (1995) *J. Exp. Biol.* 198, 11, 2413-2421.
19. Bradford, M.M. (1976) *Ana. Biochem.* 72, 248-254.
20. Rao, U.M. (1989) *Free Radical Biol. Med.* 7, 513-519.
21. Costa, V., Amorim, M.A., Reis, E., Quintanilha, A. & Moradas-Ferreira, P. (1997) *Microbiology – UK* 143, 5, 1649-1656.
22. Polla, B.S., Jacquier-Sarlin, M.R., Kantengwa, S., Mariethoz, E., Hennet, T., Russo-Marie, F. & Cossarizza, A. (1996) *Free Rad. Res.* 25, 2, 125-131.
23. Manganaro, F., Chopra, V.S., Mydlarski, M.B., Bernatchez, G. & Schipper, H.M. (1995) *Free Rad. Biol. Med.* 19, 6, 823-835.

A simple and quick method to selectively sample large quantities of leaf apoplastic proteins

S. Doherty & R.R.D. Croy*

Department of Biological Sciences, University of Durham, South Road, Durham, DH1 5BW, UK.
** Author for correspondence: E-mail: r.r.d.croy@dur.ac.uk; Fax: 0191-374-2417; Tel: 0191-374-2433*

ABSTRACT

The extracellular compartment of many plant tissues contains pockets of gas confined by the surrounding cells in the tissue and is often referred to as the apoplast. Lining the apoplast is a thin film of moisture that contains many types of proteins including structural- and defence-related proteins and enzymes. The apoplast protein mixture can be isolated largely free from intracellular contamination using vacuum infiltration. This is achieved by submerging the plant tissues in an appropriate buffer, applying a low vacuum which removes gases trapped within the apoplast. A slow release of the vacuum causes the apoplast to flood with buffer. The intercellular fluid (ICF), comprising of the buffer containing dissolved proteins, can be recovered from the apoplast by low speed centrifugation. In order to sample larger quantities of the apoplast proteins for purification and analyses, a large-scale version of this technique has been developed and optimised. We have used this technique to investigate differences in the extracellular complement of proteins in tobacco leaves.

Keywords: apoplast; cell wall; intercellular fluid; malate dehydrogenase; SDS-PAGE; tobacco; plant leaves; vacuum infiltration.

Abbreviations: ICF – Intercellular fluid; SDS-PAGE – Sodium dodecyl sulphate polyacrylamide gel electrophoresis; TE – Total extract; VI – Vacuum infiltration; RCF - Relative centrifugal field; RUBISCO – Ribulose bisphosphate carboxylase.

INTRODUCTION

The extracellular environment of plant tissues can be viewed as an extension to the cytoplasm but with a unique biochemistry and composition which alters according to changing conditions and stresses. The 'apoplast' is the term used to define the space occupied by pockets of gas transiently entrapped by the aqueous films lining the spaces between cell walls (Canny 1995). Within and exposed to these films of water a variety of proteins are found associated with the cell wall matrix or freely soluble, depending upon the local pH and ionic composition. Examples include peroxidases (Welinder 1991, Mäder 1980, Espelie *et al* 1986, Fry 1986), carbohydrate- and pectin-related enzymes (see Varner & Taylor 1989 for a review) and a repertoire of hydrolases capable of hydrolysing a wide range of glycosidic linkages present in the cell wall (Hatfield & Nevins 1987) and elsewhere.

Many common abiotic stresses such as, temperature (Marentes *et al* 1993), salinity (Holland *et al* 1993), drought (Dhindsa 1991), and wounding (Showalter 1993), alter the content and properties of the cell wall and apoplast, permitting the plant to adapt to the prevailing conditions. Similarly adjustments are evident during biotic stress which establishes initially, a rapid enhancement in the rigidity of the cell wall with a concurrent general reduction in the digestibility of the tissue (Matern *et al* 1995; Robertson *et al* 1995; Showalter 1993). This is rapidly followed by secretion of a range of pathogenesis-related proteins (Apel *et al* 1990; Konbrink *et al* 1988) and antimicrobial compounds (Dixon 1986) into the apoplast.

Vacuum infiltration (VI) is a relatively simple, yet highly effective strategy, for selectively extracting soluble and ionically-bound proteins from the extracellular compartments. It is the only method that can be used to selectively isolate extracellular components from differentiated plant tissues. Once optimised VI generally causes very little cellular damage and therefore intracellular contamination of such isolates is minimised. While there is a wide range of potentially valuable and interesting proteins and enzymes present in the apoplast the small amounts of material recovered by this technique prevent its wide application for the study of these components. We describe here the development and optimisation of a large-scale version of the Hammond-Kosack (1992) VI technique that typically can yield 30-35 ml of approximately 100μg protein/ml intercellular fluid (ICF) in an 8-hour working day. Using this modified technique we have investigated development-specific changes in the enzyme and protein complement in the apoplast of tobacco leaves.

MATERIALS AND METHODS

Plant Material

Seeds of tobacco (*Nicotiana tabacum*) *cv SR1* were sown in Levington M3 compost (Levington, UK). Seedlings that had emerged after 14 days were transferred to 2 litre pots and grown in a controlled environment room at 23/20°C (±2°C) day/night temperatures, 16h photoperiod of 100μE s^{-1} m^2 (50W.m^2) light intensity (cool-white fluorescent tubes and 70% ±5% relative humidity. Plants were fertilised every two weeks with 1% (w/v) Phostrogen (Phostrogen, UK) and watered once every three days. Unless stated otherwise all plant material used was 8 weeks old.

Total soluble protein extraction (TE)

Tobacco leaves (<5 cm and >10 cm length) were excised from plants at 8 weeks old and strips (~8-10 cm^2) were cut from between the major leaf veins using a sharp blade. The total tissue fresh weight was recorded. The tissue strips were placed in an ice-chilled mortar, with sand and liquid N_2 and ground to a fine powder. Extraction buffer (1mM DTT or 1mM DTT, 200 mM NaCl, pH 7.5) was added at a ratio of 1.5ml per gram of tissue. The tissue was further ground until a thick slurry was produced. Clarification of the TE was achieved by an initial 5 minute spin in a bench-top micro centrifuge (RCF=10,000g), followed by ultracentrifugation of the supernatant at 200,000g, for 60 minutes at 4°C. The supernatant was decanted and dialysed for 24 hours at 4°C against dH_20 and stored at –20°C or lyophilised.

Vacuum infiltration (VI)

VI was carried out in a similar manner to that of Hammond - Kosack (1992). Tobacco leaves (<5 cm and >10 cm length) were removed from 8 week old plants. Strips of leaf tissue (~8-10 cm^2) were cut from between the major leaf veins using a sharp blade and total tissue weight was recorded. The strips were washed for >20 minutes in two changes of distilled water at 4°C, with occasional mixing to remove soluble proteins from the cut cells. The tissue strips were thoroughly dried using paper towels and arranged on a nylon mesh (1m x 7 cm; mesh size ~1mm^2) which was then gently rolled to form a 'Swiss-roll' type tube as shown in Figure 1.

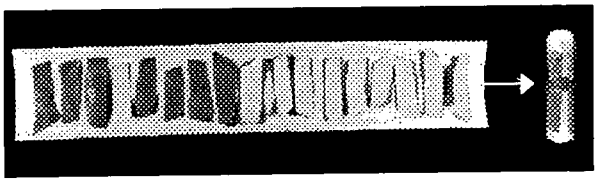

Figure 1: Arrangement of leaf strips on the nylon mesh prior to rolling into a 'Swiss-roll' as shown on the right, and secured with an elastic band.

To maintain the roll integrity during manipulations, an elastic band was loosely fixed around the nylon mesh. Several assembled rolls were then placed in chilled infiltration buffer (1 mM DTT or 1mM DTT, 200 mM NaCl, pH 7.5) in a vacuum vessel equipped with a valve suitable for the slow release of the vacuum. The rolls were kept submerged in the infiltration buffer throughout the procedure using a metal grid and a 1kg weight. Evacuation of gases trapped in the apoplast was achieved by applying a standard vacuum (8.5 x 10^4 Pa (Nm^{-2}) to the surface of the liquid and gently agitating for 30 seconds. Infiltration of the apoplast with the buffer was then achieved by slowly releasing the vacuum over a 30-second period. After infiltration the tissue rolls were removed from the buffer, wrapped in paper towels to drain off, excess liquid trapped in the nylon mesh. The rolls were then inserted into 25 ml medical sample tubes (25mm diam x 90mm long) with a 3-4 mm hole cut in the bottom. Individual sample tubes were then placed into 50 ml conical centrifuge tubes (Falcon). The tube assemblies were then centrifuged in a Sigma 204 centrifuge at up to 3000 rpm (RCF=~1500g at $R_{max=150mm}$) for 10 minutes in a swing-out rotor at 4°C. The ICF's collected in the centrifuge tube were usually russet-coloured or almost colourless. ICF's coloured green due to leaked chloroplast material indicated gross contamination with intracellular contents and were immediately discarded. ICF's were further assessed for intracellular contamination by assaying for malate dehydrogenase (MDH). ICF's with an MDH-activity >1% of the level in the leaf total extract were discarded while those with activities <1% were pooled, dialysed against distilled water, and lyophilised.

Malate Dehydrogenase and Protein Assays

Malate dehydrogenase (MDH, EC 1.1.1.37) activity was assayed in both total soluble leaf protein and ICF's according to the Biochemica Enzymes Catalogue (Boehringer Mannheim, 1st edition, 1968). The reaction mix comprised of 943µl of 0.1M phosphate buffer, pH7.5, 33µl of 2mg/ml sodium oxaloactetate in phosphate buffer, 17µl of 10mg/ml NADH (Na^+). The reaction was started by adding up to 7µl of either TE or ICF to the reaction cuvette and the decrease in absorbance at 340 nm was measured for 60 seconds. In order to 'quantify' the degree of intracellular contamination of the ICF, TE readings were standarised to 100% of the MDH-activity present in the tissue according to the formula (Hammond-Kosack, 1992): -

$$\frac{\Delta Ab^{340} \text{ of ICF} \times 100}{\Delta Ab^{340} \text{ of TE}} = \text{Relative MDH activity of ICF}$$

The protein contents of samples were assayed using Bradford microtitre plate assays using serial dilutions of a 1mg/ml BSA for calibration (Bradford 1976).

SDS-PAGE & Gel Staining

The polypeptide composition of ICF and TE samples were analysed by SDS-PAGE performed essentially as described by Laemmli (1970) using 0.75 mm-thick, 12%(w/v) acrylamide gels (acrylamide/bis-acrylamide (37.5:1) separating gels). acrylamide vertical slab gels (Bio-Rad Mini-Protean II system). Protein bands were visualised by staining with a silver staining kit (Bio-Rad), following the manufactures instructions. Native-PAGE analysis was performed as described above except samples were not denatured to ensure that the enzymes remained active. Gels were stained for superoxide dismutase (SOD) activity by incubating the gel in a solution of 50 mM Tris-HCl, pH 8.5 containing, 0.98 µM nitroblue tetrazolium, 1.57 µM phenazine methosulphate and 5.9 µM magnesium chloride with agitation under a strong light. SOD activity is distinguished as clear bands on a dark blue background (Manchenko 1994).

RESULTS

Optimisation of Vacuum Infiltration

It was clear from initial experiments that the length of time tissues are exposed to the vacuum and the level of vacuum applied both affect the efficiency of VI as well as the integrity of the cells. This was judged on basis of the observed increase in MDH activity in ICF's from tissues on prolonged exposure to the vacuum or to vacuums higher than 8.5 x 10^4 Pa (Nm^{-2}) (*data not presented*). Consequently, optimisation of the length of time that tissues can be exposed to this vacuum with minimal intracellular leakage was determined. A typical set of results is shown in figure 2. Exposing tobacco leaf tissues to the vacuum for 60-90 seconds resulted in a stable (background) level of relative MDH-activity in ICF's of between 0.2-0.4% of the MDH-activity present in the TE. Extending the vacuum exposure time to >90 seconds for this tissue, resulted in increasing ICF MDH-activity indicating greater cell disruption and leakage of intracellular components.

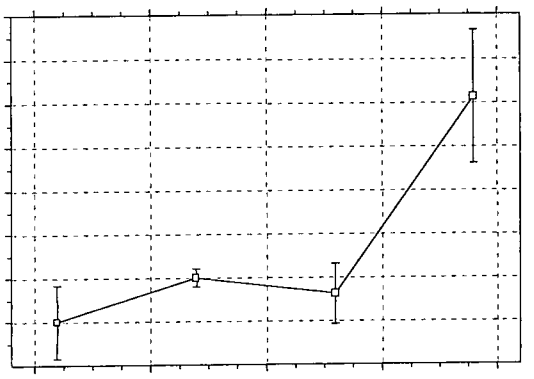

Figure 2: Change in MDH activity in ICF's with prolonged exposure to the vacuum (8.5 x 10^4 Pa). Four sets of four tissue rolls were prepared as described in the text. Each set of rolls was subjected to 30, 60, 90 or 120 seconds under vacuum. ICF's were then recovered and the MDH activities assayed. Points plotted are the means of the four results for each time point.

The Swiss-roll arrangement of tissue and nylon mesh affords some protection to the plant material and provides mechanical support during infiltration and centrifugation. However, excessive or prolonged centrifugation of the tissue rolls can cause them to be crushed at the bottom of the sample tube. Deformation of the tissue material inevitably causes cellular damage and gross leakage of intracellular components into the ICF. This was borne out experimentally as

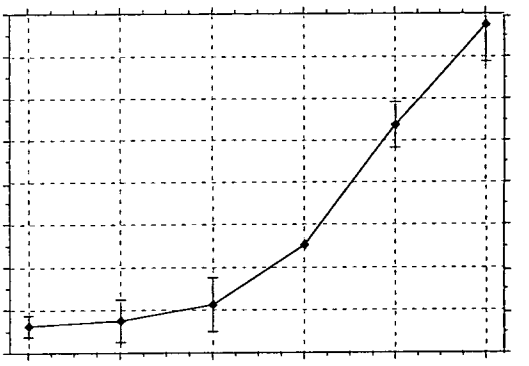

Figure 3: Increasing MDH activity in ICF's isolated at increasing centrifugation speeds (RCF). Six sets of four rolls were prepared by infiltration for 30 sec under vacuum as described in the text. ICF's were recovered by centrifuging sets of rolls at one of the following speeds (RCF): 500rpm (42g), 1000rpm (168g), 1500rpm (377g) 2000rpm (671g), 2500rpm (1048g) or 3000rpm (1509g). The points plotted are the means for the four results for each centrifuge speed.

shown in Figure 3. Relative MDH-activity in the ICF steadily increased as the RCF was increased from <50g up to >1500g; at the higher speeds, the supporting mesh tended to distort at the bottom of the sample tube. Consequently, the tissue within the mesh was crushed and the relative MDH-activity was therefore higher in these samples. At higher centrifugation speeds both the volume of ICF recovered and it's protein content were much higher than the final optimised extraction procedure (*data not shown*), however the ICF's were invariably discarded because of obvious intracellular contamination.

Both time of exposure to vacuum and centrifugation speed will influence the quality and quantity of ICF recovered from vacuum infiltrated tissues. For tobacco leaf tissue this large scale VI procedure has now been standarised to a 60-second exposure at a vacuum of 8.5 x 10^4 Pa (Nm^{-2}) with recovery of ICF's at an RCF of <200g.

Gel Analysis

As an example of the application of this modified technique, ICF and TE samples were both prepared from immature (leaves <5 cm in length, from the upper third of the plant) and mature (leaves >10 cm in length, from the bottom third of the plant) leaf tissues. The samples were then subjected to SDS-PAGE gel analysis an example of which is shown in Figure 4.

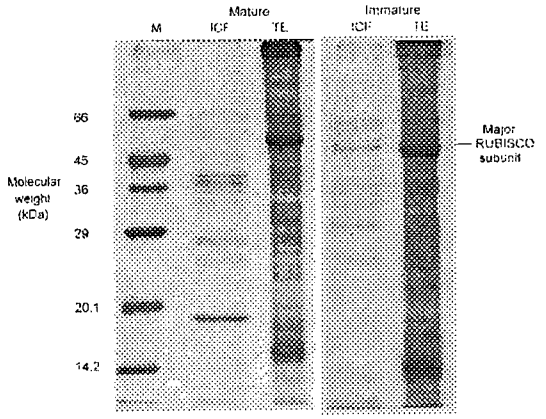

Figure 4: SDS-PAGE analyses of ICF (38μg total protein) and TE (60μg total protein) samples isolated from mature and immature tobacco leaves. (M = size marker proteins).

Examination of the silver-stained gels showed firstly that contamination of ICF samples with intracellular protein was minimal as evidenced by the conspicuous near absence of major intracellular leaf proteins such as RUBISCO, in either ICF sample. Secondly, it was obvious that there were few if any common polypeptides between the respective TE's and their ICF's again indicating the selective enrichment of components from the extracellular compartment. Thirdly, comparison of the analyses of immature and mature ICF's showed several common protein components presumably representing those constantly required throughout development. However, differences were clearly evident - bands specific to either immature or mature tissue were clearly discernable presumably reflecting protein components functioning at specific development stages in that tissue.

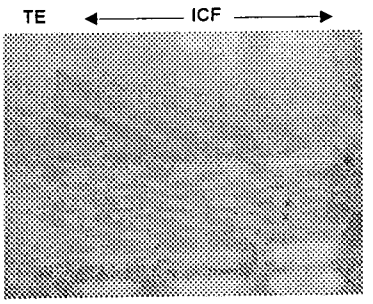

Figure 5: Native-PAGE analyses of ICF (15, 37 and 75μg total protein) and TE (16μg total protein) samples stained for the presence of SOD.

We have also investigated the distribution of the enzyme superoxide dismutase (SOD) between extracellular and intracellular compartments. Figure 5 shows *in situ* staining of a native gel containing a total protein extract and ICF from tobacco leaves. Interestingly the apoplast contains a unique complement of basic SOD isoforms which are not detectable the total extract.

DISCUSSION

It is well documented that small amounts of soluble or weakly bound proteins can be selectively sampled from the apoplast using VI followed by gentle centrifugation (Hammond-Kosack 1992; Rohringer *et al* 1983; Söding 1939; Terry & Bonner 1980). The VI procedure described here is as effective as these previous techniques at selectively enriching apoplastic material, according to contaminating enzyme assays (MDH) and gel analyses. However the scale of isolation has been increased by at least an order of magnitude such that enough ICF can now be conveniently isolated to make protein purification and proteomic analyses realistic possibilities. The amounts of protein isolated by this modified technique are in the milligram quantities, easily enough to conduct one and two dimensional PAGE analyses combined with N-terminal amino acid sequencing. The low incidence of RUBISCO sub-units in the ICF's strongly suggests that the bands observed in figure 4 all originate from the apoplast and are not due to contamination by major intracellular constituents from cellular damage or leakage.

Analyses of the ICF's from tobacco leaves from different stages of development have revealed some interesting results. Polypeptide banding patterns of the ICF's from immature and mature leaf tissues were very different, indicating that at particular developmental stages unique complements of proteins are present (figure 4). *In situ* staining for SOD enzyme activity has revealed a class of unique isoforms of SOD in the extracellular compartment. These bands represent a basic complement absent from the intracellular fraction. This result confirms the and extends the findings of Schinkel *et al.* (1998) who used vacuum infiltration to investigate the distribution of SOD in pine needles.

The large-scale variant of VI described here now provides the opportunity to isolate these unique complements of enzymes and proteins for further study.

We have successfully adapted this large-scale VI technique to barley and oil seed rape leaf materials and are currently exploring its potential application to other plant tissue types. We have successfully obtained several N-terminal sequences of apoplastic proteins from tobacco and other species, using this method (*data not shown*). Both time of exposure to vacuum and centrifugation speed to recover ICF's influence the quality and quantity of recovered from vacuum infiltrated tissue. It is clear that the best results are achieved only after some optimisation of the vacuum and centrifugation conditions for each experimental tissue. The methods described here should suffice for successful application to most plant materials. A further aspect of the methods versatility lies in the fact that many different types of buffer can be used to selectively release different fractions of apoplastic proteins (cf. Robertson et al 1998).

The authors acknowledge the financial support of the biotechnology and biological sciences research council, U.K. SD is the recipient of a BBSRC special studentship.

REFERENCES

Apel, K, Bohlmann, H, Reimann-Philipp, U (1990)
Leaf thionins, a novel class of putative defence factors
Physiologia Plantarum **80**, 315-321

Bradford, MM (1976)
A rapid and sensitive method for quantification of microgram quantities of protein utilising the principle of protein-dye binding
Ana. Biochem **72**, 248-254

Canny, MJ (1995)
Apoplastic water and solute movement - new rules for an old space.
Annual Review of Plant Physiology and Plant Molecular Biology **46**, 215-236

Cordewener, J, Booij, H, van de Zandt, H, Engelen, F, van Kammen, A, Vries, S (1991)
Tunicamycin inhibited carrot somatic embryogenesis can be restored by secreted cationic peroxidase isozymes.
Planta **184**, 478-486

Dhindsa, RS (1991)
Drought stress, enzymes of glutathione metabolism, oxidation injury, and protein synthesis in *Tortula ruralis*
Plant Physiology **95**, 648-651

Dixon, RA (1986)
The phytoalexin response: Elicitation, signalling and the control of gene expression
Biological Review of the Cambridge Philosophical Society **61**, 239-292

Espelie, KE, Franceschi, VR, Kolattukudy, PE (1986)
Immunocytochemical localisation and time course of appearance of an anionic peroxidase associated with suberisation in wound-healing potato tuber tissue
Plant Physiology **81**, 487-492

Fry, SC (1986)
Cross-linking of matrix polymers in the growing cell walls of angiosperms.
Annual Review of Plant Physiology **37**, 165-186

Hammond-Kosack (1992)
Preparation and analysis of intercellular fluid in Molecular Plant Pathology : A Practical Approach II
Edited by SJ Gurr, MJ McPherson & DJ Bowles, pp 15-21

Hartley, RD & Jones, EC (1975)
Diferulic acid as a component of cell wall of *Lilium multiforum*
Phytochemistry **15**, 1157-1160

Hatfield, RD & Nevins, DJ (1987)
Hydrolytic activity and substrate specificity of an endoglucanase from *Zea Mays* seedling cell walls.
Plant Physiology **83**, 203-207

Holland, D, Ben-Hayyim, G, Faltin, Z, Camoin, L, Strosberg, AD, Eshdat, Y (1993)
Molecular characterisation of salt-stress associated protein in citrus : protein and cDNA sequence homology to mammalian glutathione peroxidases
Plant Molecular Biology **21**, 923-927

Konbrink, E, Schroder, M & Hahlbrock, K (1988)
Several "pathogenesis-related" proteins in potato are 1,3-β-glucanases and chitinases
Procedures of the National Academy of the USA **85** pp782-786

Laemmli, UK (1970)
Cleavage of structural proteins during the assembly of the head of bacteriophage T4.
Nature **227**, 680-685

Mäder, M (1980)
Origin of the heterogeneity of peroxidase isoenzymes group G1 from *Nicotiana tabacum*
Pflanzenzphysiologia **96**, 283-296

Manchenko, GP (1994) in "Handbook of detection of enzymes on electrophoretic gels", CRC Press.

Marentes, E, Griffith, M, Mlynarz, A, Brush, RA (1993)
Proteins accumulate in the apoplast of winter rye leaves during cold-acclimation
Physiologia plantarum **87**, 499-507

Matern, U, Grimmig, B, Kneusel, RE (1995)
Plant-cell wall reinforcement in the disease resistance response - molecular composition and regulation
Canadian journal of botany-revue Canadienne de Botanique **73**, S511-S517

Rao, KV, Suprasanna, P, Reddy, GM (1990)
Biochemical changes in embryogenic and non-embryogenic calli of *Zea mays* L.
Plant Science **66**, 127-130

Robertson, D, Davies, DR, Gerrish, C, Jupe, S, Bolwell, GP (1995)
Rapid changes in oxidative metabolism as a consequence of elicitor treatment of suspension-cultured cells of French bean (*Phaseolus vulgaris* L.)
Plant Molecular Biology **27**, 59-67

Robertson, D, Davies, DR, Gerrish, C, Jupe, S, Bolwell, GP (1995)
Rapid changes in oxidative metabolism as a consequence of elicitor treatment of suspension-cultured cells of French bean (*Phaseolus vulgaris* L.)
Plant Molecular Biology **27**, 59-67

Robertson, D, Mitchel, GP, Gilroy, JS, Gernish, C, Bolwell, GP, Slabas, AR (1997)
Differential extraction and protein sequencing reveals major differences in patterns of primary cell wall proteins from plants.
J. Biol Chem **272**, 15841-15848

Rohringer, R, Ebrahim-Nesbat, F, Wolf, G (1983)
Proteins in intercellular washing fluids from leaves of barley (*Hordeum vulgare* L.)

Journal of Experimental Botany **34**, 1589-1605

Schinkel, H, Streller, S, Wingsle, G (1998) Multiple forms of extracellular superoxide dismutase in needles, stem tissues and seedlings of Scots pine. *Journal of Experimental Botany* **49**, 931-936

Showalter, AM (1993)
Structure and function of plant cell wall proteins
The Plant Cell **5**, 9-23

Söding, H (1939)
Über das Verhalten von Bakterien in lebenden Blättern
Ber Deutsch Botania Ges **57**, 465-477

Stafford, HA, Bravinder-Bree, S (1972)
Peroxidases isozymes of the first internode of sorghum. Tissue and intercellular localisation and multiple peaks of activity isolated by filtration chromotography
Plant physiology **49**, 950-956

Terry, ME, Bonner, BA (1980)
An examination of centrifugation as a method of extraction of extracellular solution from peas, and it's use for the study of IAA-induced growth
Plant Physiology **66**, 321-325

Varner, JE & Taylor, R (1989)
New ways to look at the architecture of plant cell wall. Localisation of polygalacturonate blocks in plant tissues
Plant Physiology **91** pp31-33

Welinder, KG - editors Lobarzewski, J, Greppin, H, Penel, C, Gaspar, T (1991)
The plant peroxidase superfamily: Biochemical, molecular and physiological aspects of plant peroxidases University of Geneva pp3-13

APPENDIX 2

BLAST search results

ITL4 - ATFDIVNQTYTVWA

BLASTP 2.0.14 [Jun-29-2000]

Reference:
Altschul, Stephen F., Thomas L. Madden, Alejandro A. Schäffer,
Jinghui Zhang, Zheng Zhang, Webb Miller, and David J. Lipman (1997),
"Gapped BLAST and PSI-BLAST: a new generation of protein database search
programs", Nucleic Acids Res. 25:3389-3402.

RID: 963074119-21743-13743

Query=
(13 letters)

Database: nr
517,398 sequences; 162,338,283 total letters

****

>sp|P07052|PRR2_TOBAC PATHOGENESIS-RELATED PROTEIN R MINOR FORM PRECURSOR (PR-R)
(PROB12) (THAUMATIN-LIKE PROTEIN E2)
pir||JH0231 thaumatin-like protein E2 - common tobacco
emb|CAA33292.1| (X15223) thaumatin-like protein [Nicotiana tabacum]
emb|CAA27548.1| (X03913) TMV induced protein precursor (aa 1-226) [Nicotiana
tabacum]
prf||1206322A protein,TMV induced [Nicotiana sp.]
Length = 226

Score = 27.0 bits (58), Expect = 25
Identities = 12/13 (92%), Positives = 12/13 (92%)

Query: 1 ATFDIVNQDTYTV 13
ATFDIVNQ TYTV
Sbjct: 26 ATFDIVNQCTYTV 38

****

>sp|P13046|PRR1_TOBAC PATHOGENESIS-RELATED PROTEIN R MAJOR FORM PRECURSOR
(THAUMATIN-LIKE PROTEIN E22)
pir||JH0230 pathogenesis-related protein R precursor - common tobacco
emb|CAA33293.1| (X15224) thaumatin-like protein [Nicotiana tabacum]
emb|CAA31235.1| (X12739) pathogenesis-related protein R (AA 1 - 226) [Nicotiana
tabacum]
Length = 226

Score = 25.4 bits (54), Expect = 75
Identities = 11/13 (84%), Positives = 12/13 (91%)

Query: 1 ATFDIVNQDTYTV 13
ATFDIVN+ TYTV
Sbjct: 26 ATFDIVNKCTYTV 38

****

>emb|CAB85637.1| (AJ237999) putative thaumatin-like protein [Vitis vinifera]
Length = 222

Score = 24.3 bits (51), Expect = 168
Identities = 10/13 (76%), Positives = 12/13 (91%)

Query: 1 ATFDIVNQDTYTV 13
ATFDI+N+ TYTV
Sbjct: 25 ATFDILNKCTYTV 37

****

>gb|AAB61590.1| (AF003007) VVTL1 [Vitis vinifera]
Length = 222

Score = 24.3 bits (51), Expect = 168
Identities = 10/13 (76%), Positives = 12/13 (91%)

Query: 1 ATFDIVNQDTYTV 13
ATFDI+N+ TYTV
Sbjct: 25 ATFDILNKCTYTV 37

****

>pir||PC2253 antifungal 27K protein - Diospyros texana (fragment)
gb|AAB31495.1| antifungal protein thaumatin homolog {N-terminal} [Diospyros
texana, overripe fruits, Peptide Partial, 30 aa]
Length = 30

Score = 23.9 bits (50), Expect = 220
Identities = 10/13 (76%), Positives = 11/13 (83%)

Query: 1 ATFDIVNQDTYTV 13
ATFDI N+ TYTV
Sbjct: 1 ATFDIQNKXTYTV 13

****

>pir||T04212 osmotin precursor - Arabidopsis thaliana
emb|CAB39936.1| (AL049500) osmotin precursor [Arabidopsis thaliana]
emb|CAB78208.1| (AL161532) osmotin precursor [Arabidopsis thaliana]
Length = 244

Score = 22.7 bits (47), Expect = 494
Identities = 9/13 (69%), Positives = 12/13 (92%)

Query: 1 ATFDIVNQDTYTV 13
ATF+I+NQ +YTV
Sbjct: 23 ATFEILNQCSYTV 35

□

□

□
1: PC2253 . antifungal 27K pro...[gi:1083849]PubMed, Related Sequences
□

□

□
LOCUS PC2253 30 aa PLN 24-FEB-1995
DEFINITION antifungal 27K protein - Diospyros texana (fragment).
ACCESSION PC2253
PID g1083849
VERSION PC2253 GI:1083849
DBSOURCE pir: locus PC2253;
summary: #length 30 #checksum 6033;
PIR dates: 24-Feb-1995 #sequence_revision 24-Feb-1995 #text_change
24-Feb-1995;
punctuation in sequence.
KEYWORDS .
SOURCE Diospyros texana.
ORGANISM Diospyros texana
Eukaryota; Viridiplantae; Streptophyta; Embryophyta; Tracheophyta;
euphyllophytes; Spermatophyta; Magnoliophyta; eudicotyledons; core
eudicots; Asteridae; Ericales; Ebenaceae; Diospyros.
REFERENCE 1 (residues 1 to 30)
AUTHORS Vu,L. and Huynh,Q.K.
TITLE Isolation and characterization of a 27-kDa antifungal protein from
the fruits of Diospyros texana
JOURNAL Biochem. Biophys. Res. Commun. 202 (2), 666-672 (1994)
MEDLINE 94324951
COMMENT This protein belongs to one type of antifungal proteins called
thaumatin-like protein due to the high degree of sequence homology
to the thaumatin from Thaumatococcus danielli.
FEATURES Location/Qualifiers
source 1..30
/organism="Diospyros texana"
/db_xref="taxon:37488"
Protein 1..30
/product="antifungal 27K protein"
ORIGIN
1 atfdiqnkxt ytvwaaawap sypggxkqld
//

Revised: June 5, 2000.

ITL 5 - SYQDFCVADD

BLASTP 2.0.14 [Jun-29-2000]

Reference:
Altschul, Stephen F., Thomas L. Madden, Alejandro A. Schäffer,
Jinghui Zhang, Zheng Zhang, Webb Miller, and David J. Lipman (1997),
"Gapped BLAST and PSI-BLAST: a new generation of protein database search
programs", Nucleic Acids Res. 25:3389-3402.

RID: 963077133-10221-15128

Query=
(10 letters)

Database: nr
517,398 sequences; 162,338,283 total letters

Taxonomy reports

Alignments

>gb|AAB51571.1| (U75193) germin-like protein [Arabidopsis thaliana]
gb|AAB51573.1| (U75195) germin-like protein [Arabidopsis thaliana]
emb|CAA73213.1| (Y12673) GLP3 protein [Arabidopsis thaliana]
dbj|BAA77208.1| (D89374) germin-like protein 2 precursor [Arabidopsis thaliana]
emb|CAB54516.1| (AJ132237) GER3 protein [Arabidopsis thaliana]
Length = 211

Score = 32.4 bits (69), Expect = 0.22
Identities = 9/9 (100%), Positives = 9/9 (100%)

Query: 1 SVQDFCVAD 9
SVQDFCVAD
Sbjct: 21 SVQDFCVAD 29

****

>gb|AAB51241.1| (U81163) auxin-binding protein [Prunus persica]
Length = 209

Score = 32.4 bits (69), Expect = 0.22
Identities = 9/9 (100%), Positives = 9/9 (100%)

Query: 1 SVQDFCVAD 9
SVQDFCVAD
Sbjct: 19 SVQDFCVAD 27

****

>gb|AAD00295.1| (U79114) auxin-binding protein ABP19 [Prunus persica]
Length = 209

Score = 32.4 bits (69), Expect = 0.22
Identities = 9/9 (100%), Positives = 9/9 (100%)

Query: 1 SVQDFCVAD 9
SVQDFCVAD
Sbjct: 19 SVQDFCVAD 27

****

>gb|AAB51566.1| (U75188) germin-like protein [Arabidopsis thaliana]
gb|AAB51581.1| (U75203) germin-like protein [Arabidopsis thaliana]
Length = 211

Score = 32.4 bits (69), Expect = 0.22
Identities = 9/9 (100%), Positives = 9/9 (100%)

Query: 1 SVQDFCVAD 9
SVQDFCVAD
Sbjct: 21 SVQDFCVAD 29

****

>sp|P45854|GLP1_SINAL GERMIN-LIKE PROTEIN 1 PRECURSOR
pir||T10454 germin-like protein 1 - white mustard
emb|CAA59257.1| (X84786) Glp1 [Sinapis alba]
Length = 211

Score = 32.4 bits (69), Expect = 0.22
Identities = 9/9 (100%), Positives = 9/9 (100%)

Query: 1 SVQDFCVAD 9
SVQDFCVAD
Sbjct: 21 SVQDFCVAD 29

****

>gb|AAB51750.1| (U95034) germin-like protein [Arabidopsis thaliana]
Length = 204

Score = 29.9 bits (63), Expect = 1.3
Identities = 8/9 (88%), Positives = 9/9 (99%)

Query: 1 SVQDFCVAD 9
SVQDFCVA+
Sbjct: 14 SVQDFCVAN 22

****

>sp|P46271|GLP1_BRANA GERMIN-LIKE PROTEIN PRECURSOR
pir||T07854 germin-like protein (clone BnC4) - rape
gb|AAA86365.1| (U21743) germin-like protein [Brassica napus]
Length = 207

Score = 29.9 bits (63), Expect = 1.3
Identities = 8/9 (88%), Positives = 9/9 (99%)

Query: 1 SVQDFCVAD 9
SVQDFCVA+
Sbjct: 18 SVQDFCVAN 26

****

>emb|CAA63014.1| (X91921) germin1 [Arabidopsis thaliana]
Length = 208

Score = 29.9 bits (63), Expect = 1.3
Identities = 8/9 (88%), Positives = 9/9 (99%)

Query: 1 SVQDFCVAD 9
SVQDFCVA+
Sbjct: 18 SVQDFCVAN 26

****

>gb|AAB51240.1| (U81162) auxin-binding protein [Prunus persica]
Length = 214

Score = 29.9 bits (63), Expect = 1.3
Identities = 8/8 (100%), Positives = 8/8 (100%)

Query: 2 VQDFCVAD 9
VQDFCVAD
Sbjct: 25 VQDFCVAD 32

****

SICF2 - MPVDITYLQSAVRKGRVPL

BLASTP 2.0.10 [Aug-26-1999]

Reference:
Altschul, Stephen F., Thomas L. Madden, Alejandro A. Schäffer,
Jinghui Zhang, Zheng Zhang, Webb Miller, and David J. Lipman (1997),
"Gapped BLAST and PSI-BLAST: a new generation of protein database search
programs", Nucleic Acids Res. 25:3389-3402.

Query=
(19 letters)

Database: Non-redundant GenBank CDS
translations+PDB+SwissProt+SPupdate+PIR
416,691 sequences; 127,703,076 total letters

****

emb|CAA18628.1| (AL022580) putative pectinacetylesterase protein [Arabidopsis
thaliana]
Length = 362

Score = 30.7 bits (65), Expect = 0.56
Identities = 10/11 (90%), Positives = 10/11 (90%)

Query: 5 ITYLQSAVRKG 15
ITYLQSAV KG
Sbjct: 26 ITYLQSAVAKG 36

****

sp|Q62137|JAK3_MOUSE TYROSINE-PROTEIN KINASE JAK3 (JANUS KINASE 3) (JAK-3)
>gi|2137461|pir||I58401 JAK3 - mouse >gi|537607 (L33768)
JAK3 [Mus musculus]
Length = 1299

Score = 28.2 bits (59), Expect = 3.3
Identities = 10/12 (83%), Positives = 10/12 (83%)

Query: 8 LQSAVRKGRVPL 19
L SAV KGRVPL
Sbjct: 452 LSSAVIKGRVPL 463

****

gb|AAD36370.1|AE001785_1 (AE001785) ribonuclease H-related protein [Thermotoga maritima]
Length = 223

Score = 27.3 bits (57), Expect = 5.9
Identities = 8/8 (100%), Positives = 8/8 (100%)

Query: 11 AVRKGRVP 18
AVRKGRVP
Sbjct: 9 AVRKGRVP 16

****

SICF3 - ASNGLGRTPQMGN

BLASTP 2.0.10 [Aug-26-1999]

Reference:
Altschul, Stephen F., Thomas L. Madden, Alejandro A. Schäffer,
Jinghui Zhang, Zheng Zhang, Webb Miller, and David J. Lipman (1997),
"Gapped BLAST and PSI-BLAST: a new generation of protein database search
programs", Nucleic Acids Res. 25:3389-3402.

Query=
(13 letters)

Database: Non-redundant GenBank CDS
translations+PDB+SwissProt+SPupdate+PIR

****

emb|CAB00120.1| (Z75955) similar to alpha-N-acetylgalactosaminidase; cDNA EST
EMBL:M92935 comes from this gene; cDNA EST CEMSA04R
comes from this gene [Caenorhabditis elegans]
Length = 451

Score = 30.3 bits (64), Expect = 0.76
Identities = 9/10 (90%), Positives = 9/10 (90%)

Query: 3 NGLGRTPQMG 12
NGLGRTP MG
Sbjct: 18 NGLGRTPPMG 27

****

emb|CAA64760| (X95506) alpha-galactosidase MEL [Saccharomyces sp.]
Length = 471

Score = 28.2 bits (59), Expect = 3.3
Identities = 9/10 (90%), Positives = 9/10 (90%)

Query: 3 NGLGRTPQMG 12
NGLG TPQMG
Sbjct: 24 NGLGLTPQMG 33

****

pir||JQ1021 alpha-galactosidase (EC 3.2.1.22) - yeast (Saccharomyces
cerevisiae) >gi|171924 (M58484) alpha-galactosidase
[Saccharomyces carlsbergensis]
Length = 471

Score = 28.2 bits (59), Expect = 3.3
Identities = 9/10 (90%), Positives = 9/10 (90%)

Query: 3 NGLGRTPQMG 12
NGLG TPQMG
Sbjct: 24 NGLGLTPQMG 33

****

sp|P41947|MEL6_YEAST ALPHA-GALACTOSIDASE 6 PRECURSOR (MELIBIASE 6)
(ALPHA-D-GALACTOSIDE GALACTOHYDROLASE 6)
>gi|1084809|pir||S50312 MEL6 protein - yeast
(Saccharomyces cerevisiae) >gi|547466|emb|CAA85739|
(Z37510) alpha-galactosidase [Saccharomyces cerevisiae]
Length = 471

Score = 28.2 bits (59), Expect = 3.3
Identities = 9/10 (90%), Positives = 9/10 (90%)

Query: 3 NGLGRTPQMG 12
NGLG TPQMG
Sbjct: 24 NGLGLTPQMG 33

****

Other Formats: <Picture: [FASTA Format]> <Picture: [Graphical View]>
Links: <Picture: [1 medline link]> <Picture: [1 nucleotide link]> <Picture: [92 protein neighbors]>

LOCUS CAB00120 451 aa INV 02-SEP-1999
DEFINITION similar to alpha-N-acetylgalactosaminidase; cDNA EST EMBL:M92935
comes from this gene; cDNA EST CEMSA04R comes from this gene.
ACCESSION CAB00120
PID g3878996
VERSION CAB00120.1 GI:3878996
DBSOURCE embl locus CER07B7, accession Z75955.1
KEYWORDS .
SOURCE Caenorhabditis elegans.
ORGANISM Caenorhabditis elegans
Eukaryota; Metazoa; Nematoda; Secernentea; Rhabditia; Rhabditida;
Rhabditina; Rhabditoidea; Rhabditidae; Peloderinae; Caenorhabditis.
REFERENCE 1 (residues 1 to 451)
AUTHORS Wilson,R., Ainscough,R., Anderson,K., Baynes,C., Berks,M.,
Bonfield,J., Burton,J., Connell,M., Copsey,T., Cooper,J.,
Coulson,A., Craxton,M., Dear,S., Du,Z., Durbin,R., Favello,A.,
Fulton,L., Gardner,A., Green,P., Hawkins,T., Hillier,L., Jier,M.,
Johnston,L., Jones,M., Kershaw,J., Kirsten,J., Laister,N.,
Latreille,P., Lightning,J., Lloyd,C., McMurray,A., Mortimore,B.,
O'Callaghan,M., Parsons,J., Percy,C., Rifken,L., Roopra,A.,
Saunders,D., Shownkeen,R., Smaldon,N., Smith,A., Sonnhammer,E.,
Staden,R., Sulston,J., Thierry-Mieg,J., Thomas,K., Vaudin,M.,
Vaughan,K., Waterston,R., Watson,A., Weinstock,L.,
Wilkinson-Sproat,J. and Wohldman,P.
TITLE 2.2 Mb of contiguous nucleotide sequence from chromosome III of C.
elegans
JOURNAL Nature 368 (6466), 32-38 (1994)
MEDLINE 94150718
REFERENCE 2 (residues 1 to 451)
AUTHORS Harris,B.
TITLE Direct Submission
JOURNAL Submitted (13-JUL-1996) Louis, MO 63110, USA. E-mail:
jes@sanger.ac.uk or rw@nematode.wustl.edu
COMMENT Coding sequences below are predicted from computer analysis, using
predictions from Genefinder (P. Green, U. Washington), and other
available information.
For a graphical representation of this sequence and its analysis
see:-
http://webace.sanger.ac.uk/cgi-
bin/display?db=wormace&class=Sequence &object=R07B7
Current sequence finishing criteria for the C. elegans genome
sequencing consortium are that all bases are either sequenced
unambiguously on both strands, or on a single strand with both a
dye primer and dye terminator reaction, from distinct subclones.
Exceptions are indicated by an explicit note.
IMPORTANT: This sequence is NOT necessarily the entire insert of
the specified clone. It may be shorter because we only sequence
overlapping sections once, or longer because we arrange for a small
overlap between neighbouring submissions.
This sequence is the entire insert of clone R07B7. The true right
end of clone F10C2 is at 1275 in this sequence. The start of this
sequence (1..112) overlaps with the end of sequence Z81497.
The end of this sequence (43364..43469) overlaps with the start of
sequence Z92825.
FEATURES Location/Qualifiers
source 1..451
/organism="Caenorhabditis elegans"
/db_xref="taxon:6239"
/chromosome="V"
/clone="R07B7"
Protein 1..451
/name="similar to alpha-N-acetylgalactosaminidase; cDNA
EST EMBL:M92935 comes from this gene; cDNA EST CEMSA04R
comes from this gene"
CDS 1..451
/gene="R07B7.11"
/db_xref="SPTREMBL:Q21801"
/coded_by="join(Z75955.1:28833..29013,
Z75955.1:29059..29198,Z75955.1:29270..29899,
Z75955.1:29950..30051,Z75955.1:30120..30422)"

ORIGIN

```
  1 mrlllpllfc vgafcldngl grtppmgwms wtafyceidc vkhptgcine qlykdmadql
 61 vsggydkvgy ksvhiddcws emerdshgil vanktrfpsg mkalakymhd rglkfgiyed
121 ygtktcggyp gsykhekvda qtfaawdvdy lkldgcnidq ammpigyplf ekelnetgrp
181 imyscswpay lidhpelvny nligkycntw rnfddinssw ksiisiisyy dkmqdkhipt
241 hgpgkwhdpd mlvignkgit ldmsisqftv wciwsaplim sndlriigds fkdvlknkea
301 ikinqdplgi mgrliknstd igvyvkqitp skgdkksfaf aylnrnekeg ykrieiqlas
361 igltdpagyy vhdiwshvdl gllrsgdsiv vsiapagsvf fradlaslhq pkgkrrykfd
421 nsnvvyefer eqsqlgrfdf gdylrtnrvq f
```

SICF7 – DDPD?T

No significant results

SICF8 - AVLDFCVGDLSVPDNPAG

TBLASTN 2.0.10 [Aug-26-1999]

Reference:
Altschul, Stephen F., Thomas L. Madden, Alejandro A. Schäffer,
Jinghui Zhang, Zheng Zhang, Webb Miller, and David J. Lipman (1997),
"Gapped BLAST and PSI-BLAST: a new generation of protein database search
programs", Nucleic Acids Res. 25:3389-3402.

Query=
(18 letters)

Database: Non-redundant GenBank+EMBL+DDBJ+PDB sequences
478,564 sequences; 1,310,507,524 total letters

If you have any problems or questions with the results of this search
please refer to the BLAST FAQs

****

gb|U81162|PPU81162 Prunus persica auxin-binding protein (ABP20) mRNA, complete cds
Length = 1001

Score = 37.1 bits (80), Expect = 0.026
Identities = 12/18 (66%), Positives = 14/18 (77%)
Frame = +1

Query: 1 AVLDFCVGDLSVPDNPAG 18
AV DFCV DL+ P+ PAG
Sbjct: 103 AVQDFCVADLAAPEGPAG 156

****

emb|Y15962|HVGLP1 Hordeum vulgare mRNA for germin-like protein 1
Length = 833

Score = 33.3 bits (71), Expect = 0.37
Identities = 11/15 (73%), Positives = 11/15 (73%)
Frame = +1

Query: 4 DFCVGDLSVPDNPAG 18
DFCV DLS D PAG
Sbjct: 106 DFCVADLSCSDTPAG 150

****

dbj|AB010876|AB010876 Oryza sativa OsGLP1 mRNA for germin-like protein 1, complete cds
Length = 994

Score = 30.7 bits (65), Expect = 2.2
Identities = 10/15 (66%), Positives = 11/15 (72%)
Frame = +1

Query: 4 DFCVGDLSVPDNPAG 18
DFCV DL+ D PAG
Sbjct: 181 DFCVADLTCSDTPAG 225

****

gb|AF032975|AF032975 Oryza sativa germin-like protein 5 (GER5) mRNA, complete cds
Length = 1030

Score = 30.7 bits (65), Expect = 2.2
Identities = 10/15 (66%), Positives = 11/15 (72%)
Frame = +2

Query: 4 DFCVGDLSVPDNPAG 18
DFCV DL+ D PAG
Sbjct: 182 DFCVADLTCSDTPAG 226

<Picture: Entrez protein Query>

Other Formats: <Picture: [FASTA Format]> <Picture: [Graphical View]>
Links: <Picture: [1 nucleotide link]> <Picture: [105 protein neighbors]>

```
LOCUS       AAB51240     214 aa                PLN     02-APR-1997
DEFINITION  auxin-binding protein.
ACCESSION   AAB51240
PID         g1916807
VERSION     AAB51240.1  GI:1916807
DBSOURCE    locus PPU81162 accession U81162.1
KEYWORDS    .
SOURCE      peach.
  ORGANISM  Prunus persica
            Eukaryota; Viridiplantae; Streptophyta; Embryophyta; Tracheophyta;
            euphyllophytes; Spermatophyta; Magnoliophyta; eudicotyledons; core
            eudicots; Rosidae; eurosids I; Rosales; Rosaceae; Prunus.
REFERENCE   1  (residues 1 to 214)
  AUTHORS   Ohmiya,A., Tanaka,Y., Kadowaki,K. and Hayashi,T.
  TITLE     Cloning of genes encoding auxin-binding proteins (ABP19/20) from
            peach
  JOURNAL   Unpublished
REFERENCE   2  (residues 1 to 214)
  AUTHORS   Ohmiya,A., Tanaka,Y., Kadowaki,K. and Hayashi,T.
  TITLE     Direct Submission
  JOURNAL   Submitted (05-DEC-1996) Department of Breeding, National Institute
            of Fruit Tree Science, Fujimoto 2-1, Tsukuba, Ibaraki 305, Japan
COMMENT     Method: conceptual translation.
FEATURES             Location/Qualifiers
     source          1..214
                     /organism="Prunus persica"
                     /cultivar="Akatsuki"
                     /db_xref="taxon:3760"
     Protein         1..214
                     /product="auxin-binding protein"
                     /name="cell wall protein"
     CDS             1..214
                     /gene="ABP20"
                     /coded_by="U81162.1:34..678"
ORIGIN
        1 mpqatmifpi lftfflllss snaavqdfcv adlaapegpa gfsckkpasv kvndfvfsgl
       61 giagntsnii kaavtpafva qfpgvnglgi siarldlavg gvvpfhthpg asevlivaqg
      121 ticagfvasd ntpylqtlek gdimvfpqgl lhfqvnggea palafasfgs aspglqildf
      181 alfkndlpte viaqttflda aqikklkgvl ggtn
//
```

SICF9 – AVLDFC<

Sequencing stopped because of similarity to SICF8.

See sequence search results for SICF8

SICF11 – MPDP?PTFAE

No homologies found